Assessment and Understanding of Unilateral Trans-Tibial Amputee Gait using Principal Component Analysis and Discriminant Function Analysis.

by

Maria Bisele

A thesis submitted in partial fulfilment
of the requirements of
Nottingham Trent University
for the degree of Doctor of Philosophy.

June 2018

Copyright Statement

Abstract

The general aim of this thesis was to develop analytical techniques for the assessment and understanding of lower-limb amputee (LLA) gait. The number of individuals with lower limb amputation (LLA) worldwide is growing and being able to optimise rehabilitation and prosthetic prescriptions are becoming more important. Gait analysis may be able to inform these processes, in particular at the individual level.

In study one, a machine learning algorithm was developed and optimised using Principal Component Analysis (PCA) and Discriminant Function Analysis (DFA) to distinguish between barefoot and shod running. An iterative process was used to optimise the algorithm, exploring all possible iterations of ten individuals out of twenty, finding the combination of people with the greatest generic features and thus the lowest error rate for classification. The outcome showed 93.5% classification accuracy between barefoot and shod running. This study demonstrated that an iteration procedure could optimise a machine learning algorithm to overcome the issues of overfitting, which is particularly useful when working with a small sample size as is common in gait analysis.

In study two, PCA and DFA were used to identify differences between the gait of individuals with unilateral trans-tibial amputation (UTTA) and able-bodied individuals. Different approaches were explored, establishing that PCA conducted on normalised temporal-waveforms yielded the best outcome. Results revealed that UTTA and able-bodied gait differed with regards to certain biomechanical variables, providing a better understanding of LLA function. Although differences between individuals with LLA and able-bodied individuals have previously been investigated, this study demonstrates that using multivariate statistical analyses a vast number of variables can be investigated simultaneously, identifying the hierarchy of variables and thus which need to be targeted during treatment.

Clinical diagnosis is based on individual patients, thus in study three PCA was used to determine whether one individual with a UTTA displayed unique gait characteristics when compared to a group of able-bodied individuals. Both covariance and correlation matrices were used during PCA, providing information about variation and magnitude of the data, respectively. Results revealed that each individual with UTTA has subject-specific gait characteristics, which highlights that this method can be used to identify variables which can be targeted during treatment.

In the fourth and final study, PCA was used to understand the effects of attempted symmetry on dynamic stability of individuals with UTTA. Although in rehabilitation symmetrical gait is often sought for since asymmetrical gait is said to cause long term adverse effects, results revealed that asymmetry might be playing a functional role and in fact aids better stability in UTTA gait. This

outcome may suggest that after a certain symmetry has been reached, the target of rehabilitation may need to be reconsidered to aim for better stability.

In conclusion, multivariate statistical analysis could be used to assess and understand LLA function. In a clinical setting, the ability to identify important variables during a task, particularly at patient-specific level has the potential to improve the development of treatment recommendations. Prosthetic prescription and rehabilitation processes can be tailored and in turn the outcome may be more successful which could increase the likelihood of independent living of patients and therefore improve the quality of life of individuals with LLA.

Dissemination of Research

Journal Articles (Appendix 9)

Bisele, M., Bencsik, M., Lewis, M.G., & Barnett, C.T. (2017) Optimisation of a machine learning algorithm in human locomotion using principal component and discriminant function analyses. *PloS ONE*, 12 (9), p.e0183990.

Poster Presentations

Bisele, M., Bencsik, M., Lewis, M.G., & Barnett, C.T. (2018) Should lower-limb amputee gait be assessed at individual basis to improve function? *In Proceedings of the 8th World Congress of Biomechanics, Dublin, Ireland.*

Bisele, M., Bencsik, M., Lewis, M.G., & Barnett, C.T. (2016) Application of machine learning techniques to human locomotion. *In Proceedings of the 10th Science and Technology Annual Research (STAR) conference, Nottingham Trent University.*

Oral Presentations

Bisele, M., Bencsik, M., Lewis, M.G., & Barnett, C.T. (2018) Does attempting symmetry affect dynamic balance during gait un unilateral transtibial prosthesis users? *In Proceedings of the 44th Annual Meeting and Scientific Symposium American Academy of Orthotists and Prosthetists, New Orleans, LA.*

Bisele, M., Bencsik, M., Lewis, M.G., & Barnett, C.T. (2017) How does attempting to walk symmetrically affect dynamic balance in unilateral transtibial amputees? *In Proceedings of the International Society of Prosthetics and Orthotics (ISPO) UK MS Annual Scientific Meeting and Exhibition, Clare College, Cambridge, UK.*

Bisele, M., Bencsik, M., Lewis, M.G., & Barnett, C.T. (2016) Application of machine learning techniques to human locomotion. *In Proceedings of the 10th Science and Technology Annual Research (STAR) conference, Nottingham Trent University, Nottingham, UK.*

Bisele, M., Bencsik, M., Lewis, M.G., and Barnett, C.T. (2016) Optimisation of an objective predictive machine learning algorithm in human locomotion. *In Proceedings of the BASES Biomechanics Interest Group Meeting, Liverpool John Moores, Liverpool, UK.*

Acknowledgements

"I can do all things through Christ who strengthens me." – Philippians 4:13

I would like to give a special thanks to my wonderful supervisory team, Dr Cleveland Barnett, Dr Martin Lewis and Dr Martin Bencsik. Words cannot express how grateful I am to you all. I consider myself lucky to have had the chance to work alongside you. You have been amazing teachers and mentors. I will be forever in your debt for allowing me the opportunity to do this PhD. To Dr Cleveland Barnett, thank you for your guidance throughout these years. You provided me with countless opportunities to develop and become a better researcher, and I could not thank you enough for that. To Dr Martin Lewis, thank you for your support and kindness at all times. Your genius mind has sparked a lot of ideas that kept driving this PhD forward. To Dr Martin Bencsik, thank you for your patience and the long hours you have invested in me. I could not count the number of times I came running to your office (or sent you an email) because I was stuck and you have provided guidance. None of this would have been possible without you.

To all the participants, who gave up their valuable time, thank you very much. To Jane and Miranda, thank you for supporting the recruitment of the prosthetic users.

To my office mates, you are more than just people I work with, you are amazing friends. It was a joy knowing that working meant hanging out with you all. Thank you for making this a memorable time. To Dr Edwin Abdurakman, Dr Emina Michailidou and Odette Pomenya thank you for your support and for being such wonderful friends. To Paul Lester, I cannot put into words how grateful I am for all that you have done for me. You have always taken the time to help me, if it was listening to me practice my presentations, proof reading my work or going for walks. You have been there for me during every step of this incredible journey. Thank you for your unconditional friendship and for all the coffees.

To my brothers, Amanuel and Benjamin, you have been my role models since we were young and I use to follow you around everywhere. You have inspired me to aim for extraordinary and for that I am ever thankful. To my parents, Gidies and Ensaf, there are no words to describe what you mean to me. You never doubted any of this was possible. Your unconditional love and support have pushed me to work hard and achieve my goals. This is for you.

Dedication

To my parents, Gidies and Ensaf

لوالدي

Table of Contents

List of Figures

List of Tables

Key Abbreviations

2D	Two-dimensional
3D	Three-dimensional
AMP	Amputation
ANN	Artificial Neural Networks
AP	Anterior-posterior
ASIS	Anterior superior iliac spine
AUC	Area under the curve
BoS	Base of support
BW	Backward
BW MoS	Backward margin of stability
CA	Cluster analysis
CoM	Centre of mass
CoP	Centre of pressure
CP	Cerebral palsy
CV	Cross-validation
DA	Discriminant Analysis
DFA	Discriminant Functional Analysis
DOB-SCV	Distribution optimally balanced stratified cross-validation
DoF	Degrees of freedom
HFI	Hip flexor index
HS	Heel strike
FFP	Foot-forward placement
FFT	Fast Fourier Transform
FLT	Functional linear transformation
FN	False negative
FP	False positive
FPE	Foot placement estimator
GA	Genetic algorithm
GDI	Gait Deviation Index
GGI	Gillette Gait Index
GPS	Gait Profile Score
GRF	Ground reaction force

GVS	Gait Variable Score
KNN	K-Nearest Neighbours
kPCA	Kernel based-Principal Component Analysis
LDA	Linear Discriminant Analysis
LLA	Lower-limb amputation/lower-limb amputee
LOO	Leave-one-out
LR	Logistic regression
MAP	Movement analysis profile
MCC	Matthew Correlation Coefficient
MDP	Movement Deviation Profile
ML	Medio-lateral
ML MoS	Medio-lateral margin of stability
MoS	Margin of stability
NB	Naïve Bayes
NI	Normalcy Index
NLR	Negative likelihood ratio
NORM	Self-selected speed
PAD	Peripheral arterial diseases
PC	Principal Component
PCA	Principal Component Analysis
pCoM	Centre of mass position
PSD	Power Spectral Density
PSIS	Posterior superior iliac spine
QDA	Quadratic Discriminant Analysis
QTM	Qualisys track manager
ROC	Receiver operating characteristic
ROM	Range of motion
SACH	Solid ankle cushion heel
SOM	Self-Organising Map
SV	Scalar value
SVM	Support Vector Machine
SYM_{SF}	Symmetrical step frequency
SYM_{SL}	Symmetrical step length
SYM_{SL+SF}	Symmetrical step length and step frequency

UD	Unified deformable
TF	Trans-femoral
TN	True negative
TO	Toe off
TP	True positive
TT	Trans-tibial
UK	United Kingdom
US	United States
UTFA	Unilateral trans-femoral amputation/unilateral trans-femoral amputee
UTTA	Unilateral trans-tibial amputation/unilateral trans-tibial amputee
vCoM	Centre of mass velocity
XCoM	Extrapolated centre of mass

Chapter 1: General Introduction

1.1 Introduction

Undergoing amputation is a traumatic experience. In England, approximately 5000 lower limb amputations are conducted annually, of which 90% are due to diabetes, hypertension and coronary heart disease (Ahmad *et al.,* 2014). The number of individuals with lower-limb amputation (LLA) is expected to double by 2050 due to increased adverse health issues and an increasing ageing population (Ziegler-Graham *et al.,* 2008). Therefore, individuals with LLA represent a growing problem in western society. These individuals lose musculoskeletal mechanisms, joint structures and sensory input vital for movement such as walking. Consequently, their ability to take part in activities of daily living is impacted (Pezzin *et al.,* 2000). This leads to physical and personal dependence, which can adversely affect their quality of life (Sawers & Hahn, 2011). One of the goals of prosthetic rehabilitation is for individuals with LLA to regain and maintain a certain level of function (van Velzen *et al.,* 2006), and thus be able to live independently. During rehabilitation, individuals with LLA are equipped with a prosthesis to replace the missing parts of the limb, which is then used to learn how to walk again (Barnett *et al.,* 2009). Successful prosthetic rehabilitation is associated with increased chances of living at home after the final discharge, self-care performance and improved quality of life (Dawson *et al.,* 1995).

Prosthetic rehabilitation is a complex and multifaceted procedure, which can be both physically and mentally challenging for a patient (Schaffalitzky *et al.,* 2011). The ability to walk well with a prosthesis increases the likelihood of using it following rehabilitation (Gailey, 2006). However, the number of people who can use a prosthesis efficiently ranges from 49% to 95% (Dillingham *et al.,* 2005; Karmarkar *et al.,* 2009; Schoppen *et al.,* 2003). The impact of amputation on mobility is great, especially in the elderly (van Eijk *et al.,* 2012), which make up the majority of individuals with LLA, with the average age being 70.6 years (Ahmad *et al.,* 2014). Even individuals with traumatic LLA, who tend to be younger and healthier, require time to regain pre-existing function, and it is not always achieved (van Eijk *et al.,* 2012). Research has shown that 31% of individuals with LLA are unable to live independently 24 months following amputation and 49% lose the ability to walk completely (Taylor *et al.,* 2005). Being able to predict the outcome of prosthetic rehabilitation is becoming increasingly important (Jarvis *et al.,* 2017; Leung *et al.,* 1996; van Eijk *et al.,* 2012) since it can facilitate decision-making processes early on during the rehabilitation procedure. However, predicting mobility after prosthetic rehabilitation is arduous (Sansam *et al.,* 2009).

Research studies found that prosthetic rehabilitation and the ability to walk after LLA are influenced by multiple factors, which include but are not limited to the age of the individual, level

of amputation, cause of amputation, stump factors and associated pain, cognitive and mood disturbance, dual disabilities, physical fitness, motivation, prosthetics prescriptions and rehabilitation programmes (Jarvis *et al.*, 2017; Leung *et al.*, 1996; Sansam *et al.*, 2009). There are no generic measures in place which are considered essential to evaluate prosthetic rehabilitation (Callaghan & Condie, 2003). Current prosthetic prescriptions and rehabilitation processes are based on the subjective experience of clinicians (Schaffalitzky *et al.*, 2011; van der Linde *et al.*, 2004). Even though rehabilitation goals are met, the lack of knowledge may in some cases compromise the treatment outcome. Clinical decisions supported by gait analysis, facilitate a better understanding of factors affecting gait and therefore aid more effective decision-making processes (Esquenazi, 2014). Clinical gait analysis has changed the way in which gait pathologies are treated. It helps determine the severity of a condition, provides treatment recommendations and evaluates treatment outcome (Hamill *et al.*, 2012). Using gait analysis for the assessment of individuals with LLA can help monitor prosthetic rehabilitation and therapy effectiveness (Skinner & Effeney, 1985), however, prosthetic rehabilitation is said to lack evidence-based practice (Ramstrand & Brodtkorb, 2008).

Gait analysis is commonly conducted using data acquisition tools such as motion capture systems, force platforms and electromyography (Winter, 2009). These data are often processed further using methods such as inverse dynamics (Robertson *et al.*, 2013; Winter, 2009). Subsequently, summary techniques such as gait scores and gait indices are applied, producing information that is accessible by clinical practitioners (Baker *et al.*, 2009; Schutte *et al.*, 2000; Schwartz and Rozumalski, 2008). However, the quality of the interpretation of temporal gait waveforms obtained by the acquisition tools and the processing of the data depends on the researcher's experience. Therefore, both data collection and data analysis can be subjective and highly affected by researcher bias. To overcome these issues, multivariate statistical analyses and machine learning algorithms can be used to develop automatic gait recognition tools, enabling a more objective analysis procedure (Alaqtash *et al.*, 2011a; Lakany, 2008; Simon *et al.*, 2016). In a clinical setting, an automatic gait recognition tool would not only remove researcher bias, but it could also facilitate decision-making processes. Thus, in the treatment of individuals with LLA, it may provide a guide for prosthetic prescriptions and rehabilitation programs.

Research studies commonly assess group effects, whilst clinical assessments are based on individuals. Therefore, research and clinical attempts to aid patients may appear to be operating in diverging directions, preventing a coherent inter-disciplinary approach (Schöllhorn *et al.*, 2002). Being able to identify individual gait differences, instead of focusing on typical behaviour of a group can be particularly useful, as it allows factors to be identified that can be used to tailor

a patient's treatment recommendations meeting their personal needs (Schöllhorn *et al.,* 2002). This is particularly useful in individuals with LLA since it could help tailor prosthetic prescriptions and rehabilitation programs, which may, in turn, increase the likelihood of an individual with LLA to regain the ability to walk independently after rehabilitation. Using machine learning algorithms, Schöllhorn *et al.* (2002) demonstrated that individuals exhibit unique gait characteristics, and these characteristics are not only distinctive but also persistent over the years (Horst *et al.,* 2017; 2016).

Predicting the 'right' intervention for a patient is important, but considerably more work needs to be done to develop methodological frameworks for patient-specific treatment (Hoerzer *et al.,* 2015). To be able to identify the 'right' factors that need to be targeted in an individual is the first step towards the development of this framework. Therefore, the aims of this PhD were to implement quantification methods, which would allow better assessment and understanding of LLA function. Multivariate statistical analyses and machine learning algorithms were explored to identify a technique that might allow a comparison between LLA and able-bodied gait to be made, providing an objective evaluation of LLA function. This technique was then used to compare between the gait of an individual with LLA and a group of able-bodied individuals, to determine if subject-specific gait characteristics could be identified. In addition, the technique was implemented to investigate whether it could provide a better understanding of certain functions of LLA gait such as dynamic stability.

1.2 Aims and Objectives

The general aim of this PhD was to adopt multivariate statistical analyses and machine learning algorithms to develop analytical techniques for the assessment and understanding of LLA function. The specific aims of the thesis were:

(1) To develop and optimise a machine learning algorithm using multivariate statistical analyses, namely Principal Component Analysis (PCA) and Discriminant Function Analysis (DFA) to process human locomotion.
(2) To compare the gait of individuals with unilateral trans-tibial amputation (UTTA) and able-bodied individuals using PCA and DFA to provide a better understanding of LLA function.
(3) To establish subject-specific gait characteristics of an individual with UTTA using PCA when compared to a group of able-bodied individuals.
(4) To identify the effects of attempted temporal-spatial symmetry on the dynamic stability of individuals with UTTA, and to use PCA to understand LLA function during the attempt of temporal-spatial symmetry.

1.3 Structure of Thesis

The thesis begins with a literature review in Chapter 2. In the review, topics related to the biomechanics of LLA gait, and the rationale of this PhD are outlined. Biomechanical variables of LLA gait are described, particularly focusing on variables of forward progression and dynamic stability, since these functional tasks will be a focus in this PhD research. Subsequently, multivariate statistical analyses and machine learning algorithms used in gait analysis and specifically in the assessment of LLA gait are discussed.

The general methodology is outlined in Chapter 3. Details of ethical approval and the inclusion-exclusion criteria are described here. Furthermore, biomechanical gait variables such as temporal-spatial, kinetic and kinematic variables which were collected for the research are presented. Also, acquisition tools and experimental protocol used to collect the data are described as well as processing and analysis procedures. Any additional methods that applied to a specific study are described on a study-by-study basis in the individual methodology sections.

The development and optimisation of a machine learning algorithm using PCA and DFA are described in Chapter 4. The algorithm was developed for data reduction, feature selection and classification between barefoot and shod running. Different techniques were explored in order to optimise the classification outcome, which are outlined and discussed.

In Chapter 5, PCA and DFA were applied, to compare between the gait of a group of individuals with UTTA and a group of able-bodied individuals, using various approaches to establish a robust analysis method for the assessment and understanding of LLA function. The approaches for once involved the use of different forms of biomechanical variables, i.e. entire temporal waveform vs scalar values. The influence of the number of scalar values on the discrimination procedure has also been assessed. Furthermore, the nature of biomechanical data was investigated, i.e. normalised vs non-normalised data.

In Chapter 6, the method established in Chapter 5 was applied to discriminate between the gait of one individual with UTTA and a group of able-bodied individuals. This was done to establish if an individual with UTTA displayed distinctive discriminating features, thus identifying individual gait characteristics which could potentially be used to inform patient-specific treatment. During this analysis, both the covariance and correlation matrices of PCA were utilised.

In Chapter 7, methods described and used in previous chapters were implemented to investigate the effects of attempting temporal-spatial symmetry on the dynamic stability in individuals with UTTA. Individuals with LLA are known to fall more often compared to able-bodied individuals,

which has been attributed to compromised dynamic stability, however, the control mechanisms of dynamic stability are not well understood. Hence, this study looked to provide further understanding of the underlying biomechanical variables that are involved in the maintenance of stable dynamic stability.

Finally, in Chapter 8, the PhD thesis is summarised. Furthermore, limitations, as well as future directions, are outlined, which is followed by possible implementations of findings in clinical practice, before concluding the thesis.

Chapter 2: Review of Literature

2.1 Introduction

This chapter starts with a brief description of biomechanical characteristics of able-bodied gait, followed by some statistics on individuals with LLA and a description of LLA gait, focusing on forward progression and dynamic stability. Different quantification methods of dynamic stability are described, with a detailed explanation of the extrapolated centre of mass (XCoM) and the margin of stability (MoS), which are the chosen methods for this PhD research. Subsequently, characteristics of gait data are outlined, followed by issues faced during the analysis of gait data, and methods proposed in the literature to overcome these issues. Furthermore, the use of automatic recognition tools developed using multivariate statistical analyses and machine learning algorithms are described, detailing their use in gait analysis and their application in the assessment of LLA gait.

2.2 Biomechanics of Normal Gait

Gait is a term describing locomotion characteristics such as walking and running (Fish & Nielsen, 1993). Able-bodied gait describes a series of rhythmical, alternating movements of the trunk, as well as upper-limbs and lower-limbs that lead to forward progression of the centre of gravity. Gait is usually explained in terms of components of the gait cycle starting and ending at heel strike of the same limb. As outlined in Figure 2.1, the full gait cycle is described as a stride, and a step describes heel strike to heel strike from one limb to the contralateral limb, rather than the same limb (Perry *et al.*, 2010). A gait cycle is divided into two major phases of stance and swing (Figure 2.2). The stance phase defines the period during which the foot is in contact with the ground and comprises up to 60% of the gait cycle, and the swing phase is the period during which the foot is off the ground, making up 40% of the gait cycle. Three functional goals are met during the gait cycle, i.e. weight acceptance, single limb support and limb advancement (Perry, 1992), which can be explained using eight sub-categories (Figure 2.2).

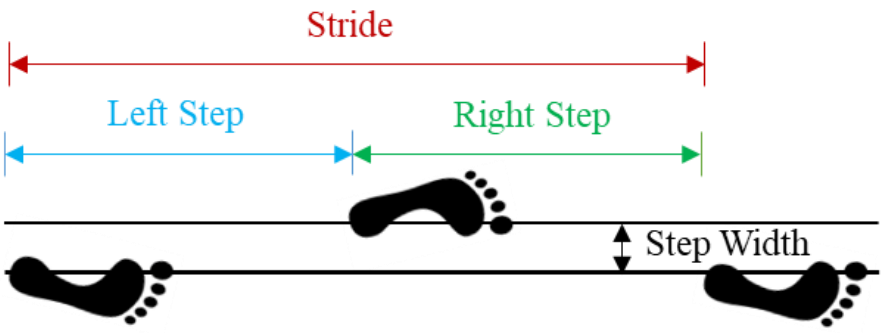

Figure 2.1 Step length, step width, stride length and foot angle during walking gait.

The eight sub-categories of the gait cycle are typically described starting with initial contact, which is often referred to as heel strike. At this instant, the foot comes into contact with the ground. Heel strike is the first phase of double limb support and stabilises the leading limb in preparation for forward progression (Perry, 1992). During heel strike, the hip is flexed to ~30°, the knee is extended between ~0-5°, the foot is at ~25° to the floor and the ankle is at a neutral position (Perry, 1992). Following heel strike, there is a rapid increase of vertical (Fz) ground reaction force (GRF) to approximately one times body weight as weight is shifted and the leading limb accepts the weight. In the anterior-posterior (Fy) GRF an increase in braking force reaches a peak just after weigh acceptance is completed. The medio-lateral (Fx) GRF increases significantly although the force is only 5% of body weight.

After initial contact, the loading response follows (Perry, 1992). During the loading response, the ankle joint plantar-flexes and the foot lowers onto the ground, the hip starts to extend, the knee flexes, and the centre of mass (CoM) propels forward and over the foot, using the heel as a rocker. The aim of this phase is shock absorption, stability during weight bearing, and preservation of forward progression. Mid-stance follows the loading response and describes the first half of single limb support (Perry, 1992). During this phase, the weight is completely aligned over the supporting foot. Thus, the body weight is fully supported by one limb, as the contralateral foot is lifting off the floor. During mid-stance, the ankle is dorsiflexed, whilst the hip and knee are extended. Following mid-stance is terminal stance which describes the second half of single limb support (Perry, 1992). It begins as the heel of the loaded limb starts lifting off the floor, and the CoM moves forward past the forefoot. During this phase, hip extension increases and the knee begins to flex again. This phase ends as the contralateral limb contacts the floor.

At this instance, pre-swing starts at the ipsilateral limb and defines the final phase of stance just before toe-off occurs (Perry, 1992). The contralateral limb is at initial contact, and the ipsilateral limb rapidly unloads the weight, transferring it to the contralateral limb, pushing the body forward. The knee extends, and the ankle plantar-flexes as the toe starts to leave the floor on the ipsilateral limb. The foot then lifts off the floor to start the initial swing phase (Perry, 1992). The hip and the knee start flexing, whilst the ankle starts to dorsiflex during this phase. The contralateral limb is at mid-stance during this instance. This phase ends as the off-loading limb is level with the contralateral limb in stance phase. The initial swing phase is followed by mid-swing, during which the hip flexes so that the limb swings forward, and the knee continues to flex (Perry, 1992). Finally, terminal swing follows, which is also referred to as late swing, where the knee is fully extended, and the ankle is dorsiflexed to neutral as the limb prepares to make contact with the ground to start the cycle again (Perry, 1992).

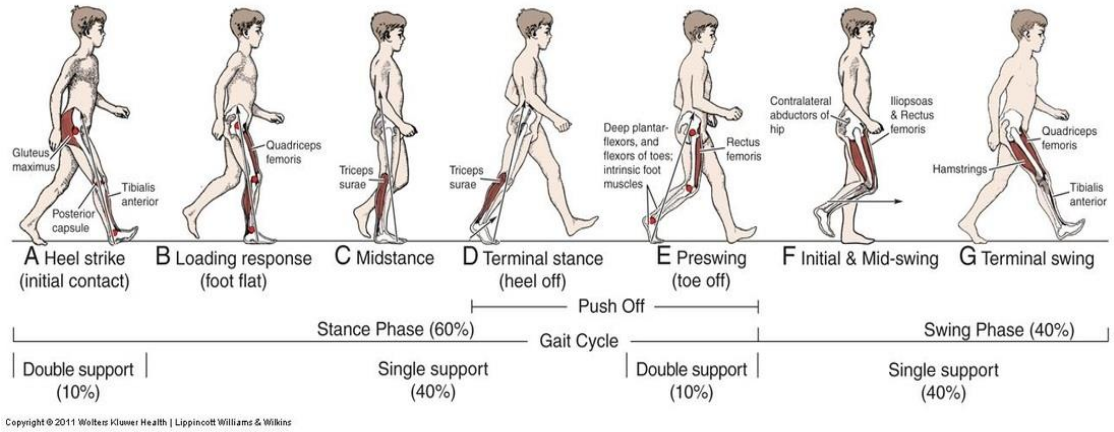

Figure 2.2 Eight phases of the gait cycle. Figure adopted from Physiopedia (2018).

2.3 Statistics of Individuals with Lower-Limb Amputation

An amputation is defined as the surgical removal of a part of the body (nhs.uk., 2018). It is a profound and life-changing event with great physical and mental impact on an individual. Every year thousands of LLAs are performed around the world, with numbers doubling in western society (Ziegler-Graham *et al.*, 2008). In England, more than 5000 new individuals with LLA are recorded per annum (Ahmad *et al.,* 2014). The most common causes for an amputation are diabetes (44%) (Ahmad *et al.,* 2014), which is at an all-time high, equating to 135 procedures each week (Diabetes UK), followed by hypertension (39%) and coronary heart disease (23%) (Ahmad *et al.,* 2014). The United States (US) has an estimated 2 million people living with an amputation, and a further 185,000 individuals scheduled to undergo an amputation annually (Ziegler-Graham *et al.,* 2008). The most common causes of limb loss in the US similar to England, are peripheral arterial diseases (PAD). At the present global estimates for the prevalence rates of PAD in adults age 70 and over stand at 3-10%, with further increases expected to reach 15-20% (Meijer *et al.,* 1998; Norgren *et al.,* 2007). Increases in life expectancy are leading to an ever-growing ageing population and associated prevalence of adverse health issues. The number of individuals predicted to suffer from limb loss by 2050 is 3.6 million people (Ziegler-Graham *et al.,* 2008). It was estimated that in the United Kingdom (UK) an amputation due to type 2 diabetes on average incurred annual hospital inpatient costs of £9546 (£6416 – £13463) (Alva *et al.,* 2015). In 2009, the annual cost of amputations in the US was estimated at $8.3 billion (Amputee Coalition, 2018) with a lifetime health care cost after LLA of around $509,275 (MacKenzie *et al.,* 2007). In conclusion, the number of individuals with LLA is increasing, placing greater cost and care demands on health systems.

2.4 Biomechanics of Lower-Limb Amputee Gait

Individuals with LLA have compromised balance, posture and gait function (Isakov *et al.,* 2000; Jayakaran *et al.,* 2012; Sadeghi *et al.,* 2000; Silverman *et al.,* 2008). The obvious mechanical difficulties result from the removal of parts of the skeletal system and the associated musculature, which are also compounded by the reduction in the somatosensory input. An amputation may occur at various levels at the upper-limbs and lower-limbs and can be classified as minor and major amputation, describing the removal of a digit such as a finger or a toe, or the removal of full parts of extremities such as an arm or shank, respectively (Assumpção *et al.,* 2009). Major limb loss accounts for more than 42% of all amputations with the majority occurring below the knee, more commonly referred to as a trans-tibial (TT) amputation, followed by above knee amputations, commonly referred to as a trans-femoral (TF) amputation. After an LLA, individuals use alternative muscle groups to create movement (van Velzen *et al.,* 2006) and thus compensatory mechanisms are adopted to achieve a certain level of function.

The compensatory gait of individuals with LLA is associated with greater energy expenditure. During locomotion, the musculoskeletal system will function to use the least amount of energy to cover the greatest distance (Waters & Mulroy, 1999). However, individuals with LLA have lower self-selected walking speed and higher energy expenditure relative to able-bodied individuals (Schmalz *et al.,* 2002). Schmalz *et al.* (2002) found oxygen consumption increased proportionally to an increase in speed, which further increased as the level of major amputation becomes higher, relative to able-bodied individuals (Figure 2.3). Greater energy expenditure was attributed to greater mechanical work required during the step-to-step transition from the prosthetic to the intact limb (Houdijk *et al.,* 2009).

The compensatory mechanisms adopted by prosthetic and intact limbs of individuals with LLA result in asymmetrical gait. Asymmetrical gait is known to cause secondary issues, some of which occur early on after the amputation, for example, lower back pain (Kulkarni *et al.,* 2005), and others which occur later in life such as hip and knee osteoarthritis (Burke *et al.,* 1978). Individuals with LLA are also 88% more likely to develop osteoporosis in the prosthetic limb due to asymmetrical gait (Burke *et al.,* 1978). During prosthetic rehabilitation, a more symmetrical gait is often desired to correct for asymmetry and thus minimise these secondary issues. Literature has shown that asymmetries tend to decrease as rehabilitation progresses, and walking ability improves (Barnett *et al.,* 2009).

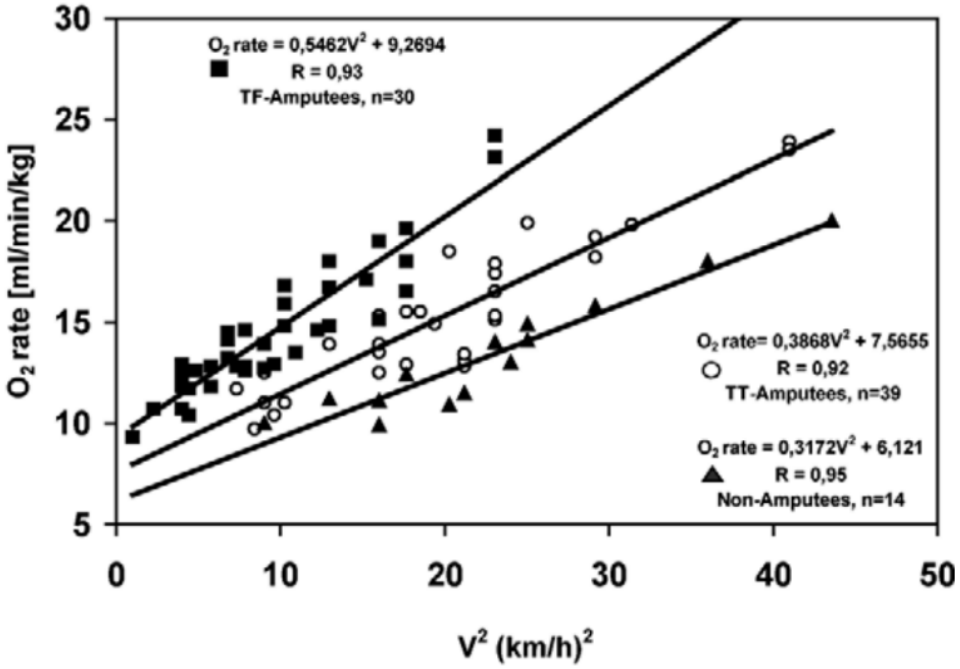

Figure 2.3 Oxygen consumption of individuals with UTFA (solid squares), individuals with UTTA (open circles) and able-bodied individuals (solid triangles), as speed increases during treadmill and level walking. Figure adopted from Schmalz *et al.* (2002).

2.4.1 Temporal-Spatial Parameters of Lower-Limb Amputee Gait

Temporal-spatial parameters describe many variables such as speed and step length, providing an initial assessment of gait. In LLA gait, temporal-spatial variables were found to differ between the intact and prosthetic limb (Isakov *et al.*, 1992; 2000) and also varied depending on individual characteristics such as level of amputation as well as prosthetic components. The self-selected walking speed of individuals with LLA tends to be lower relative to that of able-bodied individuals. However, different average results have been reported across studies for individuals with UTTA and individuals with UTFA as illustrated in Figures 2.4 and 2.5.

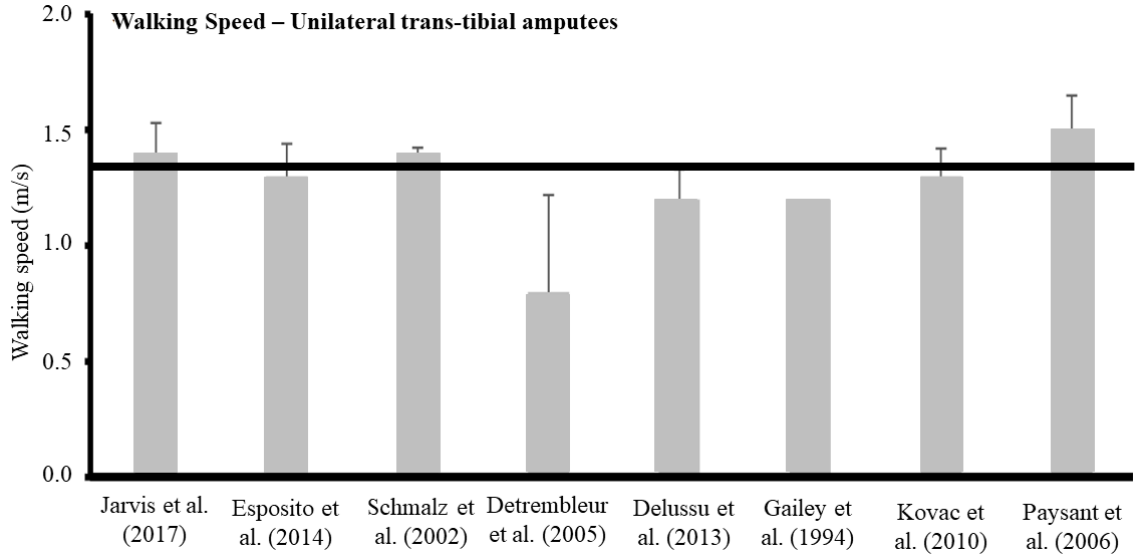

Figure 2.4 Average walking speed (m/s) of individuals with UTTA. The solid black line indicates the average speed of able-bodied individuals. Error bars show standard deviation. In all studies, speeds were identified from over ground walking except for Schmalz *et al.* (2002). The majority of the cohorts in these studies had undergone an amputation due to trauma, and their choice of prosthetic components were elastic response feet and microprocessor knee joints with some exceptions. Figure adapted from Jarvis *et al.* (2017).

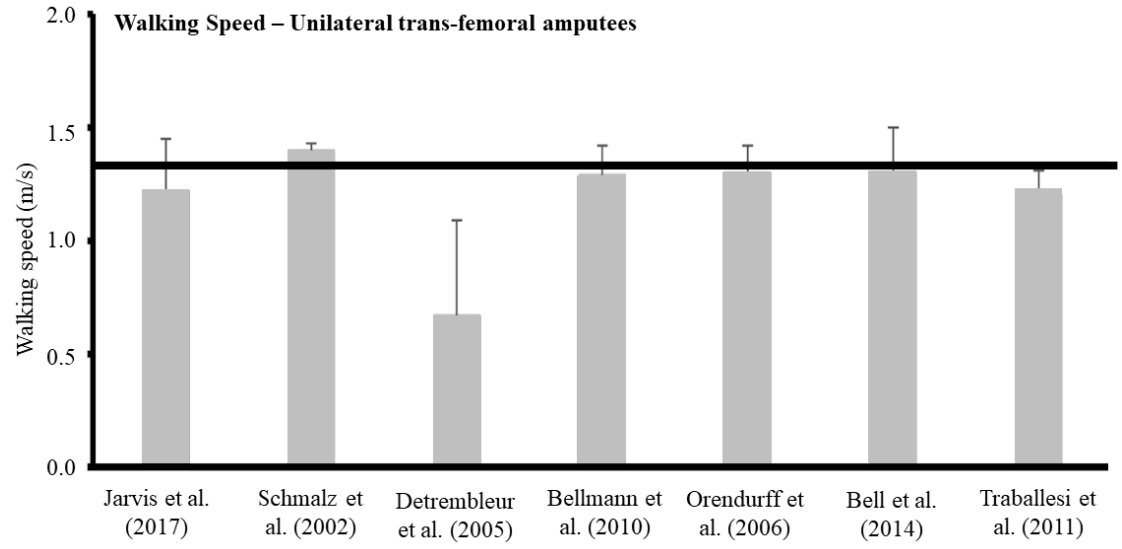

Figure 2.5 Average walking speed (m/s) of individuals with UTFA. The solid black line indicates the average speed of able-bodied individuals. Error bars show standard deviation. In all studies, speeds were identified from over ground walking except for Schmalz *et al.* (2002). The majority of the cohorts in these studies had undergone an amputation due to trauma, and their choice of prosthetic components were elastic response feet and microprocessor knee joints with some exceptions. Figure adapted from Jarvis *et al.* (2017).

Isakov *et al.* (2000) found the average speed of fourteen individuals with UTTA using patellar tendon bearing (PTB) sockets and solid ankle cushion heel (SACH) feet to be 1.25 m/s. They also found significantly larger step time and swing time on the prosthetic limb (step time 0.582±0.04s; swing time 0.438±0.04s) relative to the intact limb (step time 0.569±0.04s; swing time 0.407±0.03s). Furthermore, larger stance time and single support time on the intact limb (stance time 0.774±0.06s, single support time 0.438±0.04s) relative to the prosthetic limb (stance time 0.708±0.05s, single support time 0.407±0.03s) was found (Isakov *et al.*, 2000). The shorter single support time on the prosthetic limb was attributed to the prosthetic foot, since the rigid ankle mechanism of the SACH foot leads to quicker weight transfer from the heel to the forefoot, i.e. resulting in shorter stance duration on the prosthetic limb and shorter swing time on the intact limb. Breakey (1976) found similar results regarding the stance duration on the prosthetic limb. Highsmith *et al.* (2010) reported similar results for individuals with UTFA in step time on the prosthetic limb (0.70±0.05s) relative to the intact limb (0.60±0.06s), however, in individuals with UTTA they found step time to be shorter on the prosthetic limb (58±0.03s) relative to the intact limb (0.60±0.05s). Jarvis *et al.* (2017) also reported significantly shorter step time on the prosthetic limb (60-62% of the gait cycle) relative to the intact limb (62-66% of the gait cycle).

Longer stance time on the intact limb relative to the prosthetic limb (Board *et al.*, 2001; Breakey, 1976; Isakov *et al.*, 2000; McNealy and Gard, 2008; Sanderson and Martin, 1997; Schmid *et al.*, 2005; van der Linden *et al.*, 1999) was described as a control mechanism and was attributed to the lack of confidence in the prosthetic limb (Sanderson & Martin, 1997). It has also been identified as an attempt to protect the prosthetic limb from increased loads and forces (Hurley *et al.*, 1990; Nolan *et al.*, 2003; Powers *et al.*, 1998; Sanderson & Martin, 1997). Jarvis *et al.* (2017) however, reported that walking speed, stride length and cadence of high functioning individuals with UTTA and individuals with UTFA, who use state of the art prosthetic devices, was comparable to able-bodied individuals (Table 2.1). Rábago and Wilken (2016) used prevalence to describe gait deviations of individuals with UTTA. The measure of prevalence is described as a percentage outside normative reference ranges, where the reference range was calculated using the mean and standard deviation of a group of able-bodied individuals. Individuals with UTTA were found to have the greatest prevalence, i.e. differed from the normative reference ranges, in step time and length measurements of the intact limb, however, these deviations were not significant.

Table 2.1 Temporal-spatial variables of individuals with UTTA and individuals with UTFA of both prosthetic (PROS) and intact (NONPROS) limbs, and able-bodied individuals of both right and left limbs. Table adopted from Jarvis *et al.* (2017).

Parameter	**Individuals with UTTA**		**Individuals with UTFA**		**Able-bodied Individuals**	
	PROS	NONPROS	PROS	NONPROS	Right	Left
Speed (m/s)	1.36+5%		1.22-5%		1.29	
Stride length (m)	1.46-1%		1.42-3%		1.47	
Stride width (m)	0.13+9%		0.18+54%		0.12	
Cadence (steps/min)	112+6%		103-3%		106	
Step length	0.73+0%	0.73+1%	0.71-3%	0.72-3%	0.74	0.73
Step time (% cycle)	60.9-3%	63.8+1%	62.3-1%	64.0+1%	63.1	62.9

Temporal-spatial parameters are often used to investigate the process of rehabilitation in individuals with LLA. Baker and Hewison (1990) used speed as a performance index, demonstrating that it increases by almost 55% within the initial 15 days of rehabilitation. Barnett *et al.* (2009) also demonstrated that temporal-spatial asymmetry reduces between limbs during the rehabilitation process. Analysing temporal-spatial parameters, Isakov et al. (1996) found these variables to be symmetrical between the limbs of individuals with UTTA, unlike knee kinematic data which was found to be asymmetrical. During loading response, knee flexion increased during fast speed (1.4 $m.s^{-1}$) relative to 'normal' speed (0.9 $m.s^{-1}$) on the intact limb, but not in the prosthetic limb. Also, during toe-off, larger knee flexion was reported on the prosthetic limb relative to the intact limb due to the lack of dorsiflexion of the prosthetic foot. Schmid *et al.* (2005) found that the duration of double-support phase prior to the prosthetic limb was prolonged relative to double support prior to the intact limb, which was attributed to balance and comfort issues. However, not all studies have found this asymmetry in double-support phases (Isakov *et al.*, 1996). The temporal differences between intact and prosthetic limbs tend to reduce as walking velocity increases (Nolan *et al.,* 2003) but increase with higher prosthetic limb mass (Donker and Beek 2002; Mattes *et al.,* 2000; Nolan *et al.,* 2003).

Although individuals with UTTA and able-bodied individuals were found to have similar stance time and double support time, able-bodied individuals spend only 12% of the gait cycle having heel only contact whilst UTTA spend 20% of the gait cycle having heel only contact (Powers *et al.,* 1998). The inability of individuals with UTTA to lower the foot much more rapid after initial contact was attributed to compromised plantarflexion as a result of the stiffness of the prosthetic

ankle (Isakov *et al.*, 2000), which can be improved with better prosthetic foot devices (van der Linden *et al.*, 1999; 2004). Temporal-spatial parameters vary depending on the prosthetic foot. During the analysis of ten participants using five prosthetic feet (Carbon Copy II, Seattle, Quantum, SACH and Flex foot) at self-selected speeds, Powers *et al.* (1994) found that irrespective of the prosthetic used, the foot cadence was similar between intact and prosthetic limbs of individuals with LLA, as well as control limbs of able-bodied individuals. However, stride length was found to be larger in the Flex foot stride (1.5 m) relative to SACH (1.44 m) and Quantum (1.44 m), while the other feet were similar (Carbon Copy II = 1.46 m, Seattle = 1.47 m and control foot = 1.51 m). The Flex foot also had larger dorsiflexion (23.2º) relative to the Quantum, while the Quantum had larger dorsiflexion (19.5º) relative to the other feet (Carbon Copy II = 12.1º, Seattle = 15.1º and SACH = 12.0º). Prince *et al.* (1998) suggested that a prosthetic foot should be selected, depending on the time it takes to reach foot flat, the amount of energy recovered by the foot and other objective criteria such as maintenance.

2.4.2 Ground Reaction Forces of Lower-Limb Amputee Gait

Individuals with LLA display different GRFs relative to able-bodied individuals. Kovac *et al.* (2009) report significant asymmetries between intact and prosthetic limbs of individuals with UTTA compared to control limbs of able-bodied individuals. The vertical GRF has a typical double-peaked characteristic, where the first peak was found to increase as speed increased, but the second peak increased in the control and intact limb, but not in the prosthetic limb (b) (Sanderson & Martin, 1997). The vertically aligned prosthetic limb was notable in the anterior-posterior GRF since both breaking and propulsion phases were visibly reduced (a) (Sanderson & Martin, 1997). The lack of change in the prosthetic limb could be attributed to the lack of push-off capacity in the prosthetic ankle joint (Sanderson & Martin, 1997).

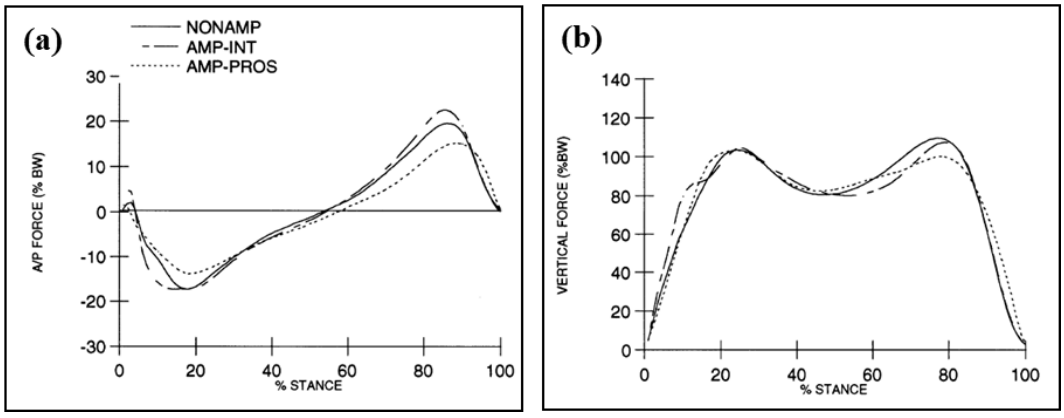

Figure 2.6 Average anterior-posterior (a) and vertical (b) components of the ground reaction force during stance phase at 1.2 m/s. Abbreviations: AMP-PROS – prosthetic limb, AMP-INT – intact limb, NONAMP – control limb. Figure adopted from Sanderson & Martin (1997).

2.4.3 Joint Kinetics and Kinematics of Lower-Limb Amputee Gait

In biomechanics, kinematics describes the movement of segments, i.e. the segment's position and orientation relative to its surroundings, whilst kinetics describes forces that cause movement, i.e. internal forces as a result of muscles and joint activity as well as external forces as a result of interaction with the surrounding environment, e.g. ground reaction forces. Depending on the level of amputation, the kinematics of an individual with LLA may be similar to that of an able-bodied individual (Sanderson & Martin, 1997). Kinematic and kinetic characteristics of UTTA gait suggest that the support functions of individuals with UTTA are similar to that of able-bodied individuals, whilst the motor functions differ (Sanderson & Martin, 1997). Individuals with UTTA lose the ankle joint and the associated ankle plantar-flexors (Sanderson and Martin, 1997; Silverman *et al.,* 2008), which are responsible for 80% of mechanical power generated at the ankle joint during walking (Winter & Sienko, 1988). These muscles are also responsible for body support, forward propulsion, leg swing initiation and medio-lateral balance during walking (Silverman *et al.,* 2008).

Individuals with LLA tend to increase the joint moment and power on the intact limb, relative to the control limbs in able-bodied individuals, to compensate for functional losses of the prosthetic limb (Nolan & Lees, 2000). The primary compensatory mechanism of individuals with LLA during self-selected walking speed is increased hip joint power on the prosthetic limb (Silverman *et al.,* 2008). They display higher amplitude and duration of hip joint power throughout the first half of the stance phase (55-60% of the gait cycle) relative to able-bodied individuals (20% of the gait cycle). This is considered the first limb propeller parameter (Sadeghi *et al.,* 2001). Hip extensor power was found to increase due to increased Gluteus Maximus activity to compensate for the lack of push-off at the ankle joint (Sadeghi *et al.,* 2001). Hip joint power before toe-off (H3S) pulls the limb upward and forward (McNealy & Gard, 2008; Sadeghi *et al.,* 2001; Seroussi *et al.* 1996). Able-bodied individuals simultaneously use their H3S and ankle joint power through the gait cycle to prepare for the swing phase. Individuals with LLA increase H3S directly before toe-off to compensate for the lack of energy generated at the ankle joint (A2S). This mechanism is associated with greater energy expenditure due to increased work at the hip joint (Silverman *et al.,* 2008; Sjödahl *et al.,* 2002; Su *et al.,* 2007; Underwood *et al.,* 2004).

Individuals with LLA adopt compensatory mechanisms in both limbs to maintain a degree of symmetry in support moments (Sanderson & Martin, 1997). Sanderson and Martin (1997) found that during early stance the support moment of the prosthetic limb reduces relative to the intact limb and the control limb because of adaptations at the knee joint. During late stance, symmetry was apparent in the support moments of hip, knee and ankle joints (Sanderson & Martin, 1997),

since individuals with UTTA generated limited ankle plantar-flexor moment, but on the intact limb the plantar-flexor moment increased to a magnitude identical to the prosthetic limb, modulating symmetry (Sanderson & Martin, 1997).

The hip joint moment in the prosthetic and intact limbs of individuals with UTTA were found to differ during the first half of the stance phase relative to the control limbs of able-bodied individuals at a speed of 1.2 m/s, but not significantly (Figure 2.7 a) (Sanderson & Martin, 1997). The amplitude of the peak extensor moment on the prosthetic limb was found to be smaller for the first half of the stance phase relative to the intact and control limbs. As speed increased the extensor moment in the control limb increased but remained unchanged in the intact limb and decreased in the prosthetic limb (Figure 2.7 b) (Sanderson & Martin, 1997).

Individuals with UTFA utilise the hip joint to assist with forward progression since knee and ankle joints are missing (McNealy & Gard, 2008; Nolan & Lees, 2000). At initial contact, the hip joint moment in the sagittal plane was found to be twice as large in individuals with UTFA relative to able-bodied individuals (McNealy & Gard, 2008). The hip moment becomes an extensor moment on the intact limb much sooner relative to the prosthetic limb (Seroussi *et al.,* 1996). Furthermore, during early stance, the work done by the concentric hip extensor was found to be larger in individuals with UTFA on the intact limb (34.2±6.6J) relative to the prosthetic limb (4.9±2.1J) and the control limb of able-bodied individuals (25.2±3.7J) (Seroussi *et al.,* 1996).

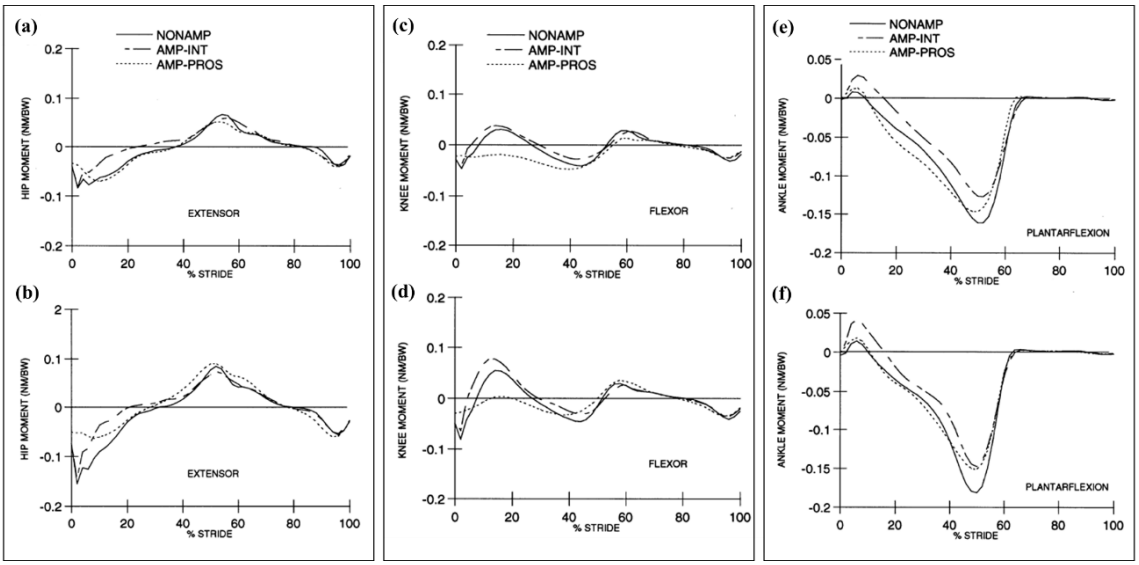

Figure 2.7 Sagittal joint moments of hip (a, b), knee (c, d) and ankle (e, f) at 1.2 m/s (a, c, e) and 1.6 m/s (b, d, f) of the prosthetic (AMP-PROS) and intact limbs (AMP-INT) relative to control limb (NONAMP). Figure adopted from Sanderson & Martin (1997).

Able-bodied individuals rely on a knee extensor moment, which controls knee flexion during weight acceptance. Individuals with UTTA have significantly smaller knee flexion moment in the prosthetic limb (Figure 2.7 c, d) (Sanderson & Martin, 1997). In the prosthetic limb of individuals with UTTA, the knee moment does not become extensor in orientation for almost the entire stance phase (Sanderson & Martin, 1997). In individuals with UTFA, the knee moment is negative preventing prosthetic knee motion during the stance phase, so there is no energy storage or return (K2S) (McNealy & Gard, 2008). Individuals with LLA experience a 63% reduction in knee power absorption during the loading response phase (K1S) on the prosthetic limb relative to the intact limb. Thus, it is assumed that the knee extensor moment is not crucial in the development of extensor support function in the prosthetic limb (Sanderson & Martin, 1997). Although knee extensor moment was found in the control limb of able-bodied individuals and the intact limb of individuals with LLA (Figure 2.7 c, d), Sanderson and Martin (1997) indicate that it may play a less dominant role in the support and propulsion during walking since it was minimal compared to the hip and the ankle joints (Figure 2.7 a, b, e, f). The hip and knee joint angles are found to be more vertically aligned in the prosthetic limb relative to the intact limb during the stance phase (Sanderson & Martin, 1997). This prevents the knee joint from collapsing and reduces loading on it, which may be due to reduced knee extensor muscle strength on the prosthetic limb, and also an indication of the lack of confidence in the ability to control the knee joint.

During the loading phase, knee flexion has a shock-absorbing effect that is important for the prevention of wear and tear (Isakov *et al.*, 1996). Control and intact knee flexion are between 15-18º, however, prosthetic knee flexion is reduced to 9-12º in individuals with UTTA (Isakov *et al.*, 1996; Powers *et al.*, 1998; Su *et al.*, 2007) and often absent or negative in individuals with UTFA (Segal *et al.*, 2006). Sanderson and Martin (1997) report minor changes in the angular position and velocity of individuals with UTTA relative to able-bodied individuals in hip, knee and ankle joints (Figure 2.8 a, c, e). Subtle differences apparent in the hip and knee joints specifically during the first part of stance phase, were the prosthetic limb retained a more extended position in both these joints resulting in the thigh being more vertical in orientation (Figure 2.8 a, c). The ankle joint demonstrated more noticeable differences in the prosthetic limb relative to the intact and control limbs, particularly during late stance and early swing, because of the substantially reduced plantar flexion (Figure 2.8 e). Postema *et al.* (1997) also reported that due to the lack of mobility in the prosthetic feet relative to a biological ankle joint, the ability for an individual with LLA to dorsiflex was limited compared to able-bodied individuals ($12.5^{o} \pm 3.1^{o}$ vs $20.2^{o} \pm 3.5^{o}$).

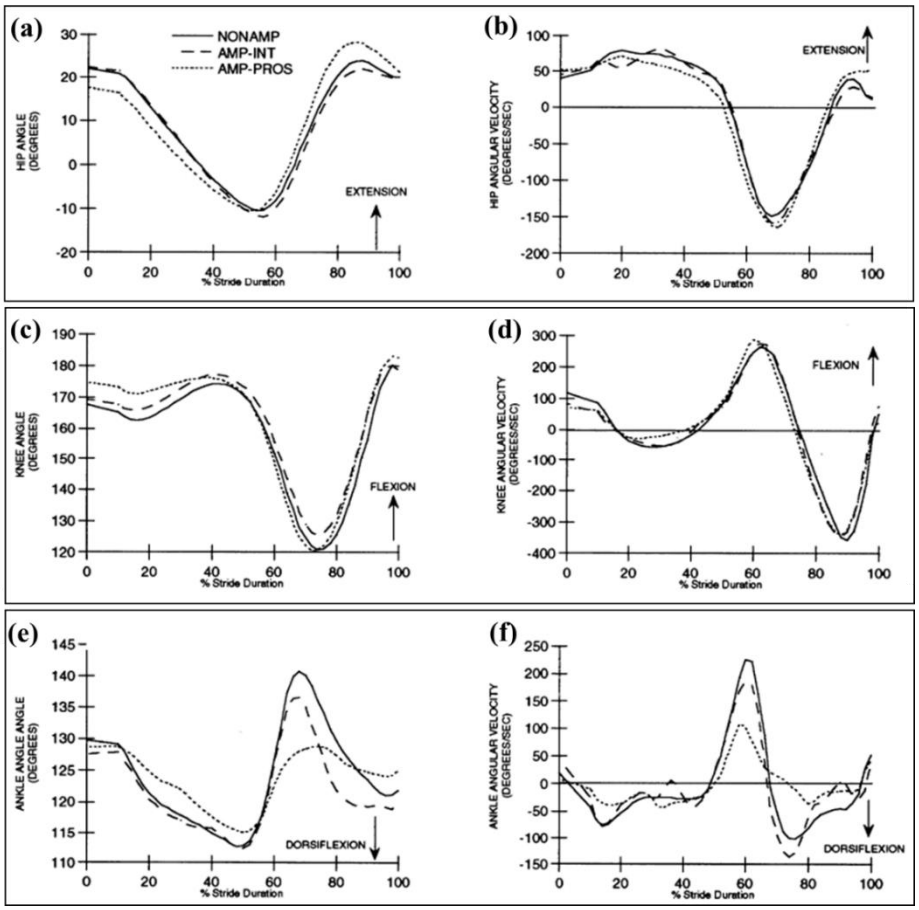

Figure 2.8 Sagittal joint angles (a, c, e) and angular joint velocity (b, d, f) of hip (a, b), knee (c, d) and ankle (e, f) at 1.2 m/s of the prosthetic (AMP-PROS) and intact limbs (AMP-INT) relative to control limb (NONAMP). Figure adopted from Sanderson & Martin (1997).

The absence of knee flexion and the lack of ankle movement during stance phase in individuals with UTTA means heel contact occurs at 20% or 44.5% of the gait cycle (Goh *et al.*, 1984; Prince *et al.*, 1998) since individuals with UTTA spend more time rotating the prosthetic foot forward until initial contact is reached. An ankle plantar-flexion indicates the foot's ability to be flat on the ground in early stance, allowing increased contact and therefore better stability. Ankle joint plantar and dorsiflexion are greatly influenced by prosthetic foot design and thus vary depending on that (Perry *et al.*, 1997; Postema *et al.*, 1997; Powers *et al.*, 1994). The majority of dynamic prosthetic feet are comprised of a blade without much articulation in the ankle joint. Therefore, the plantar-flexion during early stance occurs by heel compression and is often limited compared to the biological ankle joint (Postema *et al.*, 1997).

At self-selected walking speeds, ankle joint power is four times lower in individuals with LLA relative to ankle joint power in able-bodied individuals at slow speed. Ankle plantar flexors are a

major energy source during push-off (Seroussi *et al.,* 1996) and they are responsible for 80% of mechanical power generated at the ankle joint during walking (Winter & Sienko, 1988). Hence, individuals with LLA adopt other compensatory mechanisms to accommodate for the reduction of push-off power (Sadeghi *et al.,* 2001; Seroussi *et al.,* 1996). The three most common compensatory mechanisms are (1) increased work at the intact ankle during push-off, (2) increased concentric hip extensor muscle work at intact limb during early stance and (3) increased concentric hip extensor pull-off in the prosthetic limb (H3S) in early swing (Seroussi *et al.,* 1996). Ankle joint power is highly influenced by the prosthetic foot device (Graham *et al.,* 2007; Postema *et al.,* 1997; Seroussi *et al.,* 1996; Underwood *et al.,* 2004; van der Linden *et al.,* 1999). A dynamic prosthetic foot allows a greater power absorption (A1S) during weight acceptance, which increases dorsiflexion moment and push-off power of the prosthetic ankle (Underwood *et al.,* 2004). However, as push-off power only reaches 20% of biological ankle work it is still much lower than the ankle power generated by an able-bodied individual (Seroussi *et al.,* 1996).

The prosthetic and the intact limbs were found to have 20º, and 26º range of motion (ROM), respectively, whilst a control ankle joint has a ROM of 21º. The increased ROM in the intact limb was considered a compensatory mechanism allowing better foot clearance during swing phase due to the lack of ROM in the prosthetic ankle joint (Nolan & Lees, 2000). Due to a lack of dorsiflexion, individuals with LLA hip hike which means the pelvis is raised, raising the limb to swing it through the motion of swing phase, which helps clear the foot off the ground (Su *et al.,* 2007). During hip hiking the entire body mass against needs to be lifted up against gravity and thus its associated with greater metabolic energy cost (Su *et al.,* 2007). Furthermore, individuals with LLA have greater pelvic ROM at self-selected speed relative to pelvic ROM in able-bodied individuals during slow speed (Su *et al.,* 2007).

2.5 Stability and Balance Control in Gait

Individuals with LLA tend to fall more frequently compared to aged-matched, able-bodied individuals (Miller *et al.,* 2001a; b) . Studies report 52.4% and 80% of individuals with LLA fall within 12 months (Miller *et al.,* 2001a; b; Ülger *et al.,* 2010), with multiple falls occurring in 64% of cases (Ülger *et al.,* 2010). As a consequence of regular falls, these individuals develop a fear of falling (Miller *et al.,* 2001b), which prevents them from taking part in everyday activities, affecting their physical and mental health (Pezzin *et al.,* 2000). Falls may occur as a consequence of compromised dynamic balance and stability, and although falling is a significant problem in individuals with LLA, its underlying mechanisms are not well understood (Curtze *et al.,* 2010).

2.5.1 Conditions for Dynamic Stability

The three major systems involved in the maintenance of balance and stability are (Winter, 1995): (1) the vision system which works to anticipate and plan locomotion through observation of the surroundings and obstacle avoidance; (2) the vestibular system which is the gyro system of the human body, controlling orientation and acceleration; and (3) the somatosensory system which is a large number of sensors that take note of the position and the velocity of segments. The somatosensory system senses the contact of segments and their relation to the surrounding environment including the ground and the orientation of gravity. Research studies have investigated the role of these systems and their adaptability when one of these systems fails or is impaired (Winter, 1995).

In the literature, the inverted pendulum is a widely used model describing the postural and dynamic control of balance and stability in human locomotion (Winter, 1995). The model describes the inverted pendulum pivoted around the ankle joint, where the body is modelled as a mass m on top of a stick with length l (Figure 2.9) (Hof *et al.*, 2005). The mass m, i.e. the CoM, is the pendulum bob, which follows a sinusoidal trajectory during walking. The gravity force vector mg is located at the CoM, pointing vertically downward. The pressure of the feet is represented by a single ground reaction force vector ($-mg$), which is equal and opposite to body weight, located at the centre of pressure (CoP). The CoP varies as a result of muscle action, which can occur in the sagittal plane through ankle plantar and dorsiflexion ('ankle strategy') and in the frontal plane through the hip abductors (Winter, 1995). The CoP also defines the area of the base of support (BoS), which is approximately equal to the area under ($u_{min} - u_{max}$), and between the feet during two-feet standing. To maintain balance, the vertical projection of the CoM should be within the BoS (Hof *et al.*, 2005; Winter, 1995). Both the CoP and CoM are considered to have certain sway angles which define their limits of stability within the bounds of the BoS. If these bounds are exceeded impairments in balance and stability control may arise (Nashner, 1997).

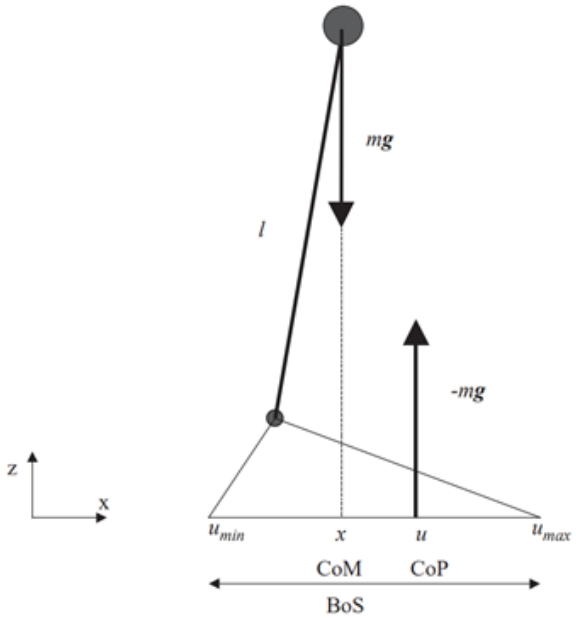

Figure 2.9 Schematic diagram of the inverted pendulum model. The vertical projection of the CoM is denoted x and the position of the COP u. Abbreviations are centre of mass (CoM), centre of pressure (CoP), base of support (BoS), mass (m), gravity (g), leg length (l). Figure adopted from Hof *et al.* (2005).

2.5.2 Extrapolated Centre of Mass and Margin of Stability as Measures of Dynamic Stability

In the literature, the classic inverted pendulum model was challenged (Pai & Patton, 1997) since in the event where the CoM is above the BoS and the CoM velocity is pointed outward, balance may be impossible and in the event where the CoM is outside the BoS and velocity is directed towards the BoS, balance could be achieved, thus the model would not hold true in dynamic situations. Hof (2008) introduced the extrapolated centre of mass (XCoM) as a simple measure of stability during walking, extending the conditions for a classical equilibrium, taking into consideration the CoM's velocity and position. The XCoM is defined as:

$$\xi = x + \frac{u_x}{\omega_0} \quad \textbf{(2.1)}$$

Where x = CoM, u = CoP and ω_0= eigenfrequency of the inverted pendulum

$$\omega_0 = \sqrt{\frac{l}{g}} \quad \textbf{(2.2)}$$

Where l = length and g = gravity

The horizontal distance between the vertical CoM projection and the CoP create a destabilising moment, which needs to be controlled by a timely displacement of the CoP. The XCoM trajectory is a straight line from the CoP to the XCoM at the time of foot contact (Hof, 2008). The CoM follows the trajectory of the XCoM in a sinusoidal manner. For stable walking, during initial contact, the CoP should be a specific distance behind and outward of the XCoM. Disturbance in CoM velocity can be compensated by a change in foot position in the same direction ('stepping strategy') (Hof, 2008).

The XCoM is used to quantify both the spatial (b) and temporal (b_τ) margin of stabilities (MoSs) (Bruijn *et al.*, 2013). The spatial MoS describes the distance between the XCoM and the border of the BoS. This can be in the medio-lateral direction or in the anterior-posterior direction. The temporal MoS, indicates the time in which the stability boundary of the BoS would be reached without intervention (Bruijn *et al.*, 2013). The MoS is used to quantify dynamic balance and describes the movement of the body relative to the BoS (Hak *et al.*, 2015) where a small MoS indicates a greater risk of losing dynamic balance control (Horak *et al.*, 2005). It is calculated using the difference between the XCoM and the limits of the BoS (Hak *et al.*, 2013a).

The MoS can be calculated in the medio-lateral (ML) direction (Equation 2.4; Figure 2.10 a) (Hof, 2007; MacAndrew-Young *et al.*, 2012), where a negative ML MoS indicates that the XCoM is located outside the lateral border of the BoS, which will lead to a deviation from a straight walking trajectory (Hak *et al.*, 2015). It can also be calculated in the backward (BW) direction (Equation 2.5; Figure 2.10 c) (Espy *et al.*, 2010; MacAndrew-Young *et al.*, 2012; Pai & Patton, 1997), where a negative BW MoS indicates that the XCoM is located posterior to the border of the BoS of the leading foot which will lead to an interruption of forward progression (Hak *et al.*, 2015).

$$XCoM = (pCoM + vCoM) \times \omega_0 \quad \textbf{(2.3)}$$

$$ML\ MoS = XCoM_{M/L} - Heel\ Position \quad \textbf{(2.4)}$$

$$BW\ MoS = XCoM_{A/P} - Heel\ Position \quad \textbf{(2.5)}$$

Where $XCoM$ = extrapolated centre of mass, $pCoM$ = position of the CoM, $vCoM$ = velocity of the CoM, ω_0= eigenfrequency of the inverted pendulum, $ML\ MoS$ = medio-lateral margin of stability, $XCoM_{M/L}$= extrapolated centre of mass in the medio-lateral direction, $BW\ MoS$ = backward margin of stability, $XCoM_{A/P}$= extrapolated centre of mass in the anterior-posterior direction.

In the Figure 2.10 (b, d), the ML MoS (a) is defined as the minimum distance in medio-lateral direction between the XCoM (dotted line) and the lateral border of the foot during heel-strike (solid line). The BW MoS (b) is defined as the distance in anterior-posterior direction between the XCoM (dotted line) and the posterior border of the leading foot during heel-strike (solid line). The XCoM is calculated as the position of the COM (pCoM) (dashed line on the graph Figure 2.10) plus its velocity (vCoM) multiplied by the square root of the leg length (l) over acceleration due to gravity (g), as defined below:

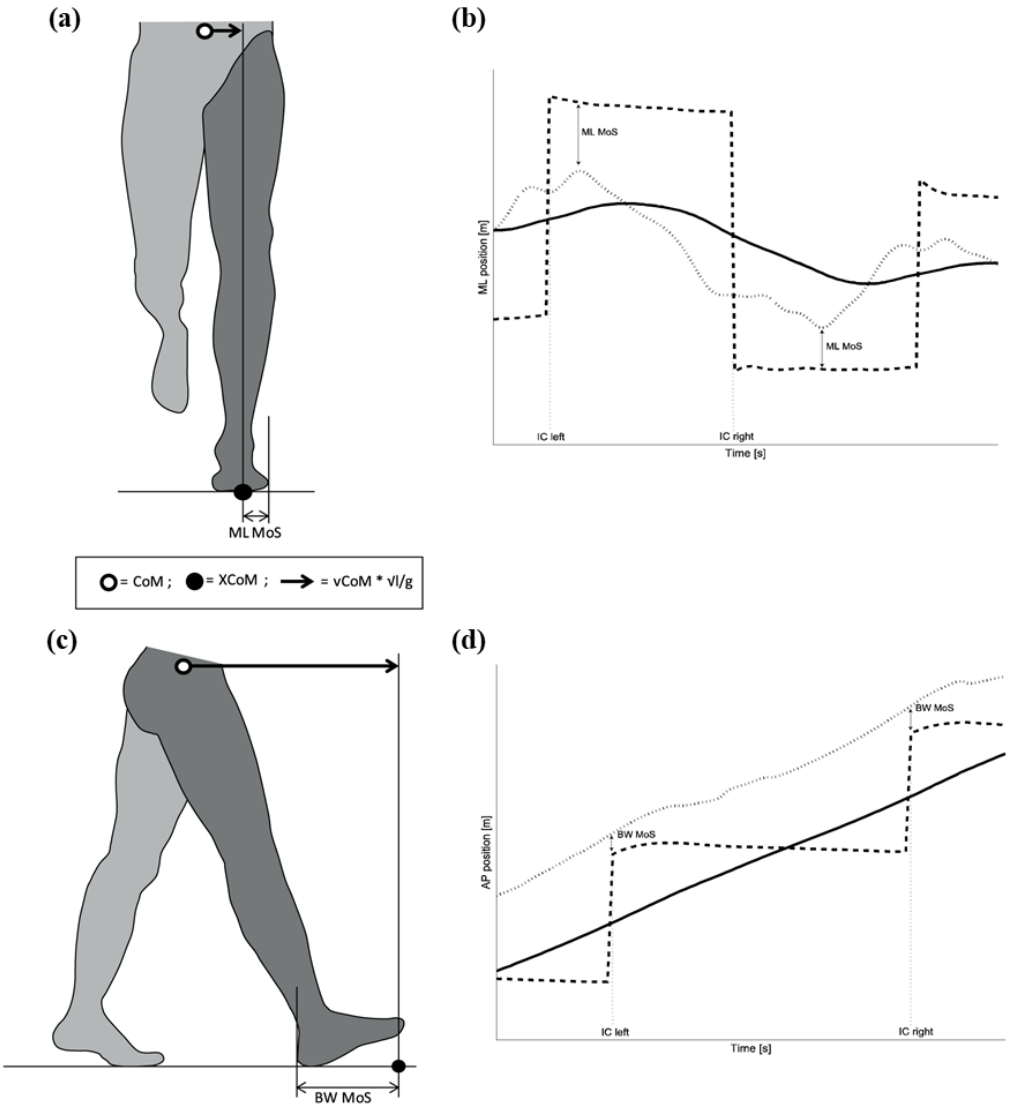

Figure 2.10 ML (a, b) and BW MoS (c, d). The graphs illustrate the MoS over a period of two steps. The trajectories of BoS (solid line), CoM (dashed line) and XCoM (dotted line). The XCoM is calculated as the position of CoM plus its velocity multiplied by ω_0, where ω_0 is defined as the square root of the leg length (l) over acceleration due to gravity (g). The MoS is calculated as the difference between the trajectory of the XCoM and the BoS, when MoS is at its minimum value. Figure adopted from Hak *et al.* (2013a).

2.5.3 Measuring the Margin of Stability in Lower-Limb Amputee Gait

During walking, most of the trunk is supported by one leg at a time, and the CoM is never over the BoS, presenting an unstable system, which can be stabilised through active control (Hof *et al.*, 2007). During walking, the CoM needs to pass the front of the stance foot during the single support phase. If this process is interrupted, dynamic balance control can be compromised, which may lead to falls if recovery fails. During walking, humans place their feet a particular distance behind, and outward of the XCoM, in doing so, the movement of the XCoM and CoM are redirected, achieving stable gait (Curtze *et al.*, 2011).

In general, individuals with LLA walk more slowly relative to able-bodied individuals (Hak *et al.*, 2013c). Comparatively, they also have different step parameters such as a lower step frequency and larger step width, but similar step length (Hak *et al.*, 2013c). The greater step width is a control for compromised balance since it keeps the CoM within safe margins from the BoS, since it increases the MoS in the ML direction (Curtze *et al.*, 2011; Hof *et al.*, 2007). Although LLA gait differs from able-bodied gait, research studies found that compensatory mechanisms to maintain dynamic balance control in response to perturbations are similar between both groups (Bolger *et al.*, 2014). In response to a decrease in dynamic balance, individuals with LLA and able-bodied individuals adapt to increase ML and BW MoS and thus control dynamic balance (Hak *et al.*, 2013a; b; Hak *et al.*, 2015). Individuals with LLA and able-bodied individuals were found to increase step frequency and step width, decrease step length and maintain constant speed in order to increase BW and ML MoS, in response to continuous perturbations through a moving walking surface (Hak *et al.*, 2013c; Hak *et al.*, 2012). In response to adaptability tasks, where participants were asked to hit targets placed in a virtual environment, individuals with LLA and able-bodied individuals decrease step length and increase step width but maintain step frequency and speed (Hak *et al.*, 2013c).

In response to multi-directional surface translation, Bolger *et al.* (2014) found that individuals with UTTA adopted different kinetic parameters relative to able-bodied individuals allowing them to achieve dynamic balance control similar to able-bodied individuals in most directions. During lateral perturbation, similar CoM but greater CoP displacement was found in individuals with LLA. This led to a greater MoS in the least stable direction. Furthermore, inter-limb differences in CoP and GRF suggested that individuals with LLA rely more on the intact limb. The limited directional force was found in the prosthetic limb relative to the intact limb, however, it was not obvious whether these are compensatory mechanisms or limitations of the prosthetic design. Some individuals with LLA exhibit exaggerated CoP, which could be a response to repeated falls or due to the limited sensorimotor information perceived, thus, exaggerating the

control response (Bolger *et al.,* 2014). However, control responses that are larger than necessary, which lie within the limits, can in the occurrence of large and continuous perturbation lead to loss of stability since further adaptation will not be possible (Bolger *et al.,* 2014). Yet exaggeration of a single and safe compensatory mechanism may eliminate the need to alter responses according to perturbations and so simplify the control mechanism (Bolger *et al.,* 2014).

When confronted with compromise in dynamic stability, it was found that forward centre of mass velocity (vCoM) and/or the forward foot placement (FFP) were increased thus increasing BW MoS (Figure 2.11) (Hof *et al.,* 2005; Hof, 2008). An increased BW MoS indicates that the CoM can easily pass the border of the BoS defined by the new stance leg, during the consecutive single support phase and thus decreases the risk of balance loss in the BW direction (Hak *et al.,* 2014). Individuals suffering from multiple morbidities such as PAD may have compromised sensorimotor function, which may prevent them from using their prosthesis adequately and thus being able to adjust FFP to control BW stability (Bolger *et al.,* 2014).

The investigation of prosthetic and intact limbs separately revealed that the step length asymmetry between the two limbs was due to asymmetry in FFP. The BW MoS was found to be larger on the intact limb compared to the prosthetic limb at initial contact but this difference was not present at the end of the double support phase. The average vCoM did not differ between steps, but the vCoM decreased during double support phase following the intact limb (Hak *et al.,* 2014). Shorter intact step length in individuals with LLA contribute to larger BW MoS at initial contact of the intact limb. The shorter step length seems to be a compensatory mechanism for the reduced BW MoS during the double support phase following the intact step. This is because the reduced ankle-push off capacity of the prosthetic limb decreases the vCoM, which limits the BW MoS during double support phase in the intact limb. Thus, the shorter step length on the intact limb is needed to decrease the risk of interruption of forward progression.

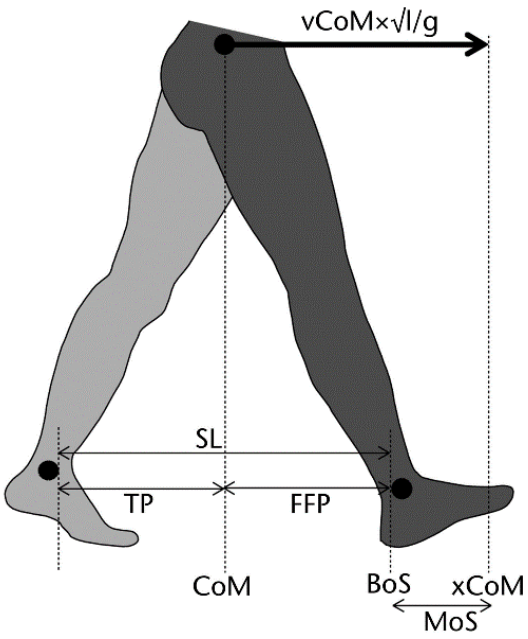

Figure 2.11 Illustration of dynamic stability, forward velocity of the COM and/or FFP in relation to the BW MoS. Figure adopted from Hak *et al.* (2014).

Investigating the recovery response after an evoked forward fall, Curtze *et al.* (2010) found that all individuals with LLA and able-bodied individuals were able to recover balance within a single step after being released from a forward-inclined orientation of 10%. Despite asymmetry in their gait, individuals with LLA were able to use either of their limbs during the recovery process. The CoP was posterior to the CoM prior to release from forward-incline orientation. After release CoM gained velocity moving apart from the XCoM, and moving the XCoM within the BoS to break the forward fall. Curtze *et al.* (2010) note that the CoP and XCoM need to coincide for a successful recovery. It is not sufficient for the CoM only to coincide with CoP since the CoM would move away due to its velocity. During the recovery process, the knee flexion on the prosthetic limb was found to be reduced at heel-strike. This has been associated with the larger step length of the prosthetic limb as the CoP cannot be actively shifted under the prosthetic foot, because of reduced active ankle control. When leading with the prosthetic limb, the heel strike interval was shorter allowing increased stability. During everyday activity, individuals with LLA encounter challenges of uneven terrain and obstacles, thus, to remain supported and stable these individuals adjust the way they walk. Both individuals with UTTA and UTFA lack active ankle control which is important for modifying CoP during heel-strike (Curtze *et al.*, 2011). During the investigation of individuals with UTTA walking on varying surfaces, no difference was found in step parameters (stride time, stance time, double-support time and step frequency), and FFP with respect to the XCoM was found to remain unchanged in lateral stability (Curtze *et al.*, 2011). However, individuals with UTFA had larger MoS on the prosthetic limb (Hof *et al.*, 2007).

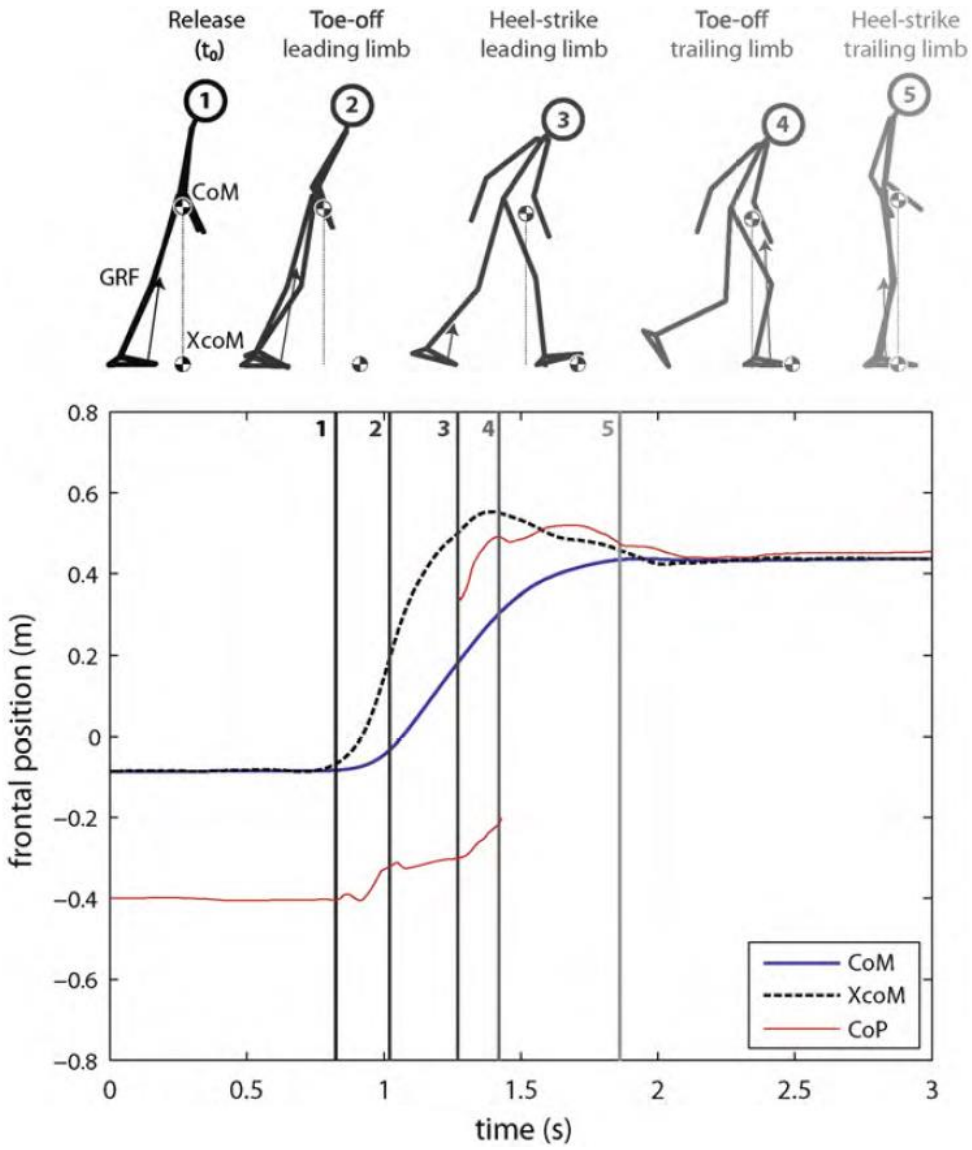

Figure 2.12 Forward position of the CoM, XCoM and CoP as a function of time after release from 10% forward-incline orientation during the investigation by Curtze *et al.* (2010). Recovery occurred within one step following (1) release at t_0, (2) toe-off leading limb, (3) heel-strike leading limb, (4) toe-off trailing limb, and heel-strike trailing limb. Figure adopted from Curtze *et al.* (2010).

2.5.4 Other Measures of Balance and Stability in Gait

2.5.4.1 Biomechanical Measurements of Stability - Stabilizing and Destabilizing Forces and Foot Placement Estimator

Duclos *et al.* (2009) introduced the concept of stabilising and destabilising forces. Stabilising forces quantify forces required to stop the CoP motion in the direction of the border of BoS and the destabilising forces are the forces needed to bring the CoP outside the BoS ignoring this velocity. Quantifying the ratio of these two forces indicates the risk of falling, where a lower ratio illustrates a greater risk.

The foot placement estimator (FPE) measures the foot position needed for stable gait (Millard *et al.*, 2009; 2012; Wight *et al.*, 2008). It is based on the assumption that the angular momentum remains intact when transitioning from one limb to the other. It estimates where the foot should be placed during the transition for the energy of the system to be equal to its peak potential energy. A pendulum gait, involving perfect interchange between potential and kinetic energy, would imply that peak potential energy is at standstill. During gait, this occurs at its apex, at mid-stance.

2.5.4.2 Examples of measures of stability derived from dynamical systems theory - Maximum Lyapunov exponent, maximum Floquet multiplier and long-range correlations

The maximum Lyapunov exponent is commonly calculated using kinematic trunk data (Kang and Dingwell, 2009) since the trunk plays a critical role in stability during upright walking (Grabiner *et al.*, 2008; MacKinnon & Winter, 1993). Studies that investigated knee osteoarthritis and anterior cruciate ligament ruptures used kinematic knee joint data (Arellano *et al.*, 2009; Fallah Yakhdani *et al.*, 2010; Gates and Dingwell, 2009; Moraiti *et al.*, 2007; Moraiti *et al.*, 2010; Segal *et al.*, 2010; Stergiou *et al.*, 2004), since the main mode of instability arose from buckling or giving way of the knee (Yakhdani *et al.*, 2010). The maximum Lyapunov exponent is calculated, identifying the nearest neighbour in a state-space for each data point (Rosenstein *et al.*, 1993) or identifying the nearest neighbour for data points along a single reference trajectory (Wolf *et al.*, 1985). Two components are reported in the literature, λ_L and λ_S, referred to as divergence exponents, where λ_L represent the time as neighbouring points reach maximum separation and the distance cannot become larger, and λ_S is the estimated maximum Lyapunov exponent. Literature suggest that the divergence measure of λ_S, but not λ_L may be a valid measure to estimate the probability of falling. Measuring walking over unstable surfaces, Chang *et al.* (2010) found increased values of λ_S, but not of λ_L. Similarly, Sloot *et al.* (2011) and van Schooten *et al.* (2011) reported increased values of λ_S, but not of λ_L, when participants were destabilised using

galvanic vestibular stimulation. Furthermore, destabilising gait using surface perturbations or visual perturbations, λ_s changed but not λ_L (Arellano *et al.,* 2009). These findings have been confirmed by Hak *et al.* (2012), which indicated that the amplitude of perturbation led to an increase of λ_s, i.e. indicating that there is a proportional relationship between the dose of perturbation and the response.

Orbital stability has been quantified using maximum Floquet multipliers, which quantifies the rate of convergence/divergence of a periodic system, in other words, the response of perturbations of a system from one gait cycle to the next (Kang & Dingwell, 2009). Research has highlighted a couple of concerns when using the maximum Lyapunov exponent and maximum Floquet multiplier as local and orbital dynamic stability measures: (1) the length of data required and (2) sensitivity of the measure. Rosenstein *et al.* (1993) suggest that the use of Lyapunov exponents are not sensitive to the length of data whilst Kang and Dingwell (2006) report that 5 minutes of continuous data was not sufficient enough. Bruijn *et al.* (2008) suggest that long data series beyond 150 strides, covering an equal number of strides for every condition, for each participant should be analysed, for an accurate estimation of balance using these measures. Local and orbital dynamic stability were influenced by speed and is therefore very sensitive to any changes in speed (England & Granata, 2007).

Research has found that gait variations are not random but instead future variations depend on past variations. These dependencies appear as long-range correlations thus they define another measure of stability. Long-range correlation can be calculated from a number of different biomechanical variables such as step length, step time, impulse, duration of contact and peak active force (Damouras *et al.,* 2010; Jordan *et al.,* 2007a; b). The calculations require a recommended 600 strides as a minimum (Damouras *et al.,* 2010). A system with a scaling exponent (α) further away from 0.5 is considered more stable. Hausdorff *et al.* (1995) reported that long-range correlations are resistant to internal and external perturbations and more tolerant to error, thus they could be used as an indicator of adaptability during gait.

2.6 Characteristics of Gait Data

Gait analysis attempts to describe the characteristics of locomotion (Kirtley, 2006; Levine *et al.*, 2012). In clinical settings, it is often used to assess the effects of conditions on gait and to understand how treatments and/or interventions influence gait (Kirtley, 2006; Levine *et al.*, 2012) such as cerebral palsy (Novacheck *et al.*, 2010), Parkinson's disease (Roiz *et al.*, 2010; Sofuwa *et al.*, 2005) and LLA (Barnett *et al.*, 2009). Gait analysis has led to improved diagnostic methods, enhanced treatment recommendations, and more effective evaluation of treatment outcomes of pathological gait (Hamill *et al.*, 2012).

During gait analysis various quantification methods are used to describe human locomotion which can be described in a three-stage system:

(1) Data acquisition tools such as motion capture systems, force platforms and electromyography are used to investigate the biomechanical and muscle activation characteristics of gait (Winter, 2009). The raw kinematic and kinetic data are often reported.

(2) Mathematical methods such as inverse dynamics are applied turning data into variables that describe biomechanical characteristics of gait, which allow further aspects of gait to be assessed such as joint angles, moments and powers (Robertson *et al.*, 2013; Winter, 2009). These are often presented in the form of temporal waveforms or time-series throughout the gait cycle with respect to time (Deluzio *et al.*, 1997; Robertson *et al.*, 2013).

(3) Application of summary techniques to simplify temporal waveforms turning them into clinically useful information such as summary scores and gait indices (Baker *et al.*, 2009; Schutte *et al.*, 2000; Schwartz & Rozumalski, 2008).

Temporal waveforms are governed by the following characteristics which need to be considered during data processing (Chau 2001a; b):

(1) High dimensionality: Data acquisition tools and further mathematical measures produce large data sets. The gait data is inter-dependent, and so it is governed by high dimensionality. Traditional statistical approaches become intractable beyond five variables, and one's visual interpretation is limited to three-dimensions. Furthermore, traditional reduction methods assume a linear relationship (Chau, 2001a).

(2) Time dependence: Data collected during self-selected speed have quasi-periodic temporal dependence which means a gait cycle has a periodic recurrence at irregular intervals. The

resulting time series are difficult to model since the traditional assumption of stationarity is not applicable.

(3) High variability: Gait data displays high intra-subject and inter-subject variabilities and also marker alignment and instrumentation cause further variability. Quantifying variability, recent studies established that some variables are repeatable whilst others substantially vary. It is difficult to control variability and so statistical conclusions during gait analysis must be interpreted with caution (Chau, 2001a).

(4) Correlation: Gait data results in temporal waveforms. During the assessment of a treatment, for example, it is common to compare temporal gait waveforms before and after the treatment to establish similarities and differences. Correlations and distances established between two points of a waveform cannot be extended to the entire curve, so mathematical derivations need to be undertaken to assess differences of entire waveforms (Chau, 2001a).

(5) Non-linear relationship: Intrinsic non-linear human movement results in the non-linear interaction of gait variables, i.e. a direct cause and effect relationship is difficult to establish analytically and exposed to subjective interpretation.

As data acquisition tools used to collect gait data and the subsequent procedures for calculating novel variables advance, they provide an ever-increasing volume of data (Deluzio *et al.,* 1997; Robertson *et al.,* 2013). This presents a limitation to clinicians and researchers when trying to interpret this data and when forming clinically useful information (Deluzio *et al.,* 1999). A widely used approach to analyse and interpret movement data is through the description of graphical profiles of temporal waveforms, using summary statistics (mean, variance, correlations) and waveform parameterisation (peak amplitude) (Alaqtash *et al.,* 2011a; Deluzio *et al.,* 1999). An example of parameterisation of gait data is shown in (Figure 2.13) which illustrates the knee angle of barefoot and shod running throughout a gait cycle, corresponding to solid and dashed waveforms, respectively. A typical discrete parameter (scalar values) would be peak knee angle as indicated by the red arrow. These values extracted from each condition are then typically compared using statistical analysis.

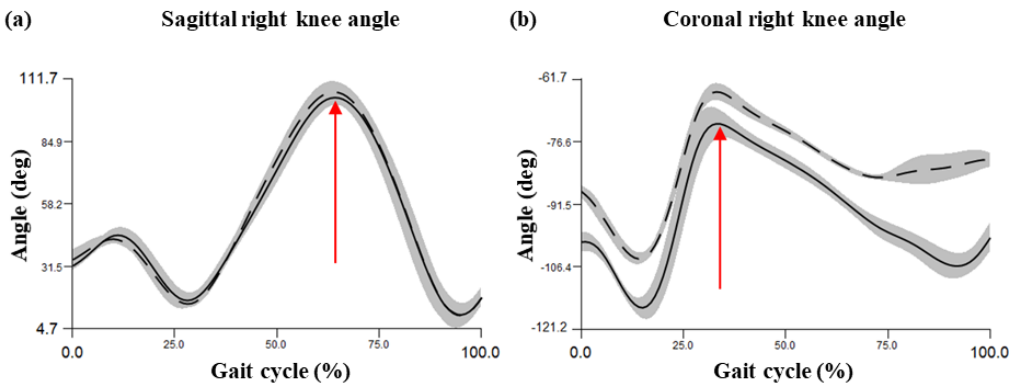

Figure 2.13 Example of knee angle parameterisation in the sagittal plane (a) and coronal plane (b).

Although these methods are typical for the analysis of gait data, there are a few disadvantages. The interpretation of graphical profiles is researcher dependent which means results will depend on the researcher's experience and will differ among various patients and between laboratories. Similarly, the choice of data collected during gait analysis is dependent upon equipment availability, and importantly, the choices of the researcher. This presents an issue in a clinical environment as the choice of parameters assessed in a patient may not necessarily be the cause of a problem, and thus results may show no significant difference, and the problem will remain undetected and untreated. Thus, both data collection and data analysis are subjective and highly affected by researcher bias.

Summary statistics and parameterisation of temporal gait waveforms often provide limited additional insight into the data beyond bivariate plots, and some gait characteristics seem to be ignored. For example, when selecting a discrete parameter, important temporal information is lost (Deluzio and Astephen, 2007) which means the relationship to time is neglected even though specific parameters may occur at a different instance in time when measurements are repeated as a result of intra-subject variation. Also, certain parameters cannot easily be identified in pathological gait (Daffertshofer *et al.*, 2004; Deluzio *et al.*, 1997) since parameters may be distorted as a result of the pathology and thus are not displayed in the same manner as measurements would be in able-bodied gait. Moreover, a linear relationship is assumed between variables, which is not the case because movement data is highly dimensional (Chau, 2001a; Daffertshofer *et al.*, 2004) thus the change of one variable can affect multiple other variables, and these effects are not necessarily proportional to the changes. Furthermore, the correlation existing between different gait variables is disregarded (Schutte *et al.*, 2000). Therefore, there is a need for efficient and robust data reduction techniques as well as methods that allow useful information to be extracted from highly correlated and time-dependent variables.

In an attempt to consider gait characteristics and interpret large amounts of complex gait data, researchers have implemented indices with the aim that a single measure could be used to represent the 'quality' of a specific gait pattern (Baker *et al.,* 2009; Schutte *et al.,* 2000; Schwartz & Rozumalski, 2008). The Gillette Gait Index (GGI) also referred to as the Normalcy Index (NI) is a widespread clinically accepted index, which is used to quantify the deviation of a patient's gait pattern from that of an able-bodied group (Schutte *et al.,* 2000). It is calculated by applying PCA to 16 biomechanical variables measured during gait analysis, where the sum of squared of these variables indicates the patient's gait deviation. The GGI has been widely used, particularly in the assessment of CP and idiopathic toe walkers (Schutte *et al.,* 2000; Trost *et al.,* 2008). It has proven effective in the diagnosis of pathologies and tracking an intervention between patients with the same pathology. A disadvantage of GGI is that the variables used during PCA are comprised of 3 temporal-spatial and 13 kinematic measurements and do not include any kinetic data. Thus, a new index was developed, which included 5 kinematic and kinetic variables, to provide an accurate description of a hip function known as the hip flexor index (HFI) (Schwartz *et al.,* 2000). The HFI has proven to be a valid method to assess hip function, but it is not necessarily considered part of the GGI category as it only focuses on one joint.

Gait Deviation Index (GDI) is another measure which was developed to quantify gait deviations of pathological gait relative to able-bodied gait (Schwartz & Rozumalski, 2008). The GDI is based on 15 gait features extracted using singular value decomposition from 9 angle variables of the pelvis and hip in the three planes of motion, of the knee and ankle joints in the sagittal plane and of foot progression. Applying this method to able-bodied individuals defines an average of non-pathological gait. The absolute distance between pathological and non-pathological gait can be quantified, indicating the extent to which the pathological gait differs. Both, the GDI and GGI were found to correlate since they are both measures of the same underlying construct, however, they measure different aspects (Schwartz *et al.,* 2000).

Gait Profile Score (GPS) is a single index outcome, similar to the GDI, but it is considered a simpler interpretation of the distance measure underlying the GDI. It provides an overall global score of the gait quality and can be deconstructed providing a gait variable score (GVS) (Baker *et al.,* 2009). The GPS is represented by the 9 variables of the GVS to generate a movement analysis profile (MAP). The MAP illustrates the variation of nine variables averaged over a gait cycle, therefore indicating which variables contribute to a high GPS score. The GPS uses features of all relevant kinematic variables from the root mean squared difference between a patient's data and the able-bodied reference data, whilst the GDI uses the first 15 gait features.

All the scores, with the exception of the HFI, consider temporal-spatial and kinematic data only, although this provides a limited evaluation of pathological gait. To provide an improved overall understanding of gait, the GDI-kinetic was introduced, considering joint kinetics rather than kinematics. This index identifies 20 gait features using singular value decomposition, whose linear combinations of the first 20 features reconstruct 91% of the data.

The indices and summary scores simplify the complexity of pathological gait data through the use of discrete parameters. Introduced by Barton *et al.* (2012), the Movement Deviation Profile (MDP) describes the deviation of a patient from normal data using a graph profile, which has shown to detect gait deviation where missed by discrete parameters. Gait data is conveyed into step-patterns using self-organising Artificial Neural Networks (ANN) or Self-Organising Map (SOM) to visualise complex gait patterns in the form of single curves (Barton *et al.,* 2006).

Over the years, many summary measures have been introduced, but unlike the ones previously mentioned, their clinical application still remains limited. For example, data reduction techniques were proposed where the combination of a score which would provide an evaluation of multiple curves and 'interpretable functions' were combined as a method (Tingley *et al.,* 2002). Aside from these summary scores and indices, in recent years biomechanics research studies started to implement alternative methods originating from computer science, psychology, cognitive science, physics and engineering, to better handle "big data" (Phinyomark *et al.,* 2017). These methods include advanced multivariate statistical analyses such as Principal Component Analysis (PCA) and machine learning techniques such as Discriminate Function Analysis (DFA), which can be used to develop automatic gait recognition tools.

2.6.1 Development of Automatic Recognition Tools using Multivariate Statistical Analyses and Machine Learning Algorithms

Automatic gait recognition tools can be developed using multivariate statistical analyses and machine learning algorithms in order to discriminate and classify data. These tools are developed using different stages of training, predictive and evaluation (Lever *et al.,* 2016a; c). (1) During the training stage a model is developed, i.e. the machine is supplied with information to learn. (2) During the prediction stage, the model developed in (1) is used to identify classes. A threshold is established to define the probability of an observation belonging to one class or the other, i.e. the classification performance of different models form the machine are assessed and/or improved. For example, as seen in Figure 2.14 the features of two classes/categories (solid and open black circles) are separated into two classes using the predicted probability. In (a) the membership of classes is perfectly separable when using a 0.5 threshold, in (b) however, the membership of

features into classes is ambiguous as shown by the 0.5 thresholds. Thus, the threshold needs to be tuned to control false positives (0.75) and false negatives (0.25) (Lever *et al.*, 2016c). (3) During the evaluation stage data that was not used for the training or the classification is used to assess how a classifier performs (Lever *et al.*, 2016a).

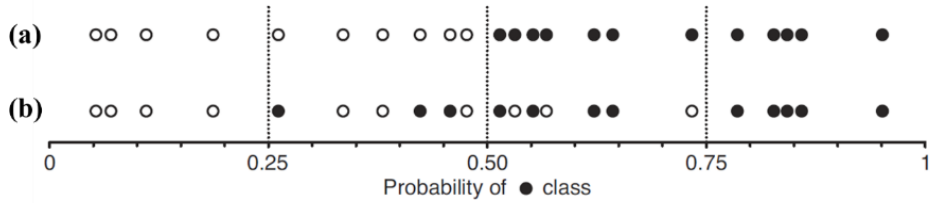

Figure 2.14 Threshold example of a classification of a data set. Figure adopted from Lever *et al.* (2016c).

Prior to the development of a machine learning algorithm, data needs to be pre-processed, which is done by reducing large volumes of data through dimensionality reduction, followed by feature selection, which can be followed by a cross-validation method and finally the classification procedure. Different methods can be implemented at any given stage of the development (Figure 2.15).

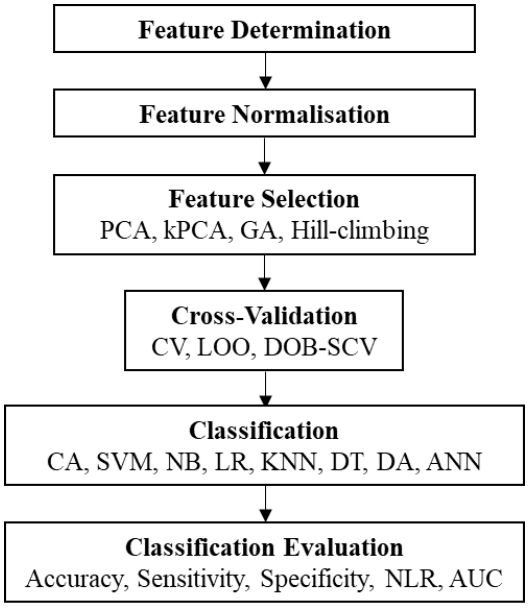

Figure 2.15 Schematic illustrating the steps in the development of an automatic recognition tool. Abbreviations are Principal Component Analysis (PCA); Kernel based-PCA (kPCA); Genetic Algorithm (GA); Cross-Validation (CV); Leave-one-out (LOO); Distribution optimally balanced stratified CV (DOB–SCV); Clustering Analysis (CA); Support Vector Machine (SVM); Naïve Bayes (NB); Logistic regression (LR); K-Nearest Neighbours (KNN); Decision Tree (DT); Discriminant Analysis (DA); Artificial Neural Networks (ANN); Negative likelihood ratio (NLR); and area under the curve (AUC). Figure adapted from Figueiredo *et al.* (2018).

2.6.1.1 Feature selection methods

When presented with large volumes of data, as is the case during gait analysis, a parsimonious representation of the data is sought. During the development of automatic pattern recognition tools, feature selection methods are used, which also improve classification outcomes (Alaqtash *et al.,* 2011a; Lee *et al.,* 2009; Muniz *et al.,* 2010a). These methods can be divided into three groups: filter methods, wrapper methods, and embedded methods (Saeys *et al.,* 2007). Filter methods process data without considering the classification algorithm that follows (Saeys *et al.,* 2007), wrapper methods use heuristic criterion to evaluate a subset of data according to the classification method that follows (Lu *et al.,* 2014; Saeys *et al.,* 2007) and embedded methods interact with the classification method. Different feature selection methods have been investigated in gait analysis, such as Principal Component Analysis (PCA) and kernel based-PCA (kPCA) which are filter methods, genetic algorithm (GA) which is a wrapper method, and hill-climbing which is an embedded method (Lu *et al.,* 2014; Martins *et al.,* 2014).

(1) Principal Component Analysis (PCA) is the orthogonal transformation of variables, i.e. dependent variables are transformed to become independent variables. It aims to establish the optimal linear transformation representing the data in the least squared sense (Yang *et al.,* 2012). Data is presented in a new coordinate system, capturing the maximum variance within the data set (Badesa *et al.,* 2014; Dillmann *et al.,* 2014; Wu *et al.,* 2007; Yang *et al.,* 2012). The different axes of the coordinate system are referred to as principal components (PCs), where the first few of PCs hold the most variance of the original data set. To reduce large data volumes, the dimensionality of the data is reduced by preserving the first two PCs and removing the remaining PCs (Lee *et al.,* 2009; Yang *et al.,* 2012). Principal Component Analysis was first applied to gait data in order to derive a method to represent signals instead of using the signals themselves (Wootten *et al.,* 1990), to reduce large volumes of data (Olney *et al.,* 1998) and to assess entire temporal waveforms of gait data retaining potentially valuable information (Deluzio *et al.,* 1997).

(2) Kernel based-PCA (kPCA) is used to map non-linear data onto a higher dimensional feature space using a kernel function such as linear, polynomial and radial basis function (RBF) (Wu *et al.,* 2007). Studies comparing different kernel functions established that a polynomial kernel achieves better performance relative to linear and RBF kernels (Liang & Lee, 2013; Wu *et al.,* 2007).

(3) Genetic algorithms (GA) are inspired by Charles Darwin's theory of natural evolution and is considered a time efficient optimisation technique (Ardestani *et al.,* 2014; Martins *et al.,* 2014). The algorithm starts with a random set of individuals called a population, where each individual of the population is characterised by a set of parameters known as genes. Each one of these genes is jointed into a string creating a chromosome (solution). A fitness function determines an individuals' probability of reproduction and only candidates with the potential to pass to the next generation as defined by the classification method are preserved, i.e. optimising the cost function (Ardestani *et al.,* 2014; Sarbaz *et al.,* 2012).

(4) Hill-climbing algorithms iteratively search for features that positively contribute to the classification procedure (Begg *et al.,* 2005). Each feature is used for initial classification and based on the performance of the classifier and the features are ranked from the highest to the lowest contributor (Chan *et al.,* 2013).

Studies demonstrated classification results improved following feature selection methods. Using PCA, Eskofier *et al.* (2011) demonstrated that the classification outcome improved from 58% to 95.8%. Using kPCA, Wu *et al.* (2007) showed that the classification outcome improved from 85% to 91% after the original dataset of 36 features was reduced to 17 features, creating a compact data set of uncorrelated features which still represented the original data set without compromise. However, other studies showed that the classification outcome did not necessarily improve following feature selection (Badesa *et al.,* 2014; Lai *et al.,* 2008). Nevertheless, the reduced data set minimised performance time, and thus also computational cost (Lai *et al.,* 2008).

Principal Component Analysis is the most common data reduction method applied in gait analysis (Badesa *et al.,* 2014; Deluzio & Astephen, 2007; Eskofier *et al.,* 2011; Figueiredo *et al.,* 2018; Lee *et al.,* 2009). However, Wu *et al.* (2007) demonstrated that kPCA extracts PCs that are more relevant to non-linear gait data in the presence of noise, relative to PCA, but it is mathematically more complicated. An issue with both PCA and kPCA is the number of PC scores retained during the analysis since the selection of PCs is fundamental to achieve the best possible classification outcome (Badesa *et al.,* 2014; Deluzio & Astephen, 2007; Eskofier *et al.,* 2011). Too many PC scores would result in overfitting of the data, and too little would result in underfitting of the data. Hill-climbing and GA aim to find a local optimum and a global minimum, respectively (Ardestani *et al.,* 2014; Martins *et al.,* 2014; Su & Wu, 2000). Genetic algorithms quantitatively and qualitatively identify the most relevant features, but the selection processes depend on other factors associated with high computational cost (Pratihar *et al.,* 2002). Compared to other methods, PCA and kPCA are less complex.

2.6.1.2 Classification methods

Machine learning algorithms have the ability to identify patterns automatically, and model complex, non-linear and high dimensional data (Alaqtash *et al.,* 2011b; Lai *et al.,* 2008; Zheng *et al.,* 2009). In gait analysis, different machine learning algorithms have been used such as Discriminant analyses (DA) which are either in the form of Linear Discriminant Analysis (LDA) or Quadratic Discriminant Analysis (QDA), Artificial Neural Networks (ANNs), Support Vector Machine (SVM), Naïve Bayes (NB), Logistic regression (LR), Clustering analysis (CA), Fuzzy logic clustering or K-Nearest Neighbours (KNN).

(1) Discriminant Analysis (DA) is a supervised machine learning algorithm that finds a linear or quadratic combination of input features in order to separate data into two or more classes. Discriminant analysis is thus referred to as Linear Discriminant Analysis (LDA) which is also known as Discriminant Function Analysis (DFA) or Quadratic Discriminant Analysis (QDA). Each feature has its own weighting factor which indicates its importance to the discrimination procedure between the classes. The intra-class and inter-class distances between the features are determined to define which class a feature belongs to (Badesa *et al.,* 2014; Harper, 2005; Lee *et al.,* 2009).

(2) Artificial Neural Networks (ANNs) are machine learning algorithms based on the biological neural system (Ardestani *et al.,* 2014). They are made up of multilayer feed-forward neural networks, which are composed of layers of interconnected sets of nodes which loosely model the neurons in a biological brain. Connections between units move forward through hidden layers of nodes to form the input to the output layer (Alaqtash *et al.,* 2011a; Chau, 2001b).

(3) Support Vector Machine (SVM) is a supervised machine learning algorithm using a kernel method to classify non-linear gait data and map it to a higher dimensional feature space (Begg & Kamruzzaman, 2005; Begg *et al.,* 2005). Classification is performed by finding the optimal hyperplanes that separate between classes.

(4) Naïve Bayes (NB) based on Bayes' theorem, assumes that all features are independent of each other (Badesa *et al.,* 2014; Chan *et al.,* 2013). It creates a probabilistic model defining the class that an input belongs to.

(5) Logistic regression (LR) transforms data into logic variables (binary variables) to maximise classification outcomes (Harper, 2005; Muniz *et al.,* 2010b).

(6) Clustering Analysis (CA) uses homogeneous groups or "clusters" to classify data. Two methods of hierarchical and non-hierarchical clustering are used to minimise variability within a class and maximise variables between classes (Kaczmarczyk *et al.,* 2009).

(7) Fuzzy Logic Clustering offers an insight into the non-linear relationship between variables (Chau, 2001a). It does not consider sharp boundaries so input data can simultaneously contribute to multiple classes (Alaqtash *et al.,* 2011b; Chau, 2001a).

(8) K-Nearest Neighbours (KNN) is a non-hierarchical clustering method. It defines the characteristics of the input data depending on similarity to their neighbours (Alaqtash *et al.,* 2011a; Badesa *et al.,* 2014).

All machine learning algorithms have benefits and limitations, hence an algorithm is chosen depending on the application. Artificial Neural Networks handle non-linear data and can learn and adapt to new data, but large volumes of variables are required for an accurate generalisation of the algorithm. It can suffer from overfitting which compromises its generalisation (Begg & Kamruzzaman, 2005; Begg *et al.,* 2005; Chau, 2001b; Lai *et al.,* 2008). Support Vector Machine, however, considers a global optimum and overfitting of the training process can be avoided (Saeys *et al.,* 2007; Wu *et al.,* 2007). It can be applied to small data, and new data can be added to the classification procedure without compromising the outcome (Begg & Kamruzzaman, 2005; Begg *et al.,* 2005; Khandoker *et al.,* 2007). Other classification methods, such as CA, are sensitive to correlated variables. This means that prior to its application, correlated variables need to be identified and removed (Kinsella & Moran, 2008). Furthermore, *a priori* rules and clusters need to be defined by the user, which may introduce bias (Chau, 2001a; Dobson *et al.,* 2007). Nevertheless, CA based on fuzzy logic clustering offers insights into non-linear relationships between variables.

Different machine learning algorithms will result in different classification outcomes due to the unique approach of each algorithm. No algorithm suits all applications (Harper, 2005) especially considering the complexity of gait data. Studies have therefore investigated different approaches to evaluate which suits their data. Comparing DA, tree-based algorithms, ANN, and LR classification methods, Harper (2005) demonstrated that no ideal approach exits, instead the performance of the classification depends on the features. Other studies suggest that the combination of different classification methods can improve the classification outcome (Pogorelc *et al.,* 2012). Classification performance depends on multiple factors such as the relevance of features, type of feature, size of the dataset, and/or number of participants (Badesa *et al.,* 2014; Begg & Kamruzzaman, 2005).

2.6.1.3 Classification evaluation

The performance of machine learning algorithms can be evaluated using different methods. The evaluation should be performed on a test set which has not been used for the training and whose classification is not known. One method involves using the confusion matrix to define accuracy, sensitivity and specificity (Lever *et al.*, 2016a). In a two-class problem, there are four possible outcomes of classification: true positive (TP), false negative (FN), true negative (TN), and false positive (FP), where accuracy (Equation 2.6) evaluates the classifier defined as the percentage of true predictions using a model of these four categories. However, high accuracy does not necessarily imply a good classifier. Thus, sensitivity (Equation 2.7) and specificity (Equation 2.8) measure the proportion of actual positives and negatives of the classifier, respectively. True positives and false positives can be captured by precision, also known as a positive predictive value, which is the proportion of predicted positives (Lever *et al.*, 2016a).

$$Accuracy\ (\%) = \frac{TN + TP}{TP + TN + FP + FN} \times 100\% \quad \textbf{(2.6)}$$

$$Sensitivity\ (\%) = \frac{TP}{TP + FN} \times 100\% \quad \textbf{(2.7)}$$

$$Specificity\ (\%) = \frac{TN}{TN + FP} \times 100\% \quad \textbf{(2.8)}$$

There are several methods to aggregate the confusion matrix. The most popular is F_β score, which controls the balance of recall and precision using β, which can be calculated as follows:

$$F_\beta = \frac{(1 + \beta^2)(Precision \times Recall)}{\beta^2 \times Precision + Recall} \quad \textbf{(2.9)}$$

Where F_β = F_β score, β = shape parameter

As β decreases, precision is given greater weight. Commonly, the F_1score is calculated with β = 1, balancing recall and precision with the equation reduced to $2TP/(2TP + FP + FN)$. The F_β does not capture the whole confusion matrix since it does not give an indication of TNs. One method to capture all data in a coefficient matrix is Matthew Correlation Coefficient (MCC), which ranges from -1 to 1, where '-1' indicates classification is always wrong, '0' indicates classification is no better than random and '+1' indicates classification is always correct.

It should be noted that no single matrix can distinguish all strengths and weakness of a classifier. Instead of evaluating a classifier using a positive or negative, a level of certainty can be used, which can be visually interpreted using a receiver operating characteristic (ROC) curve. It is also possible to determine the ratio between false and true negatives using the negative likelihood ratio (NLR) and the area under the curve (AUC) (Begg *et al.,* 2005; Chan *et al.,* 2013).

2.6.1.4 Cross-validation

After a machine learning algorithm is developed, different approaches are implemented to improve the classification performance. These include cross-validation and feature normalisation methodologies. Cross-validation (CV) methods are used to evaluate the generalisability of the classification outcome as new data is added. These methods can also minimise the likelihood of overfitting (Figueiredo *et al.,* 2018). The conventional CV method starts by dividing the data set into training and testing (predictive) data sets, based on k-fold. During the process, the cross-validation process is repeated k times until every trial is used as a testing sample at least once whilst all other trials make up the training sample. Finally, the average k results are calculated, determining the performance of the classifier (Alaqtash *et al.,* 2011a; b).

During the leave-one-out (LOO) cross-validation method data in each fold belongs to a particular participant instead of randomly assigned trials (Alaqtash *et al.,* 2011a; Badesa *et al.,* 2014). Therefore, the LOO method uses k-fold depending on the number of trials. This method is unsuitable if trials are unbalanced since that may introduce different data distributions (López *et al.,* 2014). For an unbalanced number of distribution trials, optimally balanced stratified cross-validation (DOB-SCV) should be used (López *et al.,* 2014).

Other methods to improve a classifier's accuracy and robustness is by implementing normalisation procedures. Time normalisation is an example of such method, during which each feature is expressed as a function of a gait cycle instead of time (Alaqtash *et al.,* 2011b; Eskofier *et al.,* 2011; Zhang *et al.,* 2014). Similarly, kinematic data can be standardised to a person's body weight instead of a gait cycle (Laroche *et al.,* 2014). Using a z-score to standardise data (Begg and Kamruzzaman, 2005; Hanson *et al.,* 2009; Wu and Wang, 2008) ensures that all features have a mean of zero and a variance of one (Yang *et al.,* 2012; Zhang *et al.,* 2014):

$$\frac{x - \mu}{\sigma} \qquad \textbf{(2.10)}$$

Where x = feature, μ = mean and σ = standard deviation

2.6.2 Multivariate Statistical Analysis and Machine Learning Algorithms in Gait Analysis Current Use and the Future

Automatic gait recognition tools are becoming increasingly popular in gait analysis. In a clinical setting, they can provide a quantitative, non-invasive diagnostic method, patient-specific treatment recommendations, and more effective evaluation of treatment outcomes (Alaqtash *et al.*, 2011b; Lakany, 2008; Pogorelc *et al.*, 2012). Current challenges in clinical settings are the discrimination of able-bodied gait and pathological gait and the evaluation of the progression of pathological gait (Figueiredo *et al.*, 2018). Therefore, classification methods based on statistical analysis, mathematical transformation and machine learning algorithms have been assessed in the investigation of gait data (Alaqtash *et al.*, 2011b). Using statistical analysis, the persistent challenges of an objective analysis have not been achieved and a normal distribution of data is assumed (Chau, 2001b). Mathematical transforms were limited to applications of univariate signals and guideline selection based on wavelets (Chau, 2001b). However, machine learning algorithms used to develop automatic gait recognition tools were able to detect patterns and work with complex non-linear relationships between variables (Alaqtash *et al.*, 2011b; Zheng *et al.*, 2009). They provide an objective method for the analysis of large datasets and thus eliminating researcher bias (Alaqtash, Sarkodie-Gyan, *et al.*, 2011) whilst providing a quick and cost-effective method of analysis (Alaqtash *et al.*, 2011b; Lakany, 2008; Simon, 2004). Furthermore, these algorithms could handle high-dimensional data and new data could easily be incorporated to improve the prediction performance (Alaqtash *et al.*, 2011a; Begg & Kamruzzaman, 2005 ; Zheng *et al.*, 2009). The ability to address nonlinear and high-dimensional data such as gait data and the ability to properly process new data makes machine learning algorithms a suitable method for gait analysis.

Research studies have implemented multivariate statistical analysis methods and machine learning algorithms to investigate Parkinson's disease, cerebral palsy, spinal cord injury, osteoarthritis, running injuries and stroke. The application of these advanced statistical methods was initiated due to the lack of quantitative methods in the assessment of motor symptoms in Parkinsonian gait (Palmerini *et al.*, 2011). In recent years, the use of machine learning algorithms has had many applications for the assessment of pathological gait, for example investigating the use of classifiers to detect cerebral palsy in infants (Rahmati *et al.*, 2016) and children (Kamruzzaman and Begg, 2006), determine the severity of the condition (Rozumalski and Schwartz, 2009), characterise movement patterns of stroke patients (Kaczmarczyk *et al.*, 2009) and diagnose osteoarthritis (Astephen *et al.*, 2008). Other applications included determining the risk of developing a disease or predicting the outcome of an intervention (Wei *et al.*, 2017).

In gait analysis, many studies focused on predictive tasks such as classification (80.6%) and regression (11.6%), while only a few investigated data mining such as clustering tasks (7.8%) (Halilaj *et al.*, 2018). These two machine learning approaches, predictive modelling and data mining, serve different purposes compared to more traditional statistical approaches. Predictive modelling is used to find a function/model to map input data such as kinetic or kinematic waveforms to a given output such as severity of pathology so that it can be used to make future predictions. An example of predictive modelling is powered prosthesis, which use myoelectrical sensors embedded in the prosthesis' socket to predict an individual's intention for the upcoming steps (e.g. Afzal *et al.,* 2017). Predictive modelling was also used to develop diagnosis and prognostic models, for example, of predicting falling (e.g. Wei *et al.*, 2017) or activity during outpatient treatment (e.g. Biswas *et al.*, 2013). Data mining, on the other hand, is used to discover new patterns in data. For example, using clustering analysis gait patterns of subpopulations within types of pathological gait could be identified (e.g. Rozumalski and Schwartz, 2009).

Recent investigations in the development of automatic gait recognition tool were performed on data extracted from wearable sensory systems such as footswitches and accelerometers (Taborri *et al.*, 2016). Advances in technology make these sensors smaller, lightweight and easier to take on and off. These sensors also allow measuring variables in free-living conditions which can be advantageous specifically in the advancement of robotic or powered therapies (e.g. Afzal *et al.*, 2017). Hegde *et al.*, (2018), for example, used shoe-based wearable sensors to monitor activity and gait of children with CP. Machine learning models were used to automatically classify activities of daily living. The results showed that activities could be classified with a 95.3% and 96.2% accuracy for children with and without CP, respectively. A disadvantage of wearable sensors, however, is that they only provide kinematic data. To overcome this issue Wouda *et al.* (2018) used ANN to estimate kinematic and kinematic parameters of runners using wearable sensors. Joint angles and vertical acceleration from the wearable sensors were used as input values to estimate vertical GRF. The outcome showed that sagittal knee kinematics and vertical GRF could be estimated using three inertial sensors with no significant difference to the reference data.

Although wearable sensors have their advantages, using non-ambulatory external sensors such as motion capture-systems or force platforms can provide more detailed information. These systems operate in a controlled environment (Sabatini *et al.*, 2005), which occasionally is considered a disadvantage since it can be challenging to acquire consecutive gait cycles for long-term applications in a natural environment (Alahakone *et al.*, 2010; Azhar *et al.*, 2014). However, the accuracy of these systems cannot be underestimated, as they provide comprehensive and reliable biomechanical data such as temporal-spatial, kinematic and kinetic variables (Howell et al., 2012;

Bamberg et al., 2008). Alaqtash *et al.*, (2011a), for example, have used the nearest neighbour classifier and ANN to classify GRF data of able-bodied individuals, individuals with CP and multiple sclerosis. The classification outcome yielded an accuracy of 95%, indicating that automatic gait recognition tools can be useful for clinicians in the diagnosis and identification of pathological gait. Ertelt *et al.*, (2018) used Gaussian distribution to classify the GRF patterns of athletes from different sports. The results showed that the overall prediction was 94,29% of sports and athletes. Only three out of the ten sports under investigation could not be correctly classified in all instances, whilst the other sports were 100% correctly allocation. These results can have high implications in both medical and sports fields since they have the potential to be used for the identification of gait patterns at different points during an intervention.

In previous studies, the feature space, which presents the number of variables, was generally larger than number of observations, which present the number of participants (Alaqtash *et al.*, 2011 a; b; Begg and Kamruzzaman, 2005; Eskofier *et al.*, 2013) since most studies would have fewer participants (median = 40 participants) compared to variable data points (Halilaj *et al.*, 2018). In general, the number of observations should be greater than the number of features when using machine learning otherwise there might be a risk of overfitting. Barrett and Kline (1981) recommend that the number of participants should be at least 50 for PCA. However, having said this, during gait analysis of pathological groups, the characteristics of and the location of the research site might impose constraints regarding the number of participants which can be obtained for a study.

In gait analysis, descriptive statistical methods such as peak angles are extracted from temporal waveforms. However, these methods require a priori selection of features, which depends on researchers experience and knowledge. Consequently, a large part of the temporal waveform is discarded which may hold important information. Dimensionality reduction technique could be used for feature selection and feature extraction to overcome this issue and thus full gait cycles could be implemented in the classification procedure. However, many investigations performed the machine learning procedure using discrete parameters (Begg and Kamruzzaman, 2005) and only a few have tried including entire gait waveforms (Phinyomark *et al.*, 2015). Furthermore, some studies limited their investigation to specific variables, i.e. only kinetic, kinematic or EMG (Alaqtash *et al.*, 2011a; Ertelt *et al.*, 2018), however, investigations have shown that machine learning algorithms still perform well when using different variables.

Although, some models were build using various data of kinetic, kinematic and EMG, only a limited number of studies addressed the scaling of these data (Rahmati *et al.*, 2016, Roy et al., 2013), which could adversely affect the classification outcome due to the different units and

weightings of these variables. Some studies report that variables from different planes have the potential to improve the classification results, thus providing a more comprehensive understanding of pathological gait (Schöllhorn *et al.,* 2002) but the majority of studies focused on sagittal plane data only. However, the use of data from different planes should be approached with caution since ambiguous and erroneous data such as soft tissue artefacts can negatively affect the results (Phinyomark *et al.*, 2018). Thus, more data does not necessarily mean a more accurate classification outcome would be obtained.

Machine learning algorithms are currently being trialled for a number of applications in gait analysis. Some recent studies investigated the use of machine learning in combination with modern technology to enhance medical practice. Zhan et al., (2018), for example, used machine learning and smartphones to quantify the severity of Parkinson's disease in individuals. Automatic gait recognition tools have proven to be effective in the analysis of pathological gait. However, a drawback of the methods developed thus far is the lack of inclusion of patient history (Bonnefoy-Mazure *et al.*, 2013), which needs to be addressed.

2.6.3 Application of Multivariate Statistical Analyses and Machine Learning Algorithms in Lower-Limb Amputee Gait

In LLA gait, machine learning algorithms have mainly been used to investigate powered prosthetic devices (Afzal *et al.*, 2017; Chen *et al.,* 2013; Dutta *et al.*, 2011; Hargrove *et al.*, 2015; Huang *et al.,* 2011; Joshi & Hahn, 2016; Khan *et al.*, 2018; Miller *et al.,* 2013; Pew & Klute, 2017; Simon *et al.,* 2016; Woodward *et al.,* 2016; Young *et al.,* 2013; Young *et al.,* 2014; Zheng *et al.,* 2013; Zheng & Wang, 2017). Powered prosthetic devices are becoming increasingly popular since sensors in the socket and residuum interface are used to detect changes from the muscle fibres, and depending on the signal, automatic transition between gait modes occur. The transitioning process, however, is not always smooth and thus research has used classification methods in order to identify gait modes and transition periods between gait modes to improve these devices. Gait modes have been classified using muscle synergy data from electromyography sensors (Afzal *et al.,* 2017; Miller *et al.,* 2013) and captive sensing methods (Chen *et al.,* 2013). Khan *et al.* (2018) used brain signals to detect walking intention in order to remove artefacts from physiological noises, investigating how the brain can start and stop a gait cycle on powered prosthetic devices. Seeking the highest classification outcome, studies investigated the combination of different methods (Afzal *et al.,* 2017; Chen *et al.,* 2013; Joshi & Hahn, 2016; Khan *et al.,* 2018; Miller *et al.,* 2013; Pew & Klute, 2017). Furthermore, in an attempt to reduce the time required to train and test a machine learning algorithm, Woodward *et al.* (2016) investigated the use an independent data set to test a subjects data rather than a subject's own

dependent data showing that classifiers are capable of making fast decisions. Investigating different prosthetic devices using machine learning algorithms, Lemoyne *et al.* (2015) acquired 100% classification outcome. Although the investigations of prosthetic devices are important, in the first instance individuals who can benefit from these devices need to be identifiable. Thus, classification methods should be implemented as diagnostic tools for the assessment and understanding of LLA gait. In order to do this multivariate statistical analyses and machine learning algorithms should be implemented to assess and understand differences between LLA and able-bodied gait.

Lower-limb amputee function has been described using PCA (Detrembleur *et al.,* 2005; Gao & Zhang, 2013; Mouchnino *et al.,* 2006). Quantifying symmetry, Gao and Zhang (2013) used PCA to identify important variables during a sit-to-stand and stand-to-sit tasks in an individual with UTFA. Measuring kinematics, kinetics and muscle activity, they were able to identify the most important variables determining these tasks. Using PCA, Soares *et al.* (2016) described the differences in GRF and CoP data between individuals with UTFAs and able-bodied individuals. The first three principal components (PCs) were found to explain 74.5 - 93.9% of the variance in the data. Results illustrated that the majority of differences found in the full temporal waveforms were commonly observed in areas assessed during parameterisation of waveforms (e.g. peaks). Soares *et al.* (2016) also describe the relevant sections in the temporal waveforms relative to the first three PCs. In the vertical GRF, PC1 described the sections between 20-30% and 80-95% of the stance phase, and PC2 and PC3 described the sections between 35%-75% and 7%-12% of the stance phase, respectively. While a higher magnitude was found in the vertical GRF of the control limbs relative to the prosthetic limb in PC1, PC2 and PC3 were found to be significantly different between both prosthetic and intact limbs of the individuals with UTFAs and also the control limbs able-bodied individuals.

Prosthetic rehabilitation is said to lack evidence-based practice (Ramstrand & Brodtkorb, 2008), although using gait analysis for the assessment of individuals with LLA can help monitor prosthetic rehabilitation and therapy effectiveness (Skinner & Effeney, 1985). There are no objective measures to evaluate prosthetic rehabilitation, but instead, it depends on clinicians experience (van der Linde *et al.,* 2004; Schaffalitzky *et al.,* 2011). For example, the evaluation of prosthetic alignment is based on visual interpretation of the patient's gait, which depends on the prosthetists' experience and thus is highly subjective. In an attempt to address this, Zhang *et al.,* (2018) used the machine learning algorithm SVM to detect misalignment in the prosthesis of individuals with UTTA though GRF data. The misalignment could be accurately detected 96.7%

within a subject and 88.9% between subjects, indicating that automatic gait recognition could be used in a clinical setting to detect prosthetic misalignment.

At present, limited research has investigated the use of multivariate statistical analyses and machine learning algorithms to understand LLA gait, although this can have many positive applications. Prosthetic rehabilitation is said to lack evidence-based practice and incorporation of research findings (Ramstrand & Brodtkorb, 2008). However, the implications of automatic gait recognition tools in clinical gait analysis could facilitate a better understanding of factors affecting gait and therefore aid better decision making processes early on during rehabilitation (Esquenazi, 2014), increasing the likelihood of prosthetic use after inpatient treatment. In turn, this can improve the quality of life of individuals with LLA.

Chapter 3: General Methodology

3.1 Introduction

This chapter describes common methodological procedures used across all experimental studies of this PhD. These include participant recruitment, ethical review, data acquisition, data processing and analysis techniques. Each section details the rationale and justification for the procedures. Any additional procedures, related to a particular study, are described in the methods section of the individual study.

3.2 Participants

In this research, able-bodied individuals and individuals with UTTA volunteered. Able-bodied individuals were involved in studies 1-3 presented in chapters 4-6 and were drawn from the University and local communities. Individuals with UTTA were involved in studies 2-4 presented in chapters 5-7 and were recruited from the Mobility Centre at Nottingham University Hospitals NHS Trust. Prior to volunteering in the studies, participants were given details of the studies in the participant information sheets (Appendices 5 and 6) and written informed consent (Appendices 5 and 7) was obtained from each participant on arrival to the laboratory prior to testing. Participants also completed a participant health screen form (Appendix 9) to ensure all inclusion/exclusion criteria were met, and to ensure that participants were under no risk through participation in the studies. Demographics of individuals with UTTA and details of their prosthetic components were shown in Table 3.1.

3.2.1 Ethics Approval

Ethical approval for study 1 presented in chapter 4 was obtained from Nottingham Trent University College of Science and Technology Ethical Review Committee (Humans). Ethical approval, for studies 2-4 presented in chapters 5-7, was sought from the Nottingham Trent University's College of Science and Technology Ethical Review Committee (Humans), the NHS Research Ethics Committee, the NHS Health Research Authority and the NHS Research and Development (REC reference - 16/EM/0311).

3.2.2 Inclusion/Exclusion Criteria

3.2.2.1 Experimental Study 1

Inclusion criteria for study 1 specified that participants had to be greater than 18 years of age, had no lower limb pathologies and were free of injury during the time of the study.

3.2.2.2 Experimental Study 2 – 4

Inclusion criteria for studies 2-4 specified that individuals with UTTA:

- Should have at least a year of experience using their prosthetic limb after inpatient treatment,
- Should be at least 18 years of age at the time of the study,
- Should be independent walkers, i.e. are able to walk without the use of any walking aids other than their prosthetic limb,
- Should be able to walk for 3 minute periods at once to be able to meet the walking requirements for the studies.

Exclusion criteria for studies 2-4 specified that individuals with UTTA:

- Should suffer from a medical condition that impaired balance or sensory loss including significant musculoskeletal, neurologic or cardiopulmonary conditions,
- Should have a prescription for more than five medications at the time of the research. This is because research has demonstrated that consumption of more than five medications affect walking habits (Lord & Menz, 2002),
- Should experience pain when walking at a self-selected speed,
- Should experience discomfort wearing the prosthetic limb.

Inclusion criteria for studies 2 and 3 specified that able-bodied individuals:

- Should be at least 18 years of age at the time of the study,
- Should have no lower-limb pathologies,
- Should be free of injury during the time of the study.

Exclusion criteria for studies 2 and 3 specified that able-bodied individuals:

- Should suffer from a medical condition that impaired balance or sensory loss including significant musculoskeletal, neurologic, or cardiopulmonary conditions,
- Should have a prescription for more than five medications at the time of the research,
- Should have experienced more than one fall in the 12-months prior to data collection. This is because research has demonstrated that frequent falls affect an individual's balance and stability (Melzer *et al.*, 2004)

Table 3.1 Demographics including prosthetic components of participants with UTTA.

Participant	Sex	Height (m)	Mass (kg)	Age (Years)	Cause of Amp	Time since Amp (Years)	Phantom Pain	Socket	Liner	Suspension	Foot
1	M	1.77	74.3	46	Trauma	13	Yes	Iceross carbon fibre	Iceross original	Pin	Venture 25Rt
2	M	1.67	93.3	49	Trauma	2	Yes	Carbon fibre	Endolite comfort liner	Pin	Avalon 24Rt
3	F	1.64	64.5	48	Osteosarcoma	19	Yes	Iceross laminate	Iceross sport	Pin	Avalon 24Lt
4	M	1.74	84.35	67	Failed Ankle Fusion	1	Yes	Silver carbon fibre	Iceross synergy wave	Pin	Echelon VT 27Rt
5	M	1.86	93	32	Neurofibromatosis	7	Yes	Iceross laminate	Iceross synergy wave	Pin	Senator 26Rt
6	M	1.67	88	55	Trauma	1	Yes	Laminate socket	Endolite comfort liner	Sleeve	Avalon 26Lt
7	M	1.79	95.5	70	Thrombosis	4	Yes	Laminate socket	SmartTemp cushion liner	Sleeve	Avalon 28Rt
8	M	1.77	98.3	52	Infection after Trauma	4	Yes	Laminate socket	Endolite silcare breathe liner	Sleeve	Echelon VT
9	M	1.9	87.1	28	Trauma	5	Yes	PTB socket	Gel cushion liner	Sleeve	Re-Flex Shock
10	M	1.77	89.5	53	Trauma	5	No	Laminate socket	Iceross comfort locking liner	Pin	Echelon VT
11	F	1.52	55.5	52	Osteoarthritis	1	Yes	PTB laminate socket	Pelite liner	Sleeve	Navigator 22Lt
Mean		1.74	83.9	50		5					
SD		0.11	13.6	12		5					

3.3 Data Acquisition and Processing

3.3.1 Hardware and Equipment Set-Up

Kinematic data was measured using a three-dimensional (3D) Qualisys Motion Capture System (Qualisys, Gothenburg, Sweden). The system was made up of eight Oqus 400, and one high-speed Oqus 310 cameras, and the associated hardware, and the software, Qualisys Track Manager version 2.2 (QTM v2.2) (Qualisys, Gothenburg, Sweden). Kinematic data was measured as a participant moved through the performance volume with reflective markers attached to certain body landmarks as individual cameras capture images of these reflective markers. Ground reaction force (GRF) data were measured using an AMTI OR6-7 strain gauge force platform (508x464mm) (AMTI, MA, US). The GRF was measured as a participant walked over the force platform and clear contact was made between the participant's foot and the platform. Measurements were made in three axes, namely vertical (Fz), anterior-posterior (Fy) and medio-lateral (Fx).

The cameras of the Qualisys Motion Capture System were connected in a serial fashion (Figure 3.1). Camera 1 was connected to a desktop PC (Dell OptiPlex 990, Dell, Bracknell, UK) feeding kinematic data into QTM (Qualisys, Gothenburg, Sweden). Camera 1 was also connected to the sync input of a USB analogue to digital (A-D) converter (Qualisys USB-2533, Gothenburg, Sweden). The AMTI force platform was connected to an AMTI connection box (AMTI, MSA-6) via connection cables. The AMTI connection box was fed into the A-D converter (Qualisys USB-2533, Gothenburg, Sweden) via coaxial cables and BNC connectors. The AMTI connection box was also connected to the desktop PC. Thus, for synchronisation purposes, both GRF data from the AMTI force platforms and kinematic data from the Qualisys cameras were fed into the USB A-D board and to the desktop PC. Finally, the A-D converter was connected to the desktop PC via a USB highspeed ribbon cable.

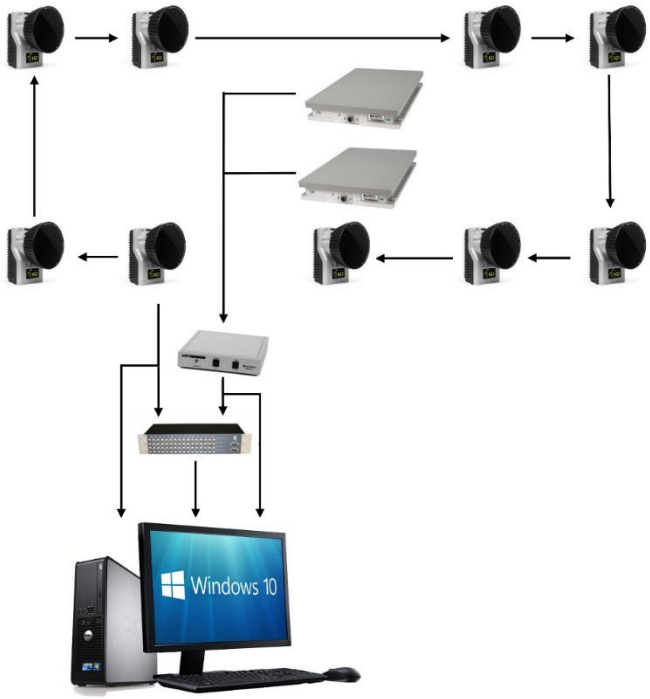

Figure 3.1 Illustration of equipment set-up.

3.3.2 Kinematic Data Acquisition

To create three-dimensional (3D) coordinates from two-dimensional (2D) images of the cameras, a linear relationship between the 2D image and 3D coordinates needs to be established (Payton & Bartlett, 2007). This was carried out through calibration of the system, ensuring that 2D images were accurately scaled to 3D coordinates. The calibration involved a series of control points on a rigid structure with known coordinates (Robertson *et al.*, 2013), which in this research was an L-shaped calibration frame with reflective markers of known dimensions (300mm & 600mm) (Figure 3.2). The frame was placed still in the performance volume so that it was seen by all cameras, whilst a T-shaped wand with markers on each end (600mm) was moved through the performance volume (Figure 3.2). The control points, i.e. the markers of the L-shaped calibration frame and the T-shaped wand were measured during movement. These measurements were utilised to scale digitised coordinates into real metric units through methods known as Functional Linear Transformation (FLT) or Direct Linear Transformation (DLT) (Robertson *et al.*, 2013).

Measurement accuracy depended on the accuracy of the calibration, which was determined by the residual error of each camera. The residual error indicates the precision of locating a marker's position. In this research, the residual error for each camera had to be <2mm in order to be accepted for data acquisition. Prior to calibration, individual cameras were checked to ensure that

no unwanted objects were obstructing the view. The calibration created a global/laboratory coordinate system (z – vertical, y – anterior/posterior and x –medial/lateral), where markers in the corners of the L-shaped frame represent the laboratory origin or zero point of the laboratory coordinate system. Markers placed on certain body landmarks of a participant created a local coordinate system. The global coordinate system is fixed whilst the local coordinate system moves dependent on participant's movements. Segment movement can be defined using both coordinate systems.

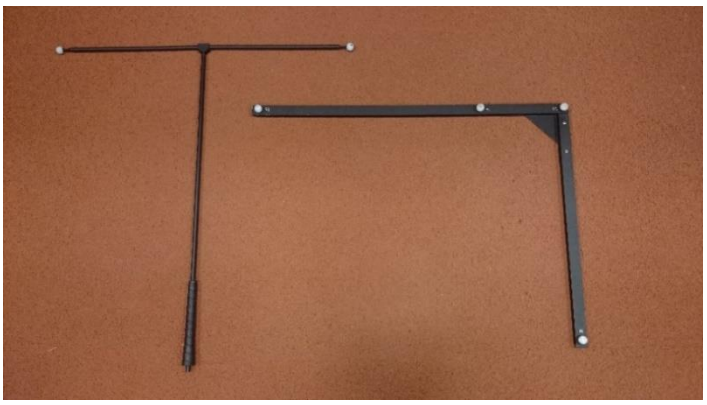

Figure 3.2 T-shaped wand (left) and L-shaped reference frame (right).

3.3.3 Biomechanical Modelling

Markers were placed on certain bony landmarks in accordance with a six-degrees of freedom (6DoF) marker model shown in Figure 3.3 and Figure 3.4. In study 1 a 36-marker model (Figure 3.3) and in studies 2-4 a 70-marker model (Figure 3.4) were used to measure kinematic data. Spherical reflective markers (14mm diameter) were attached on participants' head, upper extremities, trunk (Leardini *et al.,* 1999) and lower extremities (Cappozzo *et al.,* 1995) (Figure 3.3, Figure 3.4 and Table 3.2). Markers on the prosthetic limb of individuals with UTTA in studies 2-4 were placed, estimated depending on the intact limb due to the absence of anatomical landmarks (Powers *et al.,* 1998) to define segment geometry. The 6 DOF marker models describe segments being modelled independently of each other thus no assumptions were made regarding joint constraints (Cappozzo *et al.,* 1995; Collins *et al.,* 2009; Kirtley, 2006; Robertson *et al.,* 2014). Markers were either used as definition or tracking markers of individual segments, and at least three non-linear markers were used to define a segment's position and orientation in the 3D space. Segments were treated as objects where the inertial properties of the object depended on its shape (Hanavan, 1964), and the shape, i.e. the segment geometries were computed depending on the segment definition (Section 3.3.4).

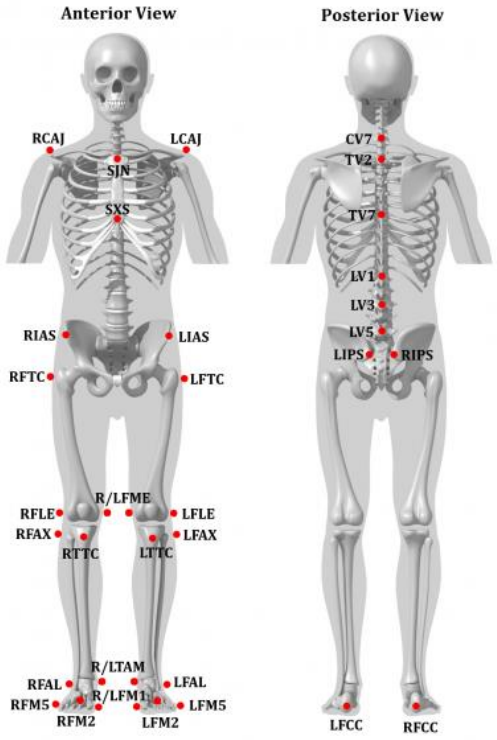

Figure 3.3 Diagram of 36-Marker Locations (Cappozzo *et al.*, 1995; Leardini *et al.*, 1999). Figure adopted from Visual3D.

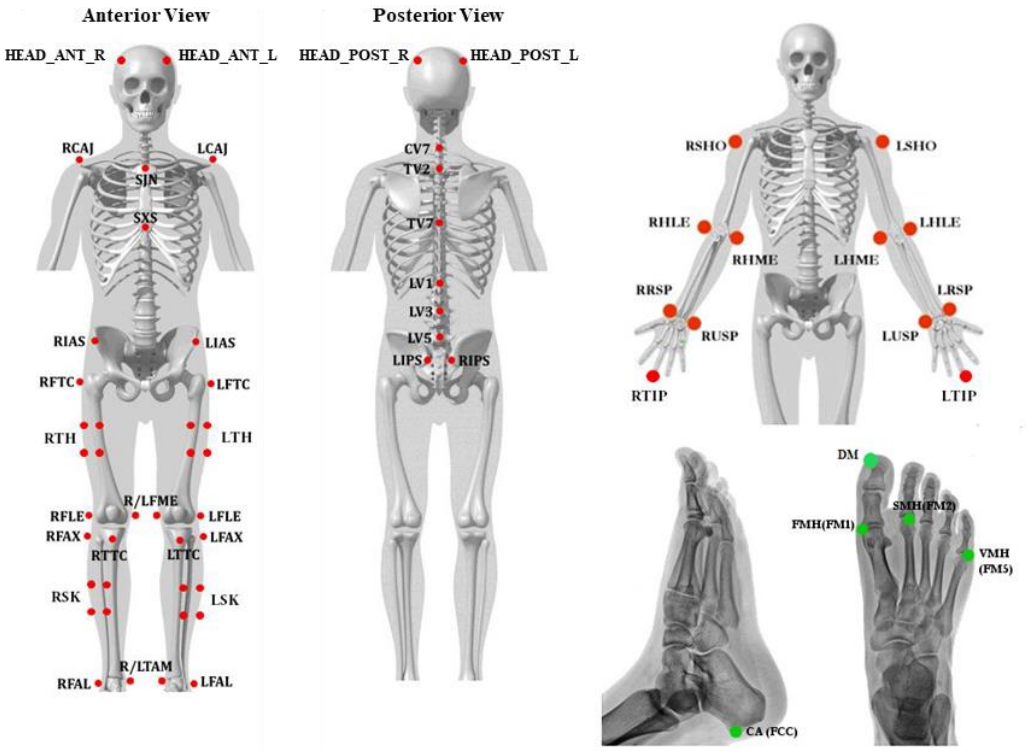

Figure 3.4 Diagram of 70-Marker Locations (Cappozzo *et al.*, 1995; Leardini *et al.*, 1999). Figure adopted from Visual3D.

Table 3.2 Anatomical positions of markers used to create a 36-marker and 70-marker model. All markers were 14mm in size.

Anatomical Position	Corresponding Marker	Study 1	Study 2 - 4
Head	HEAD_ANT_L, HEAD_ANT_R, HEAD_POST_L, HEAD_POST_R		X
Left/right acromion	LCAJ/RCAJ	X	X
Jugular notch	SJN	X	X
Xiphoid process	SXS	X	X
seventh cervical vertebrae	CV7	X	X
Second and seventh thoracic vertebrae	TV2, TV7	X	X
First, third and fifth lumbar vertebrae	LV1, LV3, LV5	X	X
Left/Right anterior superior iliac spine	LIAS/RIAS	X	X
Left/Right posterior superior iliac spine	LIPS/RIPS	X	X
Greater trochanter	LFTC/RFTC	X	X
Cluster on thigh	LTH/RTH		X
Lateral femoral epicondyle	LFLE/RFLE	X	X
Medial femoral epicondyle	LFME/RFME	X	X
Fibula head	LFAX/RFAX	X	X
Tibial tuberosity	LTTC/RTTC	X	X
Cluster on shank	LSK/RSK		X
Lateral malleolus	LFAL/RFAL	X	X
Medial malleolus	LTAM/RTAM	X	X
Calcaneus	LFCC/RFCC	X	X
1st, 2nd and 5th metatarsal head	LFM1/RFM1, LFM2/RFM2, LFM5/RFM5	X	X
Distal end of toe	LDM/RDM		X
Shoulders	LSHO/RSHO		X
Humerus lateral epicondyle	LHLE/RHLE		X
Humerus medial epicondyle	LHME/RHME		X
Ulna-Styloid process	LUSP/RUSP		X
Radius-Styloid process	LRSP/RRSP		X
Distal end of middle finger	LTIP/RTIP		X

All markers were placed bilaterally, and in the absence of anatomical landmarks, i.e. on the prosthetic leg, markers were placed estimated from the intact limb.

3.3.4 Segment Definition

3.3.4.1 Segment Definition of 36-Marker-Model

3.3.4.1.1 Thorax Segment

The thorax segment was defined using the anatomical locations of the jugular notch, the xiphoid process, the 7th cervical vertebrae and the 2nd thoracic vertebrae. The thorax was built as a cylinder where the markers of the vertebrae were considered the joint centre of the cylinder. The radii of the cylinder were defined as half the distances between the jugular notch and the 7th cervical vertebrae and the mid-point between the xiphoid process and the 2nd thoracic vertebrae, which define the proximal and distal ends of the cone, respectively. The segment was also tracked using the jugular notch, the xiphoid process, the 7th cervical vertebrae and the 2nd thoracic vertebrae.

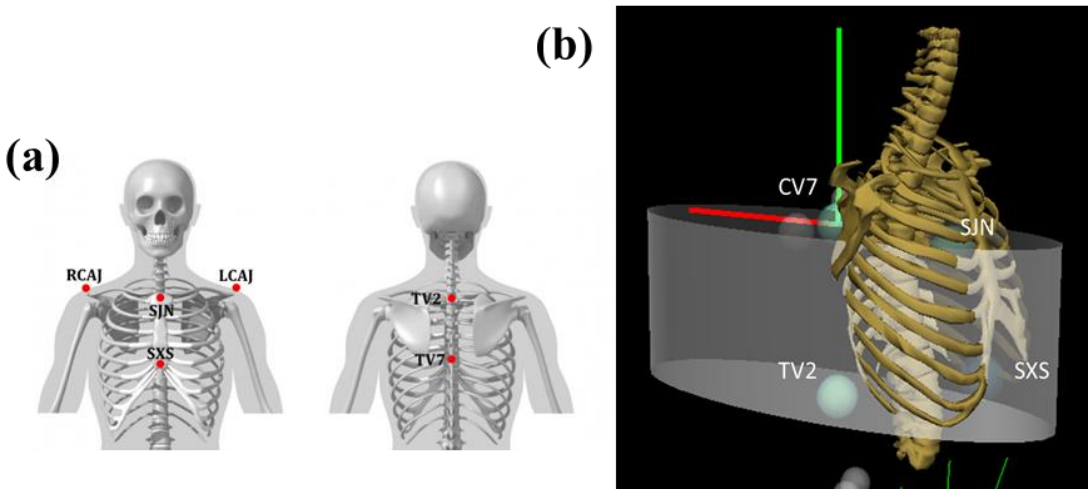

Figure 3.5 Marker location (a) and definition (b) of the thorax segment.

Table 3.3 Thorax definition in Visual3D.

Thorax segment		
Proximal joint and radius	Joint Centre - TV2	Radius - 0.5*DISTANCE(TV2,SJN)
Distal joint and radius	Joint Centre - TV7	Radius - 0.5*DISTANCE(TV7,SXS)
Extra target to define orientation	Posterior Location - SJN	

3.3.4.1.2 Coda Pelvis

The coda pelvis was defined using the anatomical locations of the Anterior Superior Iliac Spine (ASIS) and the Posterior Superior Iliac Spine (PSIS). The origin of the pelvis was created at the mid-point between the ASISs. The sacrum location was defined as the mid-point between the PSISs, and a plane from the sacrum to the ASISs defining the pelvis location. The segment was built as a cylinder and tracked using the ASISs and PSISs.

By building the pelvis the right and left hip joint centres were estimated as follows (Bell *et al.*, 1989; 1990):

$$RHJC = (0.36 \times ASIS\_Distance, -0.19 \times ASIS\_Distance, -0.3 \times ASIS\_Distance) \quad (3.1)$$

$$LHJC = (-0.36 \times ASIS\_Distance, -0.19 \times ASIS\_Distance, -0.3 \times ASIS\_Distance) \quad (3.2)$$

Table 3.4 Landmark definition for the Coda pelvis in Visual3D.

Landmark	Starting point	Ending point
SCRM	RIPS	LIPS

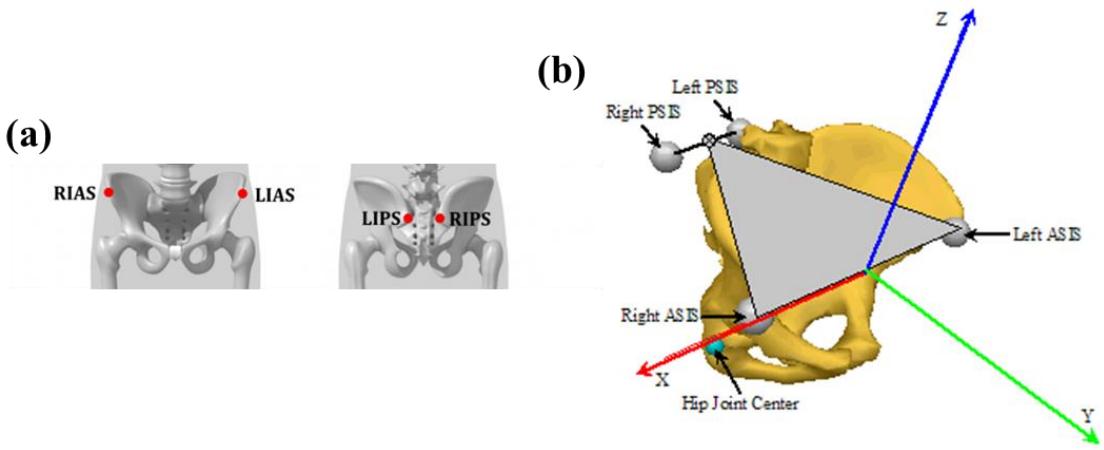

Figure 3.6 Marker location (a) and definition (b) of the coda pelvis.

3.3.4.1.3 Thigh Segment

The thigh segment was defined using the anatomical locations of the hip joint centres, greater trochanter, medial and lateral femoral epicondyle. The thighs were built as a cone, where a quarter of the distance between the hip joint centres defined the proximal radius of the cone, and the distal end of the cone was defined by the medial and lateral femoral epicondyles. The segment was tracked using the hip joint centre, greater trochanter, medial and lateral femoral epicondyle.

Table 3.5 Thigh definition in Visual3D.

Thigh segment		
Proximal joint and radius	Joint centre - RIGHT_HIP	Radius - 0.25*DISTANCE(LFTC,RLTC)
Distal joint and radius	Lateral – RFLE	Medial - RFME

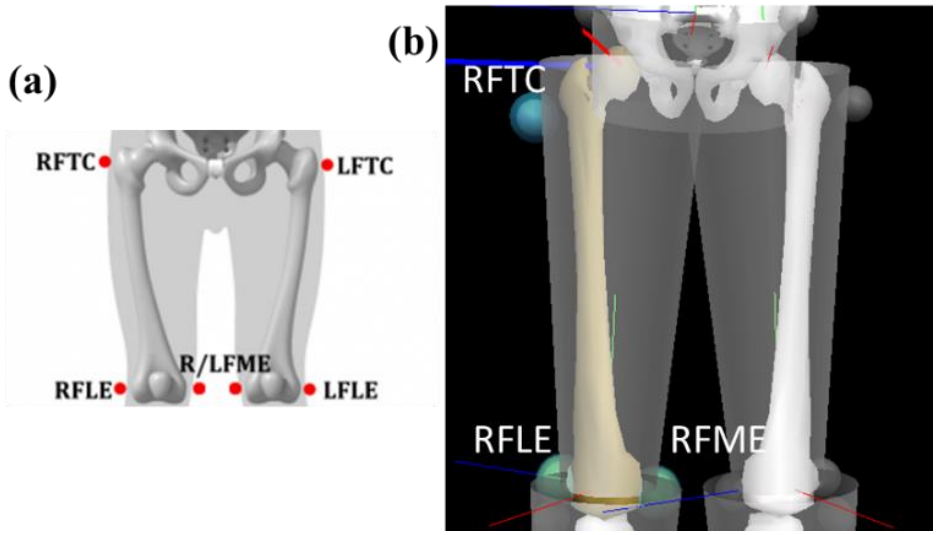

Figure 3.7 Marker location (a) and definition (b) of the thigh segment.

3.3.4.1.4 Shank Segment

The shank segment was defined using the anatomical locations of the medial and lateral femoral epicondyles, fibula head, tibial tuberosity, medial and lateral malleoli. The mid-point between the medial and lateral femoral epicondyles was used to create a landmark (RKNEE). The shank was built as a cone, where at the proximal end the joint centre was defined by the RKNEE landmarks and the fibular head as the lateral border of the cone, and the distal end of the cone was defined by the medial and lateral malleoli. The segment was tracked using the fibula head, tibial tuberosity, medial and lateral malleoli.

Table 3.6 Shank definition in Visual3D.

Shank segment		
Proximal joint and radius	Joint centre – RKNEE	Lateral - RFAX
Distal joint and radius	Lateral – RFAL	Medial - RTAM

Table 3.7 Landmark definition for the shank segment in Visual3D.

Landmark	**Starting point**	**Ending point**
RKNEE	RFLE	RFME

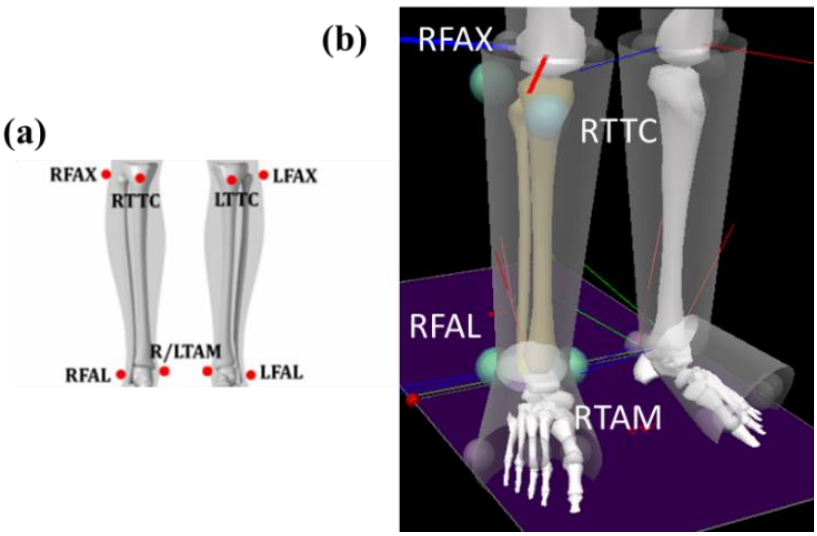

Figure 3.8 Marker location (a) and definition (b) of the shank segment.

3.3.4.1.5 Foot Segment

The foot segment was defined using the anatomical locations of the medial and lateral malleoli, calcaneus, 1st, 2nd and 5th metatarsal heads. The mid-point between the medial and lateral malleoli was used to create a landmark (RANKLE). The foot was defined as a cone where the proximal end of the cone was defined by RANKLE as the joint centre, and the radius of the cone was defined as half the distance between the malleoli. The distal end of the cone was defined by RSM_PROJ as the joint centre and the 5th metatarsal head as the lateral border of the cone. The RSM_PROJ landmark was projected on a plane from the 2nd metatarsal head, where the plane was stretched from the calcaneus and the 1st metatarsal head to the lateral point of the 5th metatarsal head. The segment was tracked using the calcaneus, 1st, 2nd and 5th metatarsal heads. The foot segment was used for kinetic calculations.

Table 3.8 Foot definition in Visual3D.

Foot segment		
Proximal joint and radius	Joint centre – RANKLE	Radius - 0.5*DISTANCE(RFAL,RTAM)
Distal joint and radius	Joint Centre - RSM_PROJ	Lateral – RFM5

Table 3.9 Landmark definition for the foot segment in Visual3D.

Landmark	**Starting point**	**Ending point**	**Lateral object**	**Projected from**
RANKLE	RFAL	RTAM		
RSM_PROJ	RFCC	RFM1	RFM5	RFM2

Figure 3.9 Marker location of the foot segment.

3.3.4.1.6 Virtual Foot Segment

The virtual foot segment, created for kinematic measurements was built similar to the foot segment, except that the joint centre at the proximal end was defined by the calcaneus instead of the mid-point between the malleoli. The virtual foot segment was used for kinematic calculations.

Table 3.10 Virtual foot definition in Visual3D.

Foot segment		
Proximal joint and radius	Joint centre – RFCC	Radius - 0.5*DISTANCE(RFAL,RTAM)
Distal joint and radius	Joint Centre - RSM_PROJ	Lateral – RFM5

3.3.4.2 Segment Definition of 70-Marker-Model

3.3.4.2.1 Head Segment

The head segment was defined as an ellipsoid by four markers on the head, and two markers on the left and right acromion. The four markers the head were in line with the forehead. Landmarks were created at the mid-point between the two front markers and two back markers of the head (HEAD_FRONT and HEAD_BACK). The proximal end of the ellipsoid was defined between the left and right acromion, while the distal end was defined between the landmarks that were defined. The segment was tracked using the four markers, which were in line with the forehead.

Table 3.11 Head definition in Visual3D.

Head		
Proximal joint and radius	Lateral - LCAJ	Medial - RCAJ
Distal joint and radius	HEAD_FRONT	HEAD_BACK

Table 3.12 Landmark definition for the head segment in Visual3D.

Landmark	**Starting point**	**Ending point**
HEAD_FRONT	HEAD_ANT_L	HEAD_ANT_R
HEAD_BACK	HEAD_POST_L	HEAD_POST_R

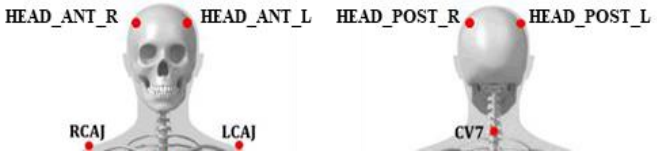

Figure 3.10 Marker location of the head segment.

3.3.4.2.2 Thorax Segment

The thorax segment was defined using the anatomical locations of the left and right acromion, jugular notch, the xiphoid process, the 7th cervical vertebrae and the 2nd thoracic vertebrae. Landmarks were created at the mid-points between the jugular notch and the 7th cervical vertebrae, and between the xiphoid process and the 2nd thoracic vertebrae. The thorax was built as a cylinder where the created landmarks defined the proximal and distal joint centres of the cylinder, and the radius of the cylinder was defined as half the distance between the left and right acromion. The segment was also tracked using the jugular notch, the xiphoid process, the 7th cervical vertebrae and the 2nd thoracic vertebrae.

Table 3.13 Thorax definition in Visual3D.

Thorax		
Proximal joint and radius	Joint centre - SJN_CV7	Radius - 0.5*DISTANCE(RCAJ,LCAJ)
Distal joint and radius	Joint centre - SXS_TV7	Radius - 0.5*DISTANCE(RCAJ,LCAJ)

Table 3.14 Landmark definition for thorax in Visual3D.

Landmark	**Starting point**	**Ending point**
SJN_CV7	SJN	CV7
SXS_TV7	SXS	TV7

3.3.4.2.3 Composite Pelvis Segment

The composite pelvis was defined using the anatomical locations of the ASIS and PSIS. The origin of the pelvis was created at the mid-point between the mid-ASISs and mid-PSIS. The length of the pelvis is defined as the distance between the origin and the midpoint between the hip joint centres, where the hip joint centres were defined as described in Section 3.3.4.1.2. The segment was built as a cylinder and tracked using the ASISs and PSISs.

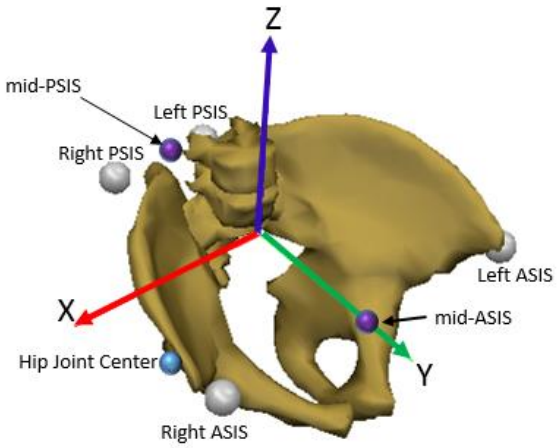

Figure 3.11 Definition of the composite pelvis.

3.3.4.2.4 Thigh Segment

The thigh segment was defined using the anatomical locations of the hip joint centres, medial and lateral femoral epicondyle. The thigh was built as a cone, where the joint centre at the proximal end was defined by the hip joint centre, and the radius was defined as a quarter of the distance between the two hip joint centres. The distal end of the cone was defined by the medial and lateral femoral epicondyles. The segment was tracked using four markers attached on a cluster to the thigh.

Table 3.15 Thigh definition in Visual3D.

Thigh segment		
Proximal joint and radius	Joint centre - RIGHT_HIP	Radius - 0.25*DISTANCE(RIGHT_HIP,LEFT_HIP)
Distal joint and radius	Lateral – RFLE	Medial - RFME

3.3.4.2.5 Shank Segment

The shank segment was defined using the anatomical locations of the medial and lateral femoral epicondyle, and the medial and lateral malleoli. The mid-point between the medial and lateral femoral epicondyles was used to create a landmark (RKNEE). The shank was built as a cone, where at the proximal end the joint centre was defined by RKNEE, and the radius was defined as half the distance between the femoral epicondyles. The distal end of the cone was defined by the medial and lateral malleoli. The segment was tracked using four markers attached on a cluster to the shank.

Table 3.16 Shank definition in Visual3D.

Shank segment		
Proximal joint and radius	Joint centre – RKNEE	Radius - 0.5*DISTANCE(RFLE,RFME)
Distal joint and radius	Lateral – RFAL	Medial - RTAM

Table 3.17 Landmark definition for the shank segment in Visual3D.

Landmark	Starting point	Ending point
RT_KNEE	RFLE	RFME

3.3.4.2.6 Foot Segment

The foot segment was defined using the anatomical locations of the medial and lateral malleoli, calcaneus, 1st, 2nd and 5th metatarsal heads. The mid-point between the medial and lateral malleoli was used to create a landmark (RANKLE). The foot was built as a cone, where the joint centre at the proximal end was defined by RANKLE, and the radius was defined by half the distance of the malleoli. The distal end of the cone was defined by the 1st and the 5th metatarsal heads. The segment was tracked using calcaneus, 1st, 2nd and 5th metatarsal heads. The foot segment was used for kinetic calculations.

Table 3.18 Foot definition in Visual3D.

Foot segment		
Proximal joint and radius	Joint centre – RANKLE	Radius - 0.5*DISTANCE(RFAL,RTAM)
Distal joint and radius	Lateral – RFM5	Medial – RFM1

Table 3.19 Landmark definition for the foot segment in Visual3D.

Landmark	Starting point	Ending point
RTANKLE	RFAL	RTAM

3.3.4.2.7 Virtual Foot Segment

The virtual foot segment was defined using the anatomical locations of the medial and lateral malleoli, calcaneus, 1st, 2nd and 5th metatarsal heads. The joint centre at the proximal end of the foot was defined by the calcaneus and the radius was 0.01. The joint centre at the distal end of the foot was defined by RSM_PROJ, and the lateral border was defined by the 5th metatarsal head. The RSM_PROJ landmark was projected on a plane from the 2nd metatarsal head, where the plane was stretched from the calcaneus and the 1st metatarsal head to the lateral point of the 5th metatarsal head. The segment was tracked using the calcaneus, 1st, 2nd and 5th metatarsal heads. The virtual foot segment was used for kinematic calculations.

Table 3.20 Landmark definition for the virtual foot segment in Visual3D.

Landmark	Starting point	Ending point	Lateral object	Project from
RSM_PROJ	RFCC	RFM5	RFM1	RFM2

3.3.4.2.8 Upper Arm Segment

The upper arm was defined using the anatomical locations of the shoulder markers, and medial and lateral Humerus epicondyles. The upper arm was built as a cone, where the joint centre at the proximal end was defined by the shoulder marker and the radius was defined as half the length between the medial and lateral Humerus epicondyles. The distal end of the cone was defined by the medial and lateral Humerus epicondyles. The segment was tracked using the shoulder marker, medial and lateral Humerus epicondyles.

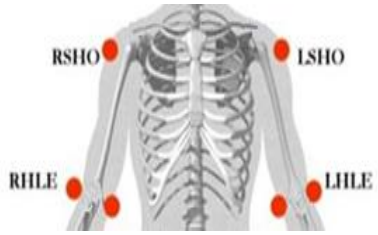

Figure 3.12 Definition of the upper arm.

3.3.4.2.9 Forearm Segment

The forearm was defined using the anatomical locations of the lateral and medial Humerus epicondyles, the Ulna-Styloid Process and Radius-Styloid Process. A landmark was defined mid-point between medial and lateral Humerus epicondyles. The forearm was built as a cone, where the joint centre at the proximal end of the cone was defined by the landmark and the radius was half the distance between the medial and lateral Humerus epicondyles. The distal end of the cone was defined by the Ulna-Styloid process and Radius-Styloid process. The segment was tracked using the medial and lateral Humerus epicondyles, the Ulna-Styloid Process and Radius-Styloid Process.

Table 3.21 Forearm definition in Visual3D.

Shank segment		
Proximal joint and radius	Joint centre – RELBOW	Radius - 0.5*DISTANCE(RHLE,RHME)
Distal joint and radius	Lateral – RRSP	Medial - RUSP

Table 3.22 Landmark definition for the forearm segment in Visual3D.

Landmark	Starting point	Ending point
RELBOW	RHLE	RHME

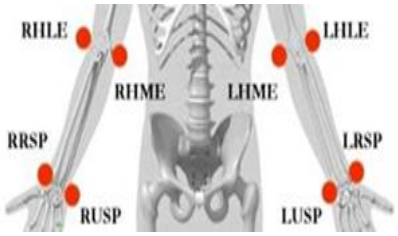

Figure 3.13 Definition of the forearm.

3.3.4.2.10 Hand Segment

The hand was defined using the anatomical locations of the Ulna-Styloid process, Radius-Styloid process and the distal end of middle finger. The hand was built as a sphere, where the proximal end of the sphere was defined by the Ulna-Styloid process and the Radius-Styloid process. The distal end of the sphere was by a joint centre along the axis of the marker on the distal end of the middle finger, and the radius was defined as half the distance between the Ulna-Styloid process and Radius-Styloid process. The segment was tracked using the Ulna-Styloid Process and Radius-Styloid Process and the marker at the distal end of the middle finger.

Table 3.23 Hand definition in Visual3D.

Shank segment		
Proximal joint and radius	Lateral – RRSP	Medial - RUSP
Distal joint and radius	Joint centre – RTIP	0.5*DISTANCE(RRSP,RUSP)

Figure 3.14 Definition of the hand.

3.3.5 Data Processing and Reduction

Following kinematic and kinetic data collection, the data was processed in QTM before .c3d files were exported for further processing in Visual3D v5 (study 1) and v6 (study 2-4) (C Motion, Germantown, MD, USA). In QTM, reflective markers were labelled using acronyms as indicated in Table 3.2. This process was done manually or using the Automatic Identification of Markers (AIM) function. Marker trajectories were checked and edited where necessary. Files were cropped to start at the heel strike on the force platform and ended at the consecutive heel strike of the same limb (study 1), or they were cropped so that the maximum number of gait cycles of either limb was captured (study 2-4). Once this process was completed, the raw marker trajectories and force data were exported form each individual data file as .c3d files for further processing in Visual3D.

In Visual3D, marker trajectories were used to model and determine segment properties such as proximal and distal ends of segments and segment geometry, as defined in Section 3.3.3. To do so, the dynamic files were imported and assigned to the appropriate static file, where the static file included all markers so that all segments could be defined. Medial and lateral landmarks defined anatomical frames from which segment coordinate systems were defined following the right-hand rule (Cappozzo *et al.*, 1995). A flexion-extension, abduction-adduction and longitudinal, Cardan rotation sequence was used to define the order of rotations to calculate joint kinematics. Gait events of heel strike (HS) and toe off (TO) were determined. Gait events were based on a kinetic and a kinematic technique (Stanhope *et al.*, 1990; Zeni *et al.*, 2008). The first technique involved kinetic data from a force platform to determine the occurrence of the required events. Based on the kinematic information of these events during force platform contact, subsequent occurrences of the same event were identified (Stanhope *et al.*, 1990). The events could only be detected where force platform data was available, thus for the events where there was no force platform contact an alternative method was used. The alternative technique was based on a coordinate based algorithm (Zeni *et al.*, 2008) and involves the determination of HS and TO depending on the maximal displacement of the heel and toe relative to the sacrum marker. Markers on the feet were characterised by a sinusoidal curve when the x-coordination of the marker was displayed against time. The peak of the curve coincides with the time during which the foot comes into contact with the ground, and the valleys coincide with the time of swing phase initiation, i.e. toe-off. A display of the foot marker relative to the sacral marker was also a sinusoidal curve with the same characteristics. Thus, the mean value of this curve was used to determine a threshold which when exceeded identifies the peaks (HS) and valleys (TO):

$$t_{HS} = (Y_{heel} - Y_{sacrum})_{max} \quad \textbf{(3.3)}$$

$$t_{TO} = (Y_{toe} - Y_{sacrum})_{max} \quad \textbf{(3.4)}$$

Kinematic data were interpolated using a spline algorithm, and both kinematic and GRF data were filtered using 4th order, zero-lag Butterworth with 6Hz and 30Hz, respectively. Butterworth filter is a low-pass filter. Thus, low frequencies remained unchanged, and high frequencies were attenuated (Robertson *et al.*, 2013). All data were normalised to 100% gait cycle. Different kinematic and kinetic variables were computed in Visual3D and exported to Excel files (Microsoft Windows, Redmond, Washington). In the Excel files, each column represented a variable, whilst each row represented a data point in time, normalised to 101 data points for 100% of the gait cycle. Data from the Excel spreadsheet was imported into MATLAB R2016a (MathWorks Inc., MA, USA) or SPSS v.23.0 (SPSS Inc., Chicago, USA) for statistical analysis.

3.3.6 Definition of Variables

3.3.6.1 Study 1

Thirty biomechanical gait variables in the form of temporal waveforms were reported for study 1 (Table 3.24).

- The ground reaction force (GRF) was calculated for each right foot contact on the force platform and normalised to body weight (BW).
- Joint angles for hip, knee and ankle joints were defined as the orientation of one segment relative to another segment, where the distal segment was calculated relative to the proximal segment. The proximal segment was considered the reference frame, i.e. the movement of the distal segment was defined by its local coordinate system. The Cardan sequence was defined as Z-X-Y, defining flexion/extension, abduction/adduction and longitudinal rotation, respectively. For ankle joint angle, a virtual foot segment was used to define the angle, removing the off-set and aligning the foot on the same plane to the lab floor. The joint angle was normalised to the standing trial.
- Joint moments for hip, knee and ankle joints were calculated as the net internal moment, where the net internal moment was balanced by the net external moment created by the GRF. Mathematically, internal and external net forces are equal and opposite to each other, i.e. the forces from the force platforms are considered internal joint forces and are used to calculate joint moments using one of many inverse dynamics calculations (moment = force × perpendicular distance). The joint moment was normalised to body mass.

- Joint powers for hip, knee and ankle joints were computed as scalar values and normalised to body mass. Joint powers are the product of moment (m_x, m_y, m_z) and angular velocity (ω_x, ω_y, ω_z):

$$Power = [Mx, My, Mz] \cdot [wx, wy, wz] \quad \textbf{(3.5)}$$

$$Power = Mx.wx + My.wy + Mz.wz \quad \textbf{(3.6)}$$

Table 3.24 Temporal waveforms of biomechanical variables reported for study 1.

No.	Temporal Waveforms of Biomechanical Variables	Units
1	Anterior-posterior GRF	BW
2	Medio-lateral GRF	BW
3	Vertical GRF	BW
4	Sagittal hip joint power	$W.kg^{-1}$
5	Frontal hip joint power	$W.kg^{-1}$
6	Transverse hip joint power	$W.kg^{-1}$
7	Sagittal hip joint moment	$N.m.kg^{-1}$
8	Frontal hip joint moment	$N.m.kg^{-1}$
9	Transverse hip joint moment	$N.m.kg^{-1}$
10	Sagittal hip joint angle	Degrees
11	Frontal hip joint angle	Degrees
12	Transverse hip joint angle	Degrees
13	Sagittal knee joint power	$W.kg^{-1}$
14	Frontal knee joint power	$W.kg^{-1}$
15	Transverse knee joint power	$W.kg^{-1}$
16	Sagittal knee joint moment	$N.m.kg^{-1}$
17	Frontal knee joint moment	$N.m.kg^{-1}$
18	Transverse knee joint moment	$N.m.kg^{-1}$
19	Sagittal knee joint angle	Degrees
20	Frontal knee joint angle	Degrees
21	Transverse knee joint angle	Degrees
22	Sagittal ankle joint power	$W.kg^{-1}$
23	Frontal ankle joint power	$W.kg^{-1}$
24	Transverse ankle joint power	$W.kg^{-1}$
25	Sagittal ankle joint moment	$N.m.kg^{-1}$
26	Frontal ankle joint moment	$N.m.kg^{-1}$
27	Transverse ankle joint moment	$N.m.kg^{-1}$
28	Sagittal ankle joint angle	Degrees
29	Frontal ankle joint angle	Degrees
30	Transverse ankle joint angle	Degrees

3.3.6.2 Study 2 – 4

Twenty biomechanical gait variables in the form of temporal waveforms were reported for the studies 2-4, and seven scalar values were reported for study 2 (Table 3.25 and Table 3.26). The GRFs, joint angles, moments and powers were computed as described in Section 3.3.6.1, with exception of the power in the prosthetic limb which was computed using unified deformable (UD) segment model (Takahashi *et al.*, 2012). Anatomically relevant models are built containing a series of rigid segments joined together via mechanical joints, but this presents an issue when modelling LLA gait since some joints are missing. Thus, the UD segment was used to compute power on the prosthetic limb since it does not require the definition of a joint.

- Centre of pressure (CoP) was computed from the force platform. The foot segment was assigned to the force, where the foot segment was defined from the ankle to the metatarsals. The signal was normalised relative to the segment's length (distance between proximal and distal ends of the segment) and width (distal radius). The CoP velocity was computed as the first derivative from the CoP position.
- Centre of mass (CoM) was defined relative to inertial properties calculated using the segment geometries as described in Sections 3.3.3 and 3.3.4.
- Speed was defined depending on stride time and length.
- Step width was defined by the medio-lateral distance between the proximal end positions of the leading foot at heel strike to the proximal end positions the heels strike of the contralateral limb (Figure 2.1). The step width was calculated by taking the cross product by taking the stride vector and the opposite step position. The left stride with was the perpendicular distance from the proximal end of the left foot segment to the right vector. The right step width was calculated as the perpendicular distance from the proximal end of the right foot segment to the left vector. Left and right stride width were reported as an average between both feet.
- Step length was defined as the distance between the proximal end position of the contralateral foot at the previous heel strike to the proximal end position of the leading foot at heel strike.
- Step frequency is the rate at which a person walks, and is better known as cadence, which is expressed in steps per minute:
    - Left steps per minute = $\frac{60}{left\ steps\ time}$
    - Right steps per minute = $\frac{60}{right\ steps\ time}$
- Net-work at the ankle was determined through the summation of positive and negative power phases. This was done using time integration. Net-work was normalised to body mass.
- The BW MoS and ML MoS of stability were computed as described in 2.5.1.1.1.

Table 3.25 Temporal waveforms of biomechanical variables reported for study 2 - 4.

No.	Temporal Waveforms of Biomechanical Variables	Units
1	Anterior-posterior GRF	BW
2	Medio-lateral GRF	BW
3	Vertical GRF	BW
4	Anterior-posterior CoP displacement	m
5	Medio-lateral CoP displacement	m
6	Vertical CoP displacement	m
7	Anterior-posterior CoP velocity	m/s
8	Medio-lateral CoP velocity	m/s
9	Vertical CoP velocity	m/s
10	Vertical CoM displacement	m
11	Vertical CoM velocity	m/s
12	Sagittal hip joint power	$W.kg^{-1}$
13	Sagittal hip joint moment	$N.m.kg^{-1}$
14	Sagittal hip joint angle	Degrees
15	Sagittal knee joint power	$W.kg^{-1}$
16	Sagittal knee joint moment	$N.m.kg^{-1}$
17	Sagittal knee joint angle	Degrees
18	Sagittal ankle joint power	$W.kg^{-1}$
19	Sagittal ankle joint moment	$N.m.kg^{-1}$
20	Sagittal ankle joint angle	Degrees

Table 3.26 Scalar values of biomechanical variables reported for study 2.

No.	Biomechanical Scalar Values	Units
1	Speed	m/s
2	Step width	m
3	Step length	m
4	Step frequency	step/min
5	Ankle net-work	$N.m.kg^{-1}$
6	BW MoS	m
7	ML MoS	m

3.4 Multivariate Statistical Analyses

In this PhD thesis multivariate statistical analyses of PCA and DFA have been used to develop a machine learning algorithm. PCA was a method of choice as it can be used to reduce high dimensionality whilst important characteristics of the data set, which contribute to its variance are still retained (Badesa *et al.,* 2014). DFA was used during the current research as compared to other machine learning algorithms it achieves maximum discrimination which helps to classify data accurately (Tharwat *et al.*, 2017). PCA is an unsupervised algorithm which in the current PhD, was used for data reduction and feature selection, whilst DFA is a supervised algorithm which was used for classification. In an unsupervised approach, classes are not defined and its entities are not known, i.e. the characteristics of the class are defined by the data structure. In a supervised approach, however, algorithms are supplied with information regarding various entities whose class is known and from this, the characteristics of each class are formed. Multivariate statistical method of DFA can be considered a machine learning algorithm, whilst PCA is not. The concept of learning has been described as the ability to develop classification rules from experience. The learning stage can be described as having a set of training objects whose classes are known, usually using a supervised algorithm, to establish prediction rules using attribute values of each class of an unknown data set (Quinlan, 1990).

3.4.1 Principal Component Analysis

Principal Component Analysis (PCA) is multivariate statistical method used to establish variation between variables. Using PCA, data is presented in a new coordinate system, capturing the maximum variance of a data set (Badesa *et al.,* 2014; Dillmann *et al.,* 2014; Wu *et al.,* 2007; Yang *et al.,* 2012). PCA can be calculated using either the covariance or correlation matrices. The matrix used depends on the nature of the data, for example, if the variables under investigation share the same units the covariance matrix should be used whilst the correlation matrix should be used when the variables have different units. PCA was first applied to biomechanical data to derive a representation of signals instead of using signals themselves (Wootten *et al.,* 1990), others used it as a data reduction method (Olney *et al.,* 1998), whilst different researchers used it to assess entire gait waveforms retaining potentially valuable information (Deluzio *et al.,* 1997).

A visual example of PCA is shown in Figure 3.15. Suppose the spheres represent two variables that make up a data set represented in a $x_1 - x_2$ coordinate system (Figure 3.15 a). The direction in which most of the variance occurs between these two variables can be captured by the axis u (Figure 3.15 b). A second axis v, perpendicular to axis u, will represent the axis holding the second most variation between the data (Figure 3.15 c). The $u - v$ coordinate system will

represent the mean of the variables, where the covariance between u and v variables would be zero. For a given data set, PCA finds the axis system defined by the principle direction of variance, i.e. $u - v$ axis, were u and v are the principle components (PCs) (Figure 3.15 d). In a larger data set, with a greater number of variables, the number of PCs would match the number of variables, creating a high-dimensional space.

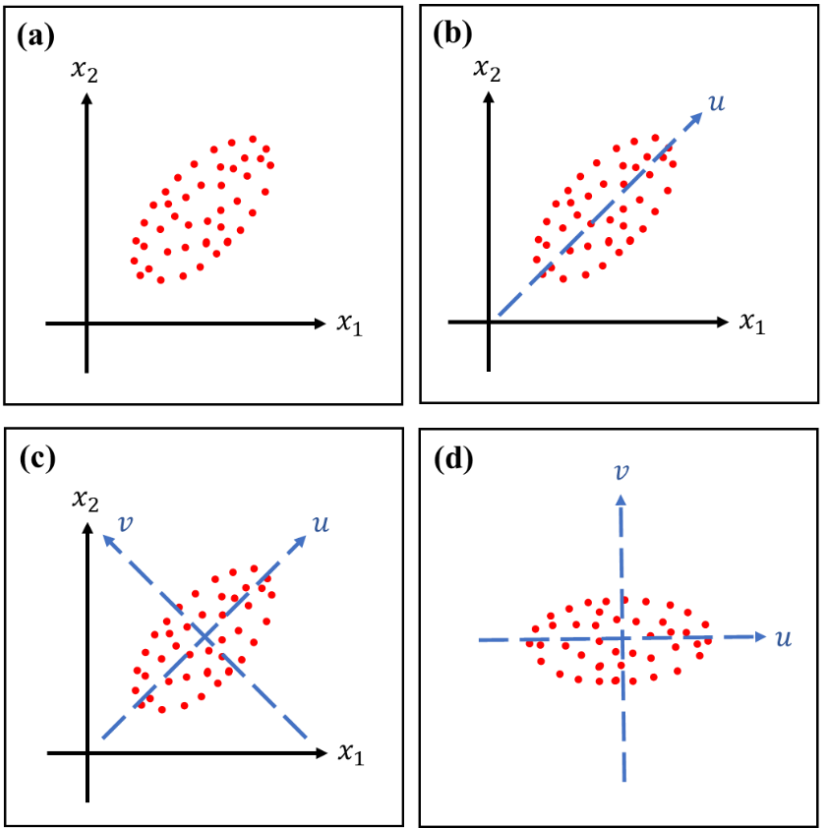

Figure 3.15. Illustration of PCA analysis. The variance of the variables is captured using PCA and represented in a new data set of PCs.

To compute PCA using covariance matrix the following methods are used (Robertson *et al.*, 2013). Firstly, the data under investigation should be represented in a matrix.

$$X = \begin{bmatrix} x_{11} & x_{12} & \dots & x_{1p} \\ x_{21} & x_{22} & \dots & x_{2p} \\ \vdots & \vdots & \ddots & \vdots \\ x_{n1} & x_{n2} & \dots & x_{np} \end{bmatrix} \quad \textbf{(3.7)}$$

To find differences in the structure of the data, the covariance of columns of X is calculated.

$$S = \begin{bmatrix} s_{11} & s_{12} & \dots & s_{1p} \\ s_{21} & s_{22} & \dots & s_{2p} \\ \vdots & \vdots & \ddots & \vdots \\ s_{n1} & s_{n2} & \dots & s_{np} \end{bmatrix} \quad \textbf{(3.8)}$$

Where:
S = covariance or correlation matrix (of columns of X)
s_{jj}= diagonal elements, that represent the variance at each instance of the temporal waveform.

Where the diagonal elements of covariance are computed as follows:

$$s_{ii} = \frac{\sum_{k=1}^{n}(x_{ki} - \bar{x}_i)^2}{n-1} \quad \textbf{(3.9)}$$

Where:
i = column
n = number of rows (participants)

The off-diagonal elements represent the covariance between each pair of time instants:

$$cov\,(i,j) = \sigma_{i,y} = s_{ij} = \frac{\sum_{k=1}^{n}(x_{ki} - \bar{x}_i)\,(x_{kj} - \bar{x}_j)}{n-1} \quad \textbf{(3.10)}$$

Where:
i and j = two columns
n = number of rows (participants)
$\bar{x}$ = mean value
σ = variance

A covariance that is not equal to zero indicates a linear relationship between two variables. The strength of the linear relationship can be defined by the correlation coefficient:

$$corr(i,j) = \rho_{i,j} = r_{ij} = \frac{s_{ij}}{s_{ii}s_{jj}}\ or\ \frac{\sigma_{i,j}}{\sigma_i\sigma_j} or\ \frac{cov(i,j)}{\sigma_i\sigma_j} \quad \textbf{(3.11)}$$

The variance of the original data (matrix X) is presented by the covariance matrix S. If the off-diagonal elements of matrix S are non-zero, they represent a correlation of the columns in matrix X. The principal components (PC) are extracted from matrix S. Since the PCs are independent of each other i.e. uncorrelated, the off-diagonal elements of the covariance matrix S are changed to equal zero. The process of changing all off-diagonal elements to zero from the covariance matrix

S to a covariance matrix D is known as diagonalisation, or also referred to as orthogonal decomposition and is given by:

$$U^T S U = D \quad \textbf{(3.12)}$$

Where:
S= covariance matrix
U= orthogonal transformation of X (columns of U are Eigenvectors of S known as loading vectors)
U^T= transpose orthogonal transformation of X
D = diagonal covariance matrix of S (Eigenvalues are stored in D which indicate variance of PCs).

If the covariance matrix of data is a diagonal matrix, such that the covariances are zero, then this means that the variances must be equal to the Eigenvalues λ. Matrix U can be seen as a orthogonal transformation matrix of the original data set in a new coordinate system. The new coordinates represent PCs which are aligned in descending order of variance in the data. The columns of U are Eigenvectors of S and are known as loading vectors which are the PCs.
The diagonal covariance matrix D has the elements λ_i, which are the Eigenvalues of S. Each Eigenvalue is a measure of variance associated with each PC. The maximum number of PCs is presented by the non-zero diagonal elements of matrix D. This is equal to fewer of participant number n or length of temporal waveform p corresponding to the rank r of matrix S.

Matrix U is the transformation of the original data set to new uncorrelated principal components (Y).

$$\underset{(nxr)}{Y} = \underset{(nxr)}{[X - \bar{X}]}\,\underset{(pxr)}{U} \quad \textbf{(3.13)}$$

In matrix Y each column is a PC and the elements of these columns are PC scores. Following the computation of PCs, they are organised in descending order of variance so that the first PC displays the maximum amount of variance in the original data followed by the second PC orthogonal to the first, and so on. The Eigenvalues λ_i which are the diagonal elements of matrix D give the variance of each PCs.

Hence PCA is a technique that conserves the variance of the original raw data through the PCs. To measure the total variation within the data the sum of variances can be computed which is corresponding to the sum of diagonal elements of S. The sum of the diagonal matrix in referred to as (tr) of a matrix therefore:

$$tr(S) = tr(D) \quad \textbf{(3.14)}$$

Quantifying the portion of total variance explained by each principal component,

$$Variation\ Explained\ by\ PCi = \frac{\lambda_i}{tr\ (S)} = \frac{\lambda_i}{\sum \lambda} \quad \textbf{(3.15)}$$

3.4.2 Discriminant Function Analysis

Fisher Discriminant Analysis, also referred to as Discriminant Function Analysis (DFA) is a multivariate statistical analysis, which is used for the development of machine learning algorithms. It is a supervised analysis, used to project data onto lower-dimensional vector and provides the highest possible discrimination between different classes. DFA attempt to express a dependent variable as a linear or quadratic combination of other variables, referred to Linear Discriminant Analysis (LDA), or Quadratic Discriminant Analysis (QDA), respectively. LDA aims to find a linear combination of input features according to a least square sense by sorting input data into two or more classes (Badesa *et al.,* 2014). Each feature has its own weighting factor which indicates its importance to the discrimination between the classes (Badesa *et al.,* 2014). The intra and inter-class distance between the features are determined to establish which class it belongs to. Discriminant Function Analysis can be calculated as follows (Badesa *et al.,* 2014; Sugavaneswaran *et al.,* 2012; Swets, 1996) (for a detailed tutorial see Tharwat *et al.,* 2017):

For two different experimental groups, i.e. a two-class problem, the features of each data set are represented in a matrix. Consider a matrix with two columns, where each column represents a vector that corresponds to a variable.

$$class\ i = \begin{bmatrix} x_{11} & x_{12} \\ x_{21} & x_{22} \\ \cdots & \cdots \\ \cdots & \cdots \\ x_{m1} & x_{m2} \end{bmatrix} class\ j = \begin{bmatrix} y_{11} & y_{12} \\ y_{21} & y_{22} \\ \cdots & \cdots \\ \cdots & \cdots \\ y_{n1} & y_{n2} \end{bmatrix} \quad \textbf{(3.16)}$$

In case where principal component Y, is unable to separate the two obvious classes, then they are projected on to Z, providing a discriminant analysis procedure:

$$Z = W^T Y \quad \textbf{(3.17)}$$

Where:
W = projection matrix

Firstly, the mean of each matrix, i.e. class is calculated, before merging them together. In case where principal components Y have not already been calculated, the covariance or correlation for each matrix must be computed. This is done in order to obtain the scatter coefficient within a group and between the groups. The scatter measure is given as:

$$S_w = \sum_i p_i \times (cov_i); S_w = \sum_j p_j \times \left(cov_j\right) \quad \textbf{(3.18)}$$

For a two-class problem with S_w as the within-class and $S_b$as the between-class scatter measure is given as:

$$S_w = \sum_{i=1}^{c} \sum_{j=1}^{n_i} \left(Y_j - M_i\right)\left(Y_j - M_i\right)^T \quad \textbf{(3.19)}$$

Where:
Y_j= principal component of class j
M_i= mean of class i

$$S_b = \sum_{i=1}^{c} (M_i - M)(M_i - M)^T \quad \textbf{(3.20)}$$

Where:
M = mean of a global mean computed from merged dataset
M_i= mean of class i

Scatter measures are then optimised using maximisation within-class and between-class covariance criteria. This is done by calculating Euclidean distances for each data point, where the Euclidean distance is defined as the straight-line difference between two points in space. Therefore, a smaller measured distance corresponds to a vector (variable) that is classified to class j.

$$D(i) = sign(S_W \times \ i + S_b) \quad \textbf{(3.21)}$$

Where:
$D(i)$ = discriminative function
i = input feature vector of class i
S_w = weighting vector
S_b = intercept

The input feature vector i is assigned to a class if $D(i)$ is positive and assigned to the other class if it is negative. Figure 3.16 shows the scatter of features and how the most discriminating features can be identified using DFA when missed by PCA. For the MATLAB codes of PCA and DFA, see Appendix 1.

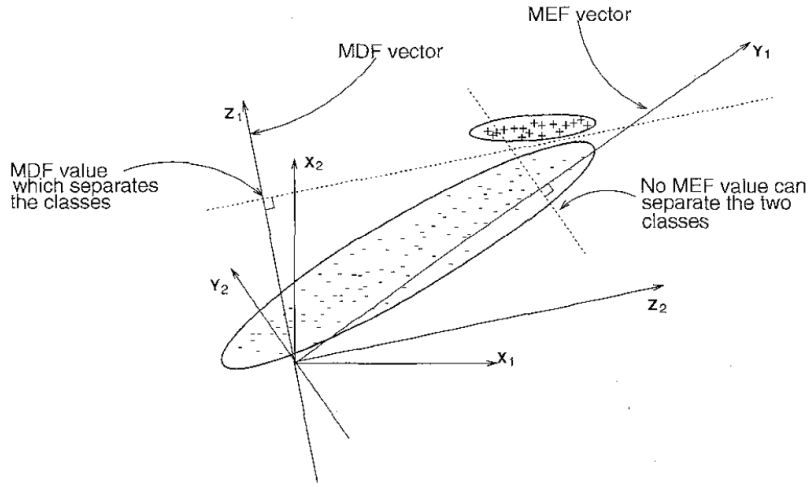

Figure 3.16 Problems with the most discriminating features (MDF) for class separation. In the x and y-axes, representing the principal components (PC), the classes are not separated. Projecting classes onto a different set of z-axes results in seperation of classes. Figure adopted from Swets (1996).

3.4.3 Display of PCA and DFA Outcomes

The PCA discrimination and DFA classification outcomes are represented using scatter plots (Figure 3.17 a, c) which illustrates the clustering or the lack of clustering between groups/conditions. Furthermore, eigenspectra (Figure 3.17 b) of PCA and DF spectra (Figure 3.17 d) of DFA show the weighing of variables, i.e. their contribution to the discrimination/ classification procedure. The length of each bar emphasises the weighwhere large and small bars represent a large and small contribution to the discrimination/ classification process, respectively.

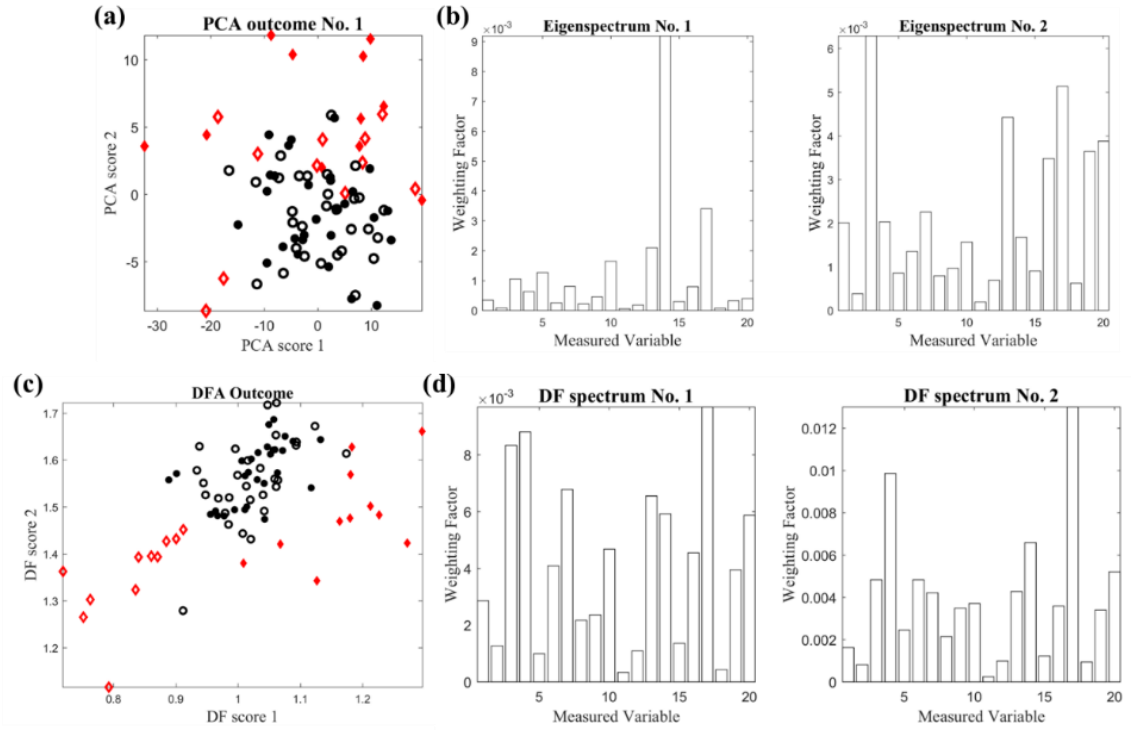

Figure 3.17 Outcome of PCA (a) and DFA (c) scatter plot, showing clustering of groups/conditions. Eigenspectra (b) and DF spectra (d) indicating the weighting factors of individual variables involved during analysis.

Chapter 4: Optimisation of a Machine Learning Algorithm in Human Locomotion.

Bisele, M., Bencsik, M., Lewis, M.G., & Barnett, C.T. (2017) Optimisation of a machine learning algorithm in human locomotion using principal component and discriminant function analyses. *PloS ONE*, 12 (9), p.e0183990.

Bisele, M., Bencsik, M., Lewis, M.G., and Barnett, C.T. (2016) Optimisation of an objective predictive machine learning algorithm in human locomotion. *In Proceedings of the BASES Biomechanics Interest Group Meeting, Liverpool John Moores, Liverpool, UK.*

4.1 Introduction

In a clinical setting, gait analysis can be particularly useful since it helps diagnose pathology, provide treatment recommendations and evaluate treatment outcomes. Data acquisition tools and processing procedures produce large amounts of gait data. This data is in the form of temporal waveforms and has typical characteristics such as high dimensionality, meaning it consists of multiple variables. A widely used approach to analyse and interpret movement data is through the description of graphical profiles of temporal waveforms, using summary statistic (mean, variance, correlations) and waveform parameterisation (peak amplitude) (Alaqtash *et al.*, 2011a; Deluzio *et al.*, 1999). However, these approaches are subject to researcher bias, and some of the gait characteristics are ignored. To overcome these drawbacks and handle data, recent studies implemented multivariate statistical analyses such as PCA and machine learning algorithms such as DFA. Principal Component Analysis is an unsupervised algorithm. It reduces data and highlights important generic features by evaluating the gross structure of a data set whilst maintaining the variance of the original data (Chau, 2001a). Discriminant Functional Analysis is a supervised algorithm, which reveals discriminating features within a data set through the evaluation of the detailed structure (von Tscharner *et al.*, 2013). Together, PCA and DFA provide a method for assessing differences between experimental groups of people/conditions. The combination of an unsupervised and a supervised algorithm can be used to develop a machine learning algorithm, which refers to the ability of a device to independently conduct discrimination on a database without the input of a researcher. Therefore, in a clinical setting, it would provide an objective method, eliminating researcher bias and without compromising gait characteristics.

Previous studies have used machine learning algorithms to identify gait differences between different groups and obtained high discrimination results such as 91.7% or 95.8% between older and younger individuals (Begg and Kamruzzaman, 2005; Eskofier *et al.*, 2011; Reid *et al.*, 2010), 98-100% between males and females (Phinyomark *et al.*, 2016), and 100% between pathological and non-pathological gait (Lemoyne *et al.*, 2015). However, experimental data sets used to develop these algorithms were made up of discrete parameters such as walking speed and maximum vertical force at heel strike (Alaqtash *et al.*, 2011a; Begg and Kamruzzaman, 2005; Wu *et al.*, 2007). Limiting the information that could be provided by entire temporal waveforms which means important discriminating features may have been neglected (Deluzio *et al.*, 1999). In some cases, high discrimination rates have been obtained, but the environment of discrimination was not challenging, as experimental groups were expected to be significantly different, e.g. experimental groups of young and older individuals (Begg & Kamruzzaman, 2005; Wu *et al.*,

2007). Sophisticated numerical methods have been employed to pre-process data and conduct discrimination (Wu *et al.,* 2007), but studies have shown that even the use of simple discrimination methods for tighter experimental conditions, enables a classification to be made (von Tscharner *et al.,* 2013). Also, the quality of the data used to train the machine learning algorithm was not considered, effecting the quality of the discrimination outcome, because different individuals will exploit features in a different manner, which means that a feature could be strongly discriminating in one individual however not in another. A group of individuals will collectively display the strongest generic discriminating features between two experimental groups of people/conditions. Therefore, depending on the individuals that have been selected to develop the training database for the machine learning algorithm, its predictive abilities will vary. Thus using an iterative process to identify the individuals that express these generic features most predominantly and using their data as the training database, will optimise the algorithm, ensuring a reliable prediction every time the machine learning algorithm is used. Therefore, the aim of this study was to develop and optimise a machine learning algorithm using multivariate statistical analyses, namely Principal Component Analysis (PCA) and Discriminant Function Analysis (DFA) for processing of human locomotion.

4.2 Methodology

4.2.1 Participants

A convenience sample of twenty recreationally active participants (14 males and 6 females; age 24±4 years; height 1.75±0.86m; mass 72.0±8.5 kg) were drawn from the University community. These individuals had no lower limb pathologies and were free of injury during the time of the study. Ethical approval was granted by the Nottingham Trent University Ethics Committee (Humans). All participants provided informed consent prior to participation.

4.2.2 Experimental Design and Data Acquisition

The study investigated participants under two different experimental conditions; running with (shod) and without shoes (barefoot). Upon arrival, the participant was briefed, and consent was acquired. All activities were completed with participants wearing lycra shorts and running shoes. To obtain kinematic data 36 spherical 14mm, reflective markers were placed directly onto the skin or clothing using bi-adhesive tape, defining trunk (Leardini *et al.,* 2011) and lower limb segments (Cappozzo *et al.,* 1995) (for marker placement, refer to Section 3.3.3). Subsequently, participants conducted a short five minute warmed-up on a treadmill at self-selected speed.

Depending on the initial condition, foot markers were placed before or after the warm-up since warm-up was performed wearing shoes.

A static trial was obtained for segment definition, followed by the dynamic trials. Dynamic trials were counterbalanced between conditions, thus participant would start with either barefoot or shod running trials. First, the participant's starting position was defined, to ensure that force platform data was obtained. During the trials participant ran at a self-selected speed along a 15m runway. This process was repeated until five successful trials (force plate contacts) were collected on the right limb for each condition. Once the intial condition was completed, the second condition followed thus shoes were either put on or taken off, followed by marker placement. Ground reaction force (GRF) was measured at 1000Hz using a single floor-mounted strain gauge force platform (AMTI, Watertown, MA, USA) and kinematics were measured at 100Hz using a nine-camera motion capture system (Qualisys, Gothenburg, SE).

4.2.3 Data Pre-Processing

Markers were labelled in QTM v2.2 (Qualisys, Gothenburg, SE) as defined in Section 3.3.3 and start and end points of a trial were adjusted to one gait cycle of the right limb. Marker trajectories and force data were exported as .c3d files and subsequently processed in Visual 3D v5 (C Motion, Inc., Germantown, MD, USA). Kinematic data were interpolated using a cubic-spline algorithm with kinematic and GRF data being subsequently filtered using 4^{th} order, zero-lag Butterworth low-pass filters with 6Hz and 30Hz cut-off frequencies, respectively. All data were normalised to 100% gait cycle. Medial and lateral landmarks defined anatomical frames from which segment coordinate systems were defined following the right-hand rule (Cappozzo *et al.,* 1995). A flexion-extension, abduction-adduction and longitudinal Cardan rotation sequence was used to define the order of rotations to calculate joint kinematics. Gait events of heel strike and toe off were determined using event detection algorithm (Stanhope *et al.,* 1990) (Section 3.3.5). Joint angles (°), joint moments ($N.m.kg^{-1}$) and joint powers ($W.kg^{-1}$) for the hip, knee and ankle joints, as well as the GRF (multiples of body weight; BW) were computed in Visual 3D (C-Motion, Inc, Germantown, USA) (Section 3.3.6). Results were reported in all three anatomical planes. Thus thirty temporal waveforms were reported for a single stride in each trial starting with heel strike of the right limb on the force platform and finished at the consecutive heel strike on the same limb. Processed data were exported from Visual3D in .c3d files, and individual signals from the .c3d files were imported to MATLAB® R2016a (MathWorks Inc., MA, USA) for further analysis.

4.3 Development of a Machine Learning Algorithm

4.3.1 Power Spectrum of Data

The machine learning algorithm was developed using DFA. Prior to DFA, PCA was used for data reduction and feature selection, followed by DFA to classifying the data. Before PCA and DFA were applied, the data were linearly interpolated to the same digital length filling any missing gaps in the data. This was done so that the power spectrum (modulus of Fast Fourier transform (FFT)) could be computed for all variables. The power spectrum removes the absolute phasing of kinetic and kinematic waveforms which if not removed could compromise the quality of the discrimination process and therefore also the machine learning algorithm since the time lag would be considered a false discrimination feature (Figure 4.1). Apart from the absolute phasing of different frequency components of the data, the rest of the temporal information of the waveforms is kept intact in the power spectra.

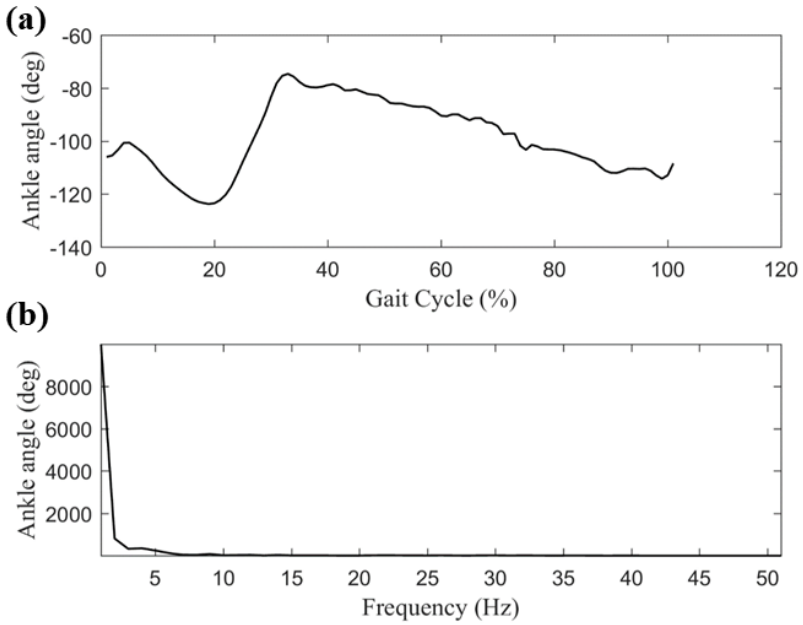

Figure 4.1 Display of ankle angle relative to time (a) and its power spectrum (b).

The Power Spectral Density (PSD) describes the contribution of power as a function of the different frequencies components (Welch, 1967; Thomson, 1982). The log of the power spectrum was also assessed, however, as it did not improve the discrimination outcome, it was not included in the procedure. The first frequency component of the power spectrum is always an average of the raw data set and has a larger magnitude than all the other frequencies. Processing the data with and without the first frequency component did not improve the discrimination outcome and thus it was not included in the discrimination process, either.

4.3.2 Application of Principal Component Analysis

After the power spectrum is applied, PCA followed. PCA is an orthogonal transformation turning dependent variables to a new set of independent variables or principal components, Z, which represent the variance observed in the original variables X (Chau, 2001a) (see Section 3.4.1). The principal components (PCs), making up the columns of the covariance and correlation matrices, are ordered in terms of decreasing variance such that the majority of variation in the data can usually be described by the first few PCs. Therefore the remaining PCs can be ignored reducing the dimensionality of the data. However, depending on the research question lower ordered PCs may provide the necessary information rather than higher ordered PCs (Phinyomark *et al.*, 2015).

4.3.2.1 Principal Component Analysis Ranking and Reduction Procedures

An input matrix M was built containing the power spectra of the kinetic and kinematic waveforms extracted from each experimental trial. The matrix was ordered as follows: for each subject, five trials of each condition existed (twenty subjects and two conditions resulted in 200 trials) and every trial was made of 30 columns with 50 row vectors, where each column represented a measured variable and each row vector represented the spectral frequency of the 3D coordinate measure of the variable. The input matrix M, originally 3D with $200 \times 30 \times 50$ points, was rearranged to be 2D, with 200×1500 points, in order to undertake the PCA on a collection of 200 trials each comprising of 1500 points. The data were summarised using PCA, involving the diagonalisation of the covariance matrix which can be either 200 x 200 or 1500 x 1500. We chose the first option so 200×1500 points became 200×200. This choice was made because there are more features (variables/parameters) than individuals thus using the unconventional method of PCA to compute the PCs substantially reduces computer memory requirements. In this particular case a small complication arises when having to access the eigenspectra. The pseudo-inverse method was further employed as the matrix requiring inversion was not square (see Appendix 1. for code) (Hua and Liu, 1998). In the PCA plot each trial was shown by a single data point i.e. 200 points (100 for barefoot and 100 shod trials). The coordinates of each data point are PC scores, these are obtained by the cross-correlation product (a.k.a. 'projection') of a given measurement (30 parameters spectra) by a given PCA eigenspectrum. However, since the PCA plot can only be shown in 2 or 3D, only two or three first PC scores are shown. In this study, the trials were shown in 2D.

As previously mentioned, higher PCs hold most of the information whilst lower ones hold increasingly noise. The numerical analysis was made immune to overfitting artefacts originating from the over-exploitation of small details, by choosing the highest explored rank (12^{th}) well

below the one still carrying information (20th). In Figure 4.2 the PCA rank is displayed using an exponentially decreasing graph. The line decreases up to rank no. 20, indicating the presence of information up to this point whilst noise is also increasing. The graph plateus beyond rank no. 20 indicating that beyond this point the data consits mainly of noise, thus a PC rank beyond this point should be avoided. Selecting too few PC scores will result in neglect of important information (underfitting) and selecting PC score too high will introduce a lot of noise (overfitting) to the discrimination procedure. The number of PC scores that need to be considered depends on the complexity of the data. For more complex data sets a higher PC score should be considered which will also be evident in the PC rank.Thus, in the current study high dimensionality was reduced from the original 1500 points (for each trial) to 8, 10 or 12 points.

The PC rank can also be displayed as an image scale (Figure 4.3), where x and y-axis are the PCs. Starting at the first PC with the highest variance, a great scatter of colours is present which gradually fades into a block colour as the presence of noise increases in the data.

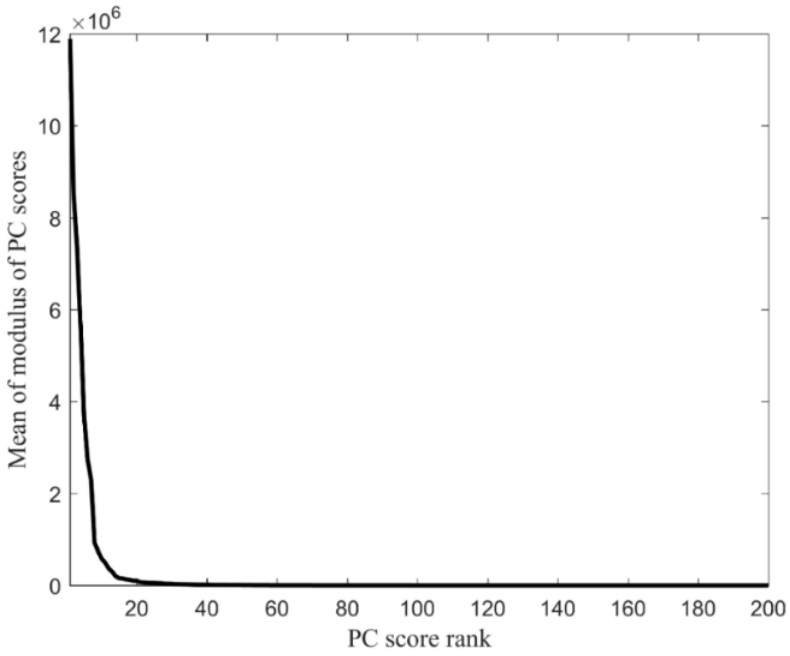

Figure 4.2 Principal components are ranked by the amount of variance they capture in the original data.

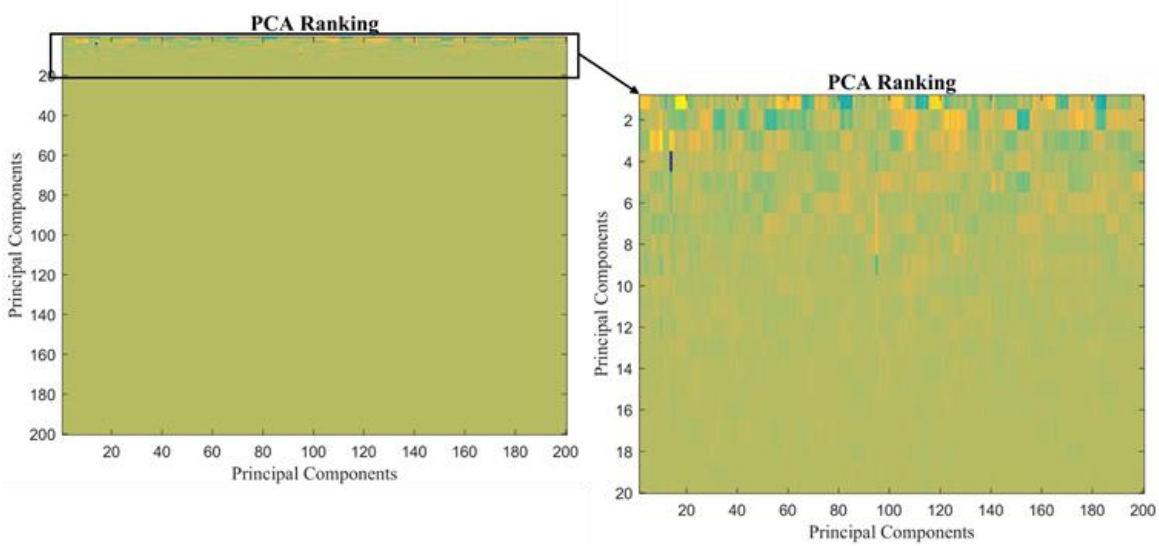

Figure 4.3 Image scale of PC ranking. The right hand image shows a zoom Section of the first 20PCs, illustrating the complexity of the data shown by the scatter before it fades into a block colour moving down the PCs that hold reduced variance.

4.3.3 Application of Discriminant Function Analysis

The reduced data set from PCA was further analysed using DFA to identify generic discriminating features between the two experimental conditions, and cluster the data as required by the goal of the study into barefoot versus shod running. Discriminant Function Analysis (DFA), also known as Linear Discriminant Analysis (LDA), is a statistical analysis which works to attain the maximum discrimination between classes. The ratio of inter-class and intra-class variance for any given database is computed to achieve maximum separation. This results in linear class boundaries thus grouping the various class clusters in a given subspace (Badesa *et al.*, 2014; Sugavaneswaran *et al.*, 2012; Swets, 1996) (see Section 3.4.2).

4.3.4 Development of the Machine Learning Algorithm

As previously mentioned a robust machine learning algorithm is developed in three stages namely training, predictive and evaluation stage (Lever *et al.*, 2016a; c). In this study, the training stage of a machine learning algorithm was optimised to distinguish between two experimental conditions, barefoot and shod running. All stages of data interpolation, application of power spectrum, dimensionality reduction and feature extraction using PCA, and classification using DFA, were combined to develop a machine learning algorithm (Figure 4.5). A machine learning algorithm is also referred to as a predictive algorithm when applied to data that did not contribute to the training stage.

Different approaches have been explored to determine which would provide the best predictive outcome (Figure 4.4). First, the discrimination was conducted on a single participant to try and discriminate between barefoot and shod running. Secondly, all participants' data were included in the discrimination process. This was followed by the selection of random biomechanical variables and a random sample of participants to investigate whether this would improve the discrimination between the experimental condition. Finally, a systematic iteration process was explored. During this process, all possible combinations of ten individuals were explored during the training stage, and an error rate was computed for each iteration to indicate the accuracy of the discrimination during the predictive stage with the remaining ten individuals. This was done for discrimination between two clouds where each cloud corresponded to one condition, and it was done for multiple clouds. In the discrimination procedure of multiple clouds, one cloud would be made up of one condition, e.g. shod trials and multiple smaller clouds corresponding to the number of the participant would make up the other condition.

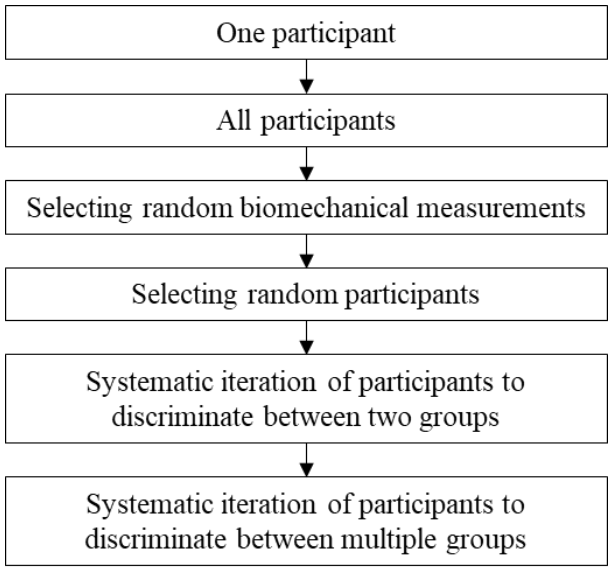

Figure 4.4 Build-up of approaches to establish the method with the highest predictive outcome.

4.3.4.1 Training and Predictive Stages

In this study, during the training stage, data from ten participants were used to direct the search for generic features and identify which of these provided the greatest discrimination between the two experimental conditions. During the predictive stage, data of the remaining ten participants that had not contributed to the training of the machine learning algorithm were used to assess whether it could automatically and correctly assign data to the group with the same generic features.

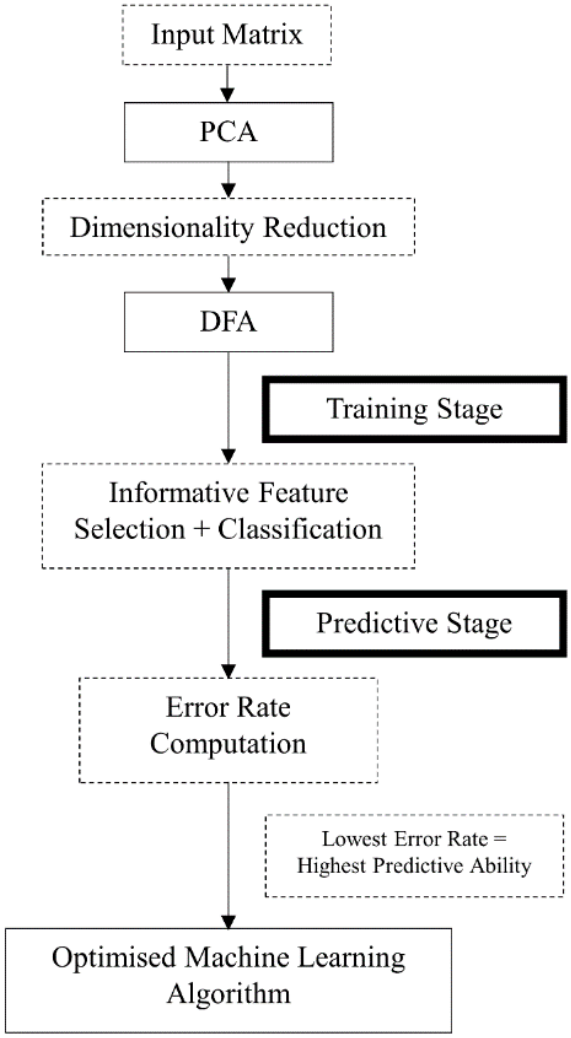

Figure 4.5 Flow-chart of the development of the machine learning algorithm.

4.3.4.2 Optimisation Process

The machine learning algorithm was trained and tested using ten participants out of a total of twenty in both stages (Figure 4.6). In order to optimise the training stage, participants that would result in the greatest classification had to be identified. This was done by exploring all possible combinations of 10 out of 20 participants; a total of 184,756 iterations were identified. An error rate was computed for each individual iteration. The best iteration corresponded to the one yielding the combination of participants with the lowest error rate since this indicates the strongest generic discriminating features to have been identified and thus optimising the algorithm. There are common gait features among individuals, however, some individuals will express these features more strongly than others, i.e. identifying the participants with the strongest expression of these features will collectively allow the identification of the generic features that discriminate between barefoot and shod running.

The error rate was calculated as follows: each trial was projected onto a two dimensional DF space, yielding a set of two DF scores. In this space, the coordinates of the two centroids of each group were calculated, and for each trial, the Euclidean distances to both centroids were further calculated. The ratio of these two distances was used to assess whether the trial ended up in the 'shod' or 'barefoot' category, with a value of 1 corresponding to the threshold dictating the membership. The trials ending up with the incorrect group were expressed as a percentage error rate, overall the 200 trials (20 individuals each undertaking 5 shod and 5 barefoot runs).

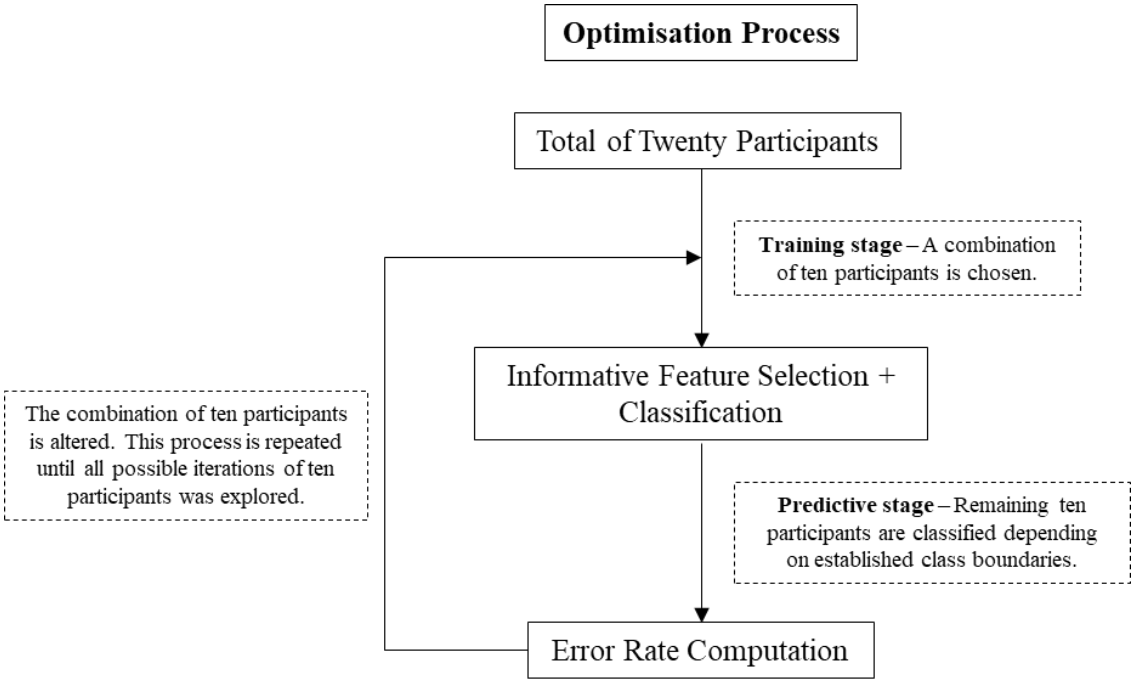

Figure 4.6 Flow-chart of the iteration process used to optimise the machine learning algorithm.

4.3.4.3 Evaluation of Classification

In this study, positive instances relate to shod running trials, and negative instances relate to barefoot running trials. The sensitivity and specificity (Equation 2.7 and Equation 2.8) refer to positive and negative instances which have been correctly identified during the predictive procedure. In this study, entrie gait waveforms have been used in the evaluation rather than discrete parameters.

4.4 Results

4.4.1 Discrimination Outcome of One Individual without Optimisation

The PCA and DFA outcomes for the discrimination between barefoot and shod running of one individual are illustrated in Figure 4.7. There was a clear classification of the experimental conditions. However, these results did not include the generic discrimination features since they were based on the data of a single individual. The PC scores considered during this discrimination were few, as the complexity of data was minimal. Figure 4.8 shows the PC rank in a scateer plot demonstaring the fading of colour after PC rank no 4, thus a score beyond this point was avoided to eliminate risks of overfitting.

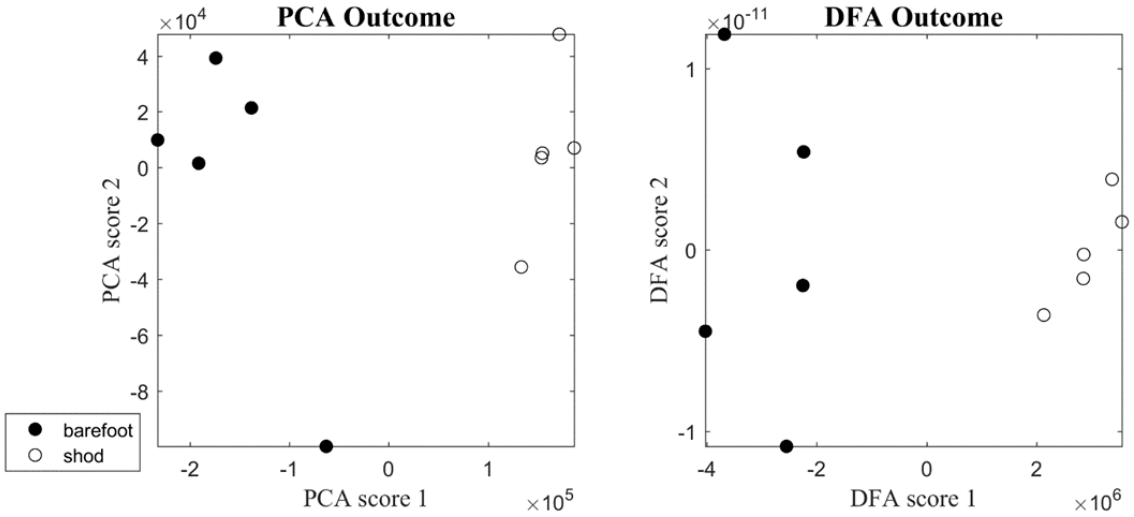

Figure 4.7 PCA and DFA outcome of one individual.

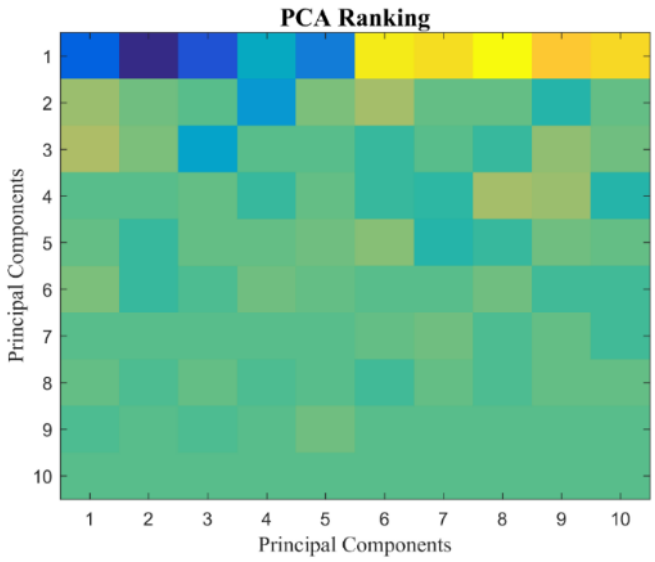

Figure 4.8 PCA ranking for one individual shown in an image scale.

4.4.2 Discrimination Outcome of a Group of Individuals without Optimisation

The outcome of the PCA search (Figure 4.9) alone results in severely overlapping clouds. This demonstrates that the discrimination sought for is not residing in the main deviations found in the data of barefoot and shod running, illustrating the challenging nature of the conditions of interest. Instead, the discrimination required resides in subtle details of the spectra, necessitating the second stage numerical search, DFA, to be applied to the data after reduction of PCA. Discriminant Function Analysis is needed depending on the ability of PCA to cluster the data. Since PCA is an unsupervised algorithm and it works to maintain the variance of the original data set, it explores the gross structure only. In a challenging environment, where differences lie within the detailed structure of the data, it will not be able to identify differences between groups/conditions. In this case, a supervised algorithm such as DFA is needed since it seeks out differences in the data by assessing the details of the structure. Visual examination undertaken of both the time courses and the spectra of the barefoot and shod conditions showed no clear common discriminating characteristics emerged despite careful inspection. Following DFA the two clouds representing each condition start classifying. Using the entire database as the training database for the discrimination exercise yielded an error rate of 24% as seen in the DFA outcome of Figure 4.9 (d). Thus, even after the numerical search, the training stage of the machine learning algorithm results in a high error rate if not optimised.

Figure 4.9 shows the outcome of PCA and DFA following classification. Each dot represents a trial of a participant and since there are 10 participants and each has conducted 10 trials (5 shod and 5 barefoot). The outcome did not improve when the first spectral frequency was included (c and d) relative to when it was not (a and b) thus it was not included in the processing procedure. Increasing the rank of the PCA scores fed to the DFA algorithm from 8 to 12 did not improve the outcome, and the data shown were obtained using 10 PCA scores.

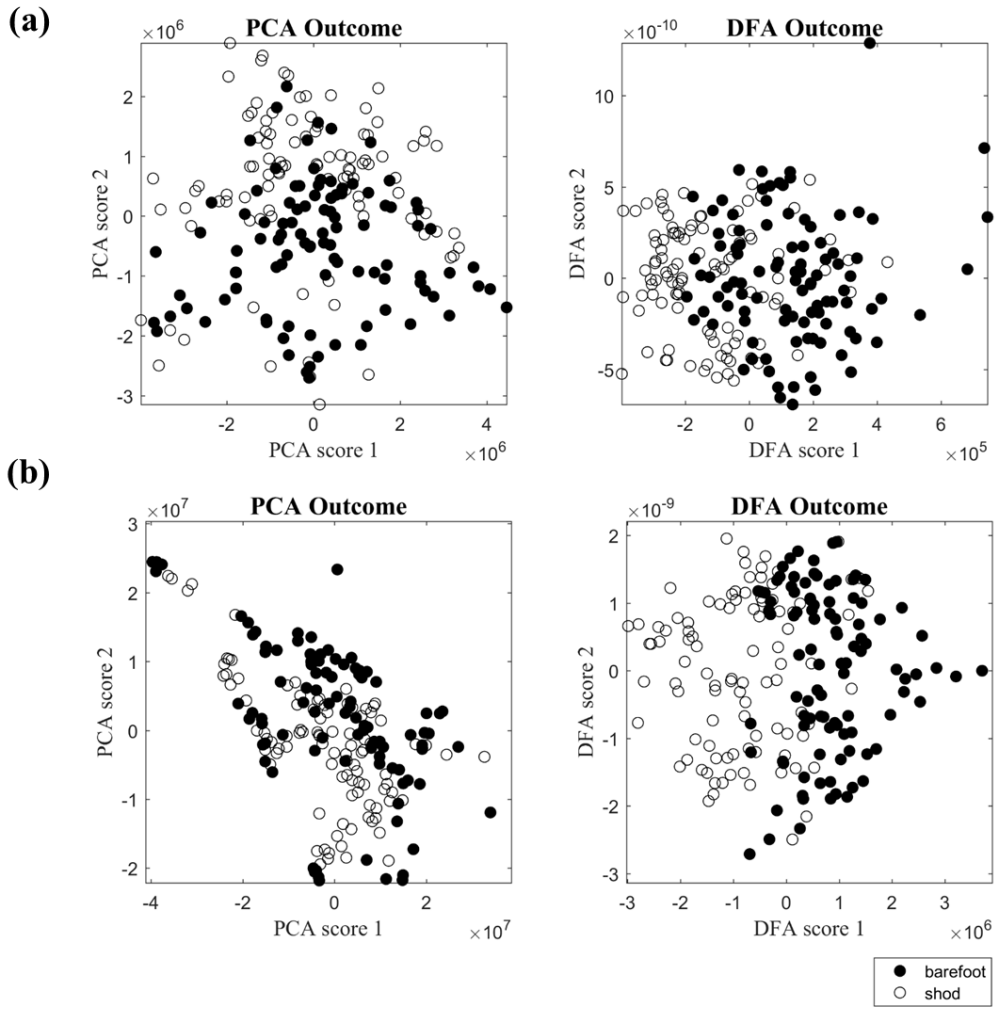

Figure 4.9 PCA (a) and DFA (b) without the first frequency component of the spectral analysis and PCA (c) and DFA (d) with the first frequency component of the spectral analysis.

4.4.3 Exploring Optimisation during Discrimination of a Multiple Class Problem

Investigating all possible iterations, as shod trials were considered as one cloud, and barefoot trials were considered multiple clouds, indicating the error rates of trials which could not be correctly classified ranged between 9% to 50%, with the majority identified to have had an error rate of 31% (Figure 4.10). Investigating all possible iterations, as barefoot trials were considered as one cloud, and shod trials were considered multiple clouds, indicating the error rates of trials which could not be correctly classified ranged between 31% to 50%, with the majority identified to have had an error rate of 50% (Figure 4.11).

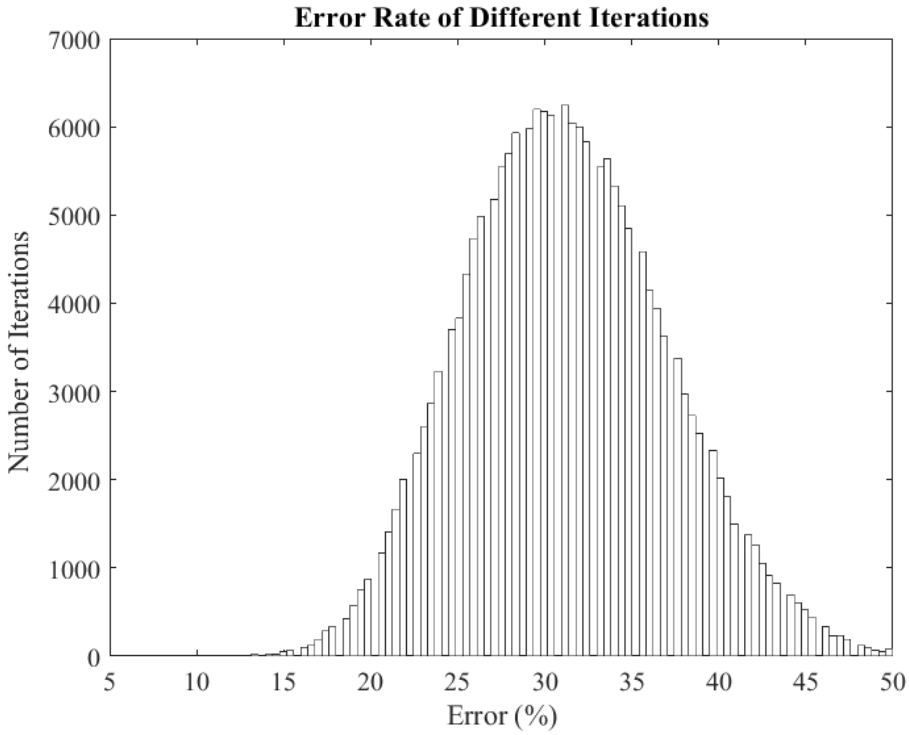

Figure 4.10 Histogram indicating the error rates of discrimination for each individual iteration during discrimination of one shod and multiple barefoot classes.

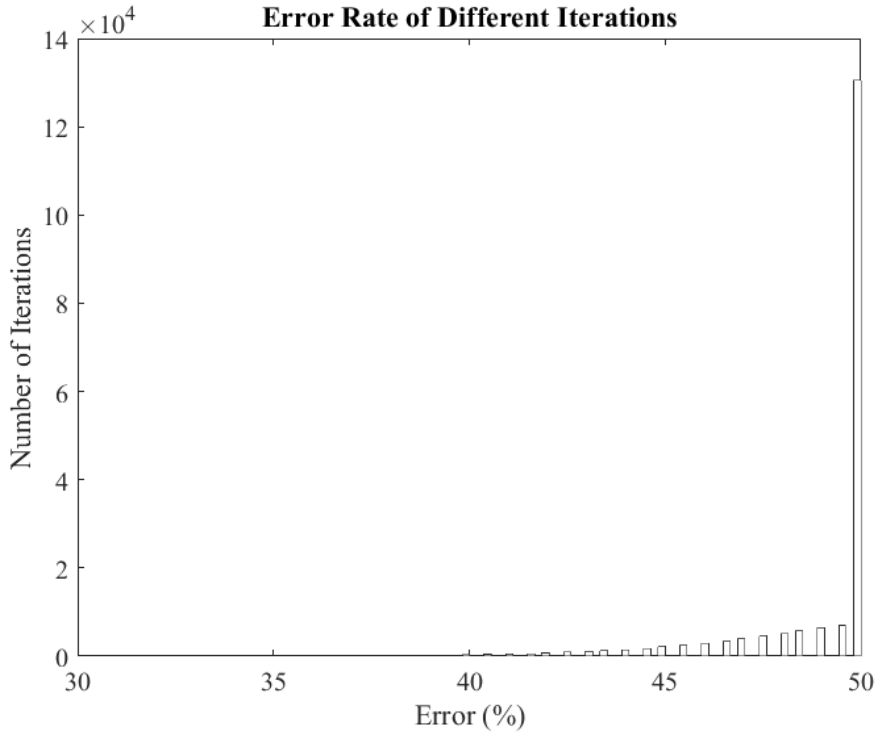

Figure 4.11 Histogram indicating the error rates of discrimination for each individual iteration during discrimination of one barefoot and multiple shod classes.

4.4.4 Exploring Optimisation during Discrimination of a Two-Class Problem

The outcome of all possible iterations, when comparing between two clouds, one corresponding to each condition, as shown in the histogram of Figure 4.12, indicated that the error rates of trials which could not be correctly classified ranged from 6.5% to 47.5%. The majority of iteration were identified to have an error rate of 22.5%. This clearly demonstrates how much the algorithm can be helped by the careful selection of the training database. As previously mentioned an iteration consisted of a different combination of 10 participants out of 20 for each the training and predicted database. The error is the percentage of trials that end up in the wrong category (shod or barefoot). The lowest error rate indicated the iteration with the strongest generic features and the highest predictive ability. Therefore, the iteration corresponding to 6.5% was used as the input for the optimised machine learning algorithm.

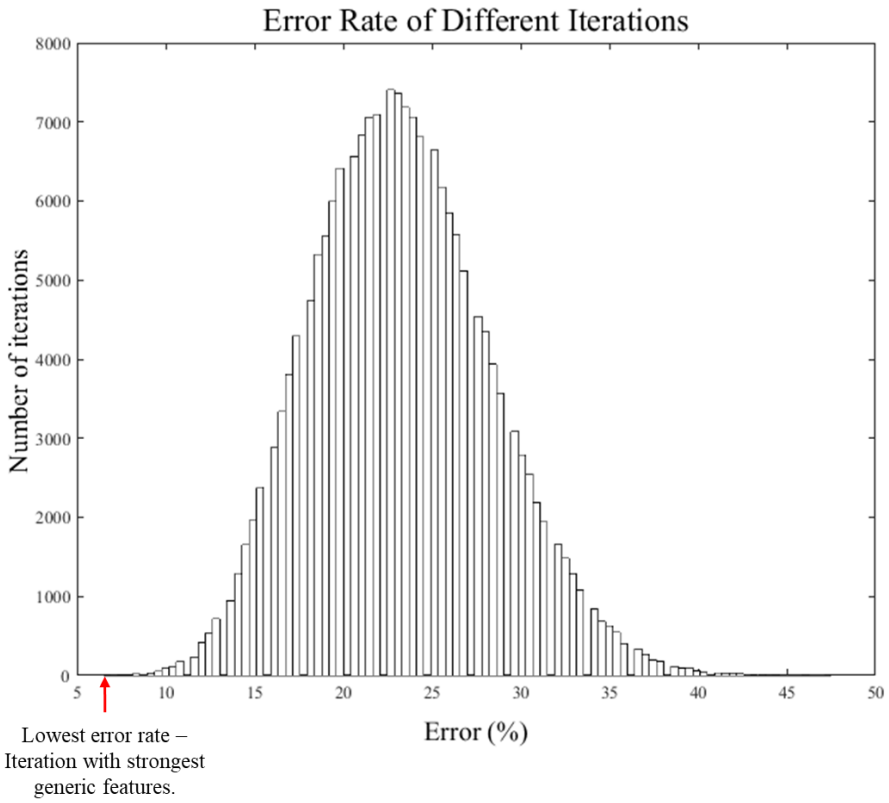

Figure 4.12 Histogram indicating the error rates of discrimination for each individual iteration during discrimination of barefoot and shod running as two separate clouds.

The optimum iteration was further used to identify the most discriminating features between the two experimental groups of barefoot and shod running using DFA. The different bar charts correspond to different DF curves were integrated over all spectral frequencies (full frequency-resolved DF curves are shown in Figure 4.13), where each bar represents a variable (Figure 4.14).

The fact that they are dissimilar justifies the benefit of undertaking the discrimination in two dimensions rather than one. The length of each bar emphasises the weight factors of individual kinetic and kinematic variables (averaged over all frequencies). Large and small bars represent a large and small contribution to the discrimination process, respectively. Since the analysis was conducted for thirty variables, there are thirty bars for each integrated DF curve. Variables corresponding to individual bars have been ordered, in decreasing order of contribution, and displayed in Figure 4.15.

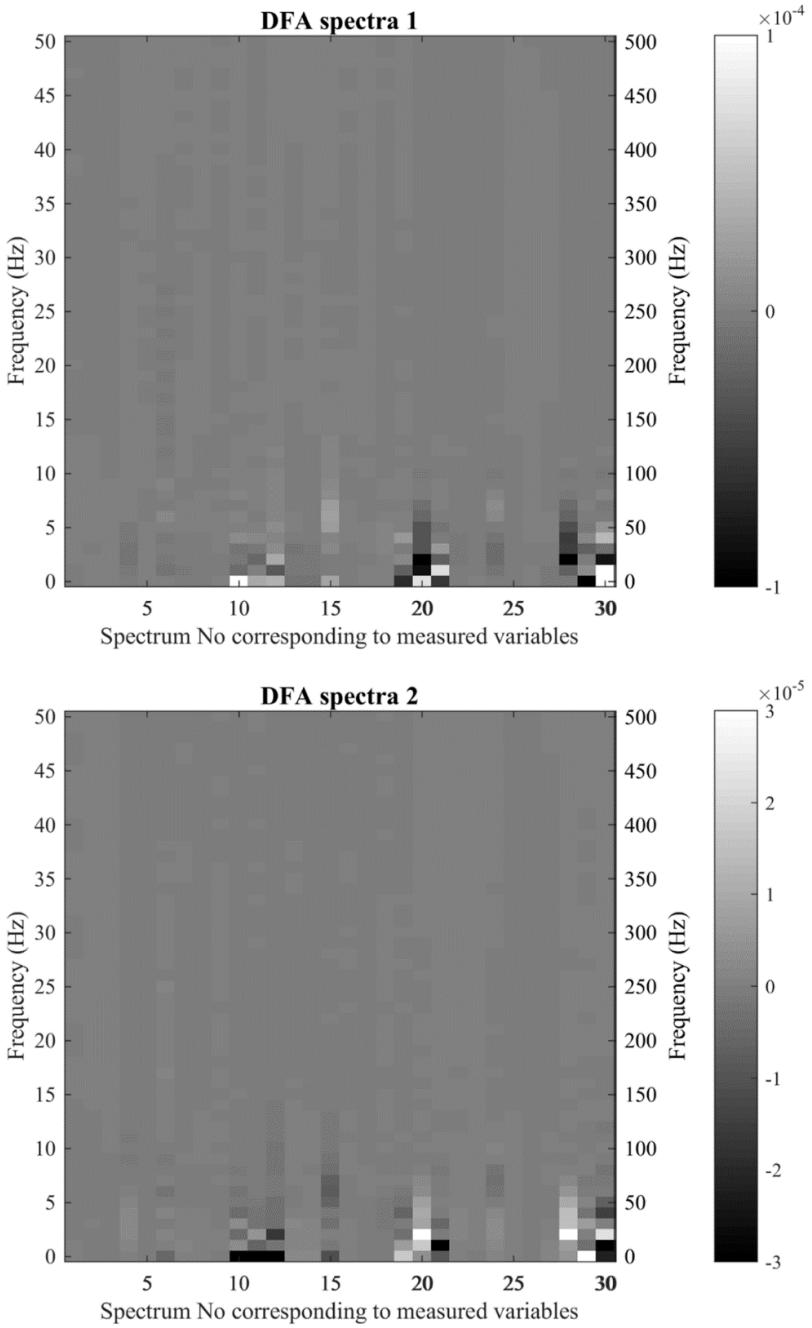

Figure 4.13 Full frequency-resolved DF curves.

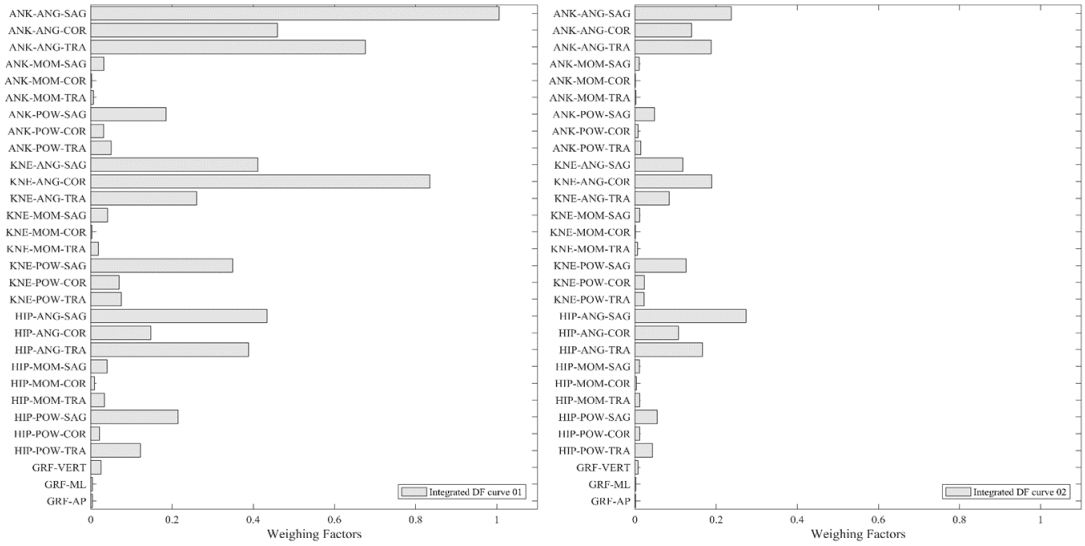

Figure 4.14 DFA discrimination is showing two bar charts where each bar is equivalent to a measured variable from a DF curve, integrated over all spectral frequencies. Abbreviations are knee (KNE), ankle (ANK), angle (ANG), moment (MOM), power (POW), anterior-posterior (AP), medio-lateral (ML) and vertical (VERT).

Rank	Integrated DF Curve 01 Variables	Integrated DF Curve 02 Variables
1	Ankle Angle in Transverse Plane	Ankle Power in Transverse Plane
2	Ankle Moment in Coronal Plane	Ankle Angle in Transverse Plane
3	Ankle Angle in Sagittal Plane	Ankle Moment in Coronal Plane
4	Ankle Angle in Coronal Plane	Ankle Angle in Sagittal Plane
5	Ankle Power in Transverse Plane	Ankle Power in Sagittal Plane
6	Ankle Moment in Transverse Plane	Ankle Angle in Coronal Plane
7	Ankle Power in Sagittal Plane	Hip Moment in Transverse Plane
8	Hip Moment in Transverse Plane	Ankle Moment in Transverse Plane
9	Ankle Moment in Sagittal Plane	Ankle Power in Coronal Plane
10	Hip Power in Transverse Plane	Ankle Moment in Sagittal Plane
11	Hip Angle in Transverse Plane	Hip Power in Transverse Plane
12	Ankle Power in Coronal Plane	Hip Angle in Transverse Plane
13	Hip Power in Sagittal Plane	Hip Power in Sagittal Plane
14	Hip Moment in Sagittal Plane	Hip Moment in Coronal Plane
15	Hip Moment in Coronal Plane	Hip Moment in Sagittal Plane
16	Hip Angle in Sagittal Plane	Hip Angle in Sagittal Plane
17	Knee Moment in Transverse Plane	Knee Moment in Transverse Plane
18	Knee Power in Transverse Plane	Hip Power in Coronal Plane
19	Knee Power in Sagittal Plane	Knee Power in Sagittal Plane
20	Knee Angle in Transverse Plane	Knee Power in Transverse Plane
21	Hip Angle in Coronal Plane	Knee Angle in Transverse Plane
22	Right Medial-Lateral GRF	Hip Angle in Coronal Plane
23	Hip Power in Coronal Plane	Right Medial-Lateral GRF
24	Knee Moment in Sagittal Plane	Knee Moment in Sagittal Plane
25	Knee Power in Coronal Plane	Knee Power in Coronal Plane
26	Knee Angle in Sagittal Plane	Knee Angle in Sagittal Plane
27	Right Anterior-Posterior GRF	Right Vertical GRF
28	Right Vertical GRF	Right Anterior-Posterior GRF
29	Knee Moment in Coronal Plane	Knee Moment in Coronal Plane
30	Knee Angle in Coronal Plane	Knee Angle in Coronal Plane

Low Contribution/ High Contribution

Figure 4.15 Measured variables in decreasing order of contribution to the discrimination process.

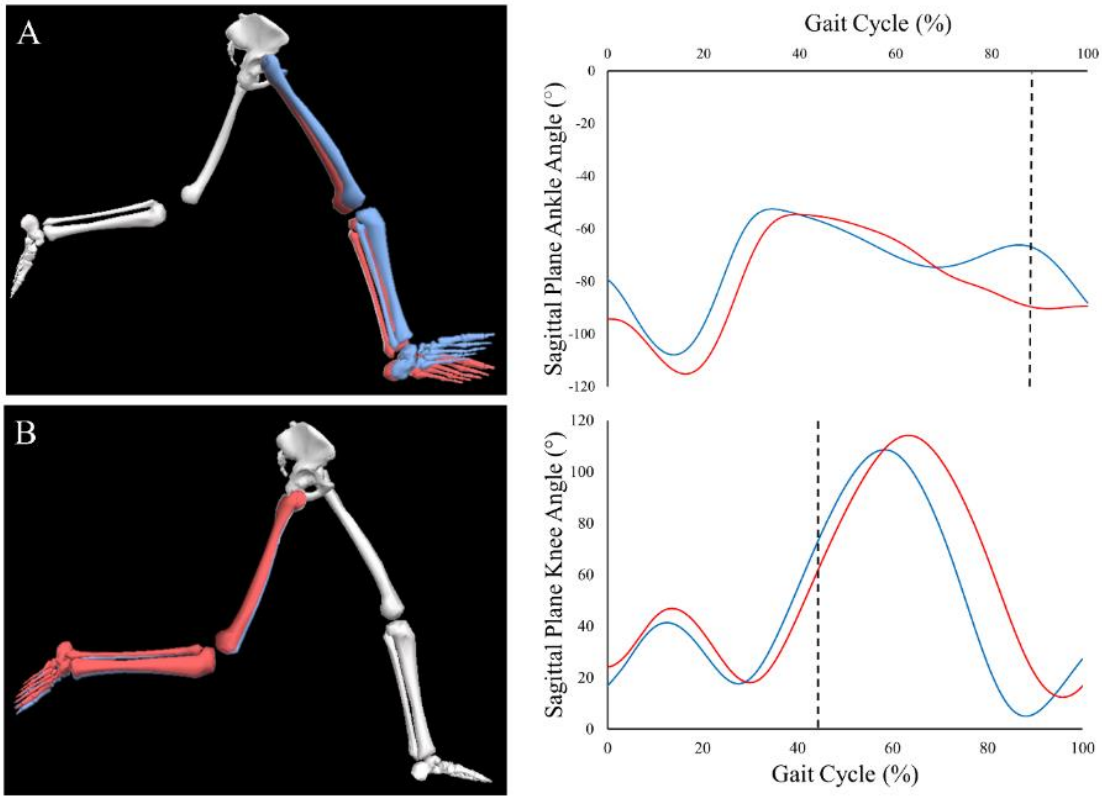

Figure 4.16 An illustrative representation of exemplary highly discriminating (A - sagittal plane ankle angle) and lower discriminating (B – sagittal plane knee angle) variables from a single participant during both shod (red limbs and lines) and barefoot (blue limbs and lines) running. Dashed lines represent the instance in the gait cycle that the illustrations are taken from.

High contribution variables included ankle angle and power in the transverse plane, ankle angle in the sagittal plane and ankle moment in the coronal plane whereas low contribution variables corresponded to knee angle and moment in the frontal plane, and medio-lateral and the anterior/posterior GRFs. An example of a highly discriminating, and a low discriminating variable is shown in Figure 4.16. The quality of the discrimination obtained with the optimised DFA is illustrated in Figure 4.17 and Figure 4.18. The quality of discrimination is evidenced by the minimal amount of overlap between the two conditions; two well-discriminated groups will not occupy the same space. The outcome of the training database alone, used to develop the algorithm is shown in Figure 4.17 (a). Once developed the predictive ability of the algorithm was assessed as illustrated in Figure 4.17 (b). It can be seen that even though there is a slightly greater scatter in the predictive outcome it does not compromise the quality of discrimination when the software was given a chance to be trained with the ideal training database, Figure 4.17 suggest that the computer was further able to correctly discriminate those individuals that have a rather ‘unique’ or ‘rare’ way to run shod and barefoot. Combining both the outcomes from the training database

and the predictive data (Figure 4.18), it is clear that both experimental conditions of barefoot and shod running were clustered in separate clouds which were shifted to the left and right side respectively, with minimal overlap between the two clouds and a slight vertical slant between the two centroids. The overlap were representative of 6.5% of the trials which could not be correctly discriminated, where 5% and 8% overlap represent predicted and training data, respectively. The discrimination occurs mostly horizontally with a slight angle indicating that the discrimination is mostly achieved through the DF score 1. Projection onto a higher dimensional space did not yield any significant discrimination. The classification evaluation reinforces these results and shows that sensitivity, i.e. true positives (shod and truly identified as shod) would be correctly identified in 90% of cases and specificity, i.e. true negatives (barefoot and correctly identified as barefoot) would be correctly identified in 91%.

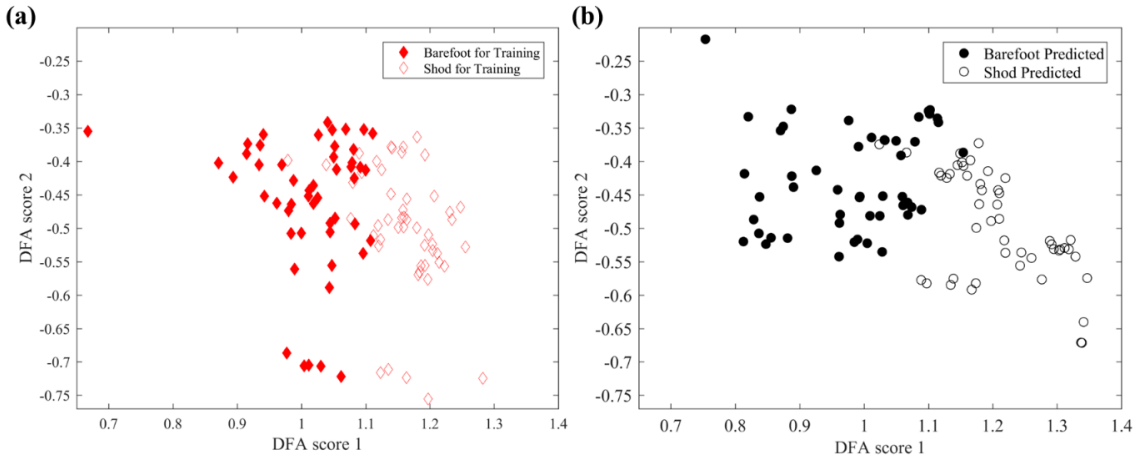

Figure 4.17 Outcome of training database (a) following discrimination, from the 10 participants with the smallest error in prediction. Outcome of discrimination for the 10 participants not used to generate the machine learning algorithm (b).

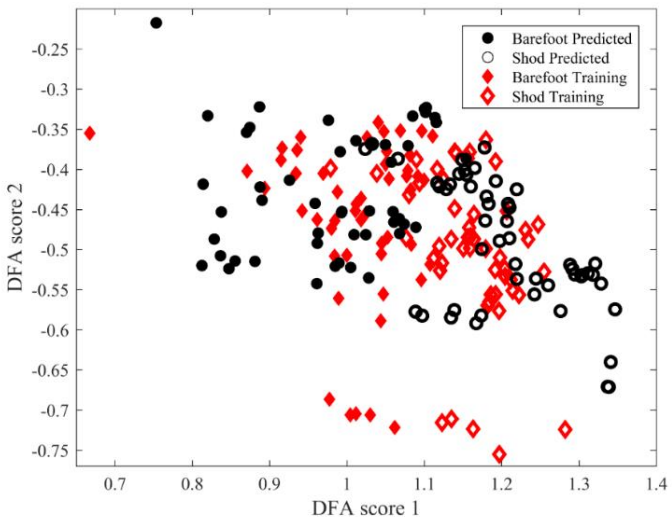

Figure 4.18 Combined display of trained and predicted data following discrimination.

4.5 Discussion and Conclusion

The aim of this study was to develop and optimise a machine learning algorithm using multivariate statistical analyses, PCA and DFA to process human locomotion. The optimisation was achieved by implementing an iterative process, where the individuals contributing to the training stage were systematically permuted, to explore all possible iterations of 10 participants out of 20. This allowed generic discriminating features to be identified between the two experimental conditions. The optimised algorithm yielded a large discrimination accuracy of 93.5%, typically 17.5 % higher than when using standard analysis.

Instead of using a cross-validation method to assess the training and predictive stage, in this study an optimisation process was developed. Previous studies have achieved large classification results however the quality of data used as a training database for the machine learning algorithms were not considered which in turn affects the reliability of their predictive outcome (Alaqtash *et al.*, 2011a; Begg & Kamruzzaman, 2005; Eskofier *et al.*, 2011; Federolf *et al.*, 2012; Kobsar *et al.*, 2015; Lemoyne *et al.*, 2015; Wu *et al.*, 2007; Phinyomark *et al.*, 2016). Factors affecting the reliability of an algorithm include data from an insufficient number of participants, i.e. too few participants. The classification results may be of great accuracy (Lemoyne *et al.*, 2015), however, the training sample may not be reflective of the generic features of a particular population, and thus the outcome may not necessarily be reliable. Using generic features to train the machine is more likely to accurately evaluate a new data set since the machine is familiar with common discriminating variables. In instances where the machine learning algorithm is facing the challenge of a mixture of highly 'generic' and highly 'singular' trials in its training database, it is suggested that by homing onto the highly generic individuals, at the stage of training the computer, substantial improvements may be achieved over the entire group, including the highly 'singular' individuals. High improvement in the software's performance was achieved by using half of the data for training, and the other half for prediction. The iterative process facilitated the identification of generic features in ten participants used for the training data. Thus, unlike other published work, the discrimination of this study is free from artefacts resulting from training the computer with trials carrying somewhat rare or unique information (Lever *et al.*, 2016a).

The relatively small group size of this study prevents an estimation to the extent to which accidental spurious information may also have been harvested in the process but limiting the process to only 10 PCA scores severely limits the likelihood of such phenomena. Since the chosen rank (10^{th}) was below the rank well below the one still carrying information (20^{th}) ensuring the numerical analysis was made immune to overfitting artefacts originating from the over-

exploitation of small details. An interesting question is whether it might be possible, in any study similar to this one, to identify the best group size to be used when optimising the training. Unfortunately, the extent to which specific volunteers provide a generic enough feature and the extent to which features of interest become spread between several PCA scores will depend on the particular study undertaken so that no general method can be recommended. A possibility to try and establish the best group size may be to use the iterative process of this study, in combination with a cross-validation method such as the leave-one-out method.

For studies with large numbers of participants, i.e. a sample size which a considered atypical in biomechanics, one way forward is perhaps to start by following this optimisation procedure with the same group sizes for training and predicting, and then further refine the collection of 'ideal' individuals by swapping one of the ten individuals with a new one to see whether improved discrimination could be obtained. This way the collection of 'ideal' generic individuals could gradually be further improved. Using a larger sample then presented in this study would provide the option to validate the machine learning algorithm since individuals who did not contribute to the training and prediction stages could be used. In such large studies, it is also possible to somewhat reduce the effect of a second possible source of overfitting artefact, that coming from (possibly high magnitude) information accidentally helping the clustering and therefore biasing it. It is possible to quantitate and minimise such overfitting artefacts (Lever *et al.*, 2016b) by splitting the individuals who did not contribute to the training into two groups respectively called 'evaluation' and 'test' sets. The trained algorithm can be optimised on the 'evaluation' set only, and those iterations are yielding a performance much lower on the 'test' set can be deemed as suffering from overfitting and dismissed. Unfortunately, such a method is not reliable on the relatively small group size of our study, and the high performance of the optimised outcome of our work suggests that we would have reached the same result if we had implemented it, as both 'evaluation' and 'test' sets would have benefitted from a similar performance.

The context of the experimental protocol influences the results of a discrimination since some experimental groups or conditions are easier to distinguish than others, in particular in instances where the two groups to be discriminated are necessarily formed from different individuals, e.g. young vs. older individuals, normal vs. pathological gait and males vs. females (Alaqtash *et al.*, 2011a; Begg & Kamruzzaman, 2005; Eskofier *et al.*, 2011; Federolf *et al.*, 2012; Kobsar *et al.*, 2015; Lemoyne *et al.*, 2015; Wu *et al.*, 2007; Phinyomark *et al.*, 2016). Thus in the development of this machine learning algorithm, the same heterogeneous sample of participants repeated both experimental conditions. This creates a more challenging environment when compared to having clearly discrete heterogeneous groups, e.g. healthy vs pathology, whose data is independent of

one another. Therefore, the outcome of the algorithm presented in this study was more likely to reflect the ability of the algorithm rather than experimental group differences.

Developing a machine learning algorithm using scalar quantities extracted from the waveforms of kinetic and kinematic variables (Alaqtash *et al.*, 2011a; Begg and Kamruzzaman, 2005; Phinyomark *et al.*, 2016; Wu *et al.*, 2007) could result in the dismissal of important temporal data, thus power spectra of full waveforms have been employed (Federolf *et al.*, 2012; Kobsar *et al.*, 2015; Reid *et al.*, 2010) since each individual feature provides complementary information (Ali & Shah, 2010). Scalar quantities have shown to result in high classification outcomes (Alaqtash *et al.*, 2011a; Begg and Kamruzzaman, 2005; Phinyomark *et al.*, 2016; Wu *et al.*, 2007), however, the outcome was highly sensitive to various factors of the discrimination procedure such as type of variables, e.g. kinematic or kinetic only, and conditions, e.g. more than two classes or groups (Schöllhorn *et al.*, 2002), since the complementary information of a full temporal waveform is missing, misclustering should be expected. In this study, the training database used to conduct a numerical search using PCA and DFA included the spectra of thirty full temporal waveforms of kinetic and kinematic variables for each trial thus the entire waveform of a variable was taken into consideration. The spectra data was used as the spectral analysis removes the phasing within the data, however this step is not needed since retrospectively it was established that the phasing in the data was removed by normalising temporal waveforms to 100% gait cycle.

Despite the use of sophisticated three-dimensional motion capture system, most studies limited the classification to data of the sagittal plane (Dobson *et al.*, 2007). However, in order to apply this type of data to clinical settings, three-dimensional data should be considered as done in this study since different planes of motion reveal additional information that will inform treatment or intervention. For example, during the assessment of the dynamic stability of individuals with LLA, it may be important to consider the frontal plane as it may help identify issues related to the medio-lateral direction.

In previous studies, ankle kinematic and kinetic variables such as plantar flexion (Lieberman *et al.*, 2010; Williams *et al.*, 2012) were shown to differ between barefoot and shod running gait (Braunstein *et al.*, 2010; Lieberman *et al.*, 2010; Williams *et al.*, 2012). Studies have also reported limited differences between barefoot and shod runners in GRFs (Divert *et al.*, 2005; Kerrigan *et al.*, 2009). Although not the specific focus of this study, the results of this study confirmed these findings, suggesting that these variables represent the key differences between shod and barefoot running gait. However, unlike previous research, the choice of variables selected in our study as an input to the machine learning algorithm were generic biomechanical features and were not

explicitly chosen, thus reducing researcher bias and reflecting the true ability of the algorithm to identify the generic discriminating features.

In order to develop a robust machine learning algorithm, three stages need to be conducted, the training, prediction and the evaluation phase (Lever *et al.*, 2016a; c). A significant limitation of this study is that the optimised machine learning algorithm was not evaluated using an independent sample. While 10 participants were used for training and the remaining 10 for predictions (testing) stages, by the time all iterations were covered, each participant was used both in stages. During the evaluation stage, the performance of the machine learning algorithm should be assessed using a truly independent test set, which was not involved in the training nor the predictive phase and whose classification outcome is not known to describe the model on unseen data. In this study, the evaluation was conducted on participants previously involved in the iterative process thus their classification outcome was known thus invalidating the evaluation outcome. However, the evaluations made for every model were on the 10 participants used for the predictive phase rather than the training phase.Therefore for future studies, an independent sample should be collected to evaluate the algorithm using a confusion matrix, i.e. accuracy, sensitivity and specificity, once trained and predictions have been made.

The development of the machine learning algorithm described has many important applications in both clinical and research settings. In clinical settings, it allows for a more comprehensive and consistent assessment process across patients by utilising a wider range of data whilst simultaneously eliminating researcher bias. Furthermore, since all discriminating features are identified, in both a clinical and research setting, it will prevent important factors being neglected and ensure accurate and reliable diagnosis. This will enable analysis methods to be more objective, consistent and reliable across institutions.

In conclusion, a machine learning algorithm, using PCA and DFA, was developed using power spectra of temporal waveforms to successfully identify barefoot and shod running gait. The predictive accuracy of the algorithm was optimised in a challenging environment by implementing an iterative process. All discriminating features between the two experimental groups were identified, and a strong machine learning algorithm was developed with a 93.5% accuracy in discriminating between conditions. This method can be implemented, to find informative features when the sample size is small and heterogeneous, as common during gait analysis and in clinical settings during the treatment of a particular patient.

Chapter 5: Identifying Gait Differences between Individuals with Unilateral Trans-Tibial Amputation and Able-Bodied Individuals.

5.1 Introduction

Gait analysis facilitates better treatment of pathological gait (Kirtley, 2006; Levine *et al.*, 2012). Using machine learning algorithms as automatic recognition tools during gait analysis can enhance subject-specific treatment methods enabling a comparison between pathological and able-bodied gait using non-invasive, quantitative methods (Alaqtash *et al.*, 2011b; Lakany, 2008). Automatic gait recognition tools enable discimination and classification of data. In clinical settings, machine learning algorithms have demonstrated the ability to classify pathologies correctly that were initially misclassified by specialists (Lakany, 2008). Thus, these algorithms provide automatic and objective methods for clinicians to use that are also quick and cost-effective (Alaqtash *et al.*, 2011a; Lakany, 2008; Simon *et al.*, 2016). The benefits of machine learning algorithms in gait rehabilitation include the ability to model complex non-linear relationships of gait data and incorporate multi-dimensional data (Figueiredo *et al.*, 2018). The ability to add new data to the machine learning algorithm means its performance can be continously improved and thus its predictive performance is also improved (Figueiredo *et al.*, 2018).

Through research, it has been suggested that multiple different variables such as temporal-spatial parameters, kinetic, kinematic and muscle activation data, should be incorporated to carry out an extensive gait analysis procedure (Figueiredo *et al.*, 2018). Since pathological gait is heterogeneous and treatment varies among patients, no machine learning algorithm fits all applications and analysis procedures, but instead, the best performing algorithm depends on the features of a data set (Harper, 2005). A good gait recognition tool should provide an accurate classification and insights into the predictive structure of the data (Breiman, 1984).

In LLA gait, machine learning algorithms have mainly been used to investigate powered prosthetic devices (Afzal *et al.*, 2017; Chen *et al.*, 2013; Dutta *et al.*, 2011; Hargrove *et al.*, 2015; Huang *et al.*, 2011; Joshi & Hahn, 2016; Khan *et al.*, 2018; Miller *et al.*, 2013; Pew & Klute, 2017; Simon *et al.*, 2016; Woodward *et al.*, 2016; Young *et al.*, 2013; Young *et al.*, 2014; Zheng *et al.*, 2013; Zheng & Wang, 2017). Although the investigations of prosthetic devices are important, in the first instance, individuals who can benefit from these devices need to be identified. For this to be feasible, multivariate statistical analyses and machine learning algorithms can be implemented as diagnostic tools to assess and understand LLA gait.

The majority of the studies that used automatic gait recognition tools during the investigation of LLA gait have focused on biomechanical gait variables recorded from wearable sensor systems such as footswitches and accelerometers (Taborri *et al.*, 2016). Recent advances in technology

make these sensors smaller, lightweight and easier to put on and off. Furthermore, these sensors allow measuring variables in free-living conditions which can be advantageous in the advancement of robotic or powered therapies (Afzal *et al.*, 2017; Chen *et al.*, 2013; Dutta *et al.*, 2011; Hargrove *et al.*, 2015; Huang *et al.*, 2011; Joshi & Hahn, 2016; Khan *et al.*, 2018; Miller *et al.*, 2013; Pew & Klute, 2017; Simon *et al.*, 2016; Woodward *et al.*, 2016; Young *et al.*, 2013; Young *et al.*, 2014; Zheng *et al.*, 2013; Zheng & Wang, 2017). Although wearable sensors have advantages, using non-ambulatory external sensors such as motion capture-systems or force platforms can provide more detailed information. These systems operate in a controlled environment (Sabatini *et al.*, 2005), which is occasionally considered a disadvantage since it can be challenging to obtain consecutive gait cycles for long-term applications in a natural environment (Alahakone *et al.*, 2010; Azhar *et al.*, 2014). However, the accuracy of these systems cannot be underestimated, as they provide comprehensive and reliable biomechanical data (Bamberg *et al.*, 2008; Howell *et al.*, 2012).

In order to improve prosthetic rehabilitation, the differences between LLA and able-bodied gait needs to be better understood. Some studies described LLA function using multivariate statistical analyses such as PCA (Detrembleur *et al.*, 2005; Gao and Zhang 2013; Mouchnino *et al.*, 2006). Trying to quantify symmetry, Gao and Zhang (2013) used PCA to identify important variables during a sit-to-stand and stand-to-sit task in an individual with UTFA. Measuring kinematic, kinetic and muscle activity, they were able to identify which variables were important during this task. Soares *et al.* (2016) used PCA to investigate whether GRF and CoP data of individuals with UTFA and able-bodied individuals can be discriminated. They report that using the first three principal components (PCs), between 74.5 - 93.9% variance of the data can be explained. The ability to compare between LLA and able-bodied gait to find differences, can assist decision-making processes during prosthetic rehabilitation. Therefore, the aim of this study was to establish differences between UTTA and able-bodied gait using PCA and DFA providing a better understanding of LLA function.

5.2 Methodology

5.2.1 Participants

A convenience sample of eleven individuals with UTTA (age 50±12years; height 1.7±0.1m; mass 83.94±13.59kg) and thirty able-bodied individuals (age 39±20years; height 1.7±0.1m; mass 73.76±14.02kg) were recruited from the university and local communities. All participants met the inclusion and exclusion criteria detailed in Section 3.2.2. Ethical approval was granted by the Nottingham Trent University's College of Science and Technology Ethical Review Committee (Humans), the NHS Research Ethics Committee, the NHS Health Research Authority and the NHS Research and Development. All participants provided written informed consent prior to participation.

5.2.2 Experimental Design and Data Acquisition

The study investigated individuals with UTTA and able-bodied individuals at self-selected walking speed. Upon arrival, the participants were briefed. All activities were completed with participants wearing lycra shorts and everyday shoes. Individuals with UTTA used their habitual prosthesis (Table 3.1). To obtain kinematic measurements 70 spherical 14mm, reflective markers were placed directly onto the skin or clothing using bi-adhesive tape, defining head, arms, trunk (Leardini *et al.,* 2011) and lower limb segments (Cappozzo *et al.*, 1995) (for marker placement, refer to Section 3.3.3). Marker placement on the prosthetic limb was estimated depending on marker placement of the intact limb (Powers *et al.,* 1998).

A static trial was obtained for segment definition, followed by the dynamic trials. First, the participant's starting position was defined, to ensure that force platform data was obtained as the participant walked along the walkway. During dynamic trials, participants walked at a self-selected speed along a 15m walkway. This process was repeated until five successful trials were collected for both limbs, where GRF was measured at 1000Hz using a single floor-mounted strain gauge force platform (AMTI, Watertown, MA, USA) and kinematics were measured at 100Hz using a nine-camera motion capture system (Qualisys, Gothenburg, SE). A successful trial was defined by a clear force plate contact.

5.2.3 Data Processing

Markers were labelled in QTM v2.2 (Qualisys, Gothenburg, SE) as defined in Section 3.3.3. and trial start and end periods were adjusted to one gait cycle of each limb starting at heel strike on the force platform. Marker trajectories and force data were exported as .c3d files and subsequently

processed in Visual3D v5 (C Motion, Inc., Germantown, MD, USA). Kinematic data were interpolated using a cubic-spline algorithm with kinematic and GRF data being subsequently filtered using 4th order, zero-lag Butterworth low-pass filters with 6Hz and 30Hz cut-off frequencies, respectively. All data were normalised to one gait cycle. Medial and lateral landmarks defined anatomical frames from which segment coordinate systems were defined following the right-hand rule (Cappozzo *et al.*, 1995). A flexion-extension, abduction-adduction and longitudinal Cardan rotation sequence was used to define the order of rotations to calculate joint kinematics. Gait events of heel strike and toe off were determined using kinetic and kinematic event detection algorithms (Stanhope *et al.*, 1990; Zeni *et al.*, 2008) (Section 3.3.5). Twenty seven biomechanical variables which are typically reported in the literature for forward progression and dynamic stability were included in the analysis (Table 3.25 and Table 3.26) since the continuous interchange between mobility and stability are essential for efficient walking (Lakany, 2008). The biomechanical variables were computed in Visual3D (C-Motion, Inc, Germantown, USA). Processed data were exported from Visual3D as .c3d files, and individual signals were imported to MATLAB® R2016a (MathWorks Inc., MA, USA) for further analysis.

5.3 Multivariate Statistical Analysis

5.3.1 Principal Component Analysis and Discriminant Function Analysis Comparing UTTA and Able-Bodied Gait

Principal Component Analysis (PCA) and Discriminant Function Analysis (DFA) were successively applied to compare the gait of a group of eleven individuals with UTTA with a group of thirty able-bodied individuals. PCA was used for data reduction and feature selection, whilst DFA was used for the classification. Twenty temporal gait waveforms (Table 3.25) and seven scalar values (discrete parameters) (Table 3.26) were reported for each limb, i.e. the prosthetic limb (PROS) and intact limb (NONPROS) of the individuals with UTTA, and the control limbs (RIGHT and LEFT) of the able-bodied individuals. Different methods were explored (Figure 5.1) to establish the most suitable technique to compare between UTTA and able-bodied gait.

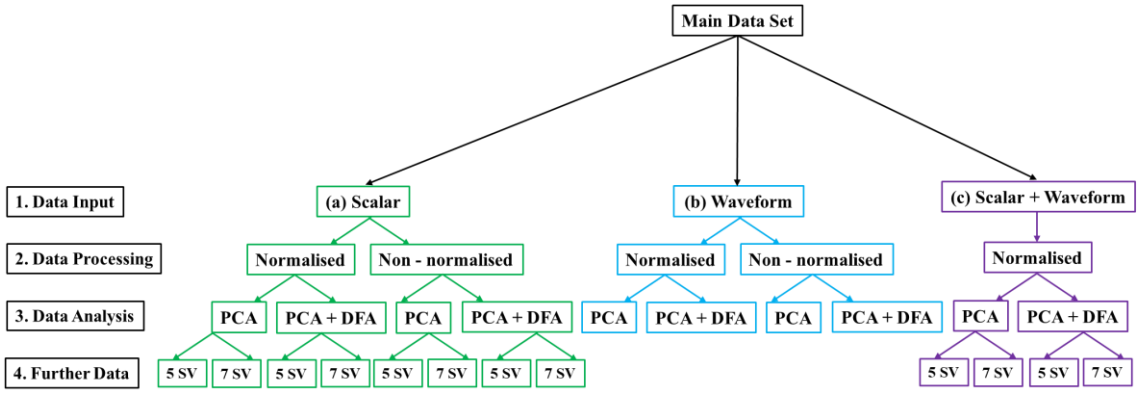

Figure 5.1 Investigative approach to establish a technique for the comparison between UTTA and able-bodied gait. Abbreviations are Principal Component Analysis (PCA), Discriminant Function Analysis (DFA), scalar values (SV).

First, the form of input data was considered i.e. scalar values (Figure 5.1 a), temporal waveform (Figure 5.1 b) or both scalar values and temporal waveforms together (Figure 5.1 c). Second, the version of input data was considered i.e. normalised or not normalised. This has been investigated because the different scaling and weighting of variables influence the outcome. Using the covariance matrix variables' weightings depend on the range of their magnitude. In biomechanics, a variable's typical magnitude may simply be based on the joint that it is derived from, some joints move through a small ROM and others through a large ROM, some are driven by small muscle groups others by large. Therefore, investigating the difference between joints may incur bias if the difference between the two groups is based on the absolute magnitude. The normalisation accounted for the variable's units, i.e. variables with the same unit were processed as a group and scaled to their specific maximum value. Thus, the using the covariance matrix the variables contribute equally, irrespective of their units, but the range of magnitude variation of a variable is retained. Third, PCA or a combination of PCA followed by DFA was considered and applied to the data. Lastly, the number of scalar values included during the analysis varied, to evaluate if additional scalar values could improve the outcome, i.e. either five biomechanical variables (step length, step frequency, ankle net-work, BW and ML MOS), or seven (including walking speed and step width) were comprised during the analysis. The five scalar values were calculated separately for each limb, whilst speed and step width were collected for the individual rather than for each limb. Speed was defined by stride time and length. To perform the analysis using two additional variables, speed and step width, the input arrays of both limbs included each of these variables so that there would be no bias due to an uneven number.

In this analysis, no power spectrum was applied to the data, as results from the previous study presented in Chapter 4, showed that it did not improve the discrimination outcome since the phasing in the data was removed by the normalisation of temporal waveforms to 100% gait cycle, done in Visual3D. Depending on the input data, i.e. temporal waveform, scalar values, or both, the input matrix *M* varied. For the temporal waveforms of each subject, one mean trial was made of 20 columns with 101 row vectors, where each column represented a variable and each row vector represented a data point in the normalised gait cycle. The original 3D input matrix *M*, for the individuals with UTTA, was 101 x 20 x 11 points for either the prosthetic or the intact limb. For the able-bodied individuals, the original 3D input matrix was 101x 20 x 30 for the right or the left limb. The third dimension represented the number of people, where one group was made up of eleven individuals with UTTA and the other group was made up of thirty able-bodied individuals. In 2D, the matrices were rearranged to 2020 x 82 points since each of the participants' limbs was considered separately. After applying PCA, this matrix was reduced to 82 x 82 points. For the scalar values, the original input matrix *M* was 5 x 82 or 7 x 82, depending on the number of scalar values. The numerical analysis was made somewhat immune to overfitting artefacts (originating from the over-exploitation of small details) by choosing the highest explored PC rank to be 10 for temporal waveforms (Figure 5.2 (a)) and 2 for scalar values (Figure 5.2 (b)). Figure 5.2 illustrates the decay of variance with the PC scores in an exponential-like decreasing curve, which indicates the information contained within each PC score. As described in Chapter 4, when a plateau is reached in the data, the content is mainly noise, and the PC scores beyond this point bring no meaningful information in the analysis.

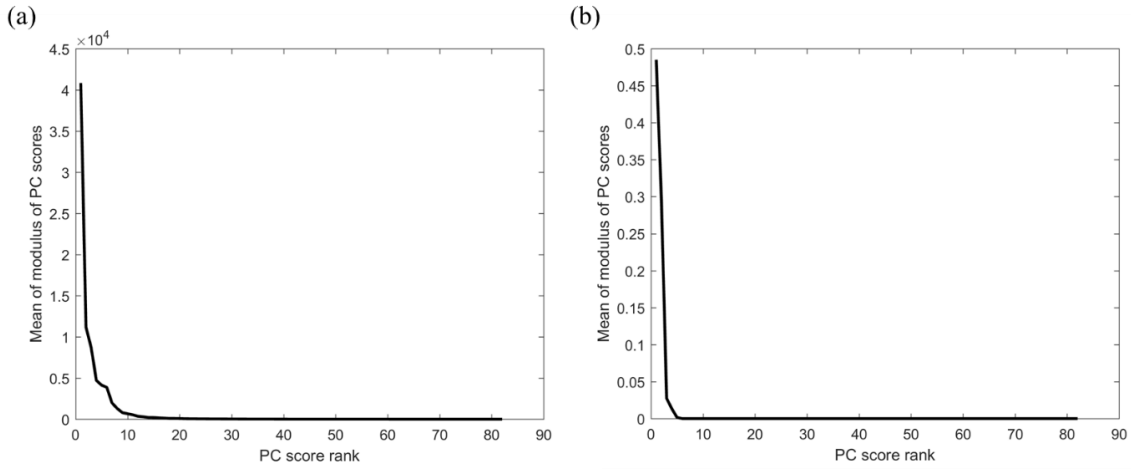

Figure 5.2 PCA ranking for temporal waveform data (a) and five scalar values (b).

5.4 Results

The overall results indicated that the prosthetic and intact limbs of the individuals with UTTA differed from the control limbs of the able-bodied individuals. Exploring different methods implied that for this application, PCA on temporal waveforms which were normalised to units provided the best outcome. The overall results are shown in Table 5.1, where in column 1 the type of data is described, i.e. temporal waveforms (a), scalar values (b) or the combination of both (c). Column 2 shows the PC holding the discriminating factors and which of the limbs differed in that dimension. Column 3 describes the main variables causing the difference between the two groups, whilst column 4 describes the DFA outcome and which limbs were clustered here, and column 5 describes the variables that caused the separate clusters in DFA.

Table 5.1 PCA and DFA outcomes of all analyses including the variables responsible for the differences and classification identified by the Eigenspectra and DF spectra, respectively.

Type of data	PCA	Variables responsible for difference	DFA	Variables responsible for classification
Not norm temp wave	PROS limb in PC2	sagittal hip joint ang sagittal knee joint ang sagittal ankle joint ang	No clustering	-
Norm temp wave	Both groups in PC2	vertical GRF sagittal hip joint mom sagittal knee joint ang	Both groups, and PROS and NONPROS separately	ML GRF vertical GRF sagittal knee joint ang
Not norm 5 SV	No difference	-	No clustering	-
Norm 5SV	PROS limb in PC1	ankle net-work ML MoS	PROS limb	ankle net-work ML MoS
Not norm 7 SV	No difference	-	No clustering	-
Norm 7 SV	PROS limb in PC1	speed ankle net-work ML MoS	PROS limb	speed ankle net-work ML MoS
Norm temp wave and 5 SV	Both groups in PC2	vertical GRF sagittal hip joint mom sagittal knee joint ang sagittal ankle joint ang ankle net-work ML MoS	Both groups, and PROS and NONPROS separately	ML GRF vertical GRF sagittal knee joint ang speed ankle net-work ML MoS
Norm Temp wave and 7 SV	Both groups in PC2	vertical GRF sagittal hip joint mom sagittal knee joint ang sagittal ankle joint ang speed ankle net-work ML MoS	Both groups, and PROS and NONPROS separately	ML GRF vertical GRF sagittal knee joint ang speed step length ankle net-work ML MoS

Abbreviations are intact limb (NONPROS), ground reaction force (GRF), margin of stability (MoS), angle (ang), medio-lateral (ML), moment (mom), normalised (norm), principal component (PC), prosthetic limb (PROS), scalar values (SV), temporal waveforms (temp wave).

5.4.1 Analyses of Normalised and Non-Normalised Temporal Waveforms

The PCA outcome is shown in four different views, where each view is between two dimensions and a dimension is a PC. The PCA outcome of the temporal waveform data without normalisation displayed no difference between the UTTA (red diamonds) and able-bodied (black circles) gait, as reflected by the lack of separation between the two clouds (Figure 5.4 a). Between PC1 and PC2 (outcome number 1), and the PC2 and PC3 (outcome number 3), the prosthetic limb (solid red diamonds) clustering at the edge of the remainder of the cloud that consisted of NONPROS (open red diamonds) and control limbs (open and solid black circles), indicating that the PROS limb differs from other limbs in PC2. The Eigenspectrum of PC2 for the temporal waveforms highlighted variables number 17, 20 and 14 (Figure 5.4 b), which corresponded to sagittal knee, ankle and hip joint angles.

The PCA outcome of temporal waveforms which were normalised to units (Figure 5.4 c) showed a difference between the gait of individuals with UTTA (red diamonds) and able-bodied individuals (black circles) in PC2 (outcome number 1 and 3) as reflected by the separation of clouds with a minimal overlap between the clusters of the groups. In outcome number 1, the groups separated horizontally, i.e. to the top and bottom of the graph and in outcome number 3 they separated vertically, i.e. to the right and left of the graph. These results also indicate that the factors responsible for the difference are held in PC2. The Eigenspectrum of PC2 for the temporal waveforms highlighted variables number 3, 17 and 13 (Figure 5.4 d), which corresponded to vertical GRF, sagittal knee joint angle and sagittal hip joint moment, respectively. The differences in the temporal waveform profile of the vertical GRF between limbs is shown in Figure 5.3.

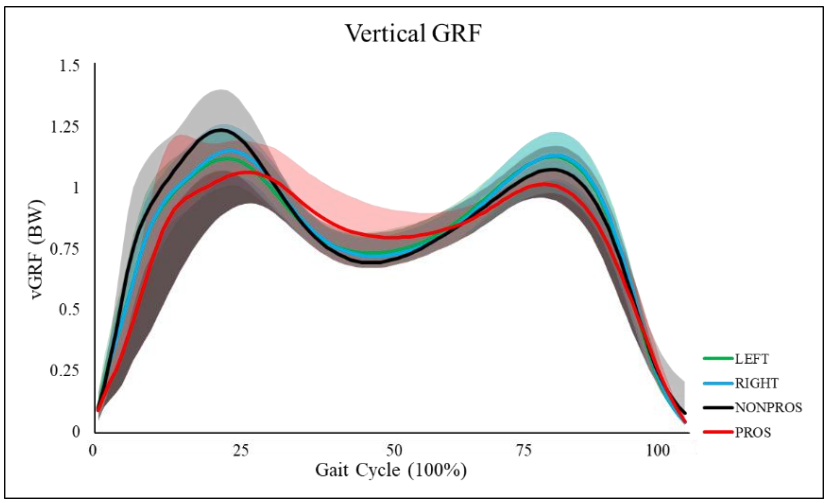

Figure 5.3 The mean ± SD of the vertical GRF temporal waveform profile of the lower-limbs of individuals with UTTA (PROS and NONPROS) and able-bodied individuals (RIGHT and LEFT).

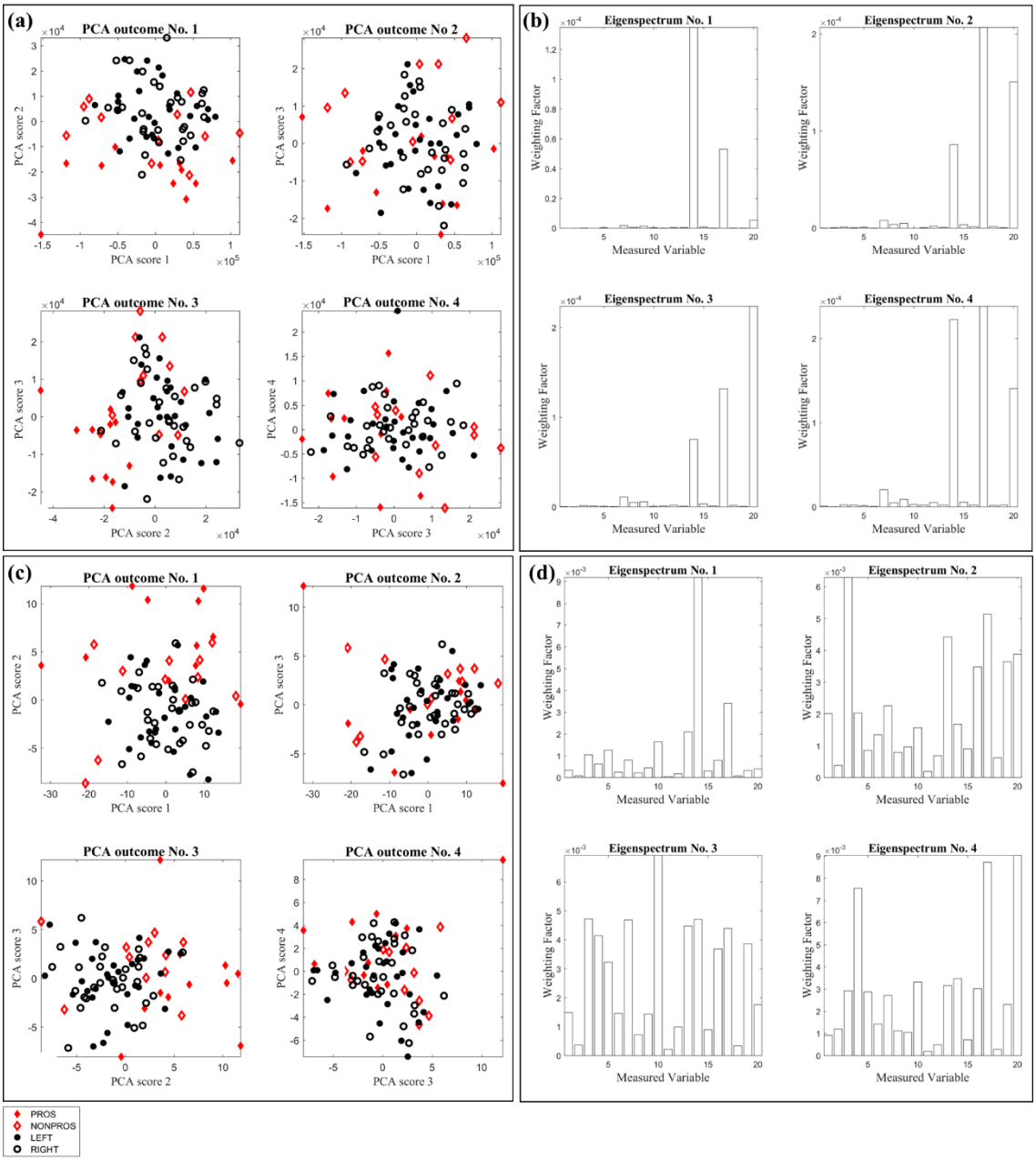

Figure 5.4 PCA outcome (a, c) and Eigenspectrum (b, d) comparing between individuals with UTTA and able-bodied individuals using temporal waveforms without (a, b) and with normalisation to units (c, d).

There was no separation between the red diamond and black circles in the DFA outcome indicating that there was no clear classification between the gait of individuals with UTTA (red diamonds) and able-bodied individuals (black circles) when the temporal waveforms were not normalised to units (Figure 5.5 a). The limbs of both groups are aligned next to each other and overlapping at a slight diagonal. The DFA outcome of the temporal waveforms, which were normalised to units (Figure 5.5 c) showed a classification between the limbs of the individuals with UTTA and able-bodied individuals. Furthermore, it showed a classification between the PROS limb (solid red diamonds) and NONPROS limb (open red diamond) which were clustered separately.

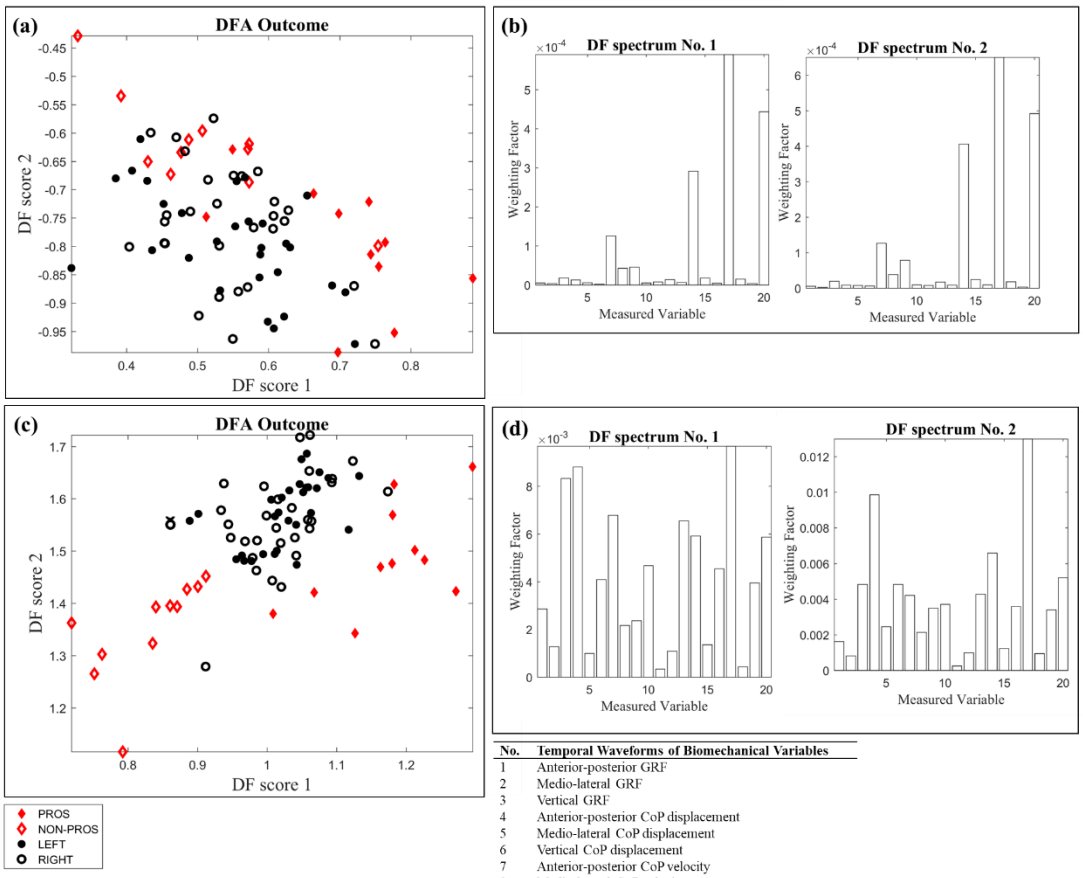

No.	Temporal Waveforms of Biomechanical Variables
1	Anterior-posterior GRF
2	Medio-lateral GRF
3	Vertical GRF
4	Anterior-posterior CoP displacement
5	Medio-lateral CoP displacement
6	Vertical CoP displacement
7	Anterior-posterior CoP velocity
8	Medio-lateral CoP velocity
9	Vertical CoP velocity
10	Vertical CoM displacement
11	Vertical CoM velocity
12	Sagittal hip joint power
13	Sagittal hip joint moment
14	Sagittal hip joint angle
15	Sagittal knee joint power
16	Sagittal knee joint moment
17	Sagittal knee joint angle
18	Sagittal ankle joint power
19	Sagittal ankle joint moment
20	Sagittal ankle joint angle

Figure 5.5 DFA classification outcome (a, c) and DF spectrum (b, d) between individuals with UTTA and able-bodied individuals using temporal waveforms without (a, b) and with normalisation to units (c, d). In the DF spectrum, each bar is equivalent to a measured variable from a DF curve, integrated over all spectral frequencies.

The DFA analysis was conducted in two dimensions. Similar to the study 1 described in Chapter 4, the DF spectra are dissimilar thus justifying the benefits to undertake the discrimination in two dimensions rather than one (Figure 5.5 b and d). The length of the bar emphasises the weight factors of the 20 individually measured variables presented in the table included in Figure 5.5. Large and small bars represent a large and small contribution to the discrimination process, respectively. The DFA outcome of temporal waveform data which was not normalised, did not classify the data thus the DF spectra did not provide any information regarding important features (Figure 5.5). The DF spectrum of the temporal waveforms which were normalised to units, however, highlighted variables number 17 and 3 (Figure 5.5 d) which corresponded to sagittal knee joint angle and vertical GRF, respectively.

5.4.2 Analyses of Five and Seven Normalised Scalar Values

The scalar values were normalised to units since previous results of the temporal waveforms demonstrated that normalisation was required to obtain accurate results. For further analysis of the scalar values without normalisation see Appendix 2. The PCA outcome of the scalar values with normalisation to units showed that the PROS limb (solid red diamonds) differed compared to the other limbs (NONPORS limb = open red diamonds, LEFT limb = closed black circle, RIGHT limb = open black circle) (Figure 5.6). The PROS limb formed a cluster at the edge of the remainder of cloud in PC1 (outcome number 1 and 2) (Figure 5.6 a). Repeating the PCA analysis with an additional two scalar values of speed and step width, did not improve clustering outcome (Figure 5.6 c). However, speed was identified as a discriminating factor as can be seen in the Eigenspectrum (Figure 5.6 d). Ankle joint net-work and ML MoS were also identified as discriminating variables between the PROS limb, and other limbs (Figure 5.6 b and d).

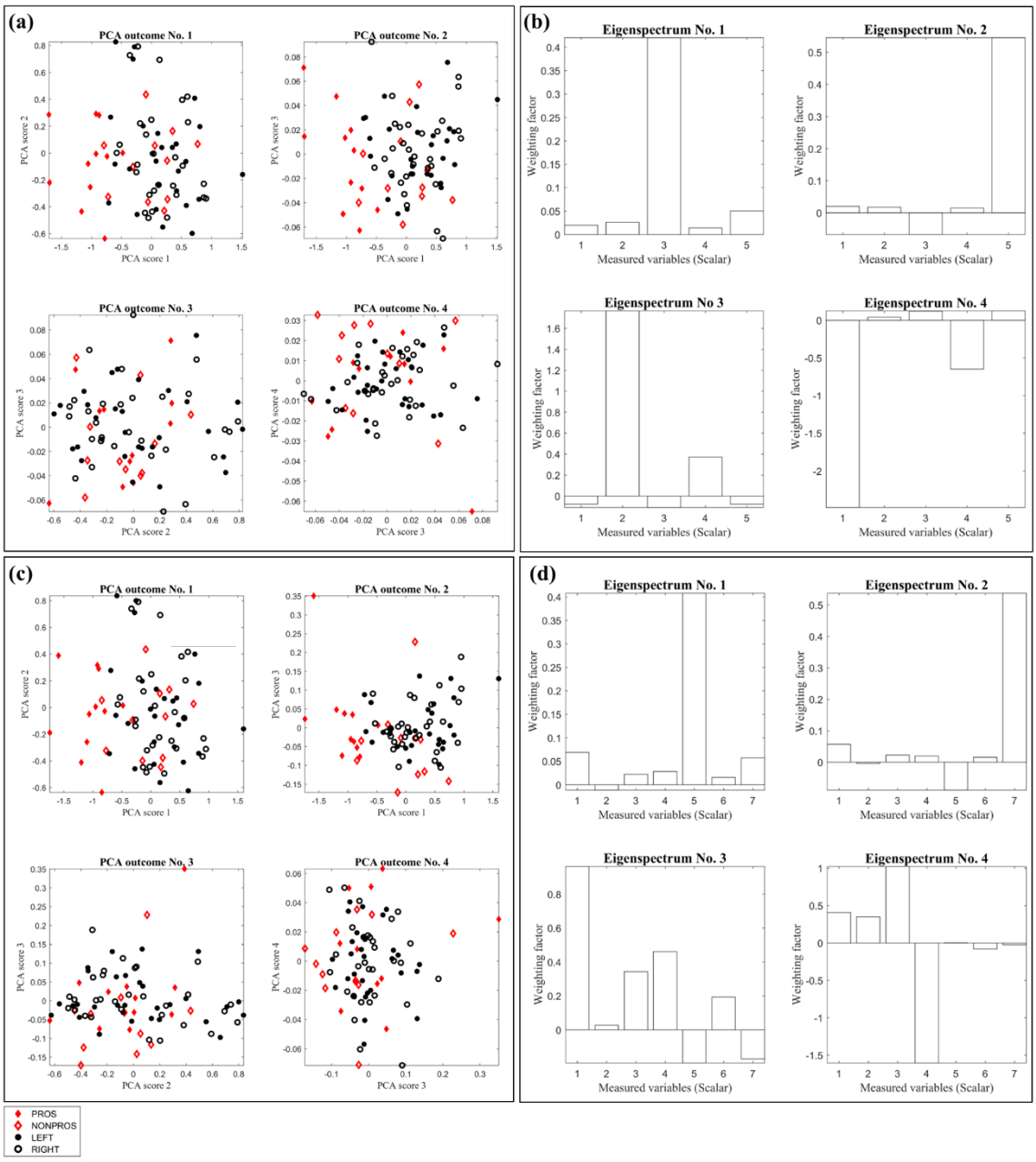

Figure 5.6 PCA outcome (a, c) and Eigenspectrum (b, d) comparing between individuals with UTTA and able-bodied individuals using five (a, b) and seven scalar values (c, d), normalised to units.

The DFA outcome for both five (Figure 5.7 a) and seven (Figure 5.7 c) scalar values, showed that the PROS limb (solid red diamonds) was classified from the remainder of the other limbs (NONPORS limb = open red diamonds, LEFT limb = closed black circle, RIGHT limb = open black circle). The discrimination of scalar values using a supervised algorithm did not improve the classification outcome but similar to the PCA outcome, speed was identified as a discriminating feature (Figure 5.7 d). Furthermore, similar to the Eigenspectra, the DF spectra highlighted ankle net-work and ML MoS to cause the classification between the PROS limb and remainder of the limbs (Figure 5.7 b).

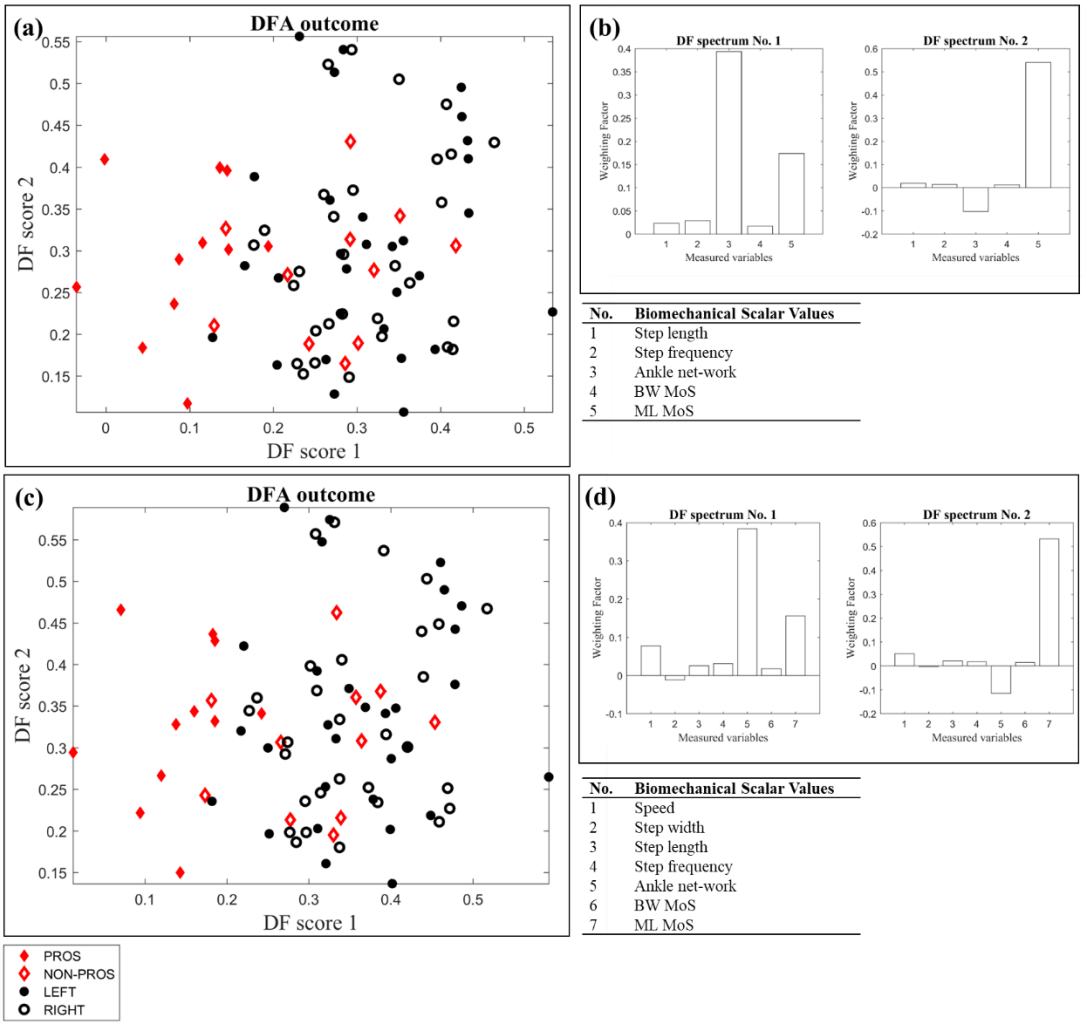

Figure 5.7 DFA classification outcome (a, c) and DF spectrum (b, d) comparing between individuals with UTTA and able-bodied individuals using five scalar values (a, b) and seven scalar values (c, d), normalised to units. In the DF spectrum, each bar is equivalent to a measured variable from a DF curve, integrated over all spectral frequencies.

5.4.3 Analyses of Temporal Waveforms and Five Scalar Values, Normalised

The PCA outcome of both, temporal waveform data and scalar values, normalised to units showed that there is a difference between UTTA (solid and open red diamonds) and able-bodied (solid and open black circles) gait in PC2 (outcome number 1 and 3, Figure 5.8 a). In outcome number 1 the groups separated horizontally, i.e. they separated to the top and bottom of the graph and in outcome number 3, they separated vertically, i.e. to the right and left of the graph. Similar results were observed in the PCA analysis of temporal waveform data alone (Section 5.4.1), suggesting that scalar values did not add any additional information to the discrimination procedure. The Eigenspectrum of PC2 for the temporal waveforms (Figure 5.8 b) highlighted variables number 3, 17, 13 and 20, which corresponded to vertical GRF, sagittal knee joint angle, sagittal hip joint moment, and sagittal ankle joint angle. The Eigenspectrum of PC for the scalar values (Figure 5.8 c) highlighted variables number 3 and 5, which corresponded ankle net-work and ML MoS (For the outcome of PCA on temporal waveform data and scalar values, which were not normalised and with 7 scalar values see Appendix 2).

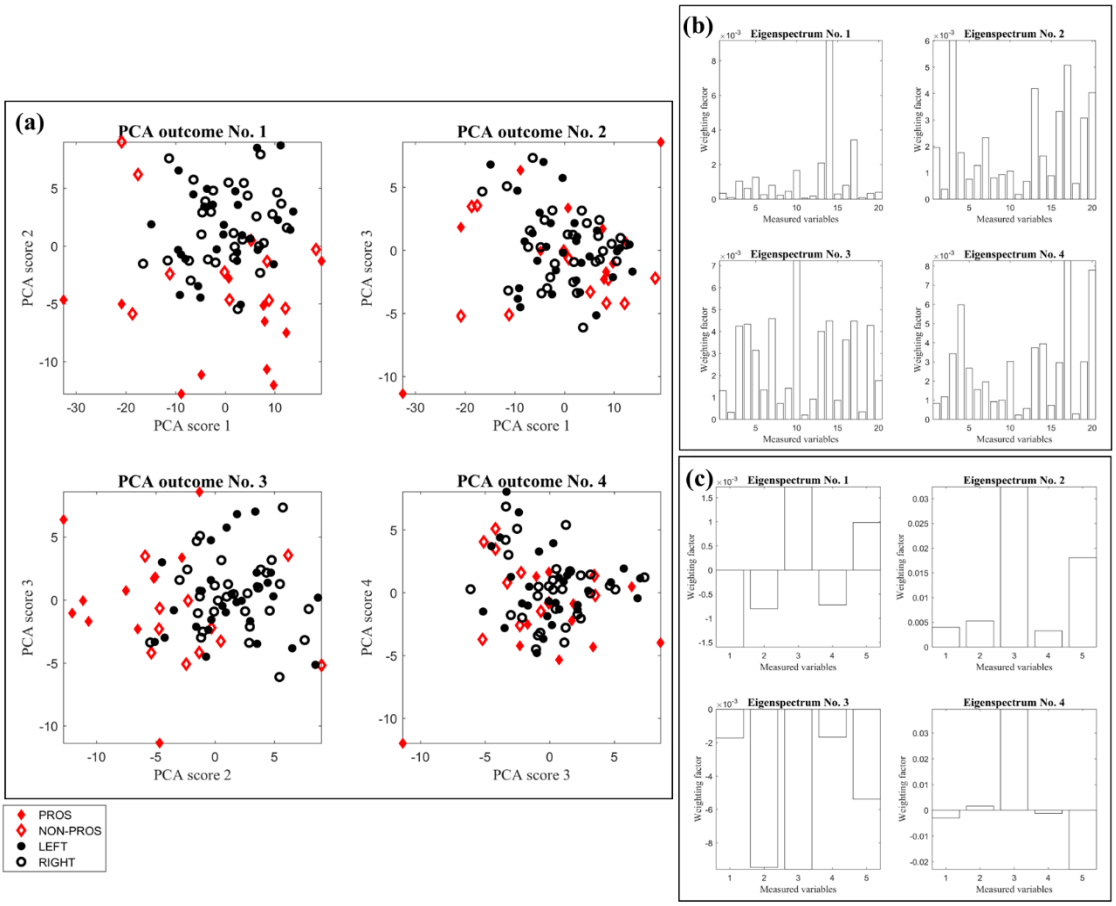

Figure 5.8 PCA outcome (a) and Eigenspectrum (b, c) comparing between individuals with UTTA and able-bodied individuals using temporal waveforms (b) and five scalar values (c), normalised to units.

The DFA outcome showed a classification between the gait of individuals with UTTA (solid and open red diamonds) and able-bodied individuals (solid and open black circles) and between the PROS and NONPROS limbs (Figure 5.8), similar to the classification of temporal waveform data alone (Section 5.4.1, Figure 5.5 c). The DF spectrum for this analysis corresponded with previous findings of individual analyses of temporal waveform data and scalar values, separately. The DF spectrum of temporal waveforms highlights variables number 17, 4 and 3, which correspond to sagittal knee joint angle, vertical GRF and medio-lateral GRF. The DF spectrum of the scalar values highlights variables 1, 3 and 5, which correspond to step length, ankle joint net-work and ML MoS. (For the outcome of DFA on temporal waveform data and scalar values, which were not normalised and with 7 scalar values see Appendix 2).

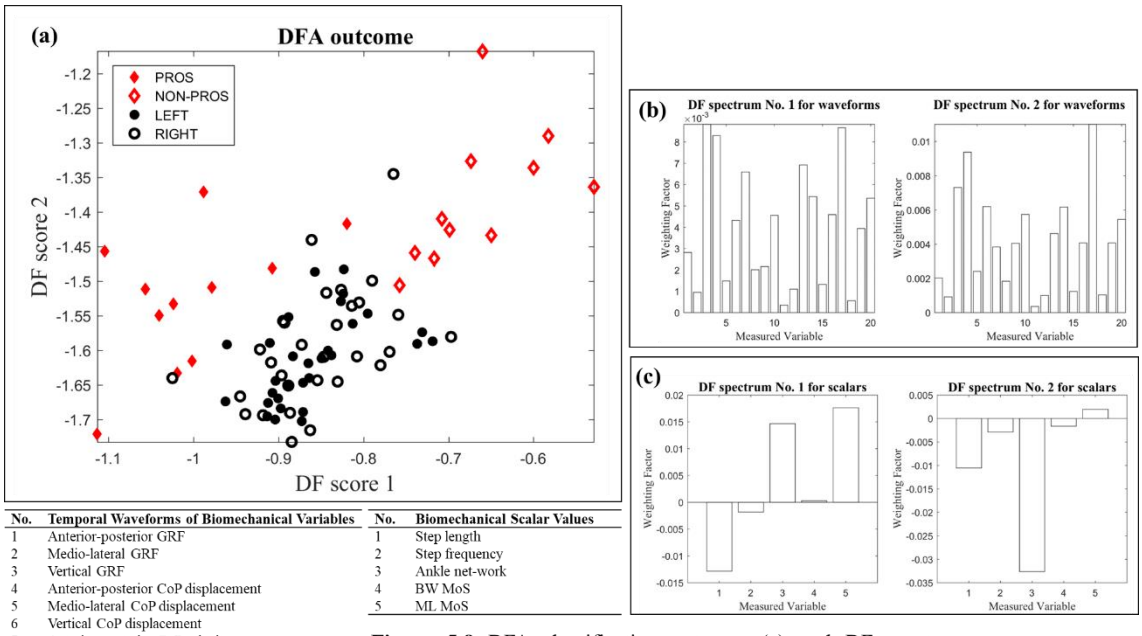

No.	Temporal Waveforms of Biomechanical Variables
1	Anterior-posterior GRF
2	Medio-lateral GRF
3	Vertical GRF
4	Anterior-posterior CoP displacement
5	Medio-lateral CoP displacement
6	Vertical CoP displacement
7	Anterior-posterior CoP velocity
8	Medio-lateral CoP velocity
9	Vertical CoP velocity
10	Vertical CoM displacement
11	Vertical CoM velocity
12	Sagittal hip joint power
13	Sagittal hip joint moment
14	Sagittal hip joint angle
15	Sagittal knee joint power
16	Sagittal knee joint moment
17	Sagittal knee joint angle
18	Sagittal ankle joint power
19	Sagittal ankle joint moment
20	Sagittal ankle joint angle

No.	Biomechanical Scalar Values
1	Step length
2	Step frequency
3	Ankle net-work
4	BW MoS
5	ML MoS

Figure 5.8 DFA classification outcome (a) and DF spectrum comparing between individuals with UTTA and able-bodied individuals using temporal waveforms (b) and five scalar values (c).

5.5 Discussion and Conclusion

The aim of this study was to establish differences between UTTA and able-bodied gait using PCA and DFA providing a better understanding of LLA function. Differences in gait between the two groups were found and attributed to vertical GRF, sagittal hip joint moment and sagittal knee joint angle. The biomechanical variables measured in this study consisted of temporal-spatial, kinetic and kinematic variables, which were commonly reported in the literature during the investigation of forward progression and dynamic stability. These variables were chosen in particular because the continuous interchange between mobility and stability is required for walking without the risk of falling (Lakany, 2008) which is a common concern for individuals with LLA (Jayakaran *et al.*, 2012). Different analysis methods were explored to establish a technique, which would allow important variables that differ between UTTA and able-bodied gait to be identified. The results demonstrated that for this particular application of multivariate statistical analyses methods, PCA on normalised temporal waveforms was the most suitable technique. However, there is not a single method that is applicable to all data and applications, instead, the best performing algorithm depends on the features of a data set (Harper, 2005).

In current methods, biomechanical variables were normalised to units, which was important as reflected by the Eigenspectra and DF spectra. This is because, using the covariance approach during PCA, the variables' weightings depend on their magnitude. In biomechanics, a variable's magnitude may be small or large depending on the joint or muscle groups driving it. Thus, investigating the difference between joints may incur bias if the difference between the two groups is based on the absolute magnitude. Hence, during the assessment of biomechanical variables using automatic gait recognition tools, normalisation of data should be incorporated.

In this study, different multivariate statistical analyses of PCA and PCA followed by DFA, have been explored. Both methods identified differences between UTTA and able-bodied gait, however, since DFA is a supervised algorithm it seeks out differences. During the treatment of pathological gait, the aim is not to seek out differences but rather find naturally occurring differences that could be treated. Therefore, using PCA alone is sufficient since it highlights differences that occur in the gross structure of the data which can also be identified in the graphical profile of temporal waveforms as highlighted in the current results. Differences in the detailed structure may imply that an issue is present, however, these differences may not be easily identified in graphical profile and thus may be more difficult to treat.

Although differences may be identified in the graphical profile of the temporal waveform and traditional statistical approaches can be used to establish if a variable differs significantly between

a group/condition, it is still advantageous to use PCA for a number of reasons: (1) Interpretation of the graphical profile of temporal waveform and the selection of discrete parameters to perform the statistical analysis are subject to researcher bias, whilst PCA is an objective measure. (2) Since PCA can be used to analyse the entire temporal waveform, characteristics of biomechanical data such as time-dependance, are considered which would otherwise be ignored if discrete parameters were used to perform traditional statistical tests. (3) Although differences could be identified in the graphical profile, PCA can be used to quantify these differences (as will be demonstrated in Chapter 6) and different parts of the profile could be ranked in terms of variance using PC scores, as demonstrated by Soares *et al.* (2016). (4) PCA enables many variables to be compared simultaneously, and it does not only reveal if variables differ between groups/conditions as traditional statistical approaches do, but it also ranks the variables in terms of variance as shown in the Eigenspectrum of the current results. Thus in clinical applications it can provide an indication of which variables need to be targeted.

The results of the PCA outcome revealed that the differences between the gait of individuals with UTTA and able-bodied individuals were in PC2, indicating that PC1 does not necessarily always hold the information of interest. Thus, although PC1 holds the majority of the variance of the original data set, it cannot be expected that it contains the variables responsible for the discrimination between experimental groups which is a common, yet false assumption. This highlights the importance of the remaining PCs, as previously discussed by Phinyomark *et al.* (2016). Having said that, variables in the first few PCs have larger weighting factors and discriminating variables in lower ranked PCs have smaller weighting factors. Thus, similar to the DFA outcome, discriminating variables in lower ranked PCs may be more difficult to identify in 2D plots of temporal waveforms.

The Eigenspectrum of the PCA with the biomechanical variables of normalised temporal waveform data highlighted that in PC2 vertical GRF, sagittal knee joint angle and sagittal hip joint moment were the main variables to cause a difference between the gait of individuals with UTTA and able-bodied individuals. Soares *et al.* (2016) previously identified that the vertical GRF discriminated in PC1 between the control limb and the prosthetic limb, while PC2 discriminated between the control limbs and both the intact and prosthetic limbs. The magnitude of the vertical GRF was found to be much smaller on the prosthetic limb, which may have been a protective mechanism to reduce loading on the residual limb. However, it should be noted that the participants in the study by Soares *et al.* (2016) were individuals with UTFA, whilst in this study, individuals with UTTA were investigated. The discrimination may have occurred at

different PC since the level of amputation differed, i.e. fewer joints remain and thus larger compensation was required.

The results showed that temporal waveforms provided more information since they span the entire gait cycle compared to scalar values (Chau, 2001a). Previous studies suggest that continuous data provide a better discriminatory approach relative to discrete parameters (Deluzio *et al.*, 1997). Schöllhorn *et al.* (2002) found that one in every three discrete parameters (scalar values) is likely to be misclassified. In this study, adding more scalar values to the analysis procedure did not improve the outcome. It should be noted, however, that although additional variables did not improve the classification outcome, one of the additional variables (speed) indicated discriminatory properties between the gait of individuals with UTTA and able-bodied individuals. Thus, the variables chosen during a discrimination procedure are of great importance. During the analysis of scalar values alone using PCA, the prosthetic limb differed from the intact limb of the individuals with UTTA and also the control limbs of the able-bodied individuals, but during the analysis of temporal waveforms alone both prosthetic and intact limbs differed from the control limbs. Using DFA did not only classify individuals with UTTA from the able-bodied individuals but also clustered prosthetic and intact limb separately. Previous studies investigating LLA gait using traditional statistics, reported similar findings, thus depending on the aims of a study, researchers may prefer to use DFA in addition to PCA since it provides a greater discrimination outcome.

The data in this study consisted of twenty temporal waveforms and seven scalar values of kinetic, kinematic and GRF variables, and demonstrates the ability of automatic gait recognition tools with large data sets. Previous research that compared between the gait of individuals with LLA and able-bodied individuals using automatic gait recognition tools limited the investigations to either kinematic, kinetic, GRF or EMG data (Miller *et al.*, 2013), but recent studies demonstrated that the classification of only kinetic or kinematic variables alone might compromise the outcome (Schöllhorn *et al.*, 2002). Assessing many variables simultaneously is not only time efficient but provides an instantaneous in-depth understanding, which can have great implications in clinical applications.

Biomechanical variables chosen for this analyses were often reported in the literature for the assessment of forward progression and dynamic stability, however, these variables were reported in the sagittal plane only. Previous studies that used automatic gait recognition report that variables from different planes have the potential to improve the classification results, thus providing a more comprehensive understanding of pathological gait (Schöllhorn *et al.*, 2002). For example, studies report that the regulation of whole-body angular momentum is important to

prevent falls, particularly in the frontal plane (Miller *et al.*, 2018). Furthermore, anterior-posterior CoM from the sagittal trajectory may provide more information regarding forward progression, however, in the current study, similar to previous research, only vertical CoM displacement and velocity were assessed, which were commonly reported for the assessment of dynamic stability. Thus, variables from different planes of motion are worthy of inclusion in future analyses.

In this study, PCA was applied for data reduction and feature selection and DFA was applied for classification and were found to effectively compare between UTTA and able-bodied gait. Other studies have compared classification performance of different machine learning algorithms such as SMV, ANN and NB in order to assess powered prosthetic devices (Afzal *et al.*, 2017; Chen *et al.*, 2013; Joshi & Hahn, 2016; Khan *et al.*, 2018; Miller *et al.*, 2013; Pew & Klute, 2017). Findings indicated that some methods provide better discrimination and classification than others. Therefore, future research should explore the use of different machine learning algorithms to investigate if these provide more information and thus a better understanding of LLA function.

In conclusion, investigating different techniques to compare UTTA and able-bodied gait in order to provide a better understanding of LLA function, has demonstrated that using PCA to assess normalised temporal waveforms of kinetic, kinematic and GRF data was an effective technique to evaluate LLA gait. It was established that both prosthetic and intact limbs differed from control limbs due to vertical GRF, sagittal knee joint angle and sagittal hip joint moment. This study demonstrates the ability of automatic gait recognition as a powerful diagnostic tool in a clinical setting.

Chapter 6: Identifying Subject-Specific Gait Characteristics of Individuals with Unilateral Trans-Tibial Amputation.

Bisele, M., Bencsik, M., Lewis, M.G., & Barnett, C.T. (2018) Should lower-limb amputee gait be assessed at individual basis to improve function? *In Proceedings of the 8th World Congress of Biomechanics, Dublin, Ireland.*

6.1 Introduction

Gait analysis is used to diagnose, assess and monitor pathological gaits (Kirtley, 2006; Levine *et al.,* 2012) such as cerebral palsy (CP) (Novacheck *et al.,* 2010), multiple sclerosis (MS), Parkinson's disease (Roiz *et al.,* 2010; Švehlík *et al.,* 2009) and other movement-related pathologies. However, it is not common practice in the treatment of individuals with LLA (Ramstrand & Brodtkorb, 2008). The treatment these individuals with LLA is influenced by multiple factors including but not limited to the age of the individual and level of amputation (Leung *et al.,* 1996), making it difficult to predict therapy outcomes. Studies suggest that there are no objective measures to evaluate prosthetic rehabilitation, but instead, it depends on clinicians experience (van der Linde *et al.,* 2004; Schaffalitzky *et al.,* 2011). Gait analysis can provide a greater understanding and inform clinical decisions more effectively (Esquenazi, 2014). In individuals with LLA, it can help monitor prosthetic rehabilitation and therapy effectiveness (Skinner & Effeney, 1985).

Research commonly focuses on group effects, whilst clinical practice is patient-specific, thus research outcomes may not always be easily integrated into clinical practice (Schöllhorn *et al.,* 2002). During the assessment of group effects, individual differences among people within the same group are not commonly investigated (Horst *et al.,* 2017). Thus, even when group effects are established, the individual variability within the groups remains unknown, making it difficult to translate group effects from research into clinical practice. Hoerzer *et al.* (2015) refer to "functional groups" which describes a group of individuals that share similar characteristics, so the response of these individuals to an intervention may be comparable. Although, participant recruitment in research projects is based on certain inclusion/exclusion criteria, participants may not necessarily fall into a "functional group", making it difficult to apply findings to clinical practice.

Using machine learning algorithms, studies found that individuals exhibit unique gait characteristics (Horst *et al.,* 2017; Schöllhorn *et al.,* 2002). These gait characteristics did not only differ between individuals but also remained constant over weeks and even months for the same participant (Horst *et al.,* 2016; 2017). This suggests that using automatic gait recognition methods such as machine learning algorithms, diagnosis and therapy procedures could be patient-specific, which would help overcome challenges as the "best" interventions for the individual could be predicted (Schöllhorn *et al.,* 2006; 2010). This method has yet to be applied to LLA gait to investigate whether individual gait characteristics can be identified. Therefore, the aim of this study was to determine subject-specific gait characteristics of one individual with UTTA using

PCA when compared to a group of able-bodied individuals. We hypothesized that (1) using PCA an individual with UTTA could be discriminated from a group of able-bodied individuals and (2) the Eigenspectrum would reveal subject-specific discrimination features that characterise the UTTA's gait.

6.2 Methodology

The methods used for this study were similar to those presented in Chapter 5. However the analysis of the data differed, since the recommendations from the previous findings were implimented (Section 5.5) and further analysis techniques using covariance and correlation matrices in PCA, were explored.

6.2.1 Participants

A convenience sample of eleven individuals with UTTA (age 50±12years; height 1.7±0.1m; mass 83.94±13.59kg) and thirty able-bodied individuals (age 39±20years; height 1.7±0.1m; mass 73.76±14.02kg) were recruited from the university and local communities. All participants met the inclusion and exclusion criteria detailed in Section 3.2.2. Ethical approval was granted by the Nottingham Trent University's College of Science and Technology Ethical Review Committee (Humans), the NHS Research Ethics Committee, the NHS Health Research Authority and the NHS Research and Development. All participants provided written informed consent prior to participation.

6.2.2 Experimental Design and Data Acquisition

The study investigated individuals with UTTA and able-bodied individuals at self-selected walking speed. Upon arrival, the participants were briefed. All activities were completed with participants wearing lycra shorts and everyday shoes. Individuals with UTTA used their habitual prosthesis (Table 3.1). To obtain kinematic measurements 70 spherical 14mm, reflective markers were placed directly onto the skin or clothing using bi-adhesive tape, defining head, arms, trunk (Leardini *et al.,* 2011) and lower limb segments (Cappozzo *et al.*, 1995) (for marker placement, refer to Section 3.3.3). Marker placement on the prosthetic limb was estimated depending on marker placement of the intact limb (Powers *et al.*, 1998).

A static trial was obtained for segment definition, followed by the dynamic trials. First, the participant's starting position was defined, to ensure that force platform data was obtained as the participant walked along the walkway. During dynamic trials, participants walked at a self-selected speed along a 15m walkway. This process was repeated until five successful trials were

collected for both limbs, where GRF was measured at 1000Hz using a single floor-mounted strain gauge force platform (AMTI, Watertown, MA, USA) and kinematics were measured at 100Hz using a nine-camera motion capture system (Qualisys, Gothenburg, SE). A successful trial was defined by a clear force plate contact.

6.2.3 Data Processing

Markers were labelled in QTM v2.2 (Qualisys, Gothenburg, SE) as defined in Section 3.3.3. and trial start and end periods were adjusted to one gait cycle of each limb starting at heel strike on the force platform. Marker trajectories and force data were exported as .c3d files and subsequently processed in Visual3D v5 (C Motion, Inc., Germantown, MD, USA). Kinematic data were interpolated using a cubic-spline algorithm with kinematic and GRF data being subsequently filtered using 4th order, zero-lag Butterworth low-pass filters with 6Hz and 30Hz cut-off frequencies, respectively. All data were normalised to one gait cycle. Medial and lateral landmarks defined anatomical frames from which segment coordinate systems were defined following the right-hand rule (Cappozzo *et al.,* 1995). A flexion-extension, abduction-adduction and longitudinal Cardan rotation sequence was used to define the order of rotations to calculate joint kinematics. Gait events of heel strike and toe off were determined using kinetic and kinematic event detection algorithms (Stanhope *et al.,* 1990; Zeni *et al.,* 2008) (Section 3.3.5). Twenty biomechanical variables which are typically reported in the literature for forward progression and dynamic stability were included in the analysis (Table 3.25) since the continuous interchange between mobility and stability are essential for efficient walking (Lakany, 2008). The biomechanical variables were computed in Visual3D (C-Motion, Inc, Germantown, USA). Processed data were exported from Visual3D as .c3d files, and individual signals were imported to MATLAB® R2016a (MathWorks Inc., MA, USA) for further analysis.

6.3 Multivariate Statistical Analysis

6.3.1 Principal Component Analysis using both Covariance and Correlation Matrices

Principal Component Analysis was applied (for data reduction and feature selection) to compare between the gait of one individual with UTTA and a group of thirty able-bodied individuals. Twenty temporal gait waveforms (Table 3.25) were reported for each limb, i.e. the prosthetic limb (PROS) and intact limb (NONPROS) of the individual with UTTA, and the control limbs (RIGHT and LEFT) of the able-bodied individuals. PCA was conducted by means of the diagonalization of the covariance matrix (a) and the correlation matrix (b).

The weightings of variables of the covariance matrix depend on their magnitude as described in Chapter 5 Section 5.3.1. Hence, using the covariance matrix, variables have been normalised depended on the variables' units, i.e. variables with the same unit were scaled to their own specific maximum. The correlation matrix is obtained by normalising the covariance matrix to the standard deviation of the data. During this normalisation procedure, variables with different variances (or dynamic ranges) are made equivalent. Although this can sometimes be considered to be a 'fairer' way of dealing with large complex data, it will bring forward the contribution of parameters that may exhibit small and irrelevant variations at the same level to those parameters that are potentially far more important. In instances where variation in the data is a valued aspect of discrimination, the covariance method is better suited to identifying differences between groups (Tinsley & Tinsley, 1987). Using the two different PCA approaches, the varying normalisation procedures will be reflected in the results.

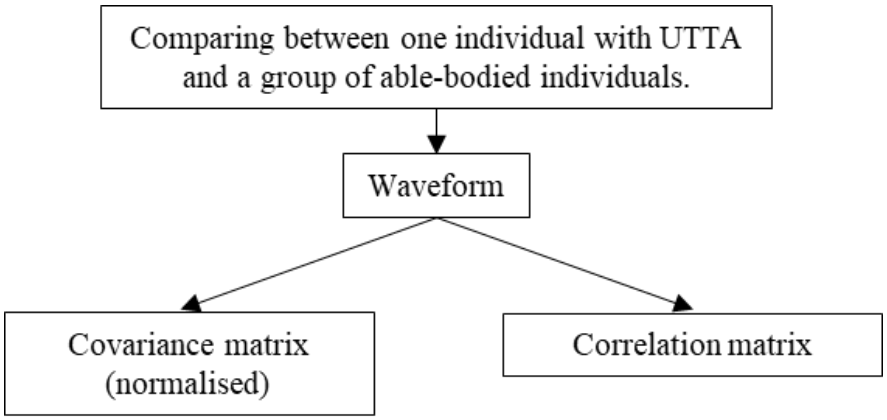

Figure 6.1 Temporal waveform data from one individual with UTTA and a group of able-bodied individuals will be compared using both, the covariance or the correlation matrices during PCA.

The input matrix M, was comprised of data from one individual with UTTA and thirty able-bodied individuals Therefore, the original 3D matrix was 101 x 20 x 62 points since one mean trial was made of 20 columns (variables) and 101 row vectors (101 data points which are equivalent to 100% of gait cycle) and the total number of limbs were 62 (the prosthetic and intact limbs of the individual with UTTA and 60 control limbs of able-bodied individuals). The 2D matrix was 2020 x 62, which was further reduced to 62 x 62 using PCA.

6.3.2 Euclidean Distances Defining Limb Variation

The distances (in PC score space) of each limb location to the origin (Figure 6.2 a) and to the cloud centre (Figure 6.2 b), were calculated to provide a measure of how different an individual limb is from these averages. The origin of PC scores coordinates is the mean value. During orthogonal transformation from the original variables into principal components, the new set of axes with rank '1', PC1, holds the maximum variance of the original data and all other axes (with PC ranks higher than 1) are orthogonal to that particular axis (and to each other). Therefore, depending on the PC rank under scrutiny, the relationship between limb location and axes will vary, and this was quantified using the Euclidean distance. This measure identifies whether a particular limb varies from the average and by how much. For example, in the second dimension, PC2, the intact and prosthetic limbs of participant X differed from the average by 2 standard deviations (2SD), whilst the control limb of participant Y varied from the average in PC4 by 2SD. The distance (in PC score space) from each limb relative to the control limbs cloud centre was also measured using the Euclidean distance using 20 ranks, indicating the difference of individual limbs relative to the average of all control limbs, since the cloud centre was quantified only using control limbs. Thus, the former measure is important because it indicates where a particular limb differs from the mean and by how much, whilst the latter measure is also important since it indicates how a particular limb differs with regards to all other control limbs. The normal distribution of the data was assessed using Kolmogorov-Smirnov test.

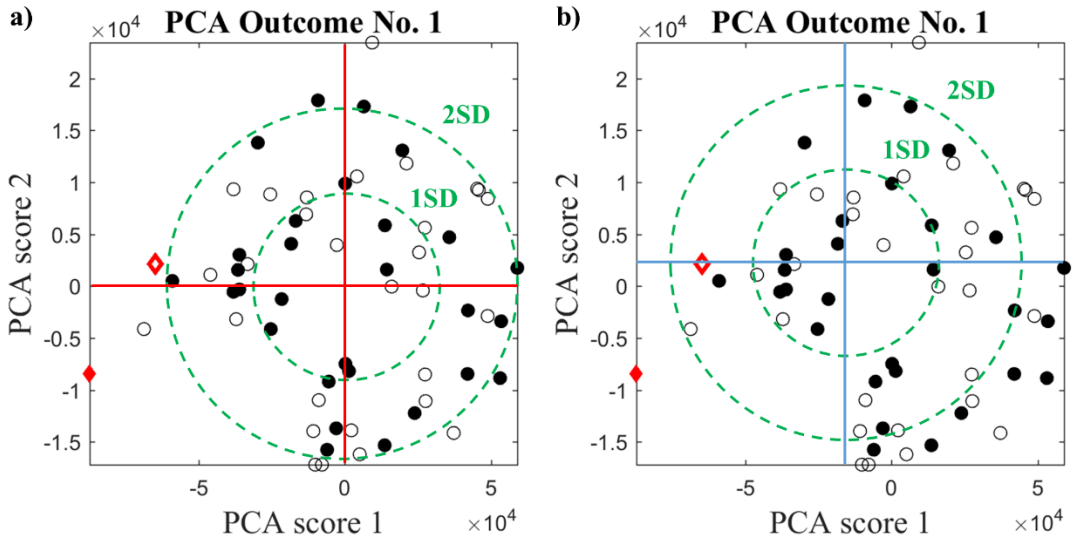

Figure 6.2 Quantification of the distance, in PC score space, of individual limbs to (a) the origin and (b) the control limbs cloud centre using Euclidean distances. The origin of the red and blue axes in (a) and (b) respectively shows where the distances are measured to. The PROS and NONPROS limbs are illustrated by full and open red diamonds and the LEFT and RIGHT control limbs are illustrated by full and open black circles. The distance from the average is measured in terms of SD (dashed green lines).

6.4 Results

The PCA outcome differed for both the correlation matrix and the covariance matrix (Figure 6.3 a and b) and differed for each individual with UTTA. Below is an example of the data for the individual with UTTA number 1. For all results of each individual with UTTA see Appendix 3. Figure 6.3 (a) shows the PCA outcome for the individual with UTTA when compared to the able-bodied individuals using covariance matrix on data normalised to units. The PCA outcome is shown in four different views between two dimensions each, where a dimension is made up of a PC component. The individual with UTTA differed from the group of able-bodied individuals in PC2 (outcome number 1 and 3). The PROS and the NONPROS limbs (solid and open red diamonds) sat at the edge of the cloud constituted of RIGHT and LEFT control limbs (solid and open black circles). In PCA outcome number 4, the PROS limb differed from the control limbs, whilst NONPROS limb was embedded within the cloud of control limbs. This demonstrated that in some instances only one of the limbs of the individual with UTTA differed not necessarily both. Therefore, the PC2 (Eig. rank 2 in Figure 6.3 a) holds discriminating features for both the PROS and NONPROS, whilst PC4 (Eig. rank 4 in Figure 6.3 a) holds discriminating features of PROS limb only. Similar to the previous study in Chapter 5, a difference did not occur in every dimension (PCs 1 and 3). In order to establish which biomechanical variables resulted in the difference between the individual with UTTA and the group of able-bodied individuals, the average Eigenspectra for the first four PCs are displayed in Figure 6.3 (b). The biomechanical variables included in the procedure are displayed in decreasing order of contribution to the discrimination, larger bars indicated larger contribution. Since the covariance matrix revealed that the PC2 discriminated between the individual with UTTA and the able-bodied individuals, the second Eigenspectrum is investigated (Eig. rank 2 in Figure 6.3 b), where the greatest contributors were variable numbers 14, 13 and 10 which corresponds to sagittal hip joint angle, sagittal hip joint moment and vertical CoM displacement. Furthermore, PC4 showed that the PROS limb differed from the control limbs, where variable numbers 7, 4 and 17 were responsible for the discrimination, which corresponded to medio-lateral CoM velocity, medio-lateral CoP displacement and sagittal knee joint angle.

Figure 6.3 (c) shows the PCA outcome for the individual with UTTA number 1 using the correlation matrix. The individual with UTTA did not differ from the able-bodied individuals when using the correlation matrix. Thus, the variables displayed in the Eigenspectrum of different PCs did not reveal any discriminatory features that provided any additional information. As previously mentioned, the different result between the covariance and the correlation matrices can be expected since the normalisation procedure between the two PCA approaches differed.

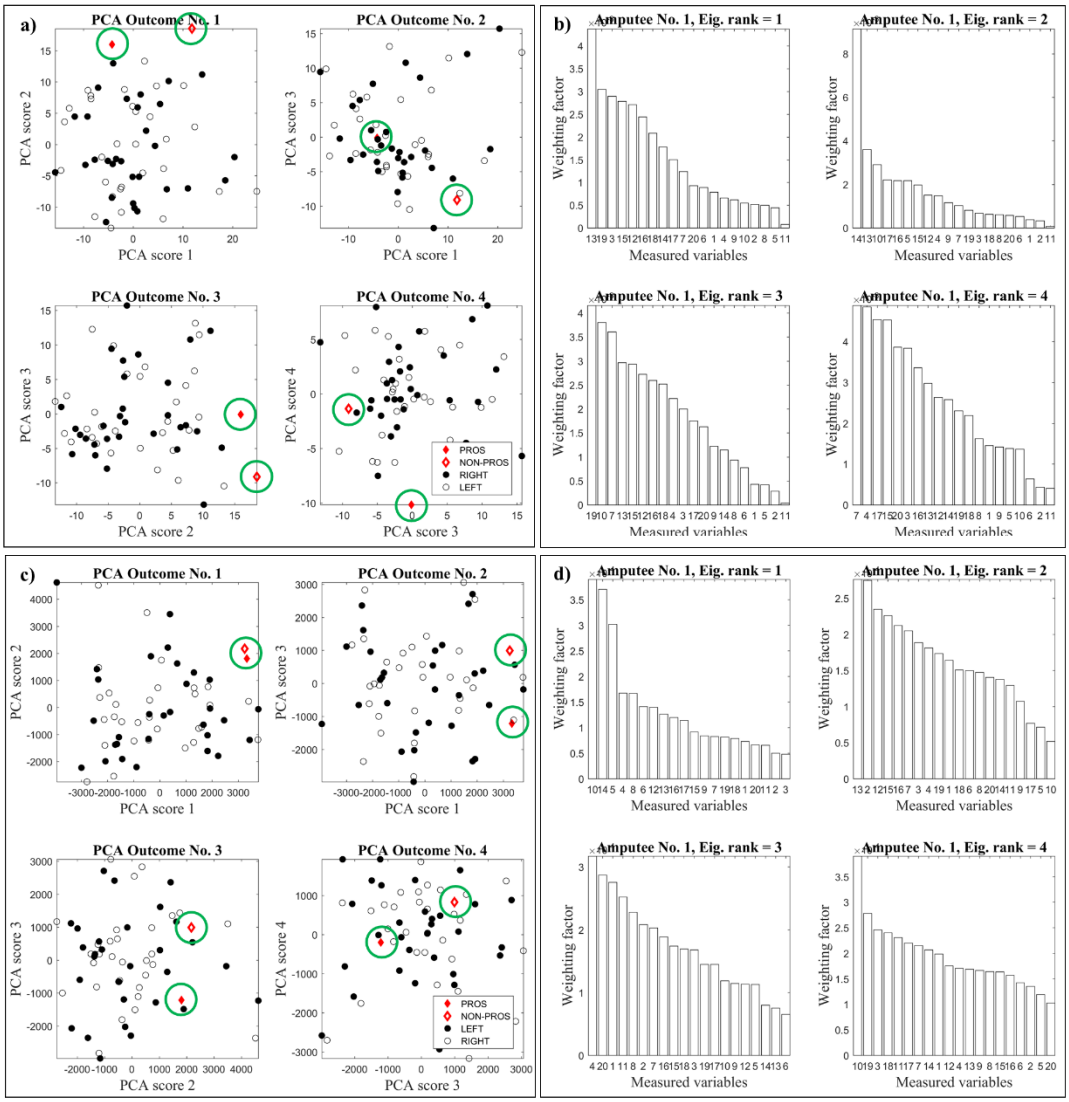

Figure 6.3 PCA outcome (a, c) and Eigenspectra (b, d) comparing between the gait of the individual with UTTA number 1 and a group of able-bodied individuals using the covariance (a, b) and the correlation (c, d) approaches.

No.	Temporal Waveforms of Biomechanical Variables
1	Anterior-posterior GRF
2	Medio-lateral GRF
3	Vertical GRF
4	Anterior-posterior CoP displacement
5	Medio-lateral CoP displacement
6	Vertical CoP displacement
7	Anterior-posterior CoP velocity
8	Medio-lateral CoP velocity
9	Vertical CoP velocity
10	Vertical CoM displacement
11	Vertical CoM velocity
12	Sagittal hip joint power
13	Sagittal hip joint moment
14	Sagittal hip joint angle
15	Sagittal knee joint power
16	Sagittal knee joint moment
17	Sagittal knee joint angle
18	Sagittal ankle joint power
19	Sagittal ankle joint moment
20	Sagittal ankle joint angle

Comparing between the gait of one individual with UTTA and the group of able-bodied individuals, the PCA outcome for each individual with UTTA varied (Table 6.1). For example, using the covariance approach both PROS and NONPROS limbs of individual number 1 differed in PC2 and the PROS limb differed in PC4 (Figure 6.3 a), but for individual number 2 only the PROS limb differed from control limbs in PC1 instead of both limbs in PC2 (Figure 6.4 a). Again, using the correlation approach individual number 1 did not differ from able-bodied individuals (Figure 6.3 c), however, in individual number 2 the PROS limb differed in PC2 (Figure 6.4 c). Furthermore, the variables responsible for the differences between the individuals with UTTA and able-bodied individuals varied, indicating that each of the individuals with UTTA displays unique gait characteristics.

The PCs that held the main discriminating features varied between individuals with UTTA. Nevertheless, the Eigenspectra corresponding to these PCs illustrated some common discriminating features among individuals (Table 6.1). The discrimination features, which occurred most commonly in both the covariance and the correlation approaches were sagittal hip joint moment (discriminating variable number 13) and sagittal hip joint angle (discriminating variable number 14). Other discriminating features were unique to one individual with UTTA and did not appear in the Eigenspectrum of many or any other individuals, for example, the sagittal ankle joint angle in individual number 11.

Table 6.1 PCs in which the prosthetic and intact limbs (PROS and NONPROS, respectively) of one individual with UTTA were discriminated from the control limbs (RIGHT and LEFT) of a group of able-bodied individuals using the covariance or the correlation approach during the PCA and the number corresponding to the top 3 variables attributed to the difference. The variables corresponding to these numbers are detailed in Table 3.25.

Individual No.	Covariance Matrix	Discriminating Variables	Correlation Matrix	Discriminating Variables
1	Both limbs in PC2	14, 13, 10	No discrimination	-
2	PROS limb in PC1	13, 19,15	PROS limb in PC2	13, 12, 16
3	PROS limb in PC1	13, 19, 3	PROS limb in PC2	2, 13, 16
4	PROS limb in PC1	13, 15, 16	PROS limb in PC2	13, 15, 12
5	Both limbs in PC1	14, 17, 10	Both limbs in PC1	14, 17, 11
6	PROS limb in PC2	14, 13, 15	No discrimination	-
7	Both limbs in PC1	14, 13, 3	Both limbs in PC1	10, 14, 5
8	Both limbs in PC1	14, 13, 15	PROS limb in PC2	14, 13, 15
9	No discrimination	-	No discrimination	-
10	NONPROS limb in PC1	13, 3, 15	No discrimination	-
11	PROS limb in PC1	13, 14, 19	Both limbs in PC3	4, 20, 10

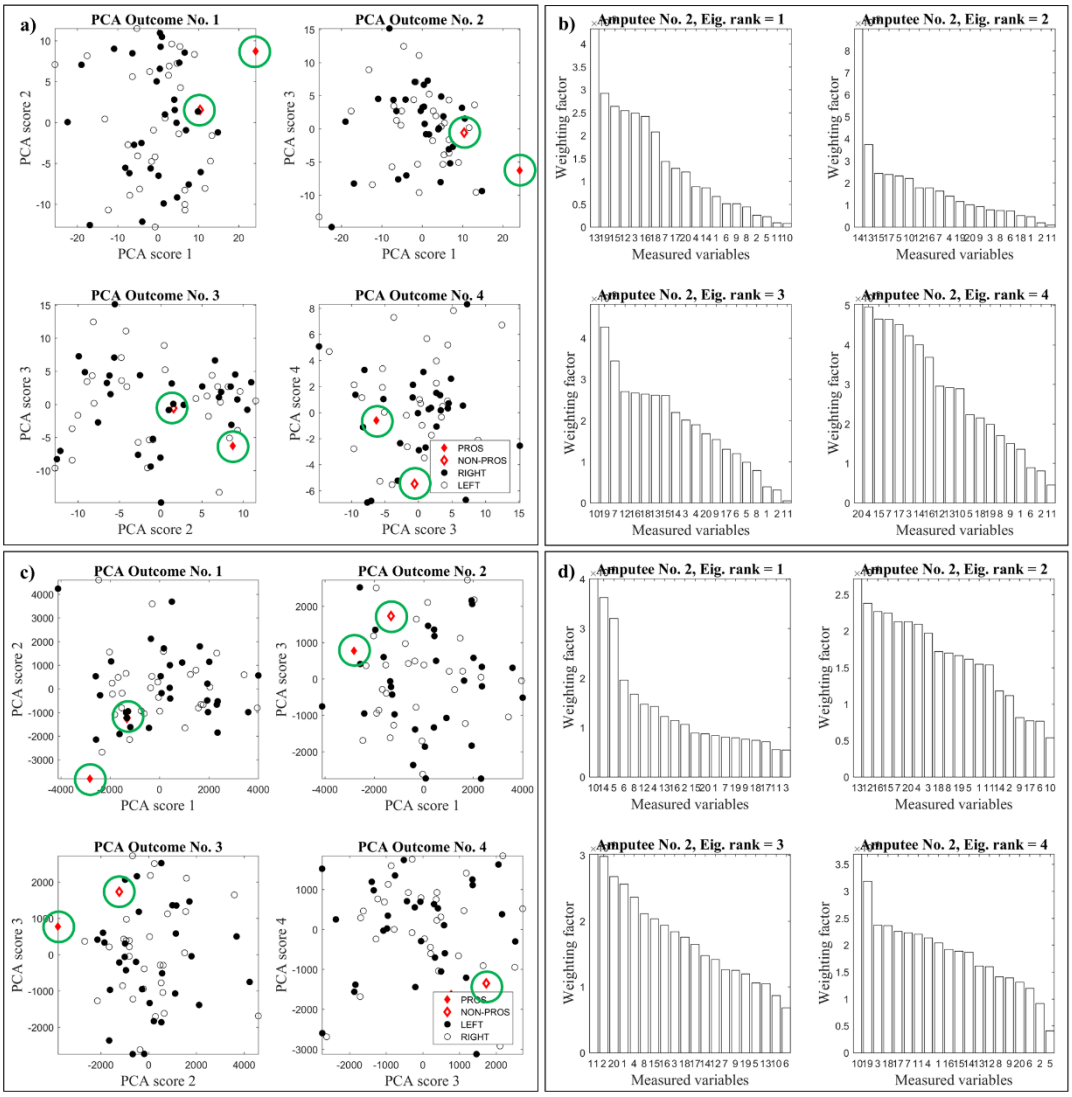

Figure 6.4 PCA outcome (a, c) and Eigenspectra (b, d) comparing between the gait of the individual with UTTA number 2 and a group of able-bodied individuals using the covariance (a, b) and the correlation (c, d) approaches.

No.	Temporal Waveforms of Biomechanical Variables
1	Anterior-posterior GRF
2	Medio-lateral GRF
3	Vertical GRF
4	Anterior-posterior CoP displacement
5	Medio-lateral CoP displacement
6	Vertical CoP displacement
7	Anterior-posterior CoP velocity
8	Medio-lateral CoP velocity
9	Vertical CoP velocity
10	Vertical CoM displacement
11	Vertical CoM velocity
12	Sagittal hip joint power
13	Sagittal hip joint moment
14	Sagittal hip joint angle
15	Sagittal knee joint power
16	Sagittal knee joint moment
17	Sagittal knee joint angle
18	Sagittal ankle joint power
19	Sagittal ankle joint moment
20	Sagittal ankle joint angle

From the PCA outcome of the individual with UTTA number 1 using the covariance approach, it was established that both PROS and NONPROS limbs differed in PC2. The average Eigenspectrum of PC2 revealed which variables were responsible for this difference. In order to quantify the relative difference between the PROS and NONPROS limbs from the control limbs, the Euclidean distance of each limb to the PC origin (0,0) was measured. In Figure 6.5 the standard deviation (SD) is shown by the dashed lines, where outer lines represent 2SD from the (0,0). If PROS and NONPROS limbs fall within ±2SD, they are considered close to average, and if they are outside of 2SD, they are considered to be outside the normal range. The red bell curve shows the distribution of data and is purely for graphical purposes.

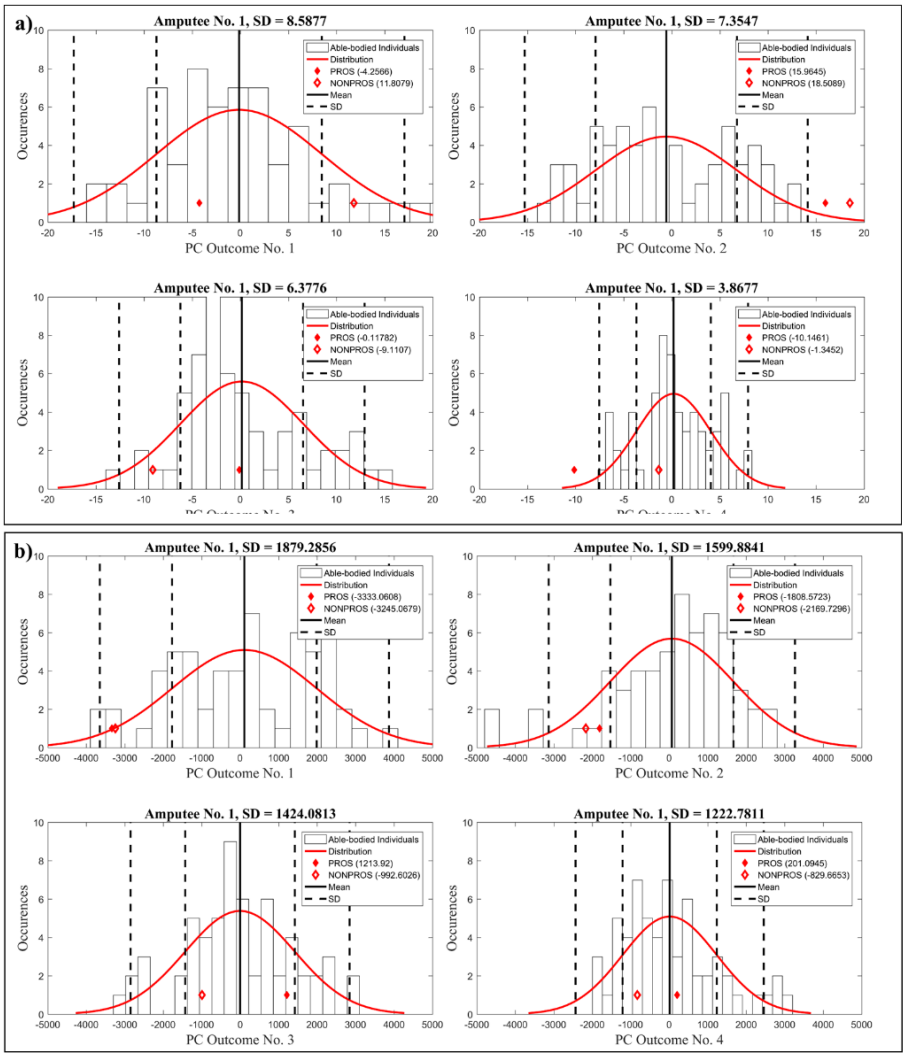

Figure 6.5 The distance of individual limbs from the origin (0,0) of PCA outcome in the first four dimensions for (a) the covariance and (b) the correlation approach. The four graphs for each approach correspond to PCs, where top left is PC1, top right PC2, bottom left PC3 and bottom right PC4. The x-axis is 1D dimension, indicating the distance in that particular dimension from (0,0), whilst the y-axis describes the number of limbs occurring at that particular distance. The PROS and NONPROS limbs are shown by the solid and open red diamonds.

Since the PCA outcome illustrated that the PROS and NONPROS limbs differed for the control limbs in PC2 using the covariance approach, it was expected that the Euclidean distance measured for the limbs in PC2 would be 2SD away, which was reflected in the results (PROS = 15.96; NONPROS = 18.51) (Figure 6.5 a). The Euclidean distance measured, revealed a greater difference for the NONPROS limb relative to the control limbs when compared to the PROS limb. Furthermore, since PC4 showed the PROS limb to differ from the control limbs whilst NONPROS limb was embedded within the cloud, the Euclidean distance measure revealed that the PROS limb lied outside 2SD (PROS = -10.15) and the NONPROS limb within 2SD (NONPROS = -1.35). For all the dimensions that did not show a difference between the individual with UTTA number 1 and able-bodied individuals the limbs were within ±1 or ±2 SD (Figure 6.5 a and b).

The distance of each limb to the centre of the cloud of control limbs was also measured using the Euclidean distance (Figure 6.6). The x-axis in Figure 6.6 shows the distance to the cloud centre (where zero is the centre) whilst the y-axis is the number of occurrences of the limbs at a particular distance. Similar to other measurements, the PROS and NONPROS limbs are represented by the solid and open red diamonds, respectively. The SD is shown by the dashed lines, where outer lines represent 2SD from the centre of the cloud. If the PROS and NONPROS fall within the 2SD, they were considered within normal range of the control limbs, and vice versa. The red bell curve shows the distribution of data and is purely for graphical purposes. Figure 6.6 shows that for the covariance matrix (a), the PROS limb lies 1SD away, and the NONPROS lies 2SD away compared to the remainder of the control limb, i.e. the NONPROS differed more than the PROS relative to the average of control limbs. With regards to the correlation matrix (b), both limbs fall between 1SD to 2SD of the control limbs, i.e. the individual with UTTA did not differ from the able-bodied individuals. For all results of each individual with UTTA see Appendix 3.

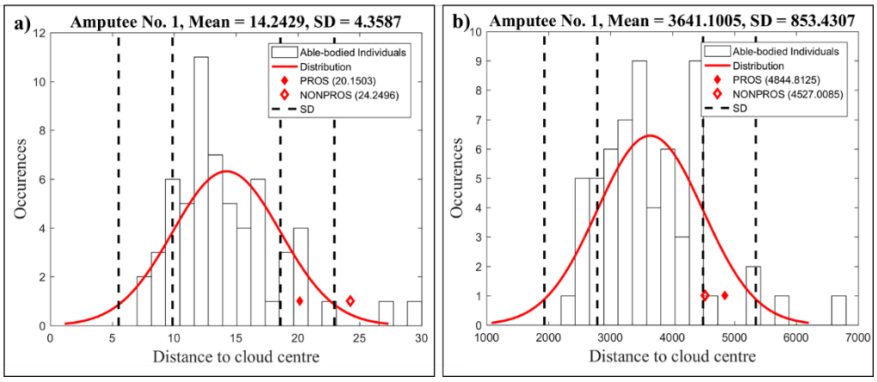

Figure 6.6 Euclidean distance of limbs from the cloud centre using (a) the covariance and (b) the correlation approach. The x-axis indicates the distance from the cloud centre, where the zero value represents the cloud centre. The y-axis defines the number of limbs that occur at that particular distance.

6.5 Discussion and Conclusion

The aim of this study was to determine subject-specific gait characteristics of one individual with UTTA using PCA when compared to a group of able-bodied individuals. The first hypothesis that using PCA could discriminate the gait of one individual with UTTA and a group of able-bodied individuals was supported. The majority of individuals with UTTA were discriminated from the group of able-bodied individuals using the covariance and correlation approaches when compared individually. However, a few were not discriminated, which may be attributed to the strong similarity between their gait and that of able-bodied individuals, perhaps because these individuals were well-established and had at least a year's worth of experience walking with a prosthetic limb. Furthermore, the PCA outcome varied, i.e. in some instances the prosthetic limb, intact limb or both limbs of the individual with UTTA were discriminated from the control limbs. Both limbs were not necessarily discriminated in all instances. These findings could be due to compensatory mechanisms adopted on each limb, i.e. if both limbs adopt compensatory mechanisms, which differ from control limbs, it can be expected that the variables between both the limbs of the UTTA differ from the control limbs of able-bodied individuals. However, if only one limb adopts compensatory mechanisms in order to generate a gait for the alternative limb similar to a control limb, only the limb with the compensatory mechanism will display different biomechanical variables.

The second hypothesis that the Eigenspectrum would reveal subject-specific discrimination features that characterise the gait of an individual with UTTA was also supported. The Eigenspectrum revealed discriminating features corresponding to each individual, of which some were common between individuals and others were specific to the particular individual, indicating that there are some generic features among individuals with UTTA but also subject-specific features, characterising unique gait. Previous research indicated that individual gait characteristics could be identified (Horst *et al.,* 2016; 2017; Schöllhorn *et al.,* 2002), but may be compromised by (a) the type of data e.g. discrete parameters rather than temporal waveforms, (b) single type of variables rather than a combination of variables e.g. only kinetic or kinematic rather than kinetic and kinematic data, and (c) the inclusion of multiple conditions in the same discrimination procedure (Schöllhorn *et al.,* 2002).

The outcome of this study also supports the idea of a "functional group" as defined by Hoerzer *et al.* (2015), since some discrimination features could be identified for a number of individuals with UTTA. These may be the consequence of the study's inclusion/exclusion criteria that specify the selection of the individuals with UTTA. In the literature, group responses have been attributed to

characteristics such as gender, anthropometrics, and age (Begg and Kamruzzaman, 2005), and are reflected in gait similarities (Hoerzer *et al.,* 2015). Individuals recruited for the experimental group of this study all had a UTTA and had used a prosthesis for at least a year after inpatient treatment. Furthermore, individuals had to be able to walk for three-minute periods at once whilst they are free from pain or other musclo-skeletal disorders. These traits can all contribute to the commonality across individuals. However, the individuals with UTTA may not necessarily have fallen into common functional groups, since other factors influence their gait such as the time since amputation, the cause of amputation and the prosthetics used.

The discrimination between an individual UTTA and the group of able-bodied individuals did not always occur in the first PC and occasionally occurred in the second or even in lower ranked PCs. In some instances, discrimination would occur in multiple different PCs, and the discrimination was for either the prosthetic, the intact or both limbs. Thus, the Eigenspectra would reveal discriminatory features for either one of the limbs or both limbs. Similar to findings of Chapter 5, although PC1 holds the greatest variance, it does not necessarily hold a particular feature of interest, as previously been reported by Phinyomark *et al.* (2015). Principal components as low as numbers 5 and 6 revealed discrimination features, however, these PCs hold features with small weighting factors relative to higher PCs such as 1 and 2.

Two different approaches of PCA were used in this study, i.e. correlation and covariance matrices. The results of the approaches differed, which was expected due to differences in the normalisation procedures. The covariance approach describes the outcome depending on the variance within variables whilst the correlation approach describes the outcome depending on the magnitude of variables. Previous studies that refer to both approaches do not explain the advantages of using one method over the other (Badesa *et al.,* 2014; Chau, 2001a; Daffertshofer *et al.,* 2004). From the result of this study, it was established that depending on the application, one may choose one method over the other, but both reveal important information and thus there is no 'ideal' method, only one that fits the purpose. In this study, in some cases, individuals with UTTA were discriminated by both matrices, in other cases, discriminating features only occurred in one matrix but not the other. Thus, where possible both approaches should be explored since differences may be due to the variance or the magnitude of certain variables.

The most common discriminating features revealed among individuals with UTTA were sagittal hip joint moment and hip joint angle. In Chapter 5, during the discrimination between a group of individuals with UTTA and a group of able-bodied individuals, sagittal hip joint moment was also identified as a discriminating factor, but sagittal hip joint angle was not. Previous studies found that the sagittal hip moment of individuals with LLA is twice as large as that of able-bodied

individuals during heel strike (McNealy & Gard, 2008). Also, a large eccentric flexor moment in the hip joint was identified during the late-mid stance phase (Lemaire *et al.*, 1993). Similar results are shown in this study, but moreover, this study has indicated the magnitude of 'importance' of any one variable. Furthermore, whilst previous studies have revealed that variables different between experimental groups, only a few variables were included during the analysis, in this study, however, a wide range of variables were explored. This indicates that the automatic gait recognition tool can be used to explore a wide range of variables simultaneously, revealing instantly more information.

As recommended by study 2 discussed in Chapter 5, the analysis was conducted by means of an unsupervised search algorithm, i.e. PCA, to investigate variables that naturally differ between one individual with UTTA and a group of able-bodied individuals rather than seeking out difference through the use of a supervised algorithm. Furthermore, continuous gait data was used in the form of temporal waveforms, which have been normalised to 100% of the gait cycle. From research, presented in Chapter 5 and other previous research (Deluzio *et al.*, 1999), temporal waveforms provide more information compared to scalar values and enable a more comprehensive and reliable discrimination procedure.

Previous research reports that the greatest discrimination at an individual level was observed when continuous data (temporal waveforms) of multiple variables (kinematics, forces and joint moments) in different planes of motion were analysed together (Schöllhorn *et al.*, 2002). In this study, similar to the one presented in Chapter 5, the data set considered different gait variables, which were commonly reported in the literature for forward progression and dynamic balance. Thus, the number of variables were limited to the sagittal plane, with a few exceptions such as the GRF. The lack of incorporation of variables from multiple planes of motion may have compromised the discrimination outcome. Thus, in future studies, variables from all anatomical planes should be included in the analysis since these may not only yield greater discrimination results but also provide a better understanding of gait as a wider spectrum of data would be investigated.

In conclusion, an individual with UTTA displays subject-specific gait characteristics which can be identified using PCA. Also, there are certain characteristics which are common in a group of individuals with UTTA. Furthermore, both the covariance approach (with normalised data to units) and the correlation approach can reveal important information, and so where possible both analyses methods should be implemented.

Chapter 7: Effects of Attempted Symmetrical Temporal-Spatial Symmetry on the Dynamic Stability of Individuals with Unilateral Trans-Tibial Amputation.

Bisele, M., Bencsik, M., Lewis, M.G., & Barnett, C.T. (2018) Does attempting symmetry affect dynamic balance during gait un unilateral transtibial prosthesis users? *In Proceedings of the 44th Annual Meeting and Scientific Symposium American Academy of Orthotists and Prosthetists, New Orleans, LA.*

Bisele, M., Bencsik, M., Lewis, M.G., & Barnett, C.T. (2017) How does attempting to walk symmetrically affect dynamic balance in unilateral transtibial amputees? *In Proceedings of the International Society of Prosthetics and Orthotics (ISPO) UK MS Annual Scientific Meeting and Exhibition, Clare College, Cambridge, UK.*

7.1 Introduction

A detrimental, functional limitation of LLA gait is impaired stability and control of balance (Jayakaran *et al.,* 2012). Individuals with LLA are known to fall more often relative to age-matched able-bodied individuals (Miller *et al.,* 2001a; b), which has been attributed to compromised dynamic balance and stability. Because of a high falling incidences, these individuals often develop a fear of falling which consequently prevents them from taking part in everyday activities (Miller *et al.,* 2001a). Although falling is a significant problem (Jayakaran *et al.,* 2012), the underlying mechanisms of it are still not well understood (Curtze *et al.,* 2010).

Walking is an unstable system, which can be stabilised through active control (Hof *et al.,* 2007). Individuals with LLA are known to walk with a lower speed, lower step frequency and higher step width relative to able-bodied individuals (Hak *et al.,* 2013c) and they have been shown to adopt compensatory mechanisms similar to able-bodied individuals in order to regulate stability by adjusting step parameters (Bolger *et al.,* 2014).

The Mos is a measure of stability, which is quantified by the distance between the CoM motion state (i.e. position and velocity) relative to the BoS. In response to a decrease in dynamic stability, individuals with LLA and able-bodied individuals have shown to increase BW and ML MoS, permitting greater stability (Hak *et al.,* 2013a; b; c; Hak et al. 2015). In response to continuous perturbations through a translating walking surface (Hak *et al.,* 2012; Hak *et al.,* 2013c), individuals with LLA and able-bodied individuals, both increased step frequency and step width, decrease step length and kept walking speed constant, which consequently increased BW MoS and ML MoS in an attempt to regulate stability more effectively (Hak *et al.,* 2013c). In a gait adaptability task, both groups decreased step length and increased step width, but did not change step frequency and step walking speed. As a result, BW MoS and ML MoS did not change (Hak *et al.,* 2013c). The BW MoS was found to be smaller for individuals with LLA relative to the able-bodied individuals, which was attributed to their naturally slower self-selected speed (Hak *et al.,* 2013c).

Compensatory mechanisms in individuals with LLA are known to result in asymmetrical gait, which is typically viewed as unwanted, since it is associated with secondary health issues such as lower back pain (Kulkarni *et al.,* 2005) and arthritis in the intact hip and knee joints (Burke *et al.,* 1978). Thus, during prosthetic rehabilitation, a more symmetrical gait is often sought to minimise these secondary issues. Previous research, however, suggests that asymmetrical step parameters, such as step length may play a functional role (Hak *et al.,* 2014). Generally, individuals with LLA were found to have a shorter step length on the intact limb relative to the prosthetic limb (Barnett

et al., 2009; Isakov *et al.,* 1996; Mattes *et al.,* 2000; Zmitrewicz *et al.,* 2006), which has been attributed to reduced push-off capacity on the prosthetic limb (Houdijk *et al.,* 2009; Zmitrewicz *et al.,* 2006). Hak *et al.* (2014), however, found that the shorter step length on the intact limb contributes to a larger BW MoS at heel strike of the intact limb. The lack of ankle push-off on the prosthetic limb during the double support phase decreases the CoM velocity limiting the increase of BW MoS during this phase. Thus, a smaller distance between the leading foot and the CoM is needed to compensate for the limited increase in BW MoS and to decrease the risk of interrupting forward progression. Therefore, in well-established individuals with LLA, temporal-spatial asymmetry aids MoS to be maintained stable (Bolger *et al.,* 2014; Hak *et al.,* 2014). However, the effects of symmetrical gait on stability, which is often desired during prosthetic rehabilitation, are unknown. Therefore, the primary aim of this study was to identify the effects of attempting temporal-spatial symmetry on the dynamic stability of individuals with UTTA and the secondary aim was to understand the biomechanical function of gait when attempting temporal-spatial symmetry.

7.2 Methodology

7.2.1 Participants

A convenience sample of eleven individuals with UTTA (age 50±12years; height 1.7±0.1m; mass 83.94±13.59kg) were recruited from the university and local communities. All participants met the inclusion and exclusion criteria detailed in Section 3.2.2. Ethical approval was granted by the Nottingham Trent University's College of Science and Technology Ethical Review Committee (Humans), the NHS Research Ethics Committee, the NHS Health Research Authority and the NHS Research and Development. All participants provided written informed consent prior to participation.

7.2.2 Experimental Design

Participants visited the biomechanics laboratory on two occasions to collect measurements for four conditions; walking at self-selected speed (NORM), walking with attempted symmetrical step length (SYM_{SL}), walking with attempted symmetrical step frequency (SYM_{SF}), and walking with both attempted symmetrical step length and step frequency (SYM_{SL+SF}). During visit 1, participants walked along a 15m walkway collecting data for the NORM condition. During visit 2, habitual step length and frequency derived from visit 1 were manipulated, so that individuals with UTTA walked at attempted symmetries. The manipulations for visit 2 were calculated using (7.1) and (7.2). For the 'new' symmetrical step length, insulating tape was used to mark the

measurements on the floor, and for the 'new' symmetrical step frequency a metronome was used. The conditions during visit 2 were randomised across participants.

$$SL_{SYM} = \frac{SL_R + SL_L}{2} \quad \textbf{(7.1)}$$

Where:
SL_{SYM} = symmetrical step length
SL_R and SL_L = right and left step length, respectively

$$SF_{SYM} = \frac{SF_R + SF_L}{2} \quad \textbf{(7.2)}$$

Where:
SF_{SYM} = symmetrical step frequency
SF_R and SF_L = right and left step frequency, respectively

7.2.3 Data Acquisition

Upon arrival, the participants were briefed. All activities were completed with participants wearing lycra shorts and everyday shoes. Individuals with UTTA used their habitual prosthesis (Table 3.1). To obtain kinematic measurements 70 spherical 14mm, reflective markers were placed directly onto the skin or clothing using bi-adhesive tape, defining head, arms, trunk (Leardini *et al.,* 2011) and lower limb segments (Cappozzo *et al.*, 1995) (for marker placement, refer to Section 3.3.3). Marker placement on the prosthetic limb was estimated based on marker placement of the intact limb (Powers *et al.,* 1998).

A static trial was obtained for segment definition, followed by the dynamic trials. First, the participant's starting position was defined, to ensure that force platform data was acquired as the participant walked along the walkway. For visit 1, during dynamic trials, participants walked at a self-selected speed along a 15m walkway (Figure 7.1 a). This process was repeated until five successful trials were collected for both limbs, where a successful trial was defined by a clear force plate contact. For visit 2, during attempted SYM_{SL} participants were asked to land with their heel on the tape markings for each step (Figure 7.1 b). The tape was placed along the 15m walkway at a set length as defined by Equation (7.1). During attempted SYM_{SF}, the metronome's frequency was defined by Equation (7.2) and participants were asked to take a step with each sound when walking along the 15m walkway (Figure 7.1 c). Finally, during attempted SYM_{SL+SF}, participants were required to take a step and land with the heel on the tape every time the

metronome sounded (Figure 7.1 d). Each condition was repeated until five successful trials were collected for each limb. Ground reaction force (GRF) was measured at 1000Hz using a single floor-mounted strain gauge force platform (AMTI, Watertown, MA, USA) and kinematics were measured at 100Hz using a nine-camera motion capture system (Qualisys, Gothenburg, SE).

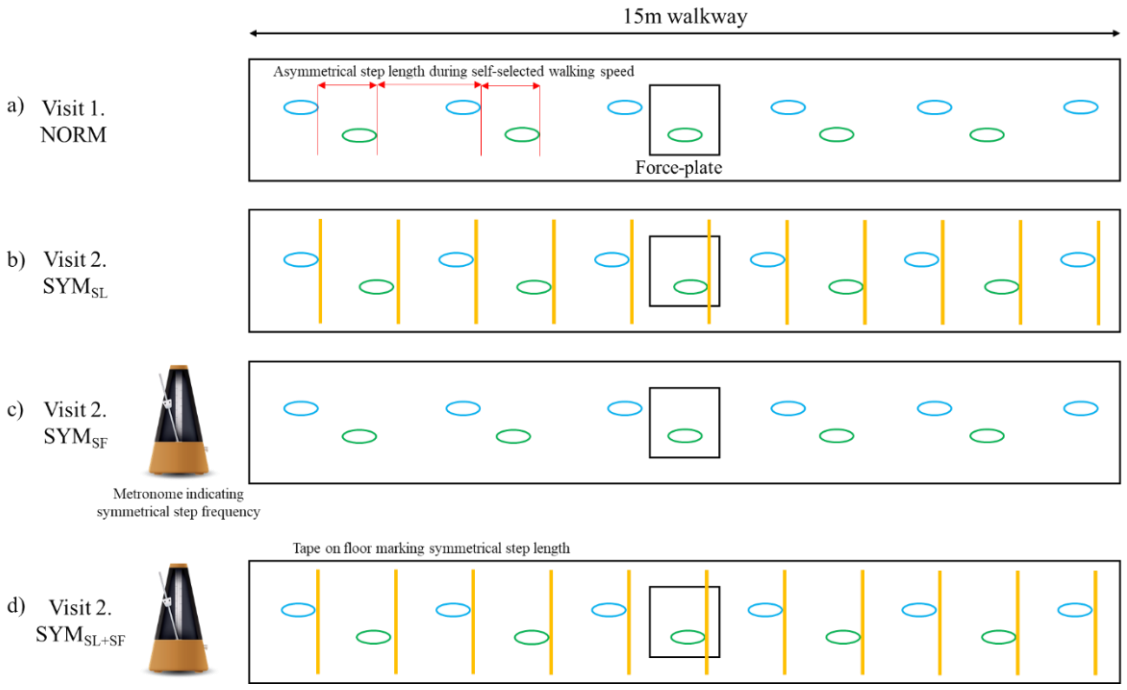

Figure 7.1 Data acquisition method. Data for four conditions were measured during two visits: NORM (a), SYM$_{SL}$ (b), SYM$_{SF}$ (c) and SYM$_{SL+SF}$ (d). The green and the blue ovals show feet placements. Abbreviations are walking at self-selected speed (NORM), walking with attempted symmetrical step length (SYM$_{SL}$), walking with attempted symmetrical step frequency (SYM$_{SF}$), and walking with both attempted symmetrical step length and step frequency (SYM$_{SL+SF}$).

7.2.4 Data Processing

Markers were labelled in QTM v2.2 (Qualisys, Gothenburg, SE) as defined in Section 3.3.3. and trial start and end periods were adjusted so that the maximum number of gait cycles of both limbs were captured. Marker trajectories and force data were exported as .c3d files and subsequently processed in Visual3D v5 (C Motion, Inc., Germantown, MD, USA). Kinematic data were interpolated using a cubic-spline algorithm with kinematic and GRF data being subsequently filtered using 4th order, zero-lag Butterworth low-pass filters with 6Hz and 30Hz cut-off frequencies, respectively. All data were normalised to one gait cycle. Medial and lateral landmarks defined anatomical frames from which segment coordinate systems were defined following the right-hand rule (Cappozzo *et al.*, 1995). A flexion-extension, abduction-adduction and longitudinal Cardan rotation sequence was used to define the order of rotations to calculate

joint kinematics. Gait events of heel strike and toe off were determined using kinetic and kinematic event detection algorithms (Stanhope *et al.,* 1990; Zeni *et al.,* 2008) (Section 3.3.5). Twenty seven biomechanical variables which are typically reported in the literature for forward progression and dynamic stability were included in the analysis (Table 3.25 and Table 3.26) since the continuous interchange between mobility and stability are essential for efficient walking (Lakany, 2008). The biomechanical variables were computed in Visual3D (C-Motion, Inc, Germantown, USA). Processed data were exported from Visual3D as .c3d files, and individual signals were imported to MATLAB® R2016a (MathWorks Inc., MA, USA) for further analysis.

7.2.5 Statistical Analysis

Two statistical analyses were performed. To answer the primary aim of this study a two-way repeated measure analysis of variance (ANOVA) was used and to answer the secondary aim of the study PCA was used. The ANOVA was used to assess the difference between the four conditions (NORM, $SYM_{SL,}$ $SYM_{SF,}$ SYM_{SL+SF}) and the two limbs (PROS and NONPROS) for BW MOS, ML MOS, step length, step frequency, step width and speed. The normality of all the data was assessed using the Shapiro – Wilk Test of Normality ($P > 0.05$). All statistical analyses were conducted in IBM SPSS v.24 (IBM, Portsmouth, UK). Where the assumption of sphericity was violated, a Greenhouse-Geisser correction factor was applied to control for Type I errors (Field, 2013). Effect sizes (partial eta squared) were calculated for each statistical comparison, and posthoc comparisons of significant effects were conducted using the Bonferroni adjustment when statistical significance was identified between conditions/limbs for any of the given variables analysed (Vincent & Weir, 2012). The alpha level (α) of statistical significance was set at $p < 0.05$. During this analysis data from, all eleven individuals with UTTA were assessed.

During the second statistical analysis the effect of the conditions on twenty biomechanical variables (Table 3.25) were assessed using PCA. Both the covariance and the correlation approaches were used as recommended in Chapter 6, since the covariance matrix identifies the differences with regards to variation, whilst the correlation matrix identifies the differences with regards to magnitude. During this analysis, only data from seven individuals with UTTA were assessed. This was due to missing data form four of the individuals. The analyses were conducted as follows:

(1) All individuals with UTTA at NORM were compared to one individual with UTTA during either $SYM_{SL,}$ SYM_{SF} or SYM_{SL+SF}.
(2) All individuals with UTTA at NORM were compared to all individuals with UTTA during either $SYM_{SL,}$ SYM_{SF} or SYM_{SL+SF}.

(3) All individuals with UTTA at NORM were compared to all individuals with UTTA during all conditions.

Procedure (3) comparing all individuals with UTTA at NORM with all individuals with UTTA during all other conditions yielded the best discrimination outcome and thus are presented in the results below. For results of procedures (1) and (2) see Appendix 4.

7.3 Results

7.3.1 Effects of Attempted Symmetry on Backward and Medio-lateral Margin of Stability

The BW MoS (a) and ML MoS (b) relative to the four conditions (NORM, $SYM_{SL,}$ $SYM_{SF,}$ SYM_{SL+SF}) are illustrated in Figure 7.2. The BW MoS of each limb appeared to increase/decrease depending on the condition, but the symmetry/asymmetry that exists between the limbs was preserved. These results could also be observed in the PCA outcome (Figure 7.3 and Figure 7.4) since individual conditions were not separated but instead clustered, possibly because of the preserved symmetry/asymmetry in the data.

The BW MoS showed a significant difference with a large effect size between PROS and NONPROS limbs ($F(1,10) = 11.44$, $p = 0.007$, $\eta_p^2 = 0.534$). The PCA outcome also highlight this difference between PROS and NONPROS limbs which formed separate clusters. The difference between the limbs were attributed to vertical GRF, and sagittal hip, knee and ankle joint angles (Figure 7.3 and Figure 7.4, Eigenspectrum number 2). The BW MoS showed a significant difference between the attempted symmetrical step parameters with medium effect ($F(1.47,14.71) = 6.01$, $p = 0.018$, $\eta_p^2 = 0.376$), where the attempted SYM_{SL} decreased the BW MoS more than any other condition, whilst the attempted SYM_{SF} increased it. The ML MOS showed no significant difference between limbs ($F(1,10) = 0.91$, $p = 0.362$, $\eta_p^2 = 0.084$) nor between conditions ($F(3,30) = 1.32$, $p = 0.285$, $\eta_p^2 = 0.117$).

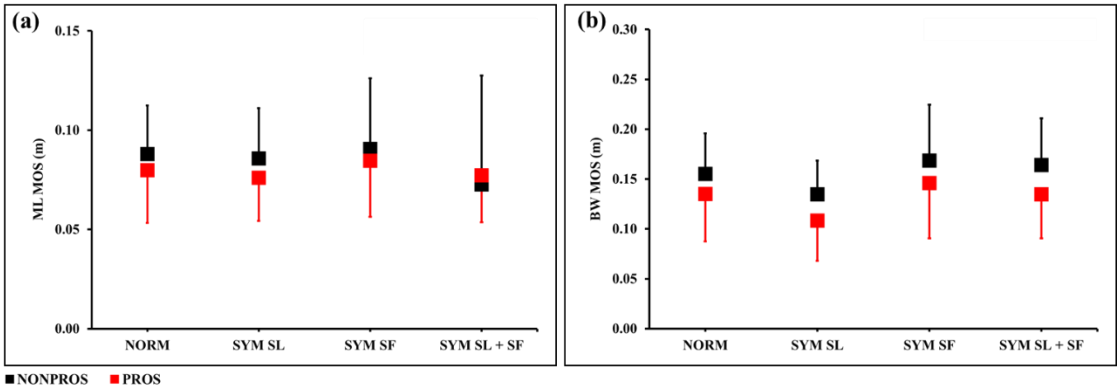

Figure 7.2 BW MoS (a) and ML MoS (b) during the four conditions of NORM, SYM_{SL}, SYM_{SF}, and SYM_{SL+SF}.

The PROS and NONPROS limbs seemed to form separate clusters for each individual with UTTA, where each cluster contained all conditions. The conditions were scattered differently for individuals, whilst some individuals were clustered relatively close together, others were separated, such as participant number 5. The Eigenspectrum of PC1 using the covariance approach identified sagittal hip joint angle (variable number 14) as a causal factor for these individual clusters for each participant, whilst the correlation approach highlighted sagittal hip joint angle (variable number 14) as well anterior-posterior GRF (variable number 1) as causal factors.

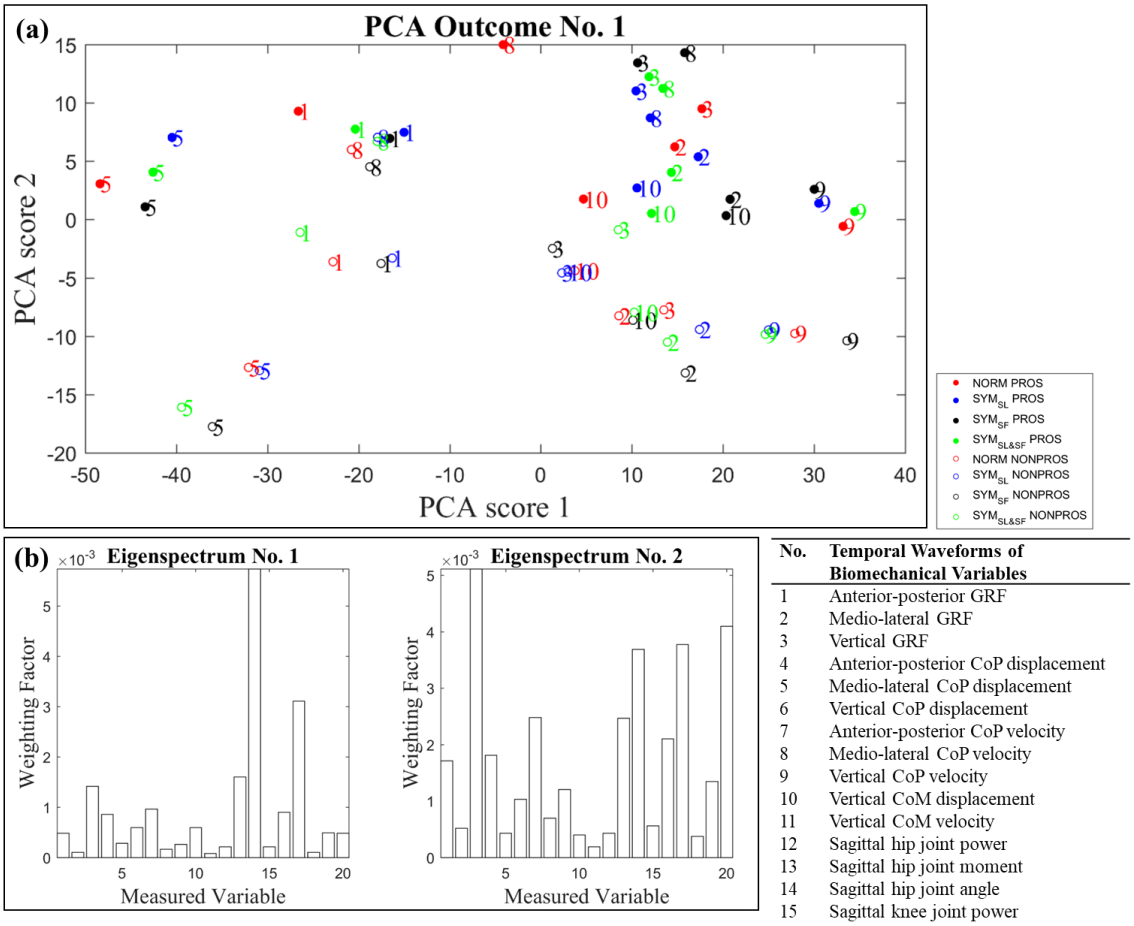

No.	Temporal Waveforms of Biomechanical Variables
1	Anterior-posterior GRF
2	Medio-lateral GRF
3	Vertical GRF
4	Anterior-posterior CoP displacement
5	Medio-lateral CoP displacement
6	Vertical CoP displacement
7	Anterior-posterior CoP velocity
8	Medio-lateral CoP velocity
9	Vertical CoP velocity
10	Vertical CoM displacement
11	Vertical CoM velocity
12	Sagittal hip joint power
13	Sagittal hip joint moment
14	Sagittal hip joint angle
15	Sagittal knee joint power
16	Sagittal knee joint moment
17	Sagittal knee joint angle
18	Sagittal ankle joint power
19	Sagittal ankle joint moment
20	Sagittal ankle joint angle

Figure 7.3 PCA outcome (a) and its Eigenspectra (b) of the covariance matrix comparing individuals with UTTA during all conditions. The different colours indicate conditions, where solid and open circles are the PROS and NONPROS limbs, respectively. The numbers refer to the individual participants.

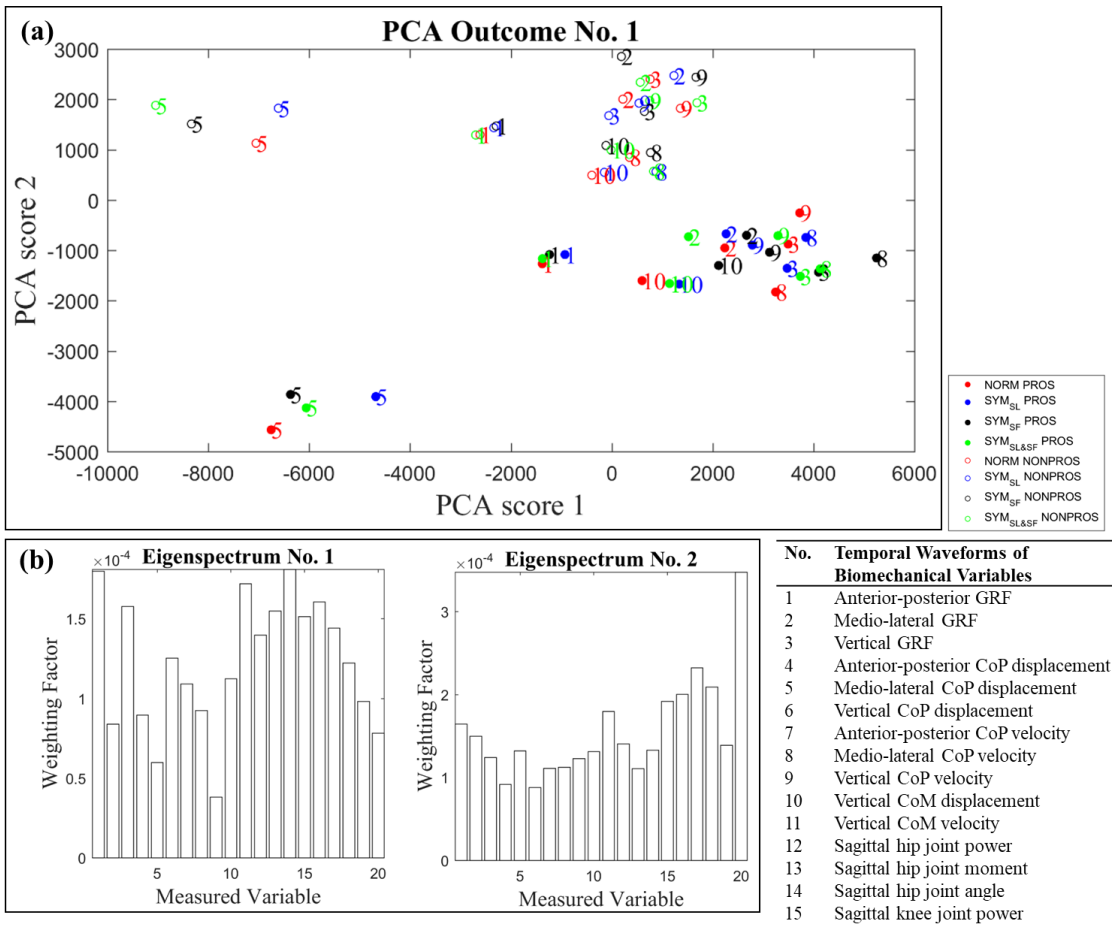

No.	Temporal Waveforms of Biomechanical Variables
1	Anterior-posterior GRF
2	Medio-lateral GRF
3	Vertical GRF
4	Anterior-posterior CoP displacement
5	Medio-lateral CoP displacement
6	Vertical CoP displacement
7	Anterior-posterior CoP velocity
8	Medio-lateral CoP velocity
9	Vertical CoP velocity
10	Vertical CoM displacement
11	Vertical CoM velocity
12	Sagittal hip joint power
13	Sagittal hip joint moment
14	Sagittal hip joint angle
15	Sagittal knee joint power
16	Sagittal knee joint moment
17	Sagittal knee joint angle
18	Sagittal ankle joint power
19	Sagittal ankle joint moment
20	Sagittal ankle joint angle

Figure 7.4 PCA outcome (a) and its Eigenspectra (b) of the correlation matrix comparing individuals with UTTA during all conditions. The different colours indicate conditions, where solid and open circles are the PROS and NONPROS limbs, respectively. The numbers refer to the individual participants.

7.3.2 Effects of Attempted Symmetry on Step Parameters

The results show that the step length was larger on the PROS limb relative to the NONPROS (F(1,10) = 9.14, p = 0.013, η_p^2 = 0.477) (Figure 7.5 a). Furthermore, the step length increased during the attempted symmetry step parameters relative to the NORM condition (F(1.24, 12.42) = 6.40, p = 0.021, η_p^2= 0.390). The Bonferroni post hoc revealed a significant difference between the NORM and attempted SYM_{SL+SF} and SYM_{SL} (p = 0.001), also between NORM and SYM_{SF} (p = .043). The step frequency was lower on the PROS limb relative to the NONPROS but there was no significant difference between them (F(1,10) = 0.53, p = 0.483, η_p^2 = 0.050). However, step frequency differed significantly between conditions with medium effect (F(1.74, 17.37) = 4.58, p = 0.029, η_p^2= 0.314). The step width did not change significantly between the four conditions (F(3,30) 0.81, p = 0.499, η_p^2 = 0.075). The effects of NORM, SYM_{SL}, SYM_{SF} and SYM_{SL+SF} on speed were not normally distributed, thus a Friedman's ANOVA was conducted. Speed differed significantly between conditions, $\chi^2(5) = 9.25$, p = 0.026 and using Wilcoxon tests there were no apparent difference between NORM and SYM_{SL} (p = 0.449), or NORM and SYM_{SF} (p = 0.059), but there was a significant difference between NORM and SYM_{SL+SF} (p = 0.011).

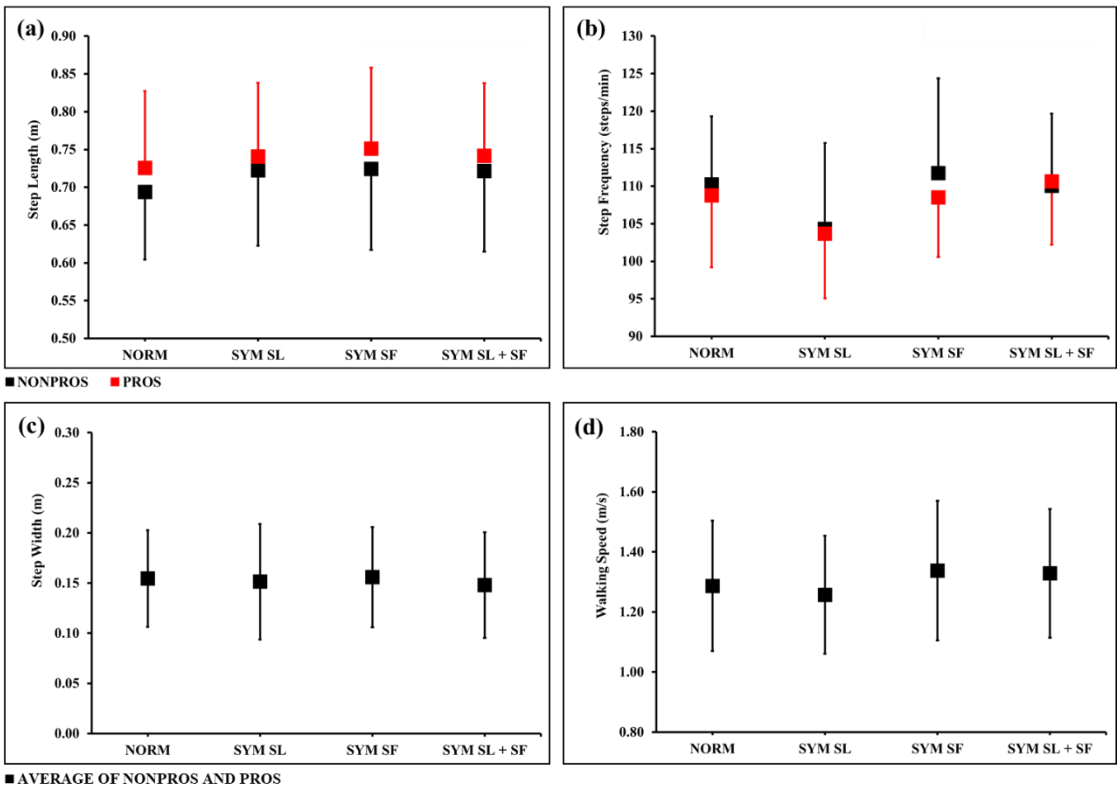

Figure 7.5 The interaction results of NORM, SYM_{SL}, SYM_{SF} and SYM_{SL+SF} on step length (a), step frequency (b), step width (c) and speed (d).

7.4 Discussion and Conclusion

The primary aim of this study was to identify the effects of attempting temporal-spatial symmetry on the dynamic stability of individuals with UTTA and the secondary aim was to understand the biomechanical function of gait when attempting temporal-spatial symmetry. The results show that although symmetrical step parameters were attempted, individuals with UTTA adjusted their limbs and asymmetry was preserved, as evident by the results for the BW MoS. The attempted symmetrical step length (SYM_{SL}) decreased the BW MoS, whereas the attempted symmetrical step frequency (SYM_{SF}) increased BW MoS, thus when combined, these symmetries appeared to counterbalance one another. Speed was found to increase during the attempt of SYM_{SF} and SYM_{SL+SF}, although not significantly during SYM_{SF}. A significant increase in speed during the attempt of SYM_{SL+SF} was probably the consequence of greater step length and step frequency during this condition, which both lead to increased velocity. Previous research suggests that greater velocity improves dynamic coordination between the limbs and thus may lead to increased stability (Donker & Beek, 2002). Furthermore, backward fall can be reduced by a decrease in step length or increase in CoM velocity (Espy *et al.*, 2010; Pai & Patton, 1997), whilst CoM velocity is directly related to increased walking speed (Hak *et al.*, 2012).

Attempted SYM_{SF} increased BW MoS. An increase in BW MoS implies that during the following single-support phase defined by the new stance limb, the CoM can pass the posterior border of the BoS, indicating that the risk of backward loss of balance decreases (Hak *et al.*, 2014). Attempting SYM_{SL}, increased the step length on the intact limb whilst the step length on the prosthetic limb remained constant, i.e. the intact limb adjusted to meet the required symmetry. However, BW MoS decreased indicating a compromise of dynamic stability. Previous findings by Hak *et al.* (2012) and Hak *et al.* (2013c) showed that in response to perturbations individuals with LLA increase step frequency and shorten step length while keeping walking speed constant. Thus, step length was shortened in order to maintain stability, rather than lengthened. Studies have implied that the shorter step length commonly found in the intact limb is a compensation for the lack of CoM velocity when stepping with the prosthetic limb due to reduced push-off capacity, which constrains the BW MoS during the double support phase of the intact limb (Hak *et al.*, 2013c). Therefore, as a result of the attempt to introduce SYM_{SL} in this study, the individuals with UTTA may have lost this compensatory mechanism since the step length on the intact limb increased. The reason for the adjustment on the intact limb rather than the prosthetic limb remains unknown and needs further investigation. A possible explanation would be the inability of the prosthetic limb to adjust to certain changes due to the restrictions proposed by the prosthesis.

The attempted symmetrical step parameters did not have a significant effect on ML MoS. In response to perturbations, individuals with LLA have shown to increase step width probably as a control mechanism to allow ML MoS to increase. Hof *et al.* (2007) state that ML MoS increased because of increased step width and step frequency, where step frequency coincides with an increased in walking speed. However, in this study, the attempted symmetrical step frequency increased the step frequency and speed but did not increase step width. Consequently, this may be why there was no change to ML MoS, which might imply that step frequency and step length are predominantly associated with forward progression and BW MoS. During the assessment of individuals with UTTA in the encounter of uneven surfaces, Curtze *et al.* (2011) reported no change in lateral MoS during the investigation of foot placement with respect to the XCoM. However, Hof *et al.* (2007) reported larger MoS on the prosthetic side during the investigation of individuals with UTFA. Thus, levels of amputation may affect foot placement, although the loss of the ankle structure affects the CoP adjustment in both individuals with UTTA and UTFA.

The PCA outcomes revealed differences between the intact and the prosthetic limb, similar to the results of Chapter 5. These differences were found to be predominantly due to vertical GRF, sagittal hip joint moment, and hip and knee joint angles when using the covariance approach. The correlation approach highlighted sagittal ankle joint angle to be the main driver for a difference between prosthetic and intact limbs. These results are similar to previous findings, which indicate that the ankle joint angle changes between limbs since the prosthetic foot component is rigid compared to the biological ankle joint. Furthermore, the PCA outcome revealed multiple smaller clusters of each individual with UTTA. The clusters were made up of the four conditions, i.e. attempted symmetrical step parameters did not change the way an individual with UTTA walks instead the individual seemed to adjust and preserve asymmetry, as seen by the shift of the limb from its NORM position to various directions in the PC space whilst remaining in close proximity. Previous studies reported similar results of individual clusters of people (Schöllhorn *et al.*, 2002; Chapter 6), and support the need for subject-specific evaluation. Using PCA for subject-specific evaluation can help improve treatment recommendations specifically prosthetic prescriptions, leading to more tailored and effective rehabilitation goals.

A limitation of this study was the small sample size (N=11) used to carry out PCA. Most research concludes that large sample size is required for an accurate analysis to be made (Halilaj *et al.*, 2018). However, in gait analysis, the sample size of populations under investigation is often small due to characteristics of pathologies since it can be difficult to find individuals who have these characteristics. The location of the investigation might place further constrain since there might not be many individuals in certain areas who have these characteristics. Although larger sample

size seems to be more reliable there must be a tradeoff with regards to sampling effort and cost. This study demonstrated that a sample size of N=11 was enough to achieve the stability of eigenvalues and eigenvectors of PCA. However further research is needed, to establish if there is a particular number of participants which would satisfy the criteria for a reliable analysis.

In conclusion, the findings of this study suggest asymmetrical temporal-spatial parameters play a functional role in LLA stability. The PCA outcome further confirmed that asymmetry was preserved during attempted symmetrical conditions since data did not cluster due to conditions, but instead, the prosthetic and intact limbs of individuals with UTTA formed multiple small clusters, suggesting that each individual with UTTA has highly individualised gait characteristics.

Chapter 8: General Discussion and Conclusions

8.1 Discussion

The general aim of this PhD was to adopt multivariate statistical analyses and machine learning algorithms to develop analytical techniques for the assessment and understanding of LLA function. The number of individuals with LLA is expected to increase drastically (Ziegler-Graham *et al.,* 2008). Individuals with LLA lose musculoskeletal mechanisms, joint structures and sensory input vital for movement such as walking, thus the ability to take part in activities of daily living is impacted (Pezzin *et al.,* 2000). Using automatic gait recognition tools in gait analysis, could provide non-invasive diagnosis methods, patient-specific treatment recommendations and evaluation of treatment outcome (Alaqtash *et al.,* 2011b; Lakany, 2008; Pogorelc *et al.,* 2012), thus it could potentially provide a guide for prosthetic prescriptions and rehabilitation programmes during the treatment of individuals with LLA.

In the first study of this thesis presented in Chapter 4, the aim was to develop and optimise a machine learning algorithm. Principal Component Analysis (PCA) was used for data reduction and feature selection, and Discriminant Function Analysis (DFA) was used for classification between barefoot and shod running. To optimise this procedure, all possible iterations of ten individuals out of a total of twenty were explored to establish which combination of participants would provide the best discrimination between the conditions. An error rate was calculated to indicate the number of trials misclassified. The combination of ten individuals with the smallest error rate (6.5% misclassified) was used to train the algorithm, thus optimising it. The best iteration correctly classified footwear condition 93.5% of the time, although the error rates ranged from 6.5% - 50% for other combinations of participants. Thus, the quality of data used to train the machine learning algorithm was improved through the identification of individuals carrying generic features. In instances where the machine learning algorithm is facing the challenge of a mixture of highly ‘generic’ and highly ‘singular’ trials in its training database, it is suggested that by homing onto the highly generic individuals, at the stage of training the computer, substantial improvements may be achieved over the entire group, including the highly ‘singular’ individuals.

The classification method used in this study was conducted in a challenging scenario of the same individual with a subtle change to their gait, as compared to examples found in the literature, which have used clearly discrete heterogeneous groups e.g. healthy vs pathology (Kobsar *et al.,* 2015; Laroche *et al.,* 2014) or young vs. old (Begg & Kamruzzaman, 2005; Eskofier *et al.,* 2013). Therefore, the outcome of the algorithm presented in this study was more likely to reflect the ability of the algorithm rather than the differences between experimental groups. Biomechanical research studies are often conducted using a small sample size, which may have subtle differences

between groups/conditions that are difficult to detect. This study demonstrated a technique that could be implemented during the development of machine learning algorithms to improve their classification performance. Individuals with LLA have shown to have kinematic variables, similar to those of able-bodied individuals (Sanderson & Martin, 1997). Thus such a method could have the potential to facilitate a better understanding of the differences between LLA and able-bodied gait.

The relatively small sample size of this study prevented an estimation to the extent to which accidental spurious information may also have been harvested in the process, i.e. overfitting the data. Nevertheless, by limiting the process to only 10 PCA scores, which was below the rank that still carried information (20^{th}), the likelihood of such phenomena was limited. This ensured the numerical analysis was made immune to overfitting artefacts originating from the over-exploitation of small details (Lever *et al.*, 2016b). Moreover, finding the generic features through the optimisation procedure would also limiting the risks of overfitting. An interesting question is whether it might be possible, in any study similar to this one, to identify the best group size to be used when optimising the training.

Previous studies have limited the amount or type of measured variables used, i.e. variables would only be measured in one plane of motion rather than all three, and only kinetic, kinematic or GRF data would be assessed instead of a combination of the three data types. This study demonstrated that it is possible to analyse large amounts of different types of data, e.g. thirty kinetic, kinematic and GRF variables in different planes of motion, and acquire a large classification accuracy. Assessing many variables simultaneously is not only time efficient but provides an instantaneous in-depth understanding. Furthermore, previous studies demonstrated that including variables from the frontal plane provide better classification results (Schöllhorn *et al.*, 2002). Thus, in order to improve the classification outcome, data from multiple planes should be included during the analysis.

Machine learning algorithms are typically developed in three stages of training, prediction and evaluation (Lever *et al.*, 2016b). A limitation of this study was the absence of the evaluation using an independent sample. An evaluation procedure provides an indication of the accuracy of a classifier's performance. In this study, the evaluation indicated that the sensitivity, i.e. true positives (shod and truly identified as shod) were correctly identified 90% of cases and the specificity, i.e. true negatives (barefoot and correctly identified as barefoot) were correctly identified 91% of cases. However, the evaluation stage was not conducted using an independent sample, but instead, the classification of the sample was known.

Machine learning algorithms can provide a better understanding of pathological gait. In LLA gait, it has been used extensively to improve prosthetic components (Afzal *et al.,* 2017; Chen *et al.,* 2013; Dutta *et al.,* 2011; Hargrove *et al.,* 2015; Huang *et al.,* 2011; Joshi and Hahn, 2016; Khan *et al.,* 2018; Miller *et al.,* 2013; Pew and Klute, 2017; Simon *et al.,* 2016; Woodward *et al.,* 2016; Young *et al.,* 2013; Young *et al.,* 2014; Zheng *et al.,* 2013; Zheng and Wang, 2017), however to be able to provide an individual with LLA with a better prosthesis, his/her function needs to be better understood to identify their requirements. Thus, in the second study (Chapter 5), different techniques were explored to compare the gait of individuals with LLA and able-bodied individuals providing a better understanding of LLA function. Using the Eigenspectra, it was highlighted that variables such as vertical GRF, sagittal hip joint moment, and sagittal knee joint angle caused the differences, providing a better understanding of what distinguishes between individuals with and without a UTTA. It was also established that in this particular application of PCA the use of normalised temporal waveforms provided a better method to identify important variables and understanding the gait differences between individuals with UTTA and able-bodied individuals:

- the normalisation ensured that all variables were considered of equal weighting regardless of the magnitude when using the covariance matrix,
- the waveforms included the information of the scalar values and also additional information which suggests that the use of scalar values extracted from the temporal gait waveforms may be redundant,
- PCA was sufficient without implementing DFA since DFA is supervised and seeks out differences, but instead, PCA highlights differences that occur in the gross structure which may be more suitable for clinical applications.

In this study highlights that no single method would be suitable in every application but instead the method depends on the features of a data set which also been previously reported by Harper (2005). The technique established in this study could be implemented to provide a better understanding of LLA gait.

Using temporal waveforms is more advantageous compared to scalar values since data spans the entire gait cycle, and so provides more information (Deluzio *et al.,* 1997). However, in cases where only scalar values (discrete parameters) are available, the researcher should be aware that misclassification may be likely to occur (Schöllhorn *et al.,* 2002). It should also be noted that the selection of relevant variables is important as demonstrated by this study. Using 7 scalar values did not improve the classification outcome, but speed which was one of the additional variables

added was identified as a discriminating variable between the gait of individuals with UTTA and able-bodied individuals.

Studies often compare the variables of groups of people/condition to investigate whether they differ or not. In this study, it was demonstrated that multivariate statistical analyses could reveal if groups differ as well as order variables that cause the differences according to their contribution to this difference by means of the weighting factors. This may have great implications as it may highlight which variables need to be addressed during an intervention. Furthermore, the results of the PCA outcome revealed that the differences between the UTTA and able-bodied gait were in lower ranked PCs, indicating that PC1 does not necessarily always hold the variables of interest, although it holds the greatest variance. This highlights the importance of the remaining PCs, as previously discussed by Phinyomark *et al.* (2016). It should be noted, however, that lower PCs holds lower variance and thus variables may have smaller weighting factors. Thus, the difference observed in the lower ranked PCs may only make up very small, almost unidentifiable sections in a 2D profile of temporal waveforms.

In this study, the main variables identified as discriminating factors between UTTA and able-bodied gait were vertical GRF, sagittal hip joint moment and sagittal knee joint angle. Previous studies found that between UTFA and able-bodied gait the vertical GRF discriminated between the control limb and the prosthetic limb in PC1, while PC2 discriminated between the control limbs and both the limbs of the individuals with UTFA (Soares *et al.*, 2016). The magnitude of the vertical GRF was found to be much smaller on the prosthetic limb, which may have been a protective mechanism to reduce loading on the residual limb. In the current study using PCA, no discrimination was observed in PC1, but a similar outcome was observed in PC2, which is most likely due to the varying levels of amputation since the current study investigated individuals with UTTA.

The biomechanical variables included in studies 2-4 presented in Chapters 5-7 were commonly reported in the literature for the assessment and investigation of forward progression and dynamic stability of LLA gait. The majority of these variables were reported in the sagittal plane. However, it has been demonstrated that data in the frontal plane improves classification outcome and provides more information (Schöllhorn *et al.*, 2002, Chapter 4). Thus, referring to a previous discussion point, data from multiple planes should be included. However, the use of data from different planes should be approached with caution since ambiguous and erroneous data such as soft tissue artefacts can negatively affect the results (Phinyomark *et al.*, 2018).

Studies have used a combination of different machine learning algorithms, seeking the highest classification outcome (Afzal *et al.,* 2017; Chen *et al.,* 2013; Joshi & Hahn, 2016; Khan *et al.,* 2018; Miller *et al.,* 2013; Pew & Klute, 2017). Thus, in future studies a combination of different methods may reveal more information and better understand of LLA gait, which could potentially help better treatment recommendations. Exploring different methods can help identify a technique to reduce time consumption during training and testing procedures of a machine learning algorithm as previously done by Woodward *et al.* (2016). In a clinical setting, a quick diagnosis would be more cost effective and could help reduce the financial burden on health institutions.

Since clinical analysis is commonly based on patient-specific assessments, the third study presented in Chapter 6 was conducted to investigate if distinct gait characteristics can be identified for one individual with UTTA. Therefore, an individual with UTTA was discriminated from a group of able-bodied individuals. The covariance and correlation approaches of PCA were used during this analysis. The results demonstrated that some characteristics were common among individuals with UTTA whilst others were specific to an individual. These findings were similar to previous research which reported subject-specific gait characteristics of able-bodied individuals (Schöllhorn *et al.,* 2002) as well as "functional groups" which describes a group of individuals that share similar characteristics (Horst *et al.,* 2017). This study demonstrates that multivariate statistical analyses could aid as a patient-specify diagnosis tool in clinical settings.

The outcome of the covariance and correlation matrices differed, which was due to the varying normalisation procedure of the two approaches. Previous studies that mentioned the use of both the covariance and the correlation matrices during gait analysis did not recommend one approach over the other (Badesa *et al.,* 2014; Chau, 2001a; Daffertshofer *et al.,* 2004). This study demonstrates the importance of using both approaches since the covariance matrix takes into consideration the range whilst the correlation matrix considers the magnitude of the data, providing important information. Thus the researcher was supplied with varying information from these approaches which were equally important since one approach indicated the differences between participants as a result of the variation of variables and the other as a result of the magnitude of variables. Therefore, where possible both approaches should be implemented.

In the literature, it is commonly reported that compensatory mechanisms in individuals with LLA lead to asymmetrical gait, which is associated with secondary health issues such as lower back pain (Kulkarni *et al.,* 2005) and arthritis in the intact hip and knee joint (Burke *et al.,* 1978). Recent studies, however, have found that asymmetrical gait may play a functional role in well-established individuals with LLA. Therefore, the fourth and final study presented in Chapter 7 investigated the effects of attempted symmetrical step parameters on the dynamic stability of

individuals with UTTA. Furthermore, the multivariate statistical analysis, PCA, was used to establish if underlying mechanisms of these effects can be identified. The main finding of this study was that asymmetry was preserved in UTTA gait although symmetrical step parameters were attempted, which was also reflected by the lack of clustering of conditions in the PCA outcome.

In previous research, it was found that individuals with LLA increased step frequency and decreased step length in order to maintain stability (Hak *et al.*, 2013c). In the current study, attempting symmetrical step length reduced BW MoS. Previous studies highlight that shorter step length on the intact limb is a compensatory mechanism attributed to reduced push-off capacity on the prosthetic limb since attempting symmetrical step length increased the step on the intact limb this mechanism was removed, explaining the reduction of BW MoS observed. Thus, the results of this study confirmed previous findings by Hak *et al.* (2013c) who suggested that temporal-spatial asymmetry may be playing a functional role.

The PCA outcome further revealed individual clusters comprised of the conditions of the same individual with UTTA, confirming previous results (Schöllhorn *et al.*, 2002; Chapter 6). The clusters also highlighted the difference between the prosthetic and the intact limb of individuals with UTTA previously seen in the DFA outcome presented in Chapter 5.

A limitation of this study was the small sample size used during PCA. However, the investigation of pathological groups in gait analysis is often performed using a small sample since characteristics of certain pathology place a constraint in finding individuals who are suited for the analysis. Although larger sample size seems to be more reliable, the first study of this PhD, presented in Chapter 4, introduces a method which could be used to optimise a machine learning algorithm and overcome the dangers of overfitting even when working with small sample size. However further research is needed, to establish the specific number of participants which would satisfy the criteria for a reliable analysis.

This thesis demonstrates that multivariate statistical analyses such as PCA can help understand certain phenomenon of gait which were previously not well understood. In a clinical environment, such findings have the potential to improve treatment recommendations. In individuals with LLA, it may assist in the choice of a suitable prosthesis or help set rehabilitation goals. Furthermore, these methods could be used to define the cost functions of a computer simulation, which can help facilitate individualised treatment by identifying the effects of certain factors on the computer simulation. In the case where the computer simulation reveals an outcome, which is sought for, it could be translated into clinical practice to inform treatment. The advantage of using multivariate

statistical analyses to inform a computer simulation means that a possible treatment outcome could be predicted, prior to applying the treatment to the patient. Thus, it can be identified if a treatment may be suitable or an alternative is required.

8.2 Conclusion

In conclusion, LLA and able-bodied gait differed as well as prosthetic and intact limbs differed. Individuals with UTTA reveal common group gait characteristics and unique subject-specific gait characteristics. Principal Component Analysis could be used to compare between individuals at group and subject-specific levels, providing a better understanding of gait. In a clinical setting, PCA may be a useful assessment tool.

Different multivariate statistical analyses and machine learning algorithms can be used to assess and understand gait, however there is not a single best method that can be standardised for all applications of gait analysis. Instead, the best performing algorithm depends on the features of a data set. The methods of this research have demonstrated that certain techniques can be implemented to improve classification accuracies of machine learning algorithms providing a better understanding of pathological gait. For example, the training and prediction data sets of a machine learning algorithm should be optimised using an iteration procedure when working with a small sample size to overcome issues of overfitting. Furthermore, entire temporal waveforms should be implemented instead of discrete parameters since they provide more information and characteristics of gait data are considered. Where entire temporal waveforms are not available the discrete parameters should be selected with care. Also, both the correlation and the covariance approaches of PCA should be implemented since they reveal information regarding magnitude and variance of the data which can both be relevant during the treatment of a patient. When using the covariance matrix, variables need to be normalised since scaling of variables will influence the classification accuracy.

This research demonstrates that in a clinical setting the analysis involving all possible variables resulted in comprehensive ranking order. This is in contrast with other studies which compared a lower number of variables, therefore, having a limited scope of the problem. The ability to investigate a large number of variables and establish the order in which these deviate from what is considered healthy for a particular group of people with pathological gait, allows treatment to be targeted at particular variables which have been highlighted as an issue. Additionally, ranking of variables can be identified at patient-specific level. These findings could have great impact in the medical world, since they present a potential for tailored treatment thus in turn the treatment outcome may be more successful improving patient’s quality of life.

Chapter 9: References

Afzal, T., Iqbal, K., White, G., & Wright, A. B. (2017) A Method for Locomotion Mode Identification Using Muscle Synergies. *IEEE Transactions on Neural Systems and Rehabilitation Engineering*, 25 (6), 608–617. Available From: https://doi.org/10.1109/TNSRE.2016.2585962

Ahmad, N., Thomas, G. N., Gill, P., Chan, C., & Torella, F. (2014) Lower limb amputation in England: prevalence, regional variation and relationship with revascularisation, deprivation and risk factors. A retrospective review of hospital data. *Journal of the Royal Society of Medicine*, 107 (12), 483–489. Available From: https://doi.org/10.1177/0141076814557301

Amputee Coalition. (2018) *Limb Loss Statistics - Amputee Coalition*. [ONLINE] Available at: https://www.amputee-coalition.org/resources/limb-loss-statistics/. [Accessed 28 June 2018].

Alahakone, A. U., Senanayake, S. M. N. A., & Senanayake, C. M. (2010) Smart wearable device for real time gait event detection during running. *IEEE Asia-Pacific Conference on Circuits and Systems, Proceedings, APCCAS*, 612–615. Available From: https://doi.org/10.1109/APCCAS.2010.5774975

Alaqtash, M., Sarkodie-Gyan, T., Yu, H., Fuentes, O., Brower, R., & Abdelgawad, A. (2011a) Automatic classification of pathological gait patterns using ground reaction forces and machine learning algorithms. *Annual International Conference of the IEEE Engineering in Medicine and Biology Society*, 453–7. Available From: https://doi.org/10.1109/IEMBS.2011.6090063

Alaqtash, M., Yu, H., Brower, R., Abdelgawad, A., & Sarkodie-Gyan, T. (2011b) Application of wearable sensors for human gait analysis using fuzzy computational algorithm. *Engineering Applications of Artificial Intelligence*, 24 (6), 1018–1025. Available From: https://doi.org/10.1016/j.engappai.2011.04.010

Ali, S. & Shah, M. (2010) Human action recognition in videos using kinematic features and multiple instance learning. *IEEE Transactions on Pattern Analysis and Machine Intelligence*, 32 (2), 288–303. Available From: https://doi.org/10.1109/TPAMI.2008.284

Alva, M. L., Gray, A., Mihaylova, B., Leal, J., & Holman, R. R. (2015) The impact of diabetes-related complications on healthcare costs: New results from the UKPDS (UKPDS 84) *Diabetic Medicine*, 32 (4), 459–466. Available From: https://doi.org/10.1111/dme.12647

Ardestani, M. M., Moazen, M., & Jin, Z. (2014) Gait modification and optimization using neural network-genetic algorithm approach: Application to knee rehabilitation. *Expert Systems with Applications*, 41 (16), 7466–7477. Available From: https://doi.org/10.1016/j.eswa.2014.06.034

Arellano, C. J., O'Connor, D. P., Layne, C., & Kurz, M. J. (2009) The independent effect of added mass on the stability of the sagittal plane leg kinematics during steady-state human walking. *Journal of Experimental Biology*, 212 (12), 1965–1970. Available From: https://doi.org/10.1242/jeb.026153

Asadi, H., Dowling, R., Yan, B., & Mitchell, P. (2014) Machine learning for outcome prediction of acute ischemic stroke post intra-arterial therapy. *PLoS ONE*, 9 (2), 14–19. Available From: https://doi.org/10.1371/journal.pone.0088225

Astephen, J.L., Deluzio, K.J., Caldwell, G.E., Dunbar, M.J. and Hubley-Kozey, C.L. (2008) Gait and neuromuscular pattern changes are associated with differences in knee osteoarthritis severity levels. *Journal of Biomechanics*, 41 (4), 868-876.

Azhar, M. A., Gouwanda, D., & Gopalai, A. A. (2014) Development of an intelligent real-time heuristic-based algorithm to identify human gait events. *In Biomedical and Health Informatics (BHI), 2014 IEEE-EMBS International Conference*, 573–576.

Badesa, F. J., Morales, R., Garcia-Aracil, N., Sabater, J. M., Casals, A., & Zollo, L. (2014) Auto-adaptive robot-aided therapy using machine learning techniques. *Computer Methods and Programs in Biomedicine*, 116 (2), 123–130. Available From: https://doi.org/10.1016/j.cmpb.2013.09.011

Baker, P. A. & Hewison, S. R. (1990) Gait recovery pattern of unilateral lower limb amputees during rehabilitation. *Prosthetics and Orthotics International*, 14 (2), 80–84. Available From: https://doi.org/10.3109/03093649009080327

Baker, R., McGinley, J. L., Schwartz, M. H., Beynon, S., Rozumalski, A., Graham, H. K., & Tirosh, O. (2009) The gait profile score and movement analysis profile. *Gait & Posture*, 30(3), 265–9. Available From: https://doi.org/10.1016/j.gaitpost.2009.05.020

Bamberg, S.J.M., Benbasat, A.Y., Scarborough, D.M., Krebs, D.E., &Paradiso, J.A. (2008) Gait analysis using a shoe-integrated wireless sensor system. *IEEE Transactions on Information Technology in Biomedicine*, 12 (4), 413-423. Available From: https://doi.org/10.1109/TITB.2007.899493

Barnett, C., Vanicek, N., Polman, R., Hancock, A., Brown, B., Smith, L., & Chetter, I. (2009) Kinematic gait adaptations in unilateral transtibial amputees during rehabilitation. *Prosthetics and Orthotics International*, 33 (2), 135–147. Available From: https://doi.org/10.1080/03093640902751762

Barrett, P.T. and Kline, P. (1981) The observation to variable ratio in factor analysis. *Personality Study & Group Behaviour*.

Barton, G. J., Hawken, M. B., Holmes, G., & Schwartz, M. H. (2015) A gait index may underestimate changes of gait: a comparison of the Movement Deviation Profile and the Gait Deviation Index. *Computer Methods in Biomechanics and Biomedical Engineering*, 18 (1), 57–63. Available From: https://doi.org/10.1080/10255842.2013.776549

Barton, G. J., Hawken, M. B., Scott, M. A., & Schwartz, M. H. (2012) Movement Deviation Profile: A measure of distance from normality using a self-organizing neural network. *Human Movement Science*, 31 (2), 284–294. Available From: https://doi.org/10.1016/j.humov.2010.06.003

Barton, G., Lees, A., Lisboa, P., & Attfield, S. (2006) Visualisation of gait data with Kohonen self-organising neural maps. *Gait & Posture*, 24 (1), 46–53. Available From: https://doi.org/10.1016/j.gaitpost.2005.07.005

Begg, R. K., Palaniswami, M., & Owen, B. (2005) Support vector machines for automated gait classification. *IEEE Transactions on Biomedical Engineering*, 52 (5), 828–838. Available From: https://doi.org/10.1109/TBME.2005.845241

Begg, R. & Kamruzzaman, J. (2005) A machine learning approach for automated recognition of movement patterns using basic, kinetic and kinematic gait data. *Journal of Biomechanics*, 38 (3), 401–408. Available From: https://doi.org/10.1016/j.jbiomech.2004.05.002

Bell, A. L., Brand, R. A., & Pedersen, D. R. (1989) Prediction of hip joint centre location from external landmarks. *Human Movement Science*, 8 (1), 3–16. Available From: https://doi.org/10.1016/0167-9457(89)90020-1

Bell, A. L., Pedersen, D. R., & Brand, R. A. (1990) A comparison of the accuracy of several hip center location prediction methods. *Journal of Biomechanics*, 23 (6), 617–621. Available From: https://doi.org/10.1016/0021-9290(90)90054-7

Biswas, D., Cranny, A., Gupta, N., Maharatna, K., Achner, J., Klemke, J., Jöbges, M. and Ortmann, S. (2015) Recognizing upper limb movements with wrist worn inertial sensors using k-means clustering classification. *Human Movement Science*, 40,.59-76.

Board, W. J., Street, G. M., & Caspers, C. (2001) A comparison of trans-tibial amputee suction and vacuum socket conditions. *Prosthetics and Orthotics International*, 25 (3), 202–209. Available From: https://doi.org/10.1080/03093640108726603

Bolger, D., Ting, L. H., & Sawers, A. (2014) Individuals with transtibial limb loss use interlimb force asymmetries to maintain multi-directional reactive balance control. *Clinical Biomechanics*, 29 (9), 1039–1047. Available From: https://doi.org/10.1016/j.clinbiomech.2014.08.007

Bonnefoy-Mazure, A., Sagawa Jr, Y., Lascombes, P., De Coulon, G. and Armand, S. (2013) Identification of gait patterns in individuals with cerebral palsy using multiple correspondence analysis. *Research in Developmental Disabilities*, 34 (9), 2684-2693.

Braunstein, B., Arampatzis, A., Eysel, P., & Brüggemann, G. P. (2010) Footwear affects the gearing at the ankle and knee joints during running. *Journal of Biomechanics*, 43 (11), 2120–2125. Available From: https://doi.org/10.1016/j.jbiomech.2010.04.001

Breakey, J. (1976) Gait of Unilateral Below-Knee Amputees. *Orthotics and Prosthetics*, 30(3), 17–24.

Brehm, M. A., Harlaar, J., & Schwartz, M. (2008) Effect of ankle-foot orthoses on walking efficiency and gait in children with cerebral palsy. *Journal of Rehabilitation Medicine*, 40 (7), 529–534. Available From: https://doi.org/10.2340/16501977-0209

Breiman, L. (1984) *Classification and Regression Trees*. Routledge. Available From: https://doi.org/10.1201/9781315139470

Bruijn, S. M., Wisse, M., Draaijers, E., van Dieën, J. H., Meijer, O. G., & Beek, P. J. (2008) The gait sensitivity norm in human walking. *In Proc. of Dynamic Walking Conf., Delft, The Netherlands, 26–29 May*.

Burke, M. J., Roman, V., & Wright, V. (1978) Bone and joint changes in lower limb amputees. *Annals of the Rheumatic Diseases*, 37 (3), 252–254. Available From: https://doi.org/10.1136/ard.37.3.252

Callaghan, B. G., & Condie, M. E. (2003) A post-discharge quality of life outcome measure for lower limb amputees: test–retest reliability and construct validity. *Clinical Rehabilitation*, 17 (8), 858–864. Available From: https://doi.org/10.1191/0269215503cr689oa

Cappozzo, A., Catan, F., Crocel, U., & Leardini, A. (1995) Position and orientation in space of bones during movement: anatomical frame definition and determination. *Clinical Biomechanics*, 10 (4), 171–178. Available From: https://doi.org/10.1016/0268-0033(95)91394-T

Chan, H., Yang, M., Wang, H., & Zheng, H. (2013) Assessing Gait Patterns of Healthy Adults Climbing Stairs Employing Machine Learning Techniques. *International Journal of Intelligent Systems*, 28 (3), 257–70. Available From: https://doi.org/10.1002/int

Chan, H., Yang, M., Zheng, H., Wang, H., Sterritt, R., & McClean, S. (2011) Machine learning and statistical approaches to assessing gait patterns of younger and older healthy adults climbing stairs. *In Natural Computation (ICNC), 2011 Seventh International Conference On*, 588–592. Available From: https://doi.org/10.1109/ICNC.2011.6022097

Chang, M. D., Sejdić, E., Wright, V., & Chau, T. (2010) Measures of dynamic stability: Detecting differences between walking overground and on a compliant surface. *Human Movement Science*, 29 (6), 977–986. Available From: https://doi.org/10.1016/j.humov.2010.04.009

Chau, T. (2001a) A review of analytical techniques for gait data. Part 1: Fuzzy, statistical and fractal methods. *Gait & Posture*, 13 (1), 49–66. Available From: https://doi.org/10.1016/S0966-6362(00)00094-1

Chau, T. (2001b) A review of analytical techniques for gait data. Part 2: neural network and wavelet methods. *Gait & Posture*, 13 (2), 102–120. Available From: https://doi.org/10.1016/S0966-6362(00)00095-3

Chen, B., Zheng, E., Fan, X., Liang, T., Wang, Q., Wei, K., & Wang, L. (2013) Locomotion mode classification using a wearable capacitive sensing system. *IEEE Transactions on Neural Systems and Rehabilitation Engineering*, 21 (5), 744–755. Available From: https://doi.org/10.1109/TNSRE.2013.2262952

Chow, D. H. K., Holmes, A. D., Lee, C. K. L., & Sin, S. W. (2006) The effect of prosthesis alignment on the symmetry of gait in subjects with unilateral transtibial amputation. *Prosthetics and Orthotics International*, 30(2), 114–128. Available From: https://doi.org/10.1080/03093640600568617

Collins, T. D., Ghoussayni, S. N., Ewins, D. J., & Kent, J. A. (2009) A six degrees-of-freedom marker set for gait analysis: Repeatability and comparison with a modified Helen Hayes set. *Gait & Posture*, 30 (2), 173–180. Available From: https://doi.org/10.1016/j.gaitpost.2009.04.004

Curtze, C., Hof, A. L., Otten, B., & Postema, K. (2010) Balance recovery after an evoked forward fall in unilateral transtibial amputees. *Gait & Posture*, 32 (3), 336–341. Available From: https://doi.org/10.1016/j.gaitpost.2010.06.005

Curtze, C., Hof, A. L., Postema, K., & Otten, B. (2011) Over rough and smooth: Amputee gait on an irregular surface. *Gait & Posture*, 33 (2), 292–296. Available From: https://doi.org/10.1016/j.gaitpost.2010.11.023

Daffertshofer, A., Lamoth, C. J. C., Meijer, O. G., & Beek, P. J. (2004) PCA in studying coordination and variability: a tutorial. *Clinical Biomechanics (Bristol, Avon)*, 19 (4), 415–28. Available From: https://doi.org/10.1016/j.clinbiomech.2004.01.005

Damouras, S., Chang, M. D., Sejdić, E., & Chau, T. (2010) An empirical examination of detrended fluctuation analysis for gait data. *Gait & Posture*, 31 (3), 336–340. Available From: https://doi.org/10.1016/j.gaitpost.2009.12.002

Dawson, I., Keller, B. P. J. A., Brand, R., Pesch-Batenburg, J., & van Bockel, J. H. (1995) Late outcomes of limb loss after failed infrainguinal bypass. *Journal of Vascular Surgery*, 21 (4), 613–622. Available From: https://doi.org/10.1016/S0741-5214(95)70193-1

Deluzio, K. J. & Astephen, J. L. (2007) Biomechanical features of gait waveform data associated with knee osteoarthritis: an application of principal component analysis. *Gait & Posture*, 25 (1), 86–93. Available From: https://doi.org/10.1016/j.gaitpost.2006.01.007

Deluzio, K. J., Wyss, U. P., Costigan, P. a., Sorbie, C., & Zee, B. (1999) Gait assessment in unicompartmental knee arthroplasty patients: Principal component modelling of gait waveforms and clinical status. *Human Movement Science*, 18 (5), 701–711. Available From: https://doi.org/10.1016/S0167-9457(99)00030-5

Deluzio, K. J., Wyss, U. P., Zee, B., Costigan, P. a., & Serbie, C. (1997) Principal component models of knee kinematics and kinetics: Normal vs. pathological gait patterns. *Human Movement Science*, 16 (2–3), 201–217. Available From: https://doi.org/10.1016/S0167-9457(96)00051-6

Detrembleur, C., Vanmarsenille, J. M., De Cuyper, F., & Dierick, F. (2005) Relationship between energy cost, gait speed, vertical displacement of centre of body mass and efficiency of pendulum-like mechanism in unilateral amputee gait. *Gait & Posture*, 21 (3), 333–340. Available From: https://doi.org/10.1016/j.gaitpost.2004.04.005

Diabetes UK. (2018) *More than 135 diabetes amputations every week | Diabetes UK*. [ONLINE] Available at: https://www.diabetes.org.uk/About_us/News/More-than-135-diabetes-amputations-every-week. [Accessed 28 June 2018].

Dillingham, T. R., Pezzin, L. E., & Shore, A. D. (2005) Reamputation, mortality, and health care costs among persons with dysvascular lower-limb amputations. *Archives of Physical Medicine and Rehabilitation*, 86 (3), 480–486. Available From: https://doi.org/10.1016/j.apmr.2004.06.072

Dillmann, U., Holzhoffer, C., Johann, Y., Bechtel, S., Gräber, S., Massing, C., Louis, A. K. (2014) Principal Component Analysis of gait in Parkinson's disease: Relevance of gait velocity. *Gait & Posture*, 39 (3), 882–887. Available From: https://doi.org/10.1016/j.gaitpost.2013.11.021

Divert, C., Mornieux, G., Baur, H., Mayer, F., & Belli, A. (2005) Mechanical comparison of barefoot and shod running. *International Journal of Sports Medicine*, 26 (7), 593–598. Available From: https://doi.org/10.1055/s-2004-821327

Dobson, F., Morris, M. E., Baker, R., & Graham, H. K. (2007) Gait classification in children with cerebral palsy: A systematic review. *Gait & Posture*, 25 (1), 140–152. Available From: https://doi.org/10.1016/j.gaitpost.2006.01.003

Donker, S. F., & Beek, P. J. (2002) Interlimb coordination in prosthetic walking: Effects of asymmetry and walking velocity. *Acta Psychologica*, 110 (2–3), 265–288. Available From: https://doi.org/10.1016/S0001-6918(02)00037-9

Duclos, C., Desjardins, P., Nadeau, S., Delisle, A., Gravel, D., Brouwer, B., & Corriveau, H. (2009) Destabilizing and stabilizing forces to assess equilibrium during everyday activities. *Journal of Biomechanics*, 42 (3), 379–382. Available From: https://doi.org/10.1016/j.jbiomech.2008.11.007

Dutta, A., Koerding, K., Perreault, E., & Hargrove, L. (2011) August. Sensor-fault tolerant control of a powered lower limb prosthesis by mixing mode-specific adaptive Kalman filters. In *Engineering in Medicine and Biology Society, EMBC, 2011 Annual International Conference of the IEEE* (3696-3699).

England, S. A. & Granata, K. P. (2007) The influence of gait speed on local dynamic stability of walking. *Gait & Posture*, 25 (2), 172–178. Available From: https://doi.org/10.1016/j.gaitpost.2006.03.003

Eskofier, B. M., Federolf, P., Kugler, P. F., & Nigg, B. M. (2013) Marker-based classification of young-elderly gait pattern differences via direct PCA feature extraction and SVMs. *Computer Methods in Biomechanics and Biomedical Engineering*, 16 (4), 435–442. Available From: https://doi.org/10.1080/10255842.2011.624515

Espy, D. D., Yang, Y., & Pai, Y. C. (2010) Control of center of mass motion state through cuing and decoupling of spontaneous gait parameters in level walking. *Journal of Biomechanics*, 43 (13), 2548–2553. Available From: https://doi.org/10.1016/j.jbiomech.2010.05.015.CONTROL

Esquenazi, A. (2014) Gait analysis in lower-limb amputation and prosthetic rehabilitation. *Physical Medicine and Rehabilitation Clinics of North America*, 25 (1), 153–67. Available From: https://doi.org/10.1016/j.pmr.2013.09.006

Federolf, P., Tecante, K., & Nigg, B. (2012) A holistic approach to study the temporal variability in gait. *Journal of Biomechanics*, 45 (7), 1127–1132. Available From: https://doi.org/10.1016/j.jbiomech.2012.02.008

Field, A., 2013. *Discovering statistics using IBM SPSS statistics*. sage.

Figueiredo, J., Santos, C.P., & Moreno, J.C. (2018) Automatic recognition of gait patterns in human motor disorders using machine learning: A review. *Medical Engineering & Physics*. Available From: https://doi.org/10.1016/j.medengphy.2017.12.006

Fish, D.J. & Nielsen, J.P. (1993) Clinical Assessment of Human Gait. *Journal of Prosthetics and Orthotics*, 5 (2), 39.

Gailey, R. S. (2006) Predictive Outcome Measures Versus Functional Outcome Measures in the Lower Limb Amputee. *American Academy of Orthotists & Prosthetists*, 18 (6), p 51-60.

Gao, F., Zhang, F., & Huang, H. (2011) Investigation of sit-to-stand and stand-to-sit in an above knee amputee. In *Engineering in Medicine and Biology Society, EMBC, 2011 Annual International Conference of the IEEE* (7340-7343). Available From: https://doi.org/doi:10.1109/IEMBS.2011.6091712

Gates, D. H. & Dingwell, J. B. (2009) Comparison of different state space definitions for local dynamic stability analyses. *Journal of Biomechanics*, 42 (9), 1345–1349. Available From: https://doi.org/10.1016/j.jbiomech.2009.03.015.Comparison

Gitter, A., Czerniecki, J. M., & DeGroot, D. M. (1991) Biomechanical analysis of the influence of prosthetic feet on below-knee amputee walking. *American Journal of Physical Medicine & Rehabilitation*, 70 (3), 142–8.

Goh, J. C. H., Solomonidis, S. E., Spence, W. D., & Paul, J. P. (1984) Biomechanical evaluation of SACH and uniaxial feet. *Prosthetics and Orthotics International*, 8 (3), 147–154. Available From: https://doi.org/10.3109/03093648409146077

Grabiner, M. D., Donovan, S., Bareither, M. Lou, Marone, J. R., Hamstra-Wright, K., Gatts, S., & Troy, K. L. (2008) Trunk kinematics and fall risk of older adults: Translating biomechanical results to the clinic. *Journal of Electromyography and Kinesiology*, 18 (2), 197–204. Available From: https://doi.org/10.1016/j.jelekin.2007.06.009

Graham, L. E., Datta, D., Heller, B., Howitt, J., & Pros, D. (2007) A Comparative Study of Conventional and Energy-Storing Prosthetic Feet in High-Functioning Transfemoral Amputees. *Archives of Physical Medicine and Rehabilitation*, 88 (6), 801–806. Available From: https://doi.org/10.1016/j.apmr.2007.02.028

Hak, L., Houdijk, H., Beek, P.J., & van Dieën, J.H. (2013a) Steps to take to enhance gait stability: the effect of stride frequency, stride length, and walking speed on local dynamic stability and margins of stability. *PLoS ONE*, 8 (12), p.e82842. Available From: https://doi.org/10.1371/journal.pone.0082842

Hak, L., Houdijk, H., Steenbrink, F., Mert, A., van der Wurff, P., Beek, P. J., & van Dieën, J. H. (2012) Speeding up or slowing down?: Gait adaptations to preserve gait stability in response to balance perturbations. *Gait & Posture*, 36 (2), 260–264. Available From: https://doi.org/10.1016/j.gaitpost.2012.03.005

Hak, L., Houdijk, H., Steenbrink, F., Mert, A., van der Wurff, P., Beek, P. J., & van Dieën, J. H. (2013b) Stepping strategies for regulating gait adaptability and stability. *Journal of Biomechanics*, 46 (5), 905–911. Available From: https://doi.org/10.1016/j.jbiomech.2012.12.017

Hak, L., Houdijk, H., van Der Wurff, P., Prins, M. R., Beek, P. J., & van Dieën, J. H. (2015) Stride frequency and length adjustment in post-stroke individuals: Influence on the margins of stability. *Journal of Rehabilitation Medicine*, 47 (2), 126–132. Available From: https://doi.org/10.2340/16501977-1903

Hak, L., van Dieen, J. H., van der Wurff, P., & Houdijk, H. (2014) Stepping Asymmetry Among Individuals With Unilateral Transtibial Limb Loss Might Be Functional in Terms of Gait Stability. *Physical Therapy*, 94 (10), 1480–1488. Available From: https://doi.org/10.2522/ptj.20130431

Hak, L., van Dieën, J. H., van Der Wurff, P., Prins, M. R., Mert, A., Beek, P. J., & Houdijk, H. (2013c) Walking in an unstable environment: Strategies used by transtibial amputees to prevent falling during gait. *Archives of Physical Medicine and Rehabilitation*, 94 (11), 2186–2193. Available From: https://doi.org/10.1016/j.apmr.2013.07.020

Halilaj, E., Rajagopal, A., Fiterau, M., Hicks, J.L., Hastie, T.J. and Delp, S.L. (2018) Machine learning in human movement biomechanics: best practices, common pitfalls, and new opportunities. *Journal of biomechanics*.

Hamill, J., Gorton, G., & Masso, P. (2012) Clinical Biomechanics: Contributions to the Medical Treatment of Physical Abnormalities. *Kinesiology Review*, 1 (1), 17–23. Available From: https://doi.org/10.1123/krj.1.1.17

Hanavan, E. P. (1964) A Mathematical Model of the human body. *Aerospace Medical Rsearch Laboratories*, 1–149.

Hanson, M. A., Powell, H. C., Barth, A. T., Lach, J., & Maïté, B. P. (2009) Neural network gait classification for on-body inertial sensors. *Proceedings - 2009 6th International Workshop on Wearable and Implantable Body Sensor Networks, BSN 2009*, 181–186. Available From: https://doi.org/10.1109/BSN.2009.48

Hargrove, L. J., Young, A. J., Simon, A. M., Fey, N. P., Lipschutz, R. D., Finucane, S. B., & Kuiken, T. A. (2015) Intuitive control of a powered prosthetic leg during ambulation: A randomized clinical trial. *JAMA - Journal of the American Medical Association*, 313 (22), 2244–2252. Available From: https://doi.org/10.1001/jama.2015.4527

Harper, P. R. (2005) A review and comparison of classification algorithms for medical decision making. *Health Policy*, 71 (3), 315–331. Available From: https://doi.org/10.1016/j.healthpol.2004.05.002

Hausdorff, J. M., Peng, C. K., Ladin, Z., Wei, J. Y., & Goldberger, A. L. (1995) Is walking a random walk? Evidence for long-range correlations in stride interval of human gait. *Journal of Applied Physiology*, 78 (1), 349–358. Available From: https://doi.org/10.1152/jappl.1995.78.1.349

Highsmith, M. J., Schulz, B. W., Hart-Hughes, S. P., Latlief, G. A., & Phillips, S. L. (2010) Differences in the Spatiotemporal Parameters of Transtibial and Transfemoral Amputee Gait. *Journal of Prosthetics and Orthotics*, 22 (1), p 26-30. Available From: https://doi.org/10.1016/S1353-8020(10)70110-3

Hoerzer, S., von Tscharner, V., Jacob, C., & Nigg, B.M. (2015) Defining functional groups based on running kinematics using Self-Organizing Maps and Support Vector Machines. *Journal of Biomechanics*, 48 (10), 2072-2079.

Hof, A. L. (2007) The equations of motion for a standing human reveal three mechanisms for balance. *Journal of Biomechanics*, 40 (2), 451–457. Available From: https://doi.org/10.1016/j.jbiomech.2005.12.016

Hof, A. L. (2008) The “extrapolated center of mass” concept suggests a simple control of balance in walking. *Human Movement Science*, 27 (1), 112–125. Available From: https://doi.org/10.1016/j.humov.2007.08.003

Hof, A. L., Gazendam, M. G. J., & Sinke, W. E. (2005) The condition for dynamic stability. *Journal of Biomechanics*, 38 (1), 1–8. Available From: https://doi.org/10.1016/j.jbiomech.2004.03.025

Hof, A. L., van Bockel, R. M., Schoppen, T., & Postema, K. (2007) Control of lateral balance in walking. Experimental findings in normal subjects and above-knee amputees. *Gait & Posture*, 25 (2), 250–258. Available From: https://doi.org/10.1016/j.gaitpost.2006.04.013

Horak, F. B., Dimitrova, D., & Nutt, J. G. (2005) Direction-specific postural instability in subjects with Parkinson’s disease. *Experimental Neurology*, 193 (2), 504–521. Available From: https://doi.org/10.1016/j.expneurol.2004.12.008

Horst, F., Kramer, F., Schäfer, B., Eekhoff, A., Hegen, P., Nigg, B.M., & Schöllhorn, W.I. (2016). Daily changes of individual gait patterns identified by means of support vector machines. *Gait & Posture*, 49, 309-314. Available From: https://doi.org/10.1016/j.gaitpost.2016.07.073

Horst, F., Mildner, M., & Schöllhorn, W.I. (2017) One-year persistence of individual gait patterns identified in a follow-up study–A call for individualised diagnose and therapy. *Gait & Posture*, 58, 476-480.

Houdijk, H., Pollmann, E., Groenewold, M., Wiggerts, H., & Polomski, W. (2009) The energy cost for the step-to-step transition in amputee walking. *Gait & Posture*, 30 (1), 35–40. Available From: https://doi.org/10.1016/j.gaitpost.2009.02.009

Howell, A. M., Kobayashi, T., Chou, T. R., Daly, W., Orendurff, M., & Bamberg, S. J. M. (2012) A laboratory insole for analysis of sensor placement to determine ground reaction force and ankle moment in patients with stroke. *Proceedings of the Annual International Conference of the IEEE Engineering in Medicine and Biology Society, EMBS*, 6394–6397. Available From: https://doi.org/10.1109/EMBC.2012.6347457

Hua, Y. and Liu, W. (1998) Generalized karhunen-loeve transform. *IEEE Signal Processing Letters*, 5 (6), 141-142.

Huang, H., Dou, Z., Zhang, F., & Nunnery, M. J. (2011) Improving the performance of a neural-machine interface for artificial legs using prior knowledge of walking environment. *Proceedings of the Annual International Conference of the IEEE Engineering in Medicine and Biology Society, EMBS*, (2), 4255–4258. Available From: https://doi.org/10.1109/IEMBS.2011.6091056

Hurley, G. R. B., Mckenney, R., Robinson, M., Zadravec, M., & Pierrynowski, M. R. (1990) The role of the contralateral limb in below-knee amputee gait. *Prosthetics and Orthotics International*, 14 (1), 33–42. Available From: https://doi.org/10.3109/03093649009080314

Isakov, E., Burger, H., Krajnik, J., Gregoric, M., & Marincek, C. (1996) Influence of speed on gait parameters and on symmetry in trans-tibial amputees. *Prosthetics and Orthotics International*, 20 (3), 153–158. Available From: https://doi.org/10.3109/03093649609164437

Isakov, E., Keren, O., & Benjuya, N. (2000) Trans-tibial amputee gait: Time-distance parameters and EMG activity. *Prosthetics and Orthotics International*, 24 (3), 216–220. Available From: https://doi.org/10.1080/03093640008726550

Isakov, E., Mizrahi, J., Ring, H., Susak, Z., & Hakim, N. (1992) Standing sway and weight-bearing distribution in people with below-knee amputations. *Archives of Physical Medicine and Rehabilitation*, 73 (2), 174–178.

Jarvis, H. L., Bennett, A. N., Twiste, M., Phillip, R. D., Etherington, J., & Baker, R. (2017) Temporal Spatial and Metabolic Measures of Walking in Highly Functional Individuals With Lower Limb Amputations. *Archives of Physical Medicine and Rehabilitation*, 98 (7), 1389–1399. Available From: https://doi.org/10.1016/j.apmr.2016.09.134

Jayakaran, P., Johnson, G. M., Sullivan, S. J., & Nitz, J. C. (2012) Instrumented measurement of balance and postural control in individuals with lower limb amputation: A critical review. *International Journal of Rehabilitation Research*, 35 (3), 187–196. Available From: https://doi.org/10.1097/MRR.0b013e3283550ff9

Jordan, K., Challis, J. H., & Newell, K. M. (2007a) Speed influences on the scaling behavior of gait cycle fluctuations during treadmill running. *Human Movement Science*, 26 (1), 87–102. Available From: https://doi.org/10.1016/j.humov.2006.10.001

Jordan, K., Challis, J. H., & Newell, K. M. (2007b) Walking speed influences on gait cycle variability. *Gait & Posture*, 26 (1), 128–134. Available From: https://doi.org/10.1016/j.gaitpost.2006.08.010

Joshi, D. & Hahn, M. E. (2016) Terrain and Direction Classification of Locomotion Transitions Using Neuromuscular and Mechanical Input. *Annals of Biomedical Engineering*, 44 (4), 1275–1284. Available From: https://doi.org/10.1007/s10439-015-1407-3

Kaczmarczyk, K., Wit, A., Krawczyk, M., & Zaborski, J. (2009) Gait classification in post-stroke patients using artificial neural networks. *Gait & Posture*, 30 (2), 207–210. Available From: https://doi.org/10.1016/j.gaitpost.2009.04.010

Kamruzzaman, J. and Begg, R.K. (2006) Support vector machines and other pattern recognition approaches to the diagnosis of cerebral palsy gait. *IEEE Transactions on Biomedical Engineering*, 53 (12), 2479-2490.

Kang, H. G. & Dingwell, J. B. (2006) A direct comparison of local dynamic stability during unperturbed standing and walking. *Experimental Brain Research*, 172 (1), 35–48. Available From: https://doi.org/10.1007/s00221-005-0224-6

Kang, H. G. & Dingwell, J. B. (2009) Dynamic Stability of Superior vs. Inferior Segments during Walking in Young and Older Adults. *Gait & Posture*, 30 (2), 260–263. Available From: https://doi.org/10.1109/TMI.2012.2196707.Separate

Karmarkar, A. M., Collins, D. M., Wichman, T., Franklin, A., Fritzgerald, S., Dicianno, B. E., & Copper, R. A. (2009) Prosthesis and wheelchair use in veterans with lower-limb amputation. *Journal of Rehabilitation Research and Development*, 46 (5), 567–576.

Kerrigan, D. C., Franz, J. R., Keenan, G. S., Dicharry, J., Della Croce, U., & Wilder, R. P. (2009) The Effect of Running Shoes on Lower Extremity Joint Torques. *PM and R*, 1 (12), 1058–1063. Available From: https://doi.org/10.1016/j.pmrj.2009.09.011

Khan, R. A., Naseer, N., Qureshi, N. K., Noori, F. M., Nazeer, H., & Khan, M. U. (2018) FNIRS-based Neurorobotic Interface for gait rehabilitation. *Journal of NeuroEngineering and Rehabilitation*, 15 (1), 1–17. Available From: https://doi.org/10.1186/s12984-018-0346-2

Khandoker, A. H., Lai, D. T. H., Begg, R. K., & Palaniswami, M. (2007) Wavelet-based feature extraction for support vector machines for screening balance impairments in the elderly. *IEEE Transactions on Neural Systems and Rehabilitation Engineering*, 15 (4), 587–597. Available From: https://doi.org/10.1109/TNSRE.2007.906961

Kinsella, S. & Moran, K. (2008) Gait pattern categorization of stroke participants with equinus deformity of the foot. *Gait & Posture*, 27 (1), 144–151. Available From: https://doi.org/10.1016/j.gaitpost.2007.03.008

Kirtley, C. (2006) *Clinical Gait Analysis: Theory and Practice*. Elsevier Health Sciences.

Kobsar, D., Osis, S. T., Hettinga, B. A., & Ferber, R. (2015) Gait biomechanics and patient-reported function as predictors of response to a hip strengthening exercise intervention in patients with knee osteoarthritis. *PLoS ONE*. Available From: https://doi.org/10.1371/journal.pone.0139923

Kovač, I., Medved, V., & Ostojić, L. (2009) Ground Reaction Force Analysis in Traumatic Transtibial Amputees' Gait. *Collegium Antropologicum*, 33 (2), 107-114.

Kulkarni, J., Gaine, W., Buckley, J., Rankine, J., & Adams, J. (2005) Chronic low back pain in traumatic lower limb amputees. *Clinical Rehabilitation*, 19 (1), 81–86. Available From: https://doi.org/10.1191/0269215505cr819oa

Lai, D. T. H., Begg, R. K., & Palaniswami, M. (2009) Computational intelligence in gait research: a perspective on current applications and future challenges. *IEEE Transactions on Information Technology in Biomedicine : A Publication of the IEEE Engineering in Medicine and Biology Society*, 13 (5), 687–702. Available From: https://doi.org/10.1109/TITB.2009.2022913

Lai, D. T. H., Begg, R. K., Taylor, S., & Palaniswami, M. (2008) Detection of tripping gait patterns in the elderly using autoregressive features and support vector machines. *Journal of Biomechanics*, 41 (8), 1762–1772. Available From: https://doi.org/10.1016/j.jbiomech.2008.02.037

Lakany, H. (2008) Extracting a diagnostic gait signature. *Pattern Recognition*, 41 (5), 1644–1654. Available From: https://doi.org/10.1016/j.patcog.2007.11.004

Laroche, D., Tolambiya, A., Morisset, C., Maillefert, J. F., French, R. M., Ornetti, P., & Thomas, E. (2014) A classification study of kinematic gait trajectories in hip osteoarthritis. *Computers in Biology and Medicine*, 55, 42–48. Available From: https://doi.org/10.1016/j.compbiomed.2014.09.012

Leardini, A., Biagi, F., Merlo, A., Belvedere, C., & Benedetti, M. G. (2011) Multi-segment trunk kinematics during locomotion and elementary exercises. *Clinical Biomechanics (Bristol, Avon)*, 26 (6), 562–71. Available From: https://doi.org/10.1016/j.clinbiomech.2011.01.015

Leardini, A., Cappozzo, A., Catani, F., Toksvig-Larsen, S., Petitto, A., Sforza, V., & Giannini, S. (1999) Validation of a functional method for the estimation of hip joint centre location. *Journal of Biomechanics*, 32 (1), 99–103. Available From: https://doi.org/10.1016/S0021-9290(98)00148-1

Lee, M., Roan, M., & Smith, B. (2009) An application of principal component analysis for lower body kinematics between loaded and unloaded walking. *Journal of Biomechanics*, 42 (14), 2226–2230. Available From: https://doi.org/10.1016/j.jbiomech.2009.06.052

Lemaire, E. D., Fisher, F. R., & Robertson, D. G. E. (1993) Gait patterns of elderly men with trans-tibial-amputations. *Prosthetics and Orthotics International*, 17 (1), 27–37. Available From: https://doi.org/10.3109/03093649309164352

LeMoyne, R., Mastroianni, T., Hessel, A., & Nishikawa, K. (2015). Implementation of machine learning for classifying prosthesis type through conventional gait analysis. In *Engineering in Medicine and Biology Society (EMBC), 2015 37th Annual International Conference of the IEEE* (202-205).

Leung, E. C., Rush, P. J., & Devlin, M. (1996) Predicting prosthetic rehabilitation outcome in lower limb amputee patients with the functional independence measure. *Archives of Physical Medicine and Rehabilitation*, 77 (6), 605–8. Available From: https://doi.org/http://dx.doi.org/10.1016/S0003-9993(96)90303-2

Lever, J., Krzywinski, M., & Altman, N. (2016a) Classification evaluation. *Nature Publishing Group*, 13 (8), 603–605. Available From: https://doi.org/10.1038/nmeth.3945

Lever, J., Krzywinski, M., & Altman, N. (2016b) Model selection and overfitting. *Nature Publishing Group*, 13 (9), 703–704. Available From: https://doi.org/10.1038/nmeth.3968

Lever, J., Krzywinski, M., & Altman, N. (2016c) Points of Significance: Logistic regression. *Nature Methods*, 13 (7), 541–542. Available From: https://doi.org/10.1038/nmeth.3904

Levine, D., Richards, J., & Whittle, M. W. (2012) *Whittle's Gait Analysis*. Elsevier Health Sciences.

Liang, Z. & Lee, Y. (2013) Eigen-analysis of nonlinear PCA with polynomial kernels. *Statistical Analysis and Data Mining: The ASA Data Science Journal*, 6 (6), 529-544. Available From: https://doi.org/10.1002/sam.11211

Lieberman, D. E., Venkadesan, M., Werbel, W. a, Daoud, A. I., D'Andrea, S., Davis, I. S., & Pitsiladis, Y. (2010) Foot strike patterns and collision forces in habitually barefoot versus shod runners. *Nature*, 463 (7280), 531–5. Available From: https://doi.org/10.1038/nature08723

López, V., Fernández, A., & Herrera, F. (2014) On the importance of the validation technique for classification with imbalanced datasets: Addressing covariate shift when data is skewed. *Information Sciences*, 257, 1–13. Available From: https://doi.org/10.1016/j.ins.2013.09.038

Lord, S. R., & Menz, H. B. (2002) Physiologic, psychologic, and health predictors of 6-minute walk performance in older people. *Archives of Physical Medicine and Rehabilitation*, 83 (7), 907–911. Available From: https://doi.org/10.1053/apmr.2002.33227

Lu, Y., Boukharouba, K., Boonært, J., Fleury, A., & Lecœuche, S. (2014) Application of an incremental SVM algorithm for on-line human recognition from video surveillance using texture and color features. *Neurocomputing*, 126, 132–140. Available From: https://doi.org/10.1016/j.neucom.2012.08.071

MacAndrew-Young, P. M., Wilken, J. M., & Dingwell, J. B. (2012) Dynamic margins of stability during human walking in destabilizing environments. *Journal of Biomechanics*, 45 (6), 1053–1059.

MacKenzie, E. J., Castillo, R. C., Jones, A. S., Bosse, M. J., Kellam, J. F., Pollak, A. N., & Burgess, A. R. (2007) Health-Care Costs Associated with Amputation or Reconstruction of a Limb-Threatening Injury. *The Journal of Bone & Joint Surgery*, 89 (8), 1685–1692. Available From: https://doi.org/10.2106/JBJS.F.01350

MacKinnon, C. D. & Winter, D. A. (1993) Control of whole body balance in the frontal plane during human walking. *Journal of Biomechanics*, 26 (6), 633–644. Available From: https://doi.org/10.1016/0021-9290(93)90027-C

Martins, M., Costa, L., Frizera, A., Ceres, R., & Santos, C. (2014) Hybridization between multi-objective genetic algorithm and support vector machine for feature selection in walker-assisted gait. *Computer Methods and Programs in Biomedicine*, 113 (3), 736–748. Available From: https://doi.org/10.1016/j.cmpb.2013.12.005

Mattes, S. J., Martin, P. E., & Royer, T. D. (2000) Walking symmetry and energy cost in persons with unilateral transtibial amputations: Matching prosthetic and intact limb inertial properties. *Archives of Physical Medicine and Rehabilitation*, 81 (5), 561–568. Available From: https://doi.org/10.1053/mr.2000.3851

McAndrew, P. M., Wilken, J. M., & Dingwell, J. B. (2011) Dynamic stability of human walking in visually and mechanically destabilizing environments. *Journal of Biomechanics*, 44 (4), 644–649. Available From: https://doi.org/10.1016/j.jbiomech.2010.11.007

McNealy, L. L., & Gard, S. A. (2008) Effect of prosthetic ankle units on the gait of persons with bilateral trans-femoral amputations. *Prosthetics and Orthotics International*, 32 (1), 111–126. Available From: https://doi.org/10.1080/02699200701847244

Meijer, W.T., Hoes, A.W., Rutgers, D., Bots, M.L., Hofman, A., & Grobbee, D.E. (1998) Peripheral arterial disease in the elderly: the Rotterdam Study. *Arteriosclerosis, Thrombosis, and Vascular Biology*, 18 (2), 185-192.

Melzer, I., Benjuya, N., & Kaplanski, J. (2004) Postural stability in the elderly: A comparison between fallers and non-fallers. *Age and Ageing*, 33(6), 602–607. Available From: https://doi.org/10.1093/ageing/afh218

Millard, M., McPhee, J., & Kubica, E. (2012) Foot Placement and Balance in 3D. *Journal of Computational and Nonlinear Dynamics*, 7 (2), 021015. Available From: https://doi.org/10.1115/1.4005462

Millard, M., Wight, D., McPhee, J., Kubica, E., & Wang, D. (2009) Human Foot Placement and Balance in the Sagittal Plane. *Journal of Biomechanical Engineering*, 131 (12), 121001. Available From: https://doi.org/10.1115/1.4000193

Miller, J. D., Beazer, M. S., & Hahn, M. E. (2013) Myoelectric walking mode classification for transtibial amputees. *IEEE Transactions on Biomedical Engineering*, 60(10), 2745–2750. Available From: https://doi.org/10.1109/TBME.2013.2264466

Miller, S.E., Segal, A.D., Klute, G.K., & Neptune, R.R. (2018) Hip Recovery Strategy Used by Below-Knee Amputees Following Mediolateral Foot Perturbations. *Journal of biomechanics*.

Miller, W. C., Deathe, A. B., Speechley, M., & Koval, J. (2001a) The influence of falling, fear of falling, and balance confidence on prosthetic mobility and social activity among individuals with a lower extremity amputation. *Archives of Physical Medicine and Rehabilitation*, 82 (9), 1238–1244. Available From: https://doi.org/10.1053/apmr.2001.25079

Miller, W. C., Speechley, M., & Deathe, B. (2001b) The prevalence and risk factors of falling and fear of falling among lower extremity amputees. *Archives of Physical Medicine and Rehabilitation*, 82 (8), 1031–1037. Available From: https://doi.org/10.1053/apmr.2001.24295

Moraiti, C. O., Stergiou, N., Vasiliadis, H. S., Motsis, E., & Georgoulis, A. (2010) Anterior cruciate ligament reconstruction results in alterations in gait variability. *Gait & Posture*, 32 (2), 169–175. Available From: https://doi.org/10.1016/j.gaitpost.2010.04.008

Moraiti, C., Stergiou, N., Ristanis, S., & Georgoulis, A. D. (2007) ACL deficiency affects stride-to-stride variability as measured using nonlinear methodology. *Knee Surgery, Sports Traumatology, Arthroscopy*, 15 (12), 1406–1413. Available From: https://doi.org/10.1007/s00167-007-0373-1

Mouchnino, L., Mille, M.L., Martin, N., Baroni, G., Cincera, M., Bardot, A., Delarque, A., Massion, J., & Pedotti, A. (2006) Behavioral outcomes following below-knee amputation in the coordination between balance and leg movement. *Gait & posture*, 24 (1), 4-13. Available From: https://doi.org/10.1016/j.gaitpost.2005.07.007

Muniz, A. M. S., Liu, H., Lyons, K. E., Pahwa, R., Liu, W., & Nadal, J. (2010a) Quantitative evaluation of the effects of subthalamic stimulation on gait in Parkinson's disease patients using principal component analysis. *The International Journal of Neuroscience*, 120 (9), 609–616. Available From: https://doi.org/10.3109/00207454.2010.504904

Muniz, A. M. S., Liu, H., Lyons, K. E., Pahwa, R., Liu, W., & Nobre, F. F., & Nadal, J. (2010b) Comparison among probabilistic neural network, support vector machine and logistic regression for evaluating the effect of subthalamic stimulation in Parkinson disease on ground reaction force during gait. *Journal of Biomechanics*, 43 (4), 720–726. Available From: https://doi.org/10.1016/j.jbiomech.2009.10.018

Nashner, L.M. (1997) Physiology of balance, with special reference to the healthy elderly. *Gait disorders of aging: falls and therapeutic strategies*, 37-53.

nhs.uk. 2018. *Amputation - NHS.UK* . [ONLINE] Available at: https://www.nhs.uk/conditions/amputation/. [Accessed 28 June 2018].

Nolan, L., & Lees, A. (2000) The functional demands on the intact limb during walking for active trans-femoral and trans-tibial amputees. *Prosthetics and Orthotics International*, 24 (2), 117–125. Available From: https://doi.org/10.1080/03093640008726534

Nolan, L., Wit, A., Dudziñski, K., Lees, A., Lake, M., & Wychowañski, M. (2003) Adjustments in gait symmetry with walking speed in trans-femoral and trans-tibial amputees. *Gait & Posture*, 17 (2), 142–151. Available From: https://doi.org/10.1016/S0966-6362(02)00066-8

Norgren, L., Hiatt, W. R., Dormandy, J. A., Nehler, M. R., Harris, K. A., Fowkes, F. G. R., & Rutherford, R. B. (2007) Inter-Society Consensus for the management of peripheral arterial disease (TASC II) *International Angiology*, 26 (2), 82–157. Available From: https://doi.org/10.1016/j.jvs.2006.12.037

Novacheck, T. F., Trost, J. P., & Sohrweide, S. (2010) Examination of the child with cerebral palsy. *The Orthopedic Clinics of North America*, 41 (4), 469–88. Available From: https://doi.org/10.1016/j.ocl.2010.07.001

Olney, S. J., Griffin, M. P., & McBride, I. D. (1998) Multivariate examination of data from gait analysis of persons with stroke. *Physical Therapy*, 78 (8), 814–28.

Pai, Y. & Patton, J. (1997) Center of Mass Velocity-Position for Balance Control Predictions. *Physical Therapy*, 30 (4), 347–354. Available From: https://doi.org/10.1016/S0021-9290(96)00165-0

Pärkkä, J., Ermes, M., Korpipää, P., Mäntyjärvi, J., Peltola, J., & Korhonen, I. (2006) Activity classification using realistic data from wearable sensors. *IEEE Transactions on Information Technology in Biomedicine : A Publication of the IEEE Engineering in Medicine and Biology Society*, 10 (1), 119–128. Available From: https://doi.org/10.1109/TITB.2005.856863

Palmerini, L., Rocchi, L., Mellone, S., Valzania, F. and Chiari, L. (2011) Feature selection for accelerometer-based posture analysis in Parkinson's disease. *IEEE Transactions on Information Technology in Biomedicine*, 15 (3), 481-490.

Payton, C. & Bartlett, R. (2007) *Biomechanical evaluation of movement in sport and exercise: the British Association of Sport and Exercise Sciences guide*. Routledge.

Perry, J., Boyd, L. A., Rao, S. S., & Mulroy, S. J. (1997) Prosthetic weight acceptance mechanics in transtibial amputees wearing the Single Axis, Seattle Lite, and Flex Foot. *IEEE Transactions on Rehabilitation Engineering*, 5 (4), 283–289. Available From: https://doi.org/10.1109/86.650279

Perry, J. (1992) Gait analysis: normal and pathological function. *Journal of Pediatric Orthopaedics*, 12 (6), p.815.

Pew, C. & Klute, G. K. (2017) Turn Intent Detection for Control of a Lower Limb Prosthesis. *IEEE Transactions on Biomedical Engineering*, 65 (4), 789–796. Available From: https://doi.org/10.1109/TBME.2017.2721300

Pezzin, L. E., Dillingham, T. R., & MacKenzie, E. J. (2000) Rehabilitation and the long-term outcomes of persons with trauma-related amputations. *Archives of Physical Medicine and Rehabilitation*, 81 (3), 292–300. Available From: https://doi.org/10.1053/apmr.2000.0810292

Phinyomark, A., Hettinga, B.A., Osis, S., & Ferber, R. (2015) Do intermediate-and higher-order principal components contain useful information to detect subtle changes in lower extremity biomechanics during running?. *Human Movement Science*, 44, 91-101. Available From: https://doi.org/10.1016/j.humov.2015.08.018

Phinyomark, A., Osis, S. T., Hettinga, B. A., Kobsar, D., & Ferber, R. (2016) Gender differences in gait kinematics for patients with knee osteoarthritis. *BMC Musculoskeletal Disorders*, 17 (1), 157. Available From: https://doi.org/10.1186/s12891-016-1013-z

Phinyomark, A., Petri, G., Ibáñez-Marcelo, E., Osis, S.T., & Ferber, R. (2018) Analysis of big data in gait biomechanics: current trends and future directions. *Journal of Medical and Biological Engineering*, 38 (2), 244-260. Available From: https://doi.org/10.1007/s40846-017-0297-2

Physiopedia. 2018. *Gait in prosthetic rehabilitation - Physiopedia*. [ONLINE] Available at: https://www.physio-pedia.com/Gait_in_prosthetic_rehabilitation. [Accessed 28 June 2018].

Pogorelc, B., Bosnić, Z., & Gams, M. (2012) Automatic recognition of gait-related health problems in the elderly using machine learning. *Multimedia Tools and Applications*, 58 (2), 333–354. Available From: https://doi.org/10.1007/s11042-011-0786-1

Postema, K., Hermens, H. J., De Vries, J., Koopman, H. F. J. M., & Eisma, W. H. (1997) Energy storage and release of prosthetic feet Part 1: biomechanical analysis related to user benefits. *Prosthetics and Orthotics International*, 21 (1), 17–27. Available From: https://doi.org/10.3109/03093649709164526

Powers, C. M., Rao, S., & Perry, J. (1998) Knee kinetics in trans-tibial amputee gait. *Gait & Posture*, 8 (1), 1–7. Available From: https://doi.org/10.1016/S0966-6362(98)00016-2

Powers, C., Torburn, L., Perry, J., & Ayyappa, E. (1994) Influence of prosthetic foot design on sound limb loading in adults with unilateral below-knee amputations. *Archives of Physical Medicine and Rehabilitation*, 75 (7), 825–829. Available From: https://doi.org/10.5555/uri:pii:0003999394901465

Pratihar, D. K., Deb, K., & Ghosh, A. (2002) Optimal path and gait generations simultaneously of a six-legged robot using a GA-fuzzy approach. *Robotics and Autonomous Systems*, 41 (1), 1–20. Available From: https://doi.org/10.1016/S0921-8890(02)00273-7

PressureRef4PIL. 2018. *Methodology - PressureRef4PIL*. [ONLINE] Available at: https://paginas.fe.up.pt/~ee10185/methodology. [Accessed 28 June 2018].

Prince, F., Winter, D.A., Sjonnensen, G., Powell, C., & Wheeldon, R.K. (1998) Mechanical efficiency during gait of adults with transtibial amputation: a pilot study comparing the SACH, Seattle, and Golden-Ankle prosthetic feet. *Journal of Rehabilitation Research and Development*, 35 (2), 177.

Quinlan, J.R. (1990) Learning logical definitions from relations. *Machine learning*,5 (3), 239-266.

Rábago, C. A., & Wilken, J. M. (2016) The Prevalence of Gait Deviations in Individuals With Transtibial Amputation. *Military Medicine*, 181 (S4), 30–37. Available From: https://doi.org/10.7205/MILMED-D-15-00505

Rahmati, H., Martens, H., Aamo, O.M., Stavdahl, Ø., Støen, R. and Adde, L. (2016) Frequency analysis and feature reduction method for prediction of cerebral palsy in young infants. *IEEE Transactions on Neural Systems and Rehabilitation Engineering*, 24 (11), 1225-1234.

Ramstrand, N. & Brodtkorb, T.H. (2008) Considerations for developing an evidenced-based practice in orthotics and prosthetics. *Prosthetics and Orthotics International*, 32 (1), 93-102. Available From: https://doi.org/10.1080/03093640701838190

Reid, S. M., Graham, R. B., & Costigan, P. A. (2010) Differentiation of young and older adult stair climbing gait using principal component analysis. *Gait & Posture*, 31 (2), 197–203. Available From: https://doi.org/10.1016/j.gaitpost.2009.10.005

Robertson, G., Caldwell, G., Hamill, J., Kamen, G., & Whittlesey, S. (2013) *Research Methods in Biomechanics, 2E*. Human Kinetics.

Roiz, R. de M., Cacho, E. W. A., Pazinatto, M. M., Reis, J. G., Cliquet, A., & Barasnevicius-Quagliato, E. M. A. (2010) Gait analysis comparing Parkinson's disease with healthy elderly subjects. *Arquivos de Neuro-Psiquiatria*, 68 (1), 81–6.

Rosenstein, M. T., Collins, J. J., & Luca De, C. J. (1993) A practical method for calculating largest Lyapunov exponents from small data sets. *Physica D: Nonlinear Phenomena*, 65 (1–2), 117–134. Available From: https://doi.org/10.1016/0167-2789(93)90009-P

Roy, S.H., Cole, B.T., Gilmore, L.D., De Luca, C.J., Thomas, C.A., Saint-Hilaire, M.M. and Nawab, S.H., (2013) High-resolution tracking of motor disorders in Parkinson's disease during unconstrained activity. *Movement Disorders*, 28 (8), 1080-1087.

Rozumalski, A. and Schwartz, M.H. (2009) Crouch gait patterns defined using k-means cluster analysis are related to underlying clinical pathology. *Gait & Posture*, 30 (2),155-160.

Sabatini, A. M., Martelloni, C., Scapellato, S., & Cavallo, F. (2005) Assessment of walking features from foot inertial sensing. *IEEE Transactions on Biomedical Engineering*, 52 (3), 486–494. Available From: https://doi.org/10.1109/TBME.2004.840727

Sadeghi, H., Allard, P., & Duhaime, M. (2001) Muscle power compensatory mechanisms in below-knee amputee gait. *American Journal of Physical Medicine & Rehabilitation*, 80 (1), 25–32.

Sadeghi, H., Allard, P., Prince, F., & Labelle, H. (2000) Symmetry and limb dominance in able-bodied gait: A review. *Gait & Posture*, 12 (1), 34–45. Available From: https://doi.org/10.1016/S0966-6362(00)00070-9

Saeys, Y., Inza, I., & Larrañaga, P. (2007) A review of feature selection techniques in bioinformatics. *Bioinformatics*, 23 (19), 2507–2517. Available From: https://doi.org/10.1093/bioinformatics/btm344

Sanderson, D. J., & Martin, P. E. (1997) Lower extremity kinematic and kinetic adaptations in unilateral below-knee amputees during walking. *Gait & Posture*, 6 (2), 126–136. Available From: https://doi.org/10.1016/S0966-6362(97)01112-0

Sansam, K., Neumann, V., O'Connor, R., & Bhakta, B. (2009) Predicting walking ability following lower limb amputation: A systematic review of the literature. *Journal of Rehabilitation Medicine*, 41 (8), 593–603. Available From: https://doi.org/10.2340/16501977-0393

Sarbaz, Y., Banaie, M., Pooyan, M., Gharibzadeh, S., Towhidkhah, F., & Jafari, A. (2012) Modeling the gait of normal and Parkinsonian persons for improving the diagnosis. *Neuroscience Letters*, 509 (2), 72–75. Available From: https://doi.org/10.1016/j.neulet.2011.10.002

Sawers, A. & Hahn, M.E. (2011) Trajectory of the center of rotation in non-articulated energy storage and return prosthetic feet. *Journal of Biomechanics*, 44 (9), 1673-1677. Available From: https://doi.org/10.1016/j.jbiomech.2011.03.028

Schaffalitzky, E., Gallagher, P., Maclachlan, M., & Ryall, N. (2011) Understanding the benefits of prosthetic prescription: exploring the experiences of practitioners and lower limb prosthetic users. *Disability and Rehabilitation*, 33 (15-16), 1314-1323.

Schmalz, T., Blumentritt, S., & Jarasch, R. (2002) Energy expenditure and biomechanical characteristics of lower limb amputee gait: *Gait & Posture*, 16 (3), 255–263. Available From: https://doi.org/10.1016/S0966-6362(02)00008-5

Schmid, M., Beltrami, G., Zambarbieri, D., & Verni, G. (2005) Centre of pressure displacements in trans-femoral amputees during gait. *Gait & Posture*, 21 (3), 255–262. Available From: https://doi.org/10.1016/j.gaitpost.2004.01.016

Schöllhorn, W. I., Beckmann, H., & Davids, K. (2010) Exploiting system fluctuations. Differential training in physical prevention and rehabilitation programs for health and exercise. *Medicina (Kaunas) REVIEWS Medicina (Kaunas)*, 4646 (66), 365–73. Available From: https://doi.org/1006-01 [pii]

Schöllhorn, W. I., Beckmann, H., Michelbrink, M., Sechelmann, M., Trockel, M., & Davids, K. (2006) Does noise provide a basis for the unification of motor learning theories? *International Journal of Sport Psychology*, 37 (2–3), 186–206.

Schöllhorn, W.I., Nigg, B.M., Stefanyshyn, D.J., & Liu, W. (2002) Identification of individual walking patterns using time discrete and time continuous data sets. *Gait & Posture*, 15 (2), 180-186.

Schoppen, T., Boonstra, A., Groothoff, J.W., de Vries, J., Göeken, L.N., & Eisma, W.H. (2003) Physical, Mental, and Social Predictors of Functional Outcome in Unilateral Lower-Limb Amputees. *Archives of Physical Medicine and Rehabilitation*, 84 (6), 803-811.

Schutte, L. M., Narayanan, U., Stout, J. L., Selber, P., Gage, J. R., & Schwartz, M. H. (2000) An index for quantifying deviations from normal gait. *Gait & Posture*, 11 (1), 25–31. Available From: https://doi.org/10.1016/S0966-6362(99)00047-8

Schwartz, M. H., Novacheck, T. F., & Trost, J. (2000) A tool for quantifying hip flexor function during gait. *Gait & Posture*, 12 (2), 122–127. Available From: https://doi.org/10.1016/S0966-6362(00)00064-3

Schwartz, M. H. & Rozumalski, A. (2008) The gait deviation index: A new comprehensive index of gait pathology. *Gait & Posture*, 28 (3), 351–357. Available From: https://doi.org/10.1016/j.gaitpost.2008.05.001

Segal, A. D., Orendurff, M. S., Czerniecki, J. M., Shofer, J. B., & Klute, G. K. (2010) Local dynamic stability of amputees wearing a torsion adapter compared to a rigid adapter during straight-line and turning gait. *Journal of Biomechanics*, 43 (14), 2798–2803. Available From: https://doi.org/10.1016/j.jbiomech.2010.05.038

Segal, A. D., Orendurff, M. S., Klute, G. K., McDowell, M. L., Pecoraro, J. A., Shofer, J., & Czerniecki, J. M. (2006) Kinematic and kinetic comparisons of transfemoral amputee gait using C-Leg and Mauch SNS prosthetic knees. *The Journal of Rehabilitation Research and Development*, 43 (7), 857. Available From: https://doi.org/10.1682/JRRD.2005.09.0147

Seroussi, R. E., Gitter, A., Czerniecki, J. M., & Weaver, K. (1996) Mechanical work adaptations of above-knee amputee ambulation. *Archives of Physical Medicine and Rehabilitation*, 77 (11), 1209–1214.

Silverman, A. K., Fey, N. P., Portillo, A., Walden, J. G., Bosker, G., & Neptune, R. R. (2008) Compensatory mechanisms in below-knee amputee gait in response to increasing steady-state walking speeds. *Gait & Posture*, 28 (4), 602–609. Available From: https://doi.org/10.1016/j.gaitpost.2008.04.005

Simon, A. M., Spanias, J. A., Ingraham, K. A., & Hargrove, L. J. (2016) Delaying ambulation mode transitions in a powered knee-ankle prosthesis. In *Engineering in Medicine and Biology Society (EMBC), 2016 IEEE 38th Annual International Conference of the* (5079-5082). Available From: https://doi.org/10.1109/EMBC.2016.7591869

Simon, S. R. (2004) Quantification of human motion: Gait analysis - Benefits and limitations to its application to clinical problems. *Journal of Biomechanics*, 37 (12), 1869–1880. Available From: https://doi.org/10.1016/j.jbiomech.2004.02.047

Sjödahl, C., Jarnlo, G. B., Söderberg, B., & Persson, B. M. (2002) Kinematic and kinetic gait analysis in the sagittal plane of trans-femoral amputees before and after special gait re-education. *Prosthetics and Orthotics International*, 26 (2), 101–112. Available From: https://doi.org/10.1080/03093640208726632

Skinner, H. B. & Effeney, D. J. (1985) Gait analysis in amputees. *American Journal of Physical Medicine*, 64 (2), 82–9.

Sloot, L. H., van Schooten, K. S., Bruijn, S. M., Kingma, H., Pijnappels, M., & van Dieën, J. H. (2011) Sensitivity of local dynamic stability of over-ground walking to balance impairment due to galvanic vestibular stimulation. *Annals of Biomedical Engineering*, 39 (5), 1563–1569. Available From: https://doi.org/10.1007/s10439-010-0240-y

Soares, D. P., Castro, M. P. de, Mendes, E. A., & Machado, L. (2016) Principal component analysis in ground reaction forces and center of pressure gait waveforms of people with transfemoral amputation. *Prosthetics and Orthotics International*, 40(6), 729–738. Available From: https://doi.org/10.1177/0309364615612634

Sofuwa, O., Nieuwboer, A., Desloovere, K., Willems, A.-M., Chavret, F., & Jonkers, I. (2005) Quantitative gait analysis in Parkinson's disease: comparison with a healthy control group. *Archives of Physical Medicine and Rehabilitation*, 86 (5), 1007–13. Available From: https://doi.org/10.1016/j.apmr.2004.08.012

Stanhope, S. J., Kepple, T. M., McGuire, D. A., & Roman, N. L. (1990) Kinematic-based technique for event time determination during gait. *Medical & Biological Engineering & Computing*, 28 (4), 355–360. Available From: https://doi.org/10.1007/BF02446154

Stergiou, N., Moraiti, C., Giakas, G., Ristanis, S., & Georgoulis, A. D. (2004) The effect of the walking speed on the stability of the anterior cruciate ligament deficient knee. *Clinical Biomechanics*, 19 (9), 957–963. Available From: https://doi.org/10.1016/j.clinbiomech.2004.06.008

Su, F. C. & Wu, W. L. (2000) Design and testing of a genetic algorithm neural network in the assessment of gait patterns. *Medical Engineering & Physics*, 22 (1), 67–74. Available From: https://doi.org/10.1016/S1350-4533(00)00011-4

Su, P. F., Gard, S. A., Lipschutz, R. D., & Kuiken, T. A. (2007) Gait characteristics of persons with bilateral transtibial amputations. *The Journal of Rehabilitation Research and Development*, 44 (4), 491. Available From: https://doi.org/10.1682/JRRD.2006.10.0135

Sugavaneswaran, L., Umapathy, K., & Krishnan, S. (2012) Ambiguity domain-based identification of altered gait pattern in ALS disorder. *Journal of Neural Engineering*, 9 (4), p.046004. Available From: https://doi.org/10.1088/1741-2560/9/4/046004

Švehlík, M., Zwick, E. B., Steinwender, G., Linhart, W. E., Schwingenschuh, P., Katschnig, P., & Enzinger, C. (2009) Gait Analysis in Patients With Parkinson's Disease Off Dopaminergic Therapy. *Archives of Physical Medicine and Rehabilitation*, 90 (11), 1880–1886. Available From: https://doi.org/10.1016/J.APMR.2009.06.017

Swets, D. L. (1996) Using discriminant eigenfeatures for image retrieval. *IEEE Transactions on Pattern Analysis and Machine Intelligence*, 18 (8), 831–836. Available From: https://doi.org/10.1109/34.531802

Taborri, J., Palermo, E., Rossi, S., & Cappa, P. (2016) Gait partitioning methods: A systematic review. *Sensors (Switzerland)*, 16 (1), 40–42. Available From: https://doi.org/10.3390/s16010066

Takahashi, K. Z., Kepple, T. M., & Stanhope, S. J. (2012) A unified deformable (UD) segment model for quantifying total power of anatomical and prosthetic below-knee structures during stance in gait. *Journal of Biomechanics*, 45 (15), 2662–2667. Available From: https://doi.org/10.1016/j.jbiomech.2012.08.017

Taylor, S. M., Kalbaugh, C. A., Blackhurst, D. W., Hamontree, S. E., Cull, D. L., Messich, H. S., & Youkey, J. R. (2005) Preoperative clinical factors predict postoperative functional outcomes

after major lower limb amputation: An analysis of 553 consecutive patients. *Journal of Vascular Surgery*, 42 (2), 227–234. Available From: https://doi.org/10.1016/j.jvs.2005.04.015

Tharwat, A., Gaber, T., Ibrahim, A. and Hassanien, A.E. (2017) Linear discriminant analysis: A detailed tutorial. *AI communications*, 30 (2), 169-190.

Thomson, D. J. (1982) Spectrum Estimation and Harmonic Analysis. *Proceedings of the IEEE*, 70 (9), 1055–1096. Available From: https://doi.org/10.1109/PROC.1982.12433

Tingley, M., Wilson, C., Biden, E., & Knight, W.R. (2002) An index to quantify normality of gait in young children. *Gait & Posture*, 16 (2), 149-158.

Tinsley, H.E. & Tinsley, D.J. (1987) Uses of factor analysis in counseling psychology research. *Journal of Counseling Psychology*, 34 (4), p.414.

Trost, J. P., Schwartz, M. H., Krach, L. E., Dunn, M. E., & Novacheck, T. F. (2008) Comprehensive short-term outcome assessment of selective dorsal rhizotomy. *Developmental Medicine and Child Neurology*, 50 (10), 765–771. Available From: https://doi.org/10.1111/j.1469-8749.2008.03031.x

Ülger, Ö., Topuz, S., & Bayramlar, K. (2010) Risk factors, frequency, and causes of falling in geriatric persons who has had a limb removed by amputation. *Topics in Geriatric*, 26 (2), 156–163.

Underwood, H. A., Tokuno, C. D., & Eng, J. J. (2004) A comparison of two prosthetic feet on the multi-joint and multi-plane kinetic gait compensations in individuals with a unilateral trans-tibial amputation. *Clinical Biomechanics*, 19 (6), 609–616. Available From: https://doi.org/10.1016/j.clinbiomech.2004.02.005

van der Linde, H., Hofstad, C. J., Geurts, A. C. H., Postema, K., Geertzen, J. H. B., & van Limbeek, J. (2004) A systematic literature review of the effect of different prosthetic components on human functioning with a lower-limb prosthesis. *Journal of Rehabilitation Research and Development*, 41 (4), 555–570.

van der Linden, M. L., Solomonidis, S. E., Spence, W. D., Li, N., & Paul, J. P. (1999) A methodology for studying the effects of various types of prosthetic feet on the biomechanics of trans-femoral amputee gait. *Journal of Biomechanics*, 32 (9), 877–889. Available From: https://doi.org/10.1016/S0021-9290(99)00086-X

van Eijk, M.S., van der Linde, H., Buijck, B., Geurts, A., Zuidema, S., & Koopmans, R. (2012) Predicting prosthetic use in elderly patients after major lower limb amputation. *Prosthetics and Orthotics International*, 36 (1), 45-52. Available From: https://doi.org/10.1177/0309364611430885

van Schooten, K. S., Sloot, L. H., Bruijn, S. M., Kingma, H., Meijer, O. G., Pijnappels, M., & van Dieën, J. H. (2011) Sensitivity of trunk variability and stability measures to balance impairments induced by galvanic vestibular stimulation during gait. *Gait & Posture*, 33 (4), 656–660. Available From: https://doi.org/10.1016/j.gaitpost.2011.02.017

van Velzen, J. M., van Bennekom, C. A., Polomski, W., Slootman, J. R., van der Woude, L. H., & Houdijk, H. (2006) Physical capacity and walking ability after lower limb amputation: a systematic review. *Clinical Rehabilitation*, 20 (11), 999–1016. Available From: https://doi.org/10.1177/0269215506070700

Vincent, W. & Weir, J. (2012) *Statistics in Kinesiology 4th Edition*. Human Kinetics.

von Tscharner, V., Enders, H., & Maurer, C. (2013) Subspace Identification and Classification of Healthy Human Gait. *PLoS ONE*, 8 (7), 1–8. Available From: https://doi.org/10.1371/journal.pone.0065063

Waters, R. L. & Mulroy, S. (1999) The energy expenditure of normal and pathologic gait. *Gait & Posture*, 9 (3), 207–231. Available From: https://doi.org/10.1016/S0966-6362(99)00009-0

Wei, T.S., Liu, P.T., Chang, L.W. and Liu, S.Y. (2017) Gait asymmetry, ankle spasticity, and depression as independent predictors of falls in ambulatory stroke patients. *PLoS One*, 12 (5), e0177136.

Welch, P. D. (1967) The Use of Fast Fourier Transform for the Estimation of Power Spectra: A Method Based on Time Averaging Over Short, Modified Periodograms. *IEE Transactions on Audio and Electroacoustics*, 15 (2), 70–73.

Wight, D. L., Kubica, E. G., & Wang, D. W. L. (2008) Introduction of the Foot Placement Estimator: A Dynamic Measure of Balance for Bipedal Robotics. *Journal of Computational and Nonlinear Dynamics*, 3 (1), 011009. Available From: https://doi.org/10.1115/1.2815334

Williams, D. S. B., Green, D. H., & Wurzinger, B. (2012) Changes in lower extremity movement and power absorption during forefoot striking and barefoot running. *International Journal of Sports Physical Therapy*, 7 (5), 525–32.

Winter, D. A. (1995) Human blance and posture control during standing and walking. *Gait & Posture*, 3 (4), 193–214. Available From: https://doi.org/10.1016/0966-6362(96)82849-9

Winter, D. A. & Sienko, S. E. (1988) Biomechanics of below-knee amputee gait. *Journal of Biomechanics*, 21 (5), 361–367. Available From: https://doi.org/10.1016/0021-9290(88)90142-X

Winter, D. A. (2009) *Biomechanics and Motor Control of Human Movement*. John Wiley & Sons. Available From: https://doi.org/10.1002/9780470549148

Wolf, A., Swift, J., Swinney, H. L., Vastano, J., Wolf, A., Swift, J., & Lyapunov, D. (1985) Determining Lyapunov exponents from a time series. *Physica D: Nonlinear Phenomena*, 16 (3), 285–317.

Woodward, R. B., Spanias, J. A., & Hargrove, L. J. (2016) User intent prediction with a scaled conjugate gradient trained artificial neural network for lower limb amputees using a powered prosthesis. In *Engineering in Medicine and Biology Society (EMBC), 2016 IEEE 38th Annual International Conference of the* (6405-6408). Available From: https://doi.org/10.1109/EMBC.2016.7592194

Wootten, M. E., Kadaba, M. P., & Cochran, G. V. B. (1990) Dynamic electromyography. I. Numerical representation using principal component analysis. *Journal of Orthopaedic Research*, 8 (2), 247–258. Available From: https://doi.org/10.1002/jor.1100080214

Wouda, F.J., Giuberti, M., Bellusci, G., Maartens, E., Reenalda, J., Van Beijnum, B.J.F. and Veltink, P.H. (2018) Estimation of vertical ground reaction forces and sagittal knee kinematics during running using three inertial sensors. *Frontiers in physiology*, 9, 218.

Wu, J. & Wang, J. (2008) PCA-based SVM for automatic recognition of gait patterns. *Journal of Applied Biomechanics*, 24 (1), 83–87. Available From: https://doi.org/10.1123/jab.24.1.83

Wu, J., Wang, J., & Liu, L. (2007) Feature extraction via KPCA for classification of gait patterns. *Human Movement Science*, 26 (3), 393–411. Available From: https://doi.org/10.1016/j.humov.2007.01.015

Yakhdani, H.R.F., Bafghi, H.A., Meijer, O.G., Bruijn, S.M., van den Dikkenberg, N., Stibbe, A.B., van Royen, B.J., & van Dieën, J.H. (2010) Stability and variability of knee kinematics during gait in knee osteoarthritis before and after replacement surgery. *Clinical Biomechanics*, 25 (3), 230-236. Available From: https://doi.org/10.1016/j.clinbiomech.2009.12.003

Yang, M., Zheng, H., Wang, H., McClean, S., Hall, J., & Harris, N. (2012) A machine learning approach to assessing gait patterns for Complex Regional Pain Syndrome. *Medical Engineering and Physics*, 34 (6), 740–746. Available From: https://doi.org/10.1016/j.medengphy.2011.09.018

Young, A. J., Simon, A., & Hargrove, L. J. (2013) An intent recognition strategy for transfemoral amputee ambulation across different locomotion modes. In *Engineering in medicine and biology society (EMBC), 2013 35th Annual International Conference of the IEEE* (1587-1590). Available From: https://doi.org/10.1109/EMBC.2013.6609818

Young, A. J., Simon, A. M., Fey, N. P., & Hargrove, L. J. (2014) Intent recognition in a powered lower limb prosthesis using time history information. *Annals of Biomedical Engineering*, 42 (3), 631–641. Available From: https://doi.org/10.1007/s10439-013-0909-0

Zeni, J. A., Richards, J. G., & Higginson, J. S. (2008) Two simple methods for determining gait events during treadmill and overground walking using kinematic data. *Gait & Posture*, 27 (4), 710–714. Available From: https://doi.org/10.1016/j.gaitpost.2007.07.007

Zhan, A., Mohan, S., Tarolli, C., Schneider, R.B., Adams, J.L., Sharma, S., Elson, M.J., Spear, K.L., Glidden, A.M., Little, M.A. and Terzis, A. (2018). Using smartphones and machine learning to quantify Parkinson disease severity: the mobile Parkinson disease score. *JAMA neurology*, 75 (7), 876-880.

Zhang, X., Fiedler, G., Cao, Z. and Liu, Z. (2018) A support vector machine approach to detect trans-tibial prosthetic misalignment using 3-Dimensional ground reaction force features: A proof of concept. *Technology and Health Care*, (Preprint), 1-7.

Zhang, J., Lockhart, T. E., & Soangra, R. (2014) Classifying Lower Extremity Muscle Fatigue during Walking using Machine Learning and Inertial Sensors. *Annual Biomedical Engineering*, 42 (3), 600–612. Available From: https://doi.org/10.1007/s10439-013-0917-0.Classifying

Zheng, E., Wang, L., Luo, Y., Wei, K., & Wang, Q. (2013) Non-contact capacitance sensing for continuous locomotion mode recognition: design specifications and experiments with an amputee. In *Rehabilitation Robotics (ICORR), 2013 IEEE International Conference on* (1-6) Available From: https://doi.org/10.1109/ICORR.2013.6650410

Zheng, E. & Wang, Q. (2017) Noncontact capacitive sensing-based locomotion transition recognition for amputees with robotic transtibial prostheses. *IEEE Transactions on Neural Systems and Rehabilitation Engineering*, 25 (2), 161–170. Available From: https://doi.org/10.1109/TNSRE.2016.2529581

Zheng, H., Yang, M., Wang, H., & McClean, S. (2009) Machine Learning and Statistical Approaches to Support the Discrimination of Neuro-degenerative Diseases Based on Gait Analysis. In *Intelligent Patient Management* (57–70) Berlin, Heidelberg: Springer Berlin Heidelberg. Available From: https://doi.org/10.1007/978-3-642-00179-6_4

Ziegler-Graham, K., MacKenzie, E.J., Ephraim, P.L., Travison, T.G., & Brookmeyer, R. (2008) Estimating the prevalence of limb loss in the United States: 2005 to 2050. *Archives of Physical Medicine and Rehabilitation*, 89 (3), 422-429. Available From: https://doi.org/10.1016/j.apmr.2007.11.005

Zmitrewicz, R. J., Neptune, R. R., Walden, J. G., Rogers, W. E., & Bosker, G. W. (2006) The Effect of Foot and Ankle Prosthetic Components on Braking and Propulsive Impulses During Transtibial Amputee Gait. *Archives of Physical Medicine and Rehabilitation*, 87 (10), 1334–1339. Available From: https://doi.org/10.1016/j.apmr.2006.06.013

Chapter 10: Appendices

Appendix 1 – Multivariate Statistical Analyses Codes

Appendix 1.1 Principal Component Analysis Code

Appendix 1.1.1 – Covariance Approach

The following code was written in Matlab and illustrates how to upload data using the `dlmread` function, followed by developing a training data base and reshaping the data prior to the application of PCA.

```
%Upload data
folder_data = 'E:\Experimental Studies\Forward Progression and Dynamic
Balance\Results';

% Select an amputee at a timE:
amputee_array = [1:6 8:12];
Volunteers_No = 11;


%Select Group - PROSParticipants
counter = 1;
for person_No = amputee_array

    File_name1 = ['PROSParticipant00',num2str(person_No),'_NormalPROS.txt'];
    File_name2 =
['PROSParticipant00',num2str(person_No),'_NormalNONPROS.txt'];

    A_pro = dlmread([folder_data,'\',File_name1],'\t','B6..AO106');
    A_non_pro = dlmread([folder_data,'\',File_name2],'\t','B6..AO106');

    A_pro = A_pro(:,[1:3 7:9 13:15 19:2:40]);
    A_non_pro = A_non_pro(:,[1:3 7:9 13:15 19:2:40]);

    %Define measurement (columns in matrix)
    for measurement_No = 1:size(A_pro,2)
        training_data_base_non_pro(:,measurement_No,counter) =
A_non_pro(:,measurement_No);
        training_data_base_pro(:,measurement_No,counter) =
A_pro(:,measurement_No);
    end
    counter = counter+1;
end


training_data_base(:,:,1:Volunteers_No) = training_data_base_pro;
training_data_base(:,:,(Volunteers_No+1):2*Volunteers_No) =
training_data_base_non_pro;

%Define condition - PROSParticipants
PROSNormal = size(training_data_base,3);


%Upload data
folder_data = 'E:\Experimental Studies\Forward Progression and Dynamic
Balance\Results';

% Select total number of volunteers:
No_volunteers = 30;
counter = 1;
%Select Group - PROSParticipants
for person_No = [1 3 5:32]

    File_name3 = ['CONParticipant00',num2str(person_No),'_NormalL.txt'];
```

```
    File_name4 = ['CONParticipant00',num2str(person_No),'_NormalR.txt'];

    A_right = dlmread([folder_data,'\',File_name3],'\t','B6..AO106');
    A_left = dlmread([folder_data,'\',File_name4],'\t','B6..AO106');

    A_right =  A_right(:,[1:3 7:9 13:15 19:2:40]);
    A_left = A_left(:,[1:3 7:9 13:15 19:2:40]);

    %Define measurement (columns in matrix)
    for measurement_No = 1:size(A_left,2)
        training_data_base_left(:,measurement_No,counter) =
A_left(:,measurement_No);
        training_data_base_right(:,measurement_No,counter) =
A_right(:,measurement_No);
    end
    %
    counter = counter + 1;
end

training_data_base(:,:,(PROSNormal+1):(PROSNormal + No_volunteers)) =
training_data_base_right;
training_data_base(:,:,(PROSNormal + 1 + No_volunteers):(PROSNormal +
2*No_volunteers)) = training_data_base_left;

% Normalise the measurements:
training_data_base = normalise_data(training_data_base);

%Reshape the data so that one 'run' ends up being one long array of
numbers(all measurements are put into one string of data):
reshaped_training_data_base =
reshape(training_data_base,size(training_data_base,1)*size(training_data_base,
2),size(training_data_base,3));

%Undertake Principal Component Analysis of the training data base:

% Centre the data set:
temp2 = mean(reshaped_training_data_base,2);
centred_data_set = (reshaped_training_data_base -
temp2*ones(1,size(reshaped_training_data_base,2)))';

% Calculate the PCA scores and eigenvectors:
L = centred_data_set*centred_data_set'; % L is the covariance matrix C=A*A'.
[V D] = eig(L); % Diagonal elements of D are the eigenvalues for both L=A'*A
and C=A*A'.

% Calculate the pseudo inverse (because centred_data_set2'*V is not a
% square matrix) to access the eigenvectors:
temp = centred_data_set'*V;
eigendata = pinv(temp');

% Calculate the PCA scores for all measurements:
scores = temp'*centred_data_set';
scores = flipud(scores);
eigendata = fliplr(eigendata);
```

Appendix 1.1.1.1 – Normalisation of Data for Covariance Matrix

Since the data is comprised of variables with different units, this needs to be accounted for,thus the data has been normalised using following code.

```
function y = normalise_data(X);

% data in body weight:
max_magnitude = max(max(max(abs(X(:,[1:3],:)))));
for limb = 1:size(X,3)
  X(:,1:3,limb) = (1/max_magnitude)*X(:,1:3,limb);
end

% data in meters:
max_magnitude = max(max(max(abs(X(:,[4:6 10],:)))));
for limb = 1:size(X,3)
  X(:,[4:6 10],limb) = (1/max_magnitude)*X(:,[4:6 10],limb);
end

% data in meters/s:
max_magnitude = max(max(max(abs(X(:,[7:9 11],:)))));
for limb = 1:size(X,3)
  X(:,[7:9 11],limb) = (1/max_magnitude)*X(:,[7:9 11],limb);
end

% data in Watt/kg:
max_magnitude = max(max(max(abs(X(:,[12 15 18],:)))));
for limb = 1:size(X,3)
  X(:,[12 15 18],limb) = (1/max_magnitude)*X(:,[12 15 18],limb);
end

% data in N.m/kg:
max_magnitude = max(max(max(abs(X(:,[13 16 19],:)))));
for limb = 1:size(X,3)
  X(:,[13 16 19],limb) = (1/max_magnitude)*X(:,[13 16 19],limb);
end

% data in degrees:
max_magnitude = max(max(max(abs(X(:,[14 17 20],:)))));
for limb = 1:size(X,3)
  X(:,[14 17 20],limb) = (1/max_magnitude)*X(:,[14 17 20],limb);
end

y = X;
```

Appendix 1.1.2 – Correlation Approach

Principal Component Analysis can be computed using a covariance and correlation matrices. The following code illustrates how to implement the correlation matrix. If the variables to hand have different units one may choose to use the correlation matrix instead of normalising the data to units and using the covariance matrix. The normalisation procedure for both methods differs thus the answers will differ.

```
% Divide by the standard deviation in order to diagonalise the correlation
matrix rather than the covariance matrix:
%centred_data_set2 =
centred_data_set./((std(centred_data_set')')*ones(1,size(centred_data_set,2)))
;
centred_data_set =
centred_data_set./(ones(size(centred_data_set,1),1)*std(centred_data_set));


centred_data_set(isinf(centred_data_set)) = 0;
centred_data_set(isnan(centred_data_set)) = 0;


% Calculate the PCA scores and eigenvectors:
L = centred_data_set*centred_data_set'; % L is the correlation matrix C=A*A'.
[V D] = eig(L); % Diagonal elements of D are the eigenvalues for both L=A'*A
and C=A*A'.


% Calculate the pseudo inverse (because centred_data_set2'*V is not a
% square matrix) to access the eigenvectors:
temp = centred_data_set'*V;
eigendata = pinv(temp');


% Calculate the PCA scores for all measurements:
scores = temp'*centred_data_set';
scores = flipud(scores);
eigendata = fliplr(eigendata);
```

Appendix 1.2 Discriminant Functional Analysis Code

The following code was used to compute DFA.

```
function [U,V,eigenvals] = DFA(X,group,maxfac)
%[U,V,eigenvals] = DFA(X,group,maxfac)
% Performs DISCRIMINANT FUNCTION ANALYSIS
%
% INPUT VARIABLES
%
% X       = data matrix that contains m groups
%         Dim(X) = [N x M]. All columns must be independent.
% group     = a vector containing a number corresponding
%         to a group for every row in X. If you have
%         m groups there will be numbers in the range
%         1:m in this vector.
% maxfac     = the maximum number of DFA factors extracted
%
% OUTPUT VARIABLES
%
% U       = DFA scores matrix (Dim(U) = [N x maxfac])
%         the eigenvalues are multiplied with each column
%         in this matrix.
% V       = DFA loadings matrix, Dim(V) = [M x maxfac]
% eigenvals   = a vector of DFA eigenvalues
%
%
% Copyright, B.K. Alsberg, 1996

[T,W]=TW_gen(X,group);

B = T-W;

invW = inv(W);
P = invW*B;

[vec1,val]=eig(P);
d=(diag(val))';
eigenvals = d(1:maxfac);

% Here we sort the eigenvectors w.r.t. the eigenvalues:
[dummy,idx]=sort(-eigenvals);
vec = vec1(:,idx);
eigenvals = eigenvals(idx);
```

```
%% V is the matrix of canonical variates directions
V = vec(:,1:maxfac);

%% U is the matrix of scores
U = X*V;

% new line to multiply eigenvalues to DFA directions:
U = U*diag(eigenvals);
U = real(U);
```

Appendix 1.3 – Euclidean Distance Codes

The following code was used to calculate the standard deviation in order to quantify deviation.

Appendix 1.3.1 – Euclidean Distance from Centre of Cloud

```
  figure(5)
  clf
  for PC_score = 1:6
    subplot(2,3,PC_score)
    %subplot(2,2,PC_score)
    imagesc(reshaped_eigendata(:,:,PC_score))
    xlabel('Measured variables','FontName','Times','FontSize',15)
    ylabel('Gait cycle','FontName','Times','FontSize',15)
    title(['Amputee No. ',num2str(amputee_No),', Eig. rank =
',num2str(PC_score)],'FontName','Times','FontSize',15)
  end
```

Appendix 1.3.2 – Euclidean Distance from Origin of Principal Components

```
  figure(6)
  clf
  for PC_score = 1:6
    subplot(2,3,PC_score)
    %subplot(2,2,PC_score)
    temp = mean(abs(reshaped_eigendata(:,:,PC_score)));
    [a b] = sort(temp,'descend');
    bar(temp(b),'w')
    set(gca,'XTick',(1:20))
    for uu = 1:20
      lab{uu} = num2str(b(uu));
    end
    set(gca,'XTicklabel',lab')
    xlabel('Measured variables','FontName','Times','FontSize',15)
    ylabel('Weighting factor','FontName','Times','FontSize',15)
    title(['Amputee No. ',num2str(amputee_No),', Eig. rank =
',num2str(PC_score)],'FontName','Times','FontSize',15)
    axis tight
  end
```

Appendix 2 – Supplementary Results of Study 2 Presented in Chapter 5

Appendix 2.1 – Results of Scalar Values, Not Normalised

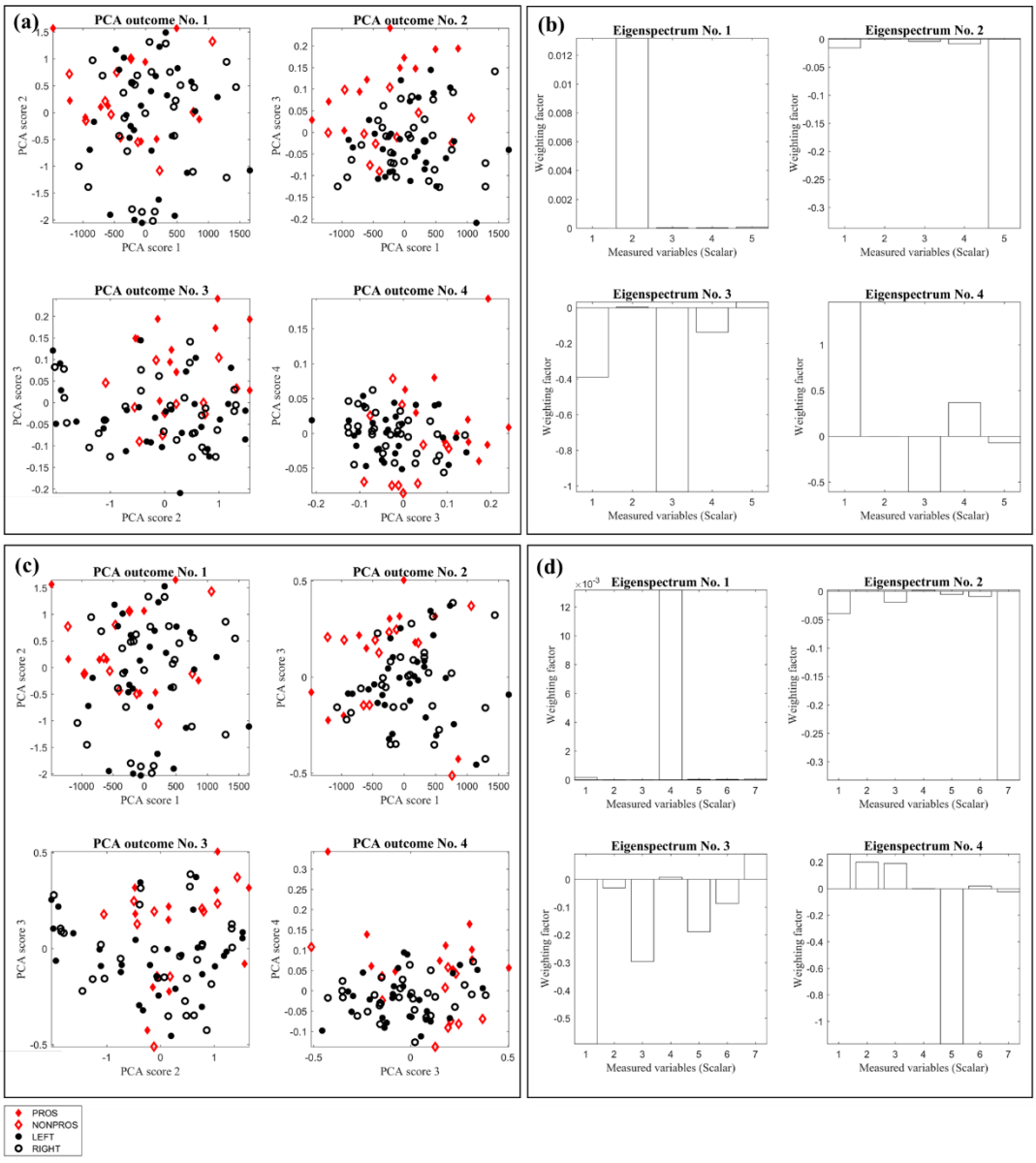

Figure 10.1 PCA outcome (a, c) and Eigenspectrum (b, d) comparing between individuals with UTTA and able-bodied individuals using five scalar values (a, b) and seven scalar values (c, d) not normalised to units.

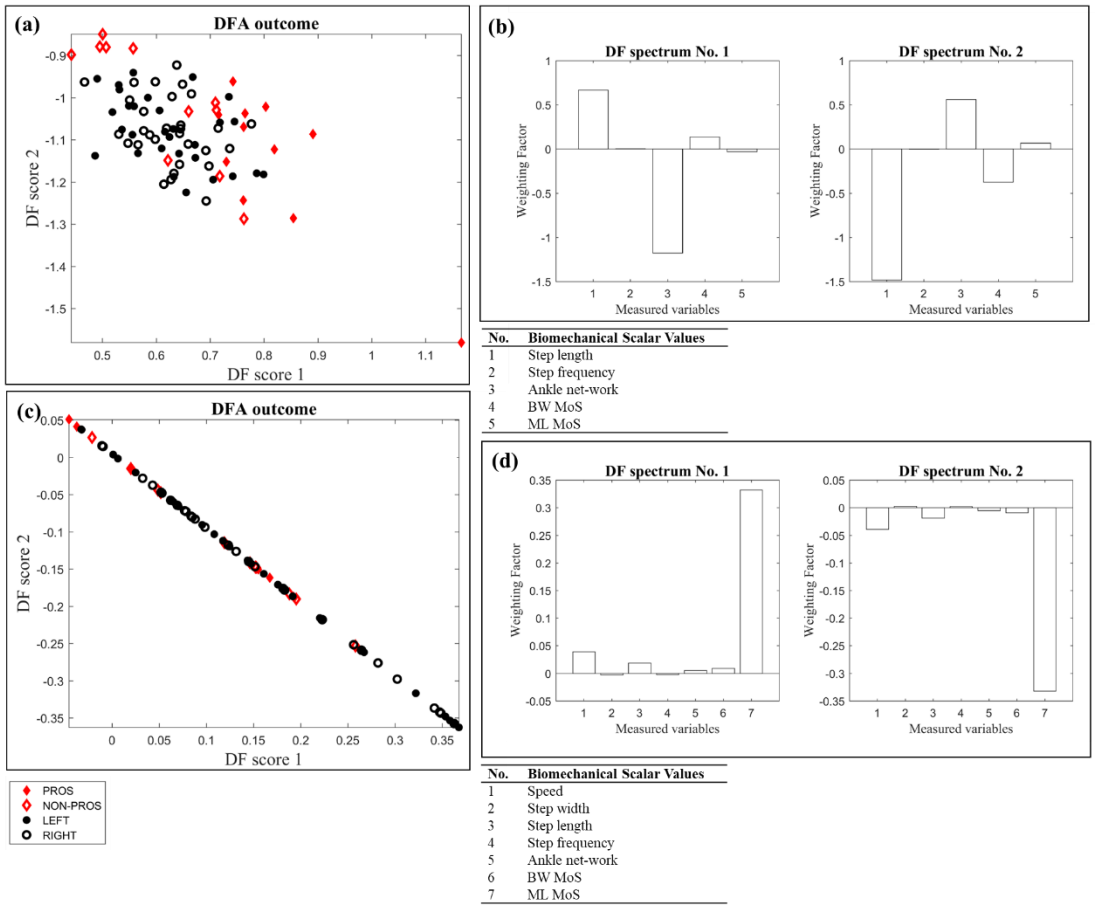

Figure 10.2 DFA classification outcome (a, c) and DF spectrum (b, d) of individuals with UTTA and able-bodied individuals using five scalar values (a, b) and seven scalar values (c, d), not normalised to units. In the DF spectrum, each bar is equivalent to a measured variable from a DF curve, integrated over all spectral frequencies.

Appendix 2.2 – Results of Temporal Waveforms and Seven Scalar Values, Normalised

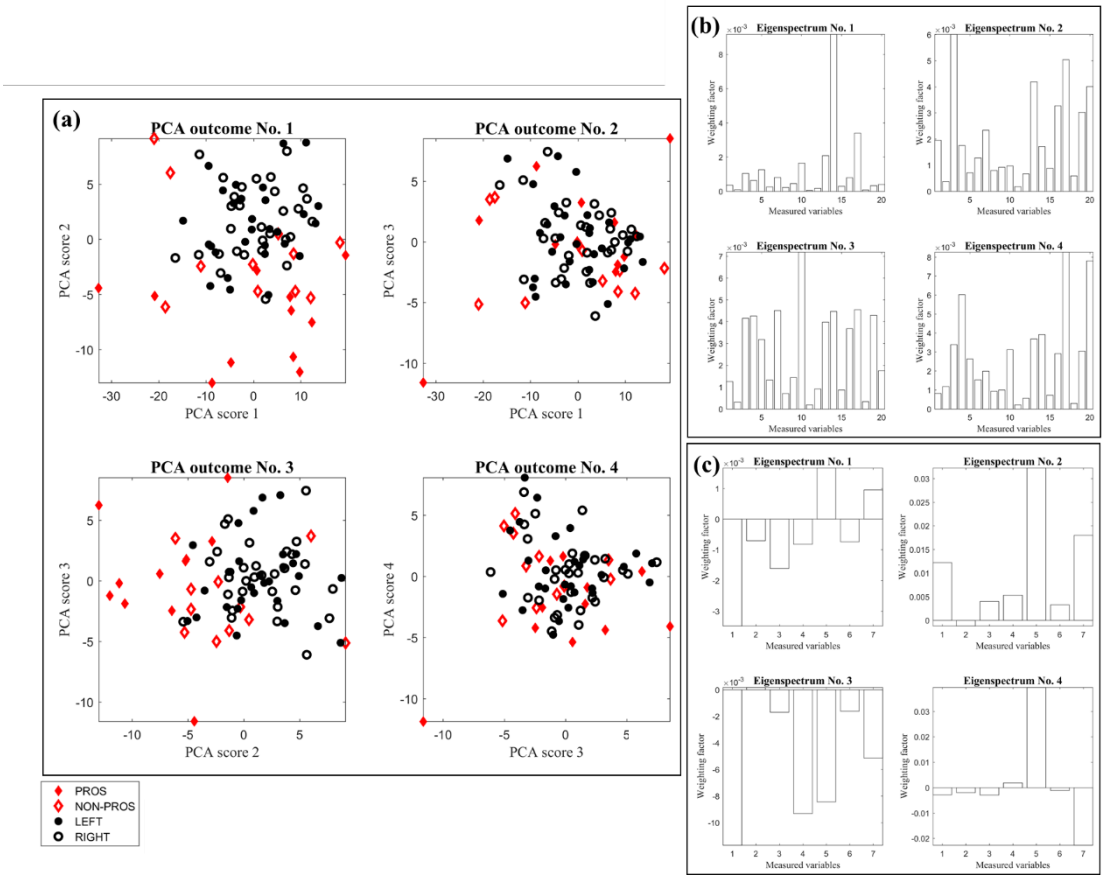

Figure 10.3 PCA (a) outcome and Eigenspectrum (b, c) of individuals with UTTA and able-bodied individuals using temporal waveforms and seven scalar values, normalised to units.

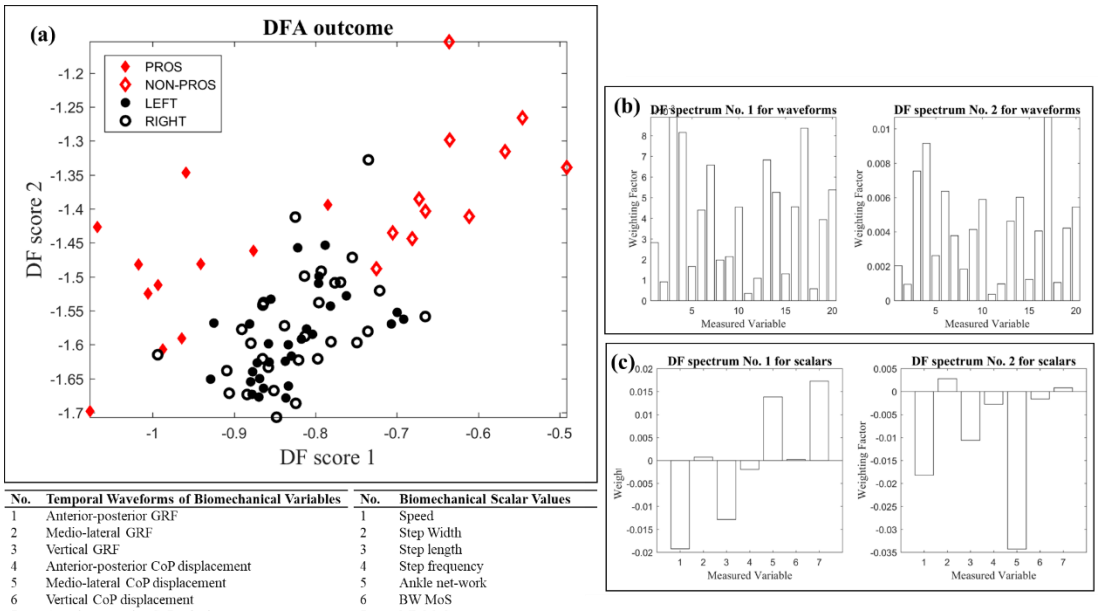

No.	Temporal Waveforms of Biomechanical Variables
1	Anterior-posterior GRF
2	Medio-lateral GRF
3	Vertical GRF
4	Anterior-posterior CoP displacement
5	Medio-lateral CoP displacement
6	Vertical CoP displacement
7	Anterior-posterior CoP velocity
8	Medio-lateral CoP velocity
9	Vertical CoP velocity
10	Vertical CoM displacement
11	Vertical CoM velocity
12	Sagittal hip joint power
13	Sagittal hip joint moment
14	Sagittal hip joint angle
15	Sagittal knee joint power
16	Sagittal knee joint moment
17	Sagittal knee joint angle
18	Sagittal ankle joint power
19	Sagittal ankle joint moment
20	Sagittal ankle joint angle

No.	Biomechanical Scalar Values
1	Speed
2	Step Width
3	Step length
4	Step frequency
5	Ankle net-work
6	BW MoS
7	ML MoS

Figure 5.8 DFA classification outcome (a) and DF spectrum comparing between individuals with UTTA and able-bodied individuals using temporal waveforms (b) and seven scalar values (c).

Appendix 3 – Supplementary Results of Study 3 Presented in Chapter 6

Appendix 3.1 – Covariance and Correlation Matrices for Comparing One Individuals with Unilateral Trans-Tibial Amputation with a Group of Able-Bodied Individuals

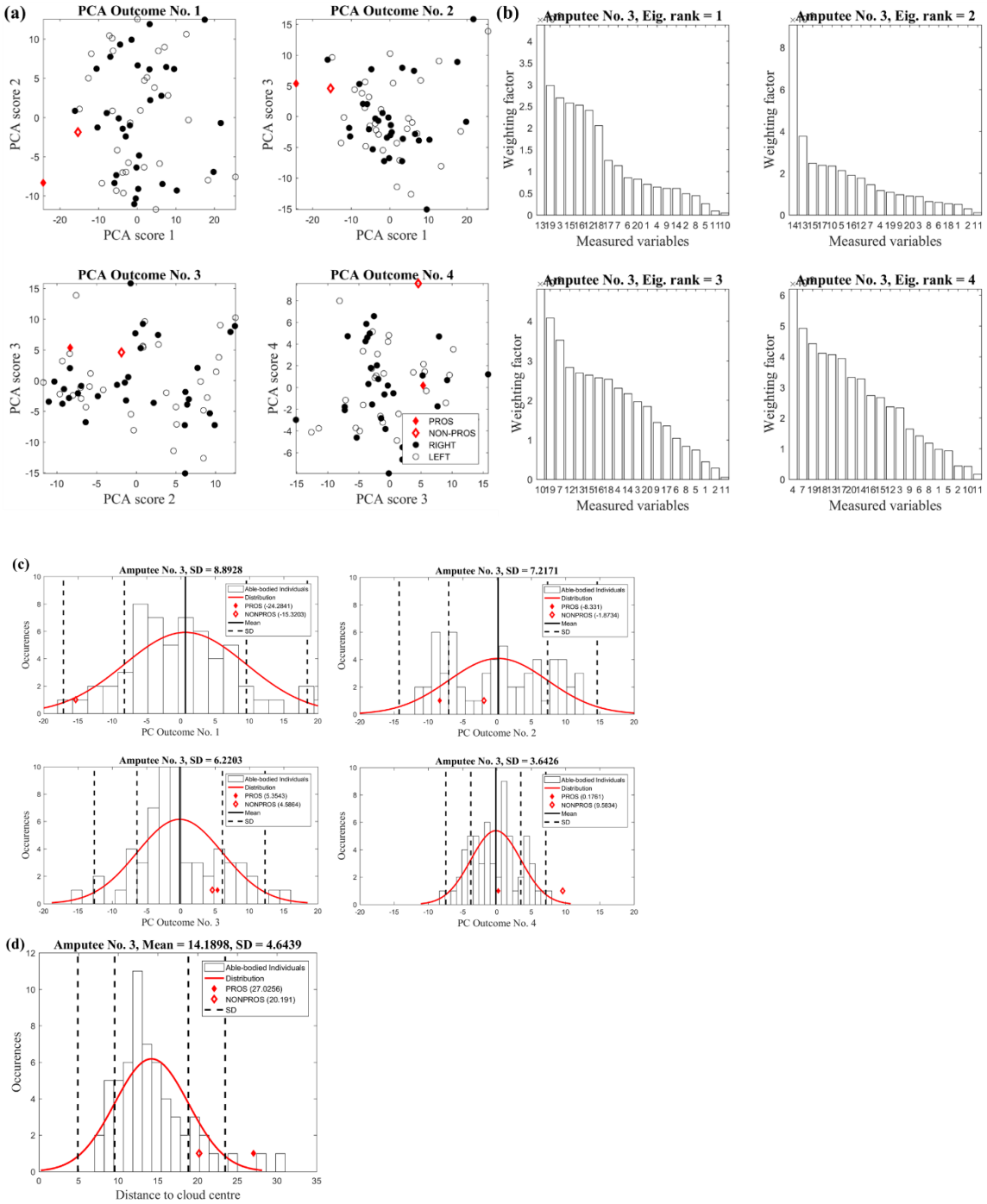

Figure 10.5 PCA outcome using the covariance approach with data normalised to units (a), the corresponding Eigenspectra (b), the Euclidian distance from the origin of the principal component (c) and the Euclidian distance from the centre of the cloud of individual with UTTA number 3.

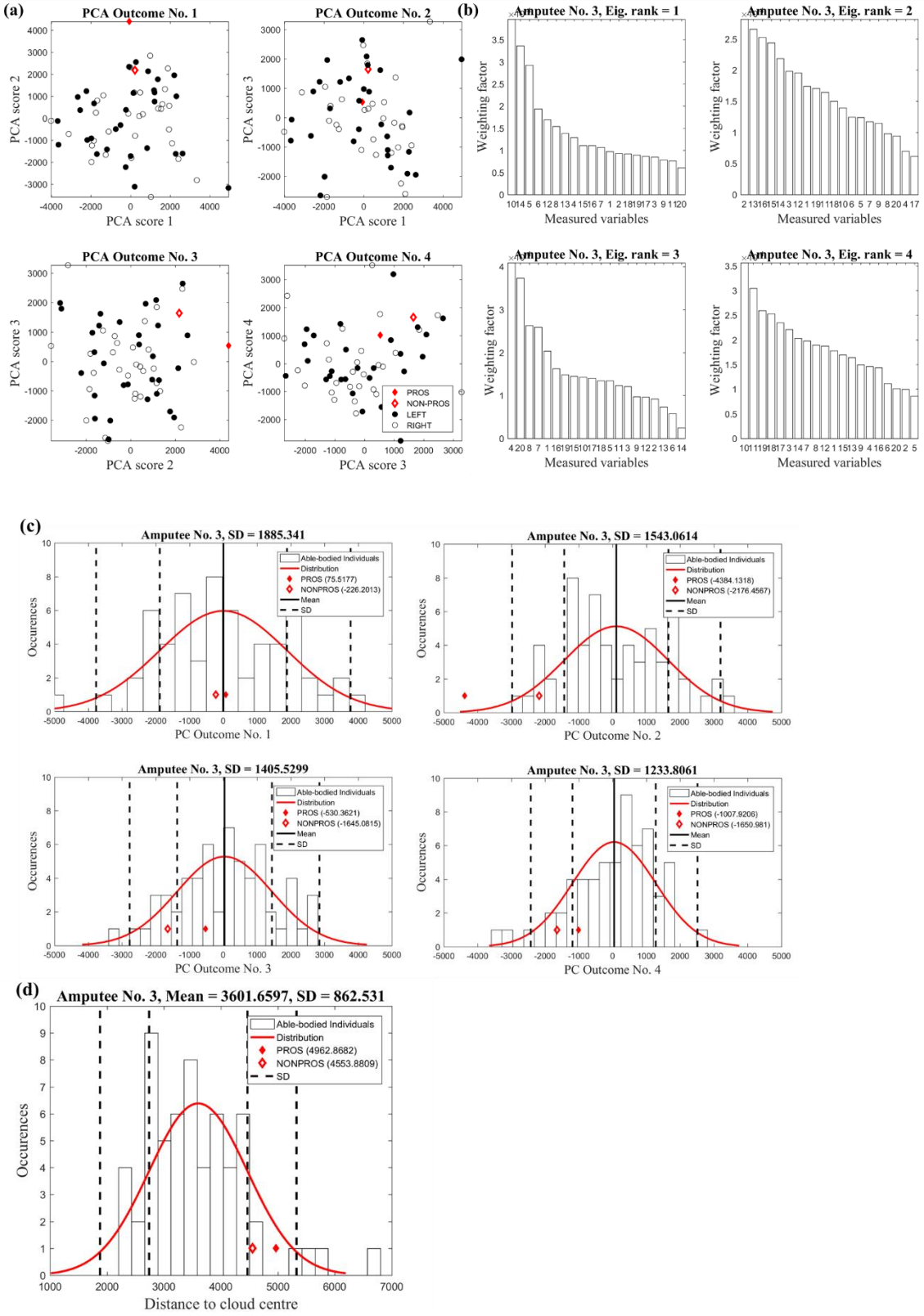

Figure 10.6 PCA outcome using the correlation approach (a), the corresponding Eigenspectra (b), the Euclidian distance from the origin of the principal component (c) and the Euclidian distance from the centre of the cloud of individual with UTTA number 3.

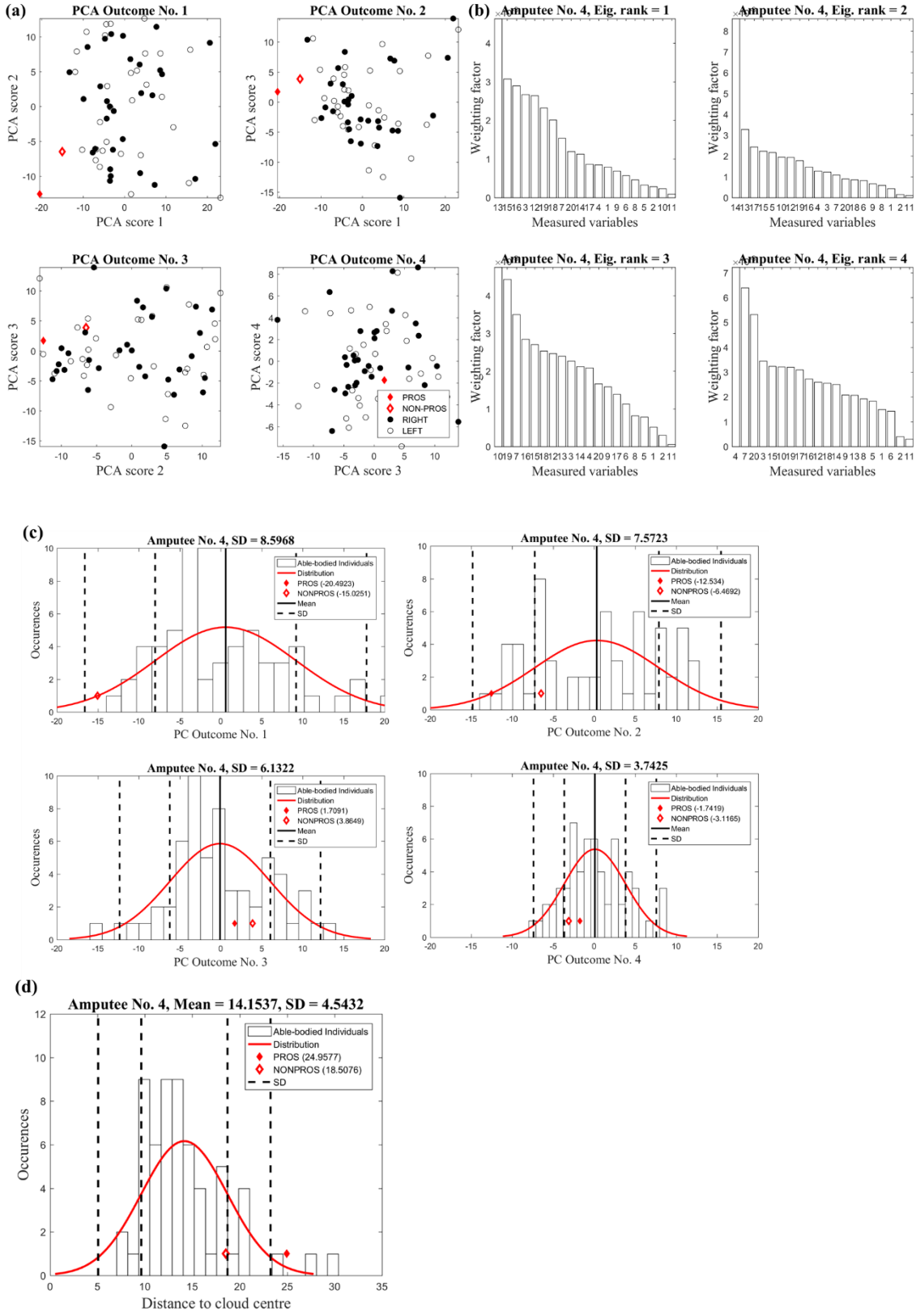

Figure 10.7 PCA outcome using the covariance approach with data normalised to units (a), the corresponding Eigenspectra (b), the Euclidian distance from the origin of the principal component (c) and the Euclidian distance from the centre of the cloud of individual with UTTA number 4.

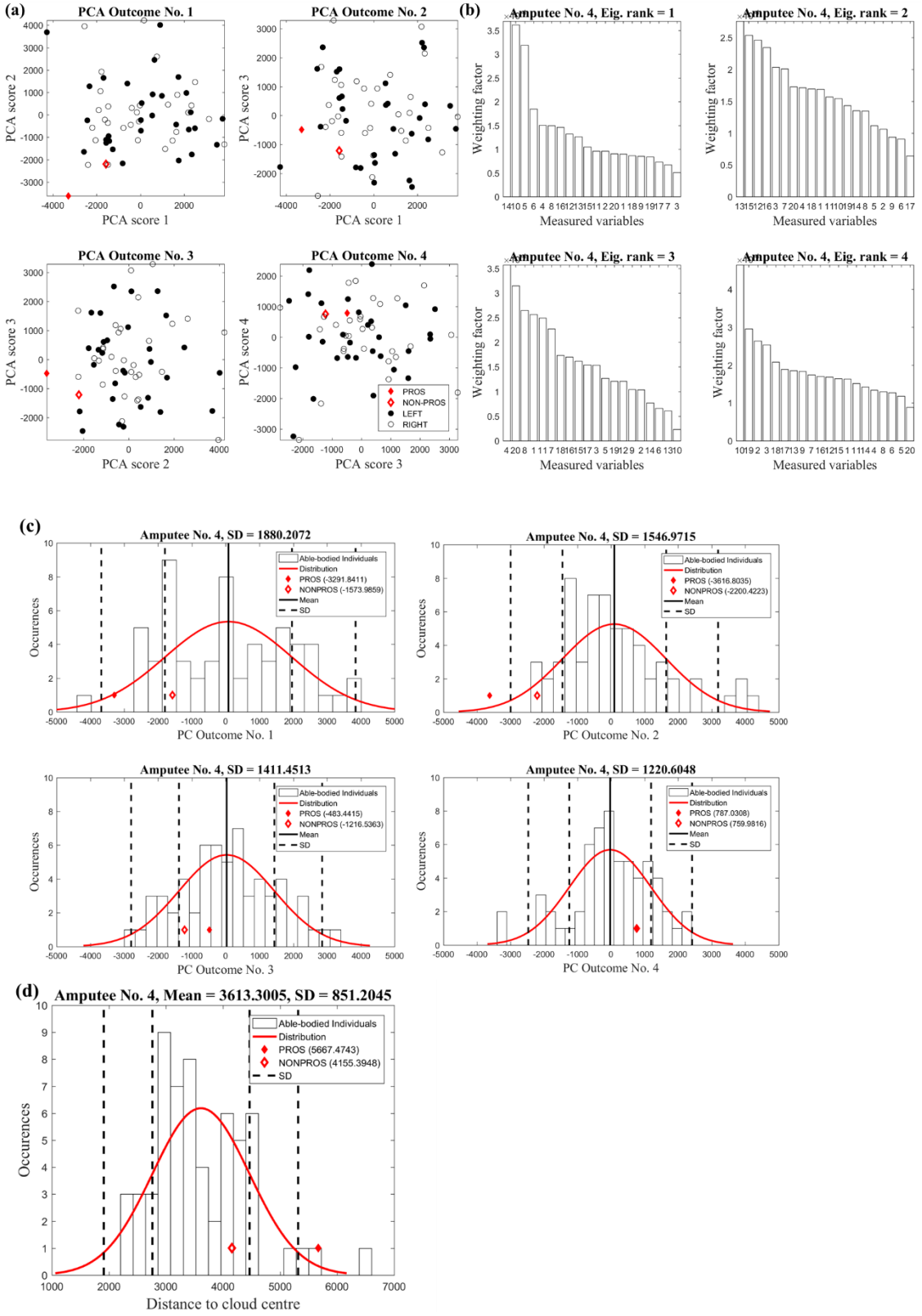

Figure 10.8 PCA outcome using the correlation approach (a), the corresponding Eigenspectra (b), the Euclidian distance from the origin of the principal component (c) and the Euclidian distance from the centre of the cloud of individual with UTTA number 4.

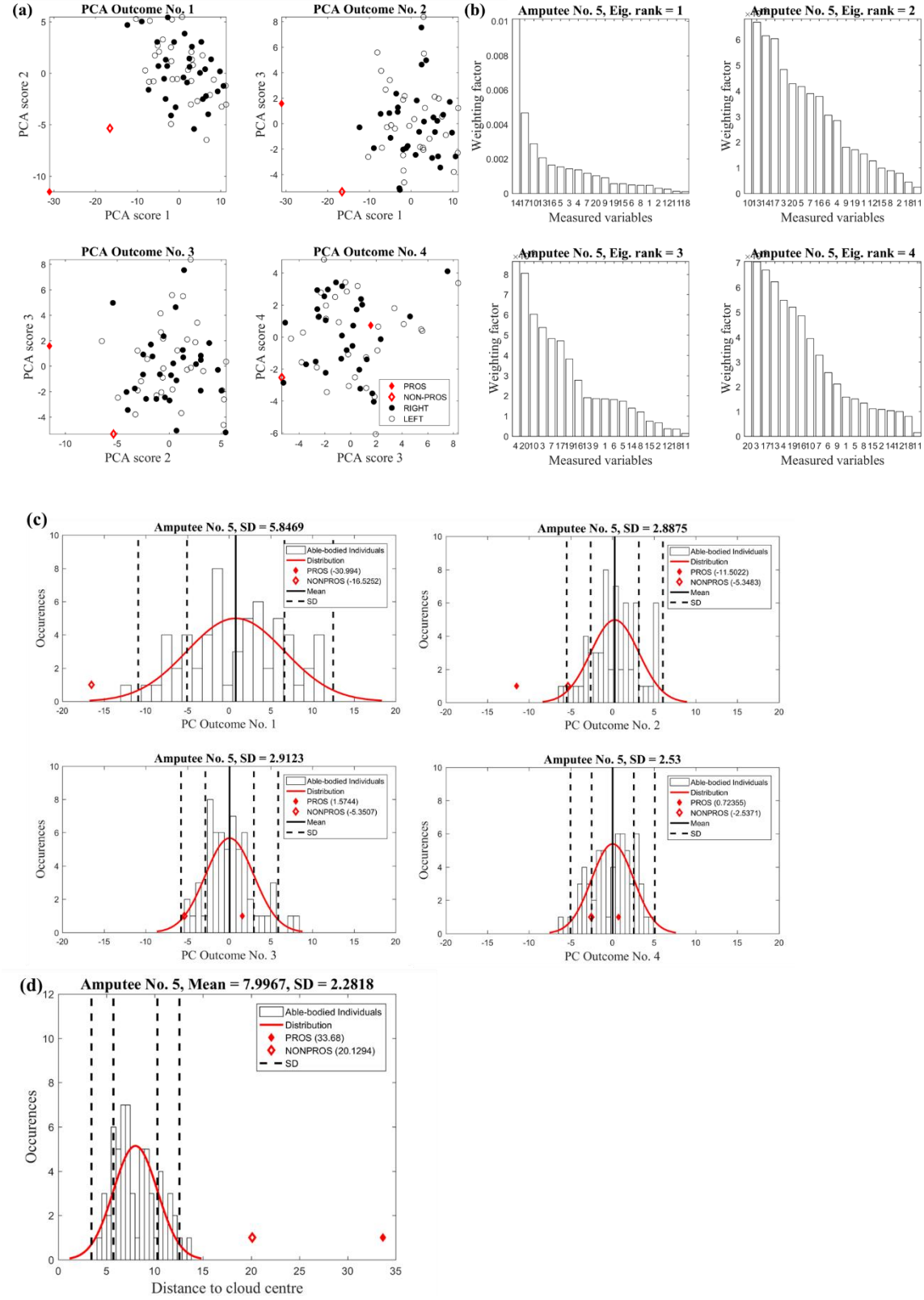

Figure 10.9 PCA outcome using the covariance approach with data normalised to units (a), the corresponding Eigenspectra (b), the Euclidian distance from the origin of the principal component (c) and the Euclidian distance from the centre of the cloud of individual with UTTA number 5.

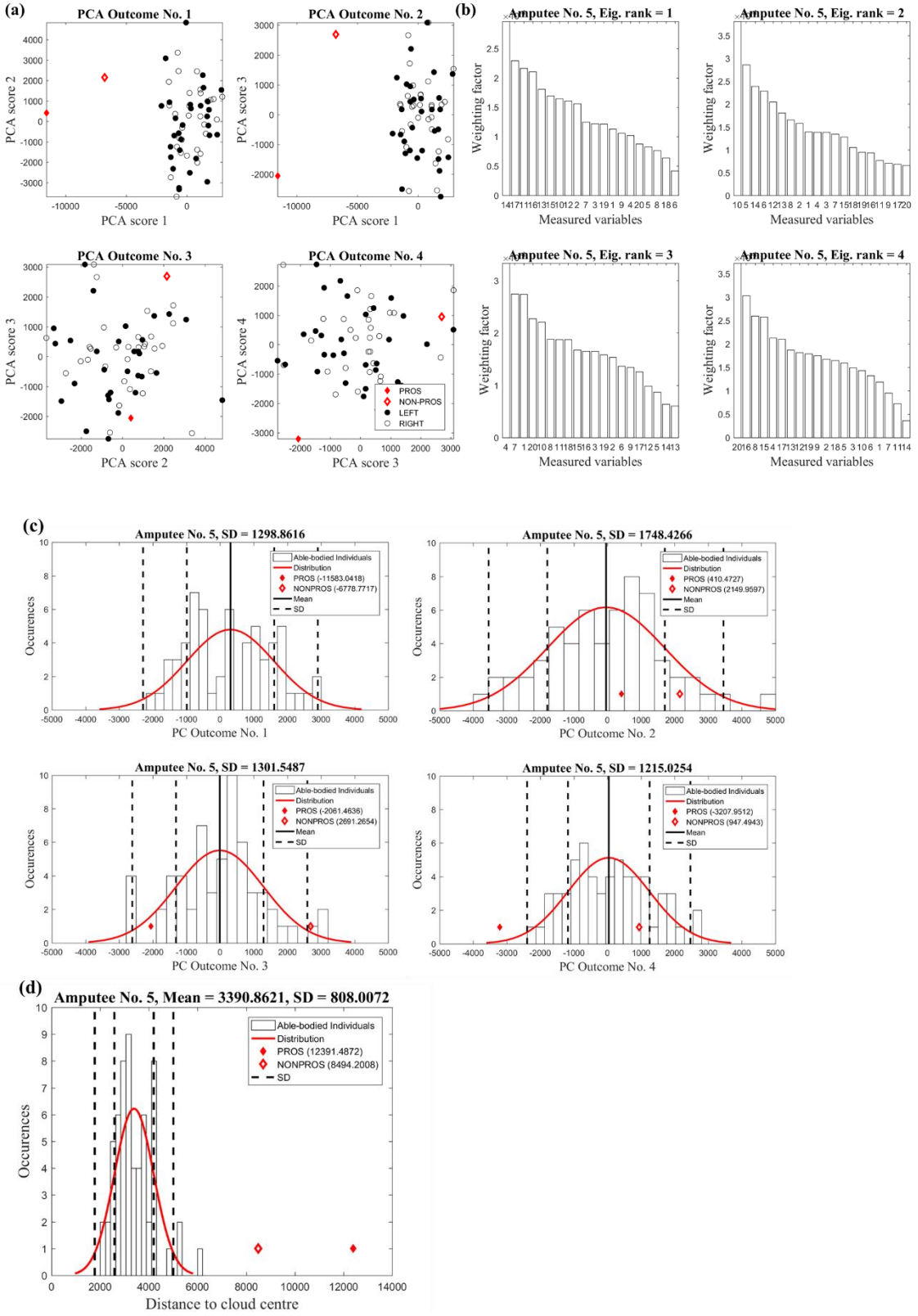

Figure 10.10 PCA outcome using the correlation approach (a), the corresponding Eigenspectra (b), the Euclidian distance from the origin of the principal component (c) and the Euclidian distance from the centre of the cloud of individual with UTTA number 5.

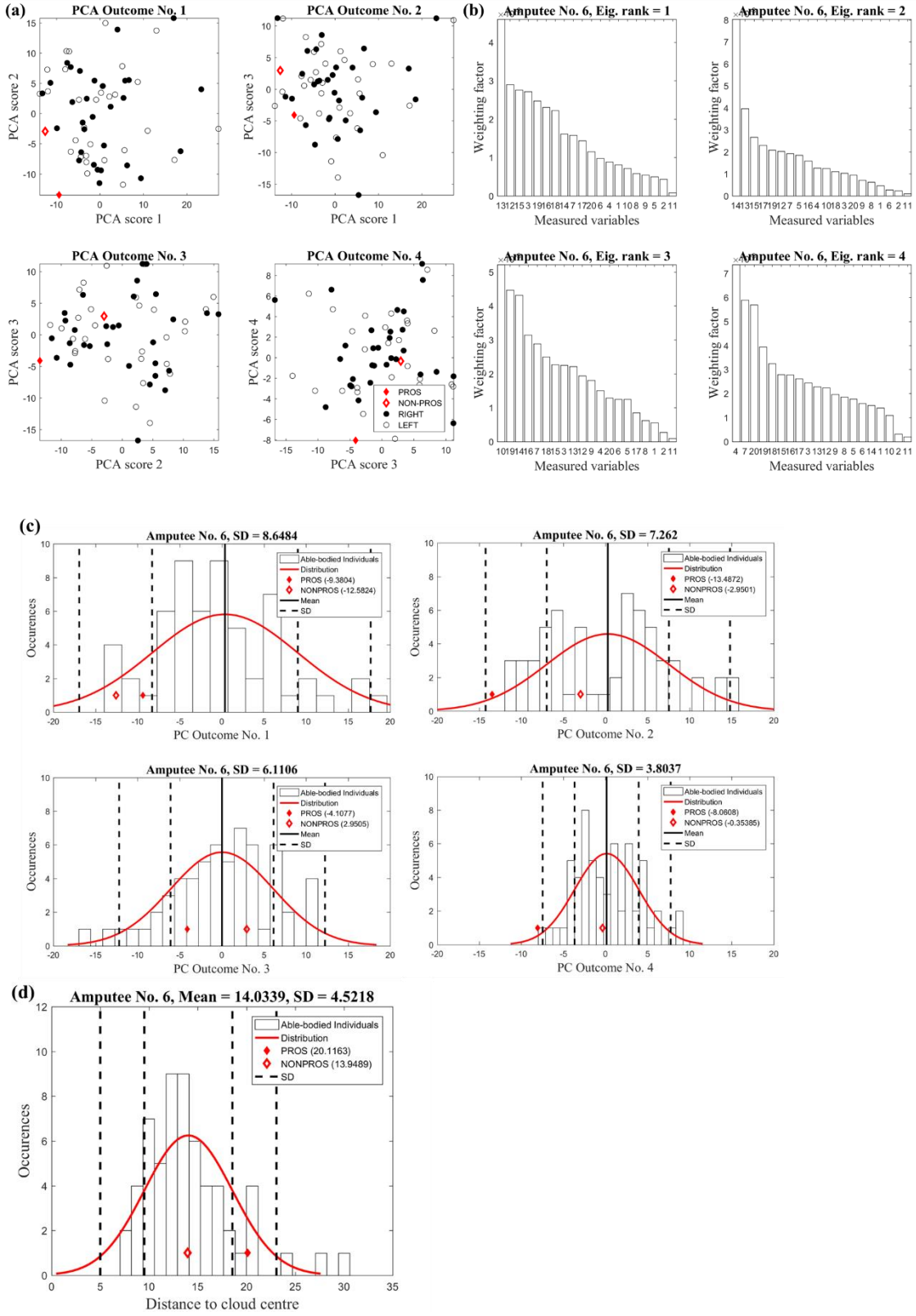

Figure 10.11 PCA outcome using the covariance approach with data normalised to units (a), the corresponding Eigenspectra (b), the Euclidian distance from the origin of the principal component (c) and the Euclidian distance from the centre of the cloud of individual with UTTA number 6.

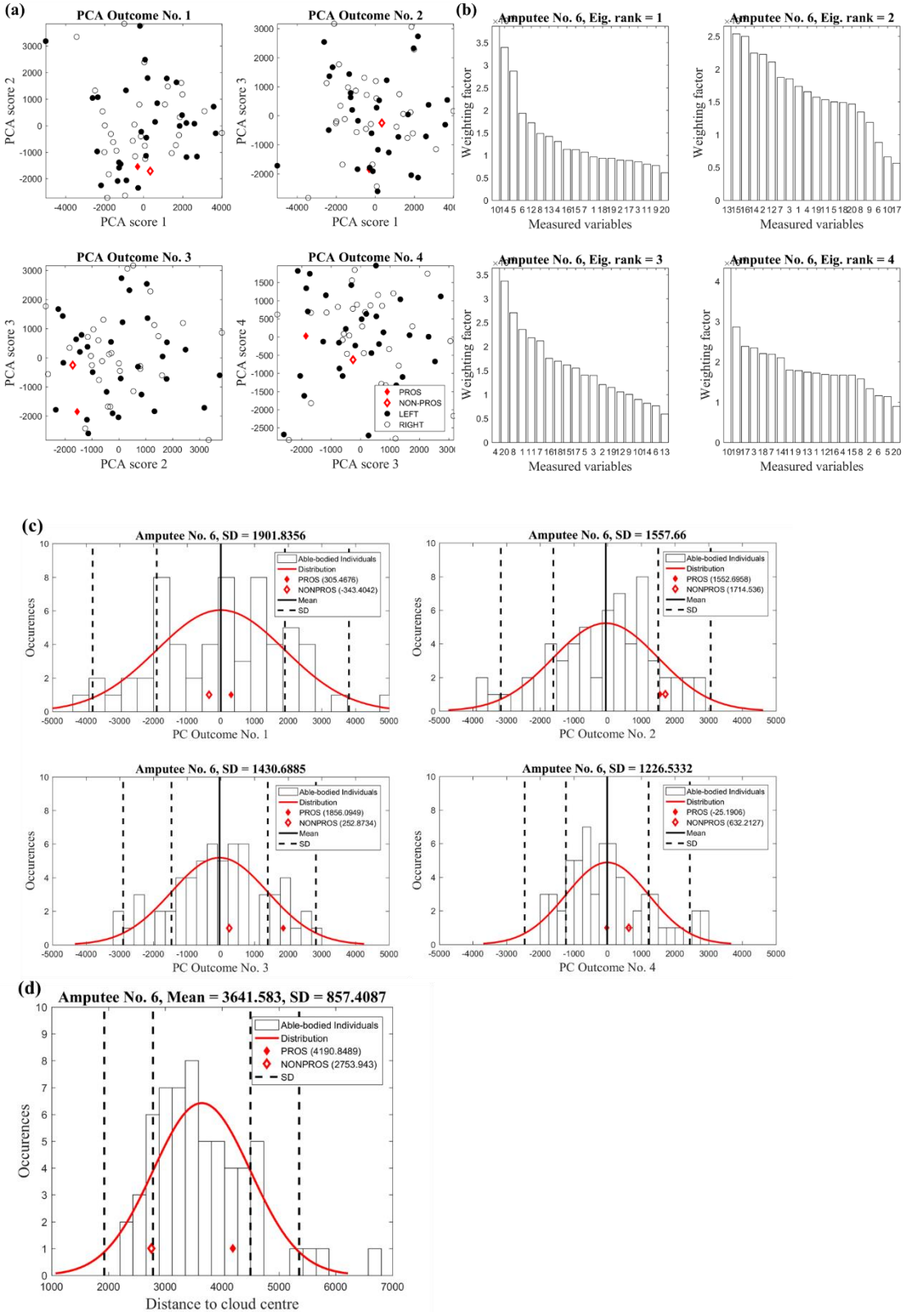

Figure 10.12 PCA outcome using the correlation approach (a), the corresponding Eigenspectra (b), the Euclidian distance from the origin of the principal component (c) and the Euclidian distance from the centre of the cloud of UTTA individual with number 6.

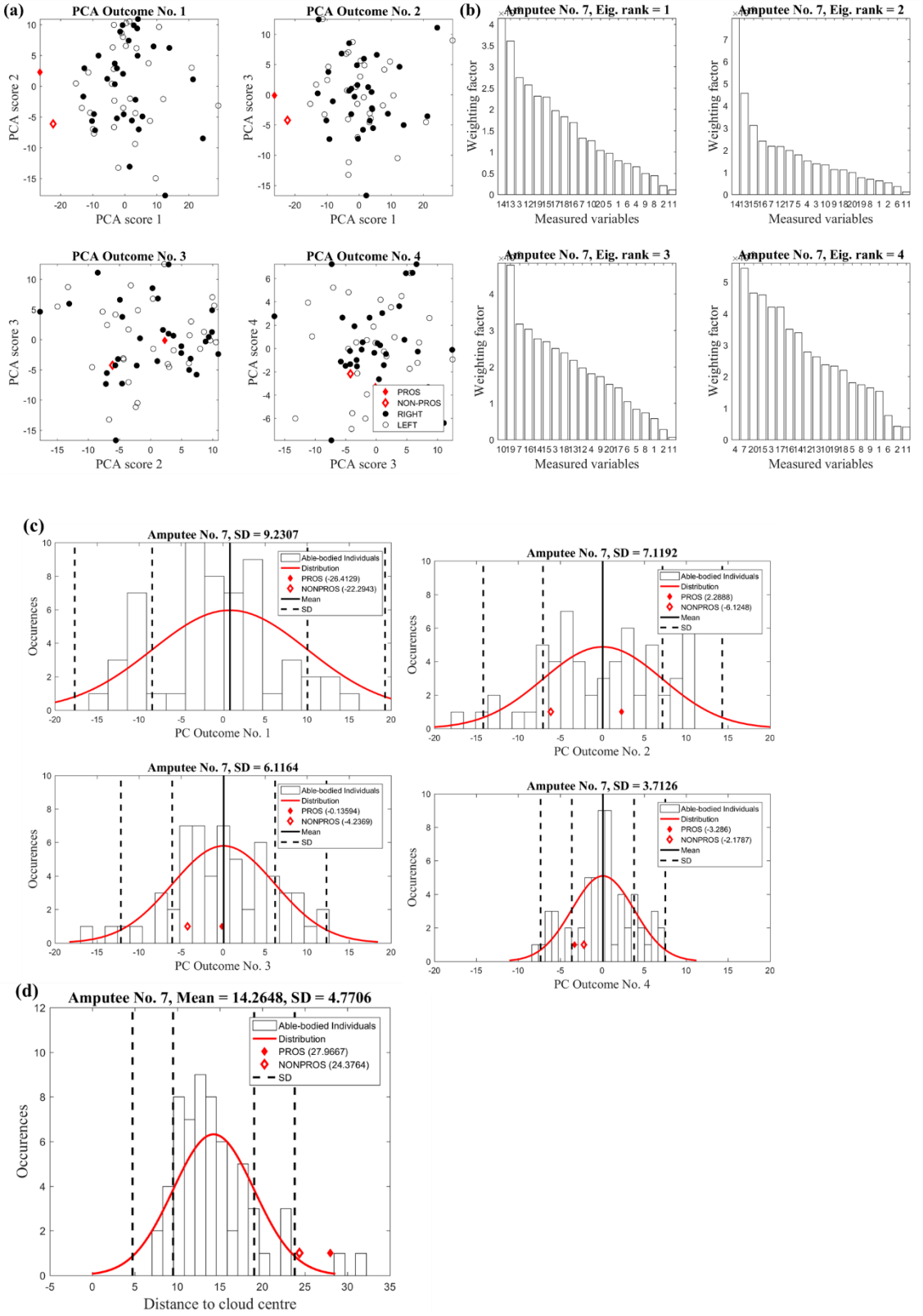

Figure 10.13 PCA outcome using the covariance approach with data normalised to units (a), the corresponding Eigenspectra (b), the Euclidian distance from the origin of the principal component (c) and the Euclidian distance from the centre of the cloud of individual with UTTA number 7.

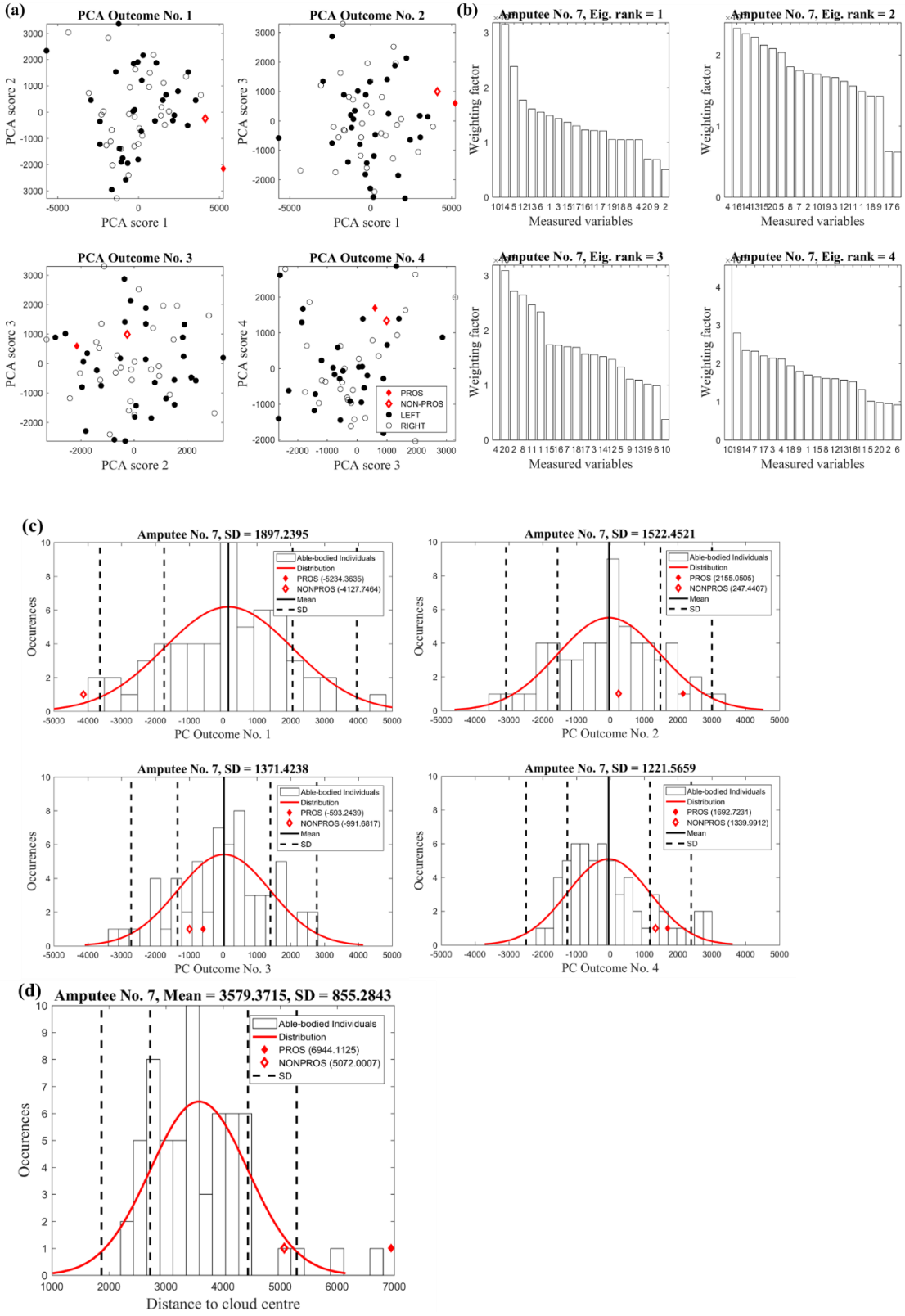

Figure 10.14 PCA outcome using the correlation approach (a), the corresponding Eigenspectra (b), the Euclidian distance from the origin of the principal component (c) and the Euclidian distance from the centre of the cloud of individual with UTTA number 7.

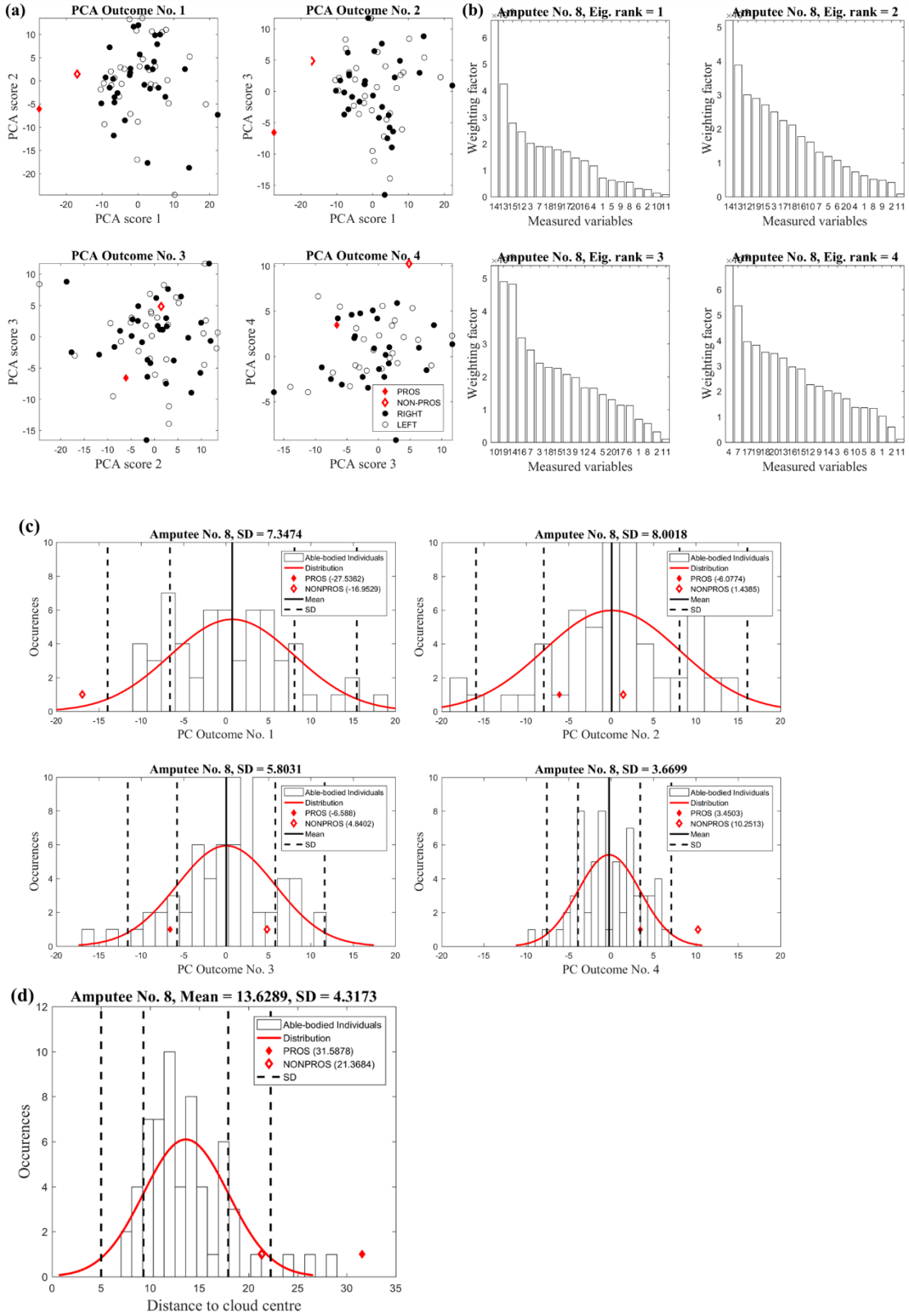

Figure 10.15 PCA outcome using the covariance approach with data normalised to units (a), the corresponding Eigenspectra (b), the Euclidian distance from the origin of the principal component (c) and the Euclidian distance from the centre of the cloud of individual with UTTA number 8.

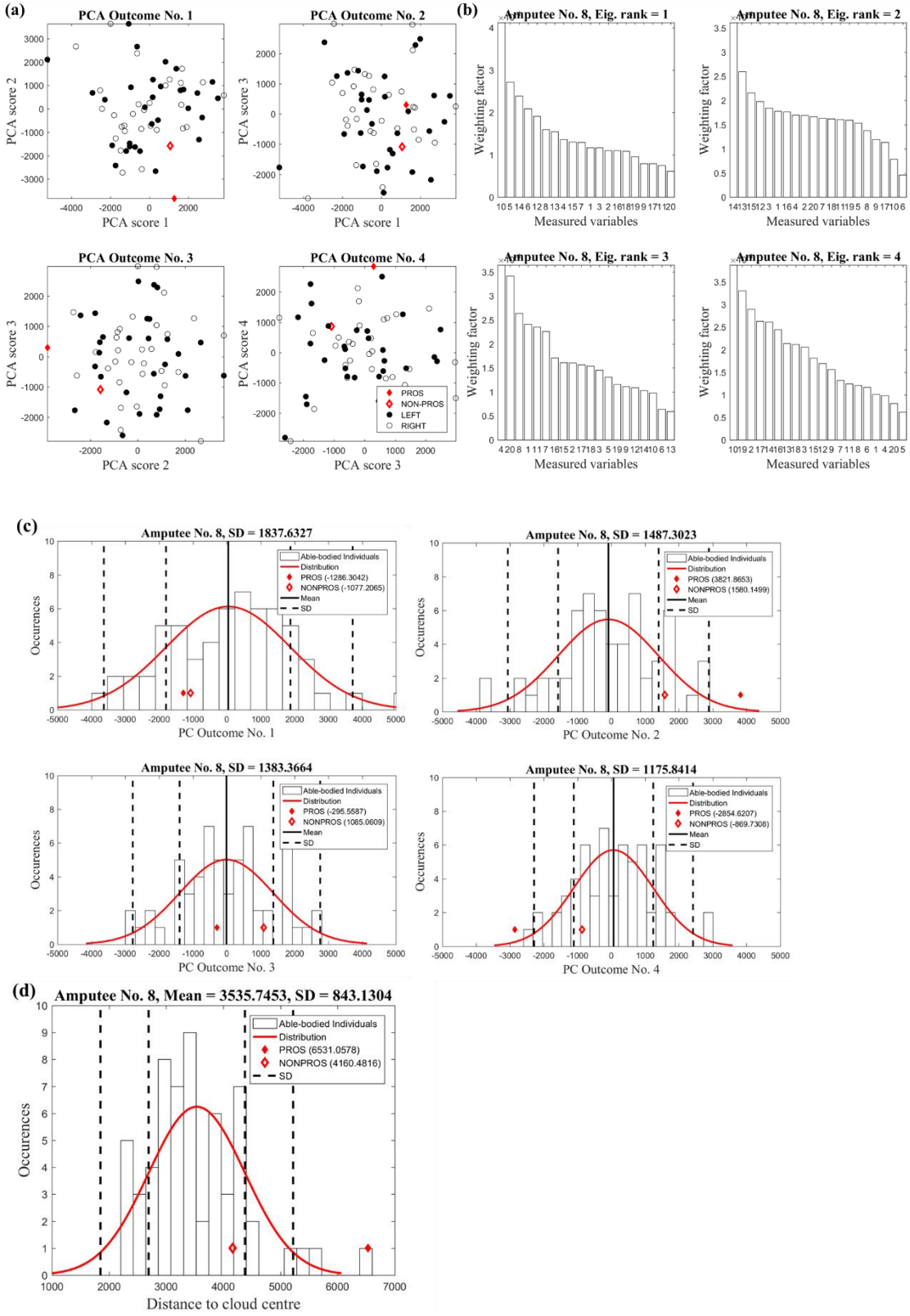

Figure 10.16 PCA outcome using the correlation approach (a), the corresponding Eigenspectra (b), the Euclidian distance from the origin of the principal component (c) and the Euclidian distance from the centre of the cloud of individual with UTTA number 8.

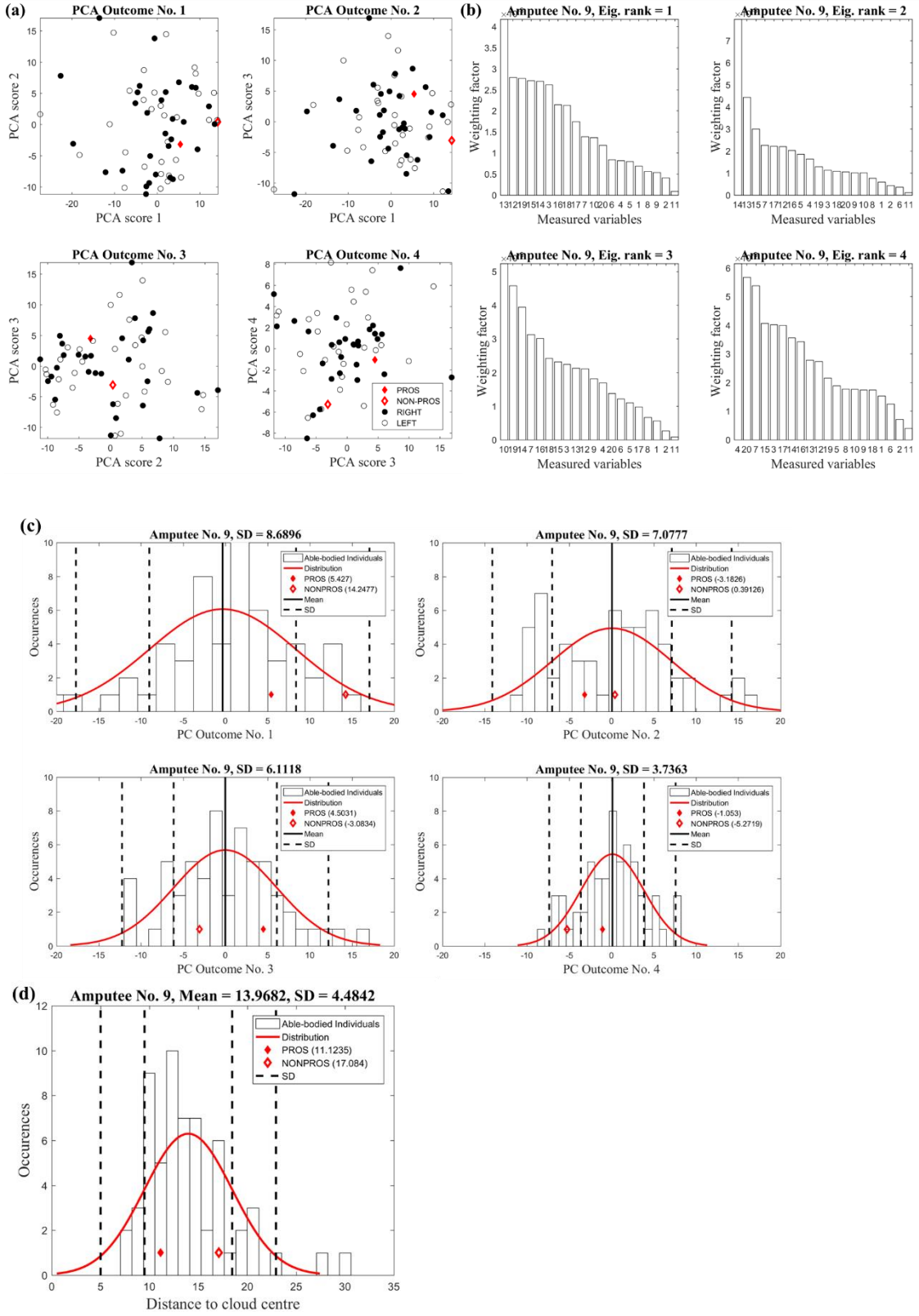

Figure 10.17 PCA outcome using the covariance approach with data normalised to units (a), the corresponding Eigenspectra (b), the Euclidian distance from the origin of the principal component (c) and the Euclidian distance from the centre of the cloud of individual with UTTA number 9.

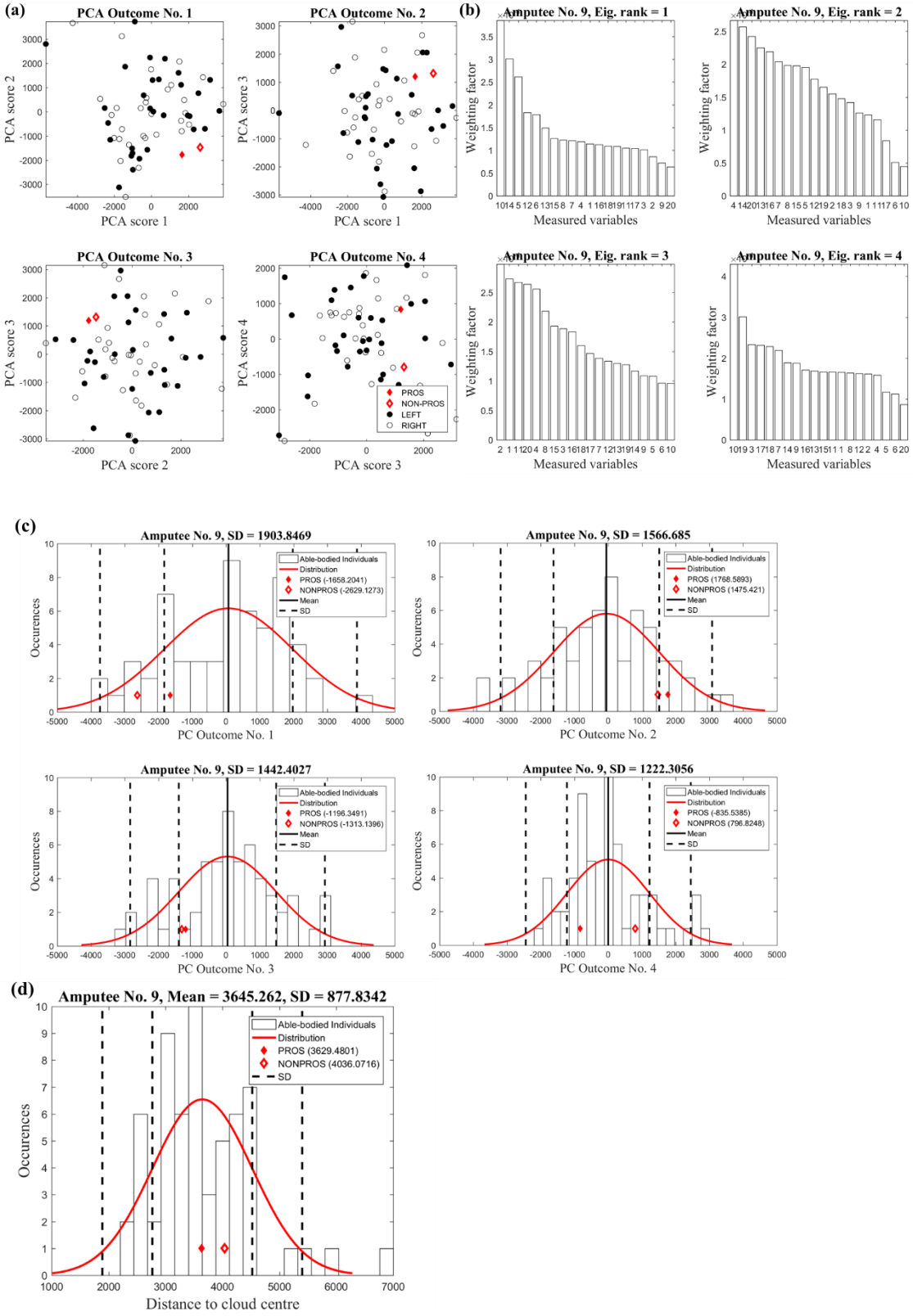

Figure 10.18 PCA outcome using the correlation approach (a), the corresponding Eigenspectra (b), the Euclidian distance from the origin of the principal component (c) and the Euclidian distance from the centre of the cloud of individual with UTTA number 9.

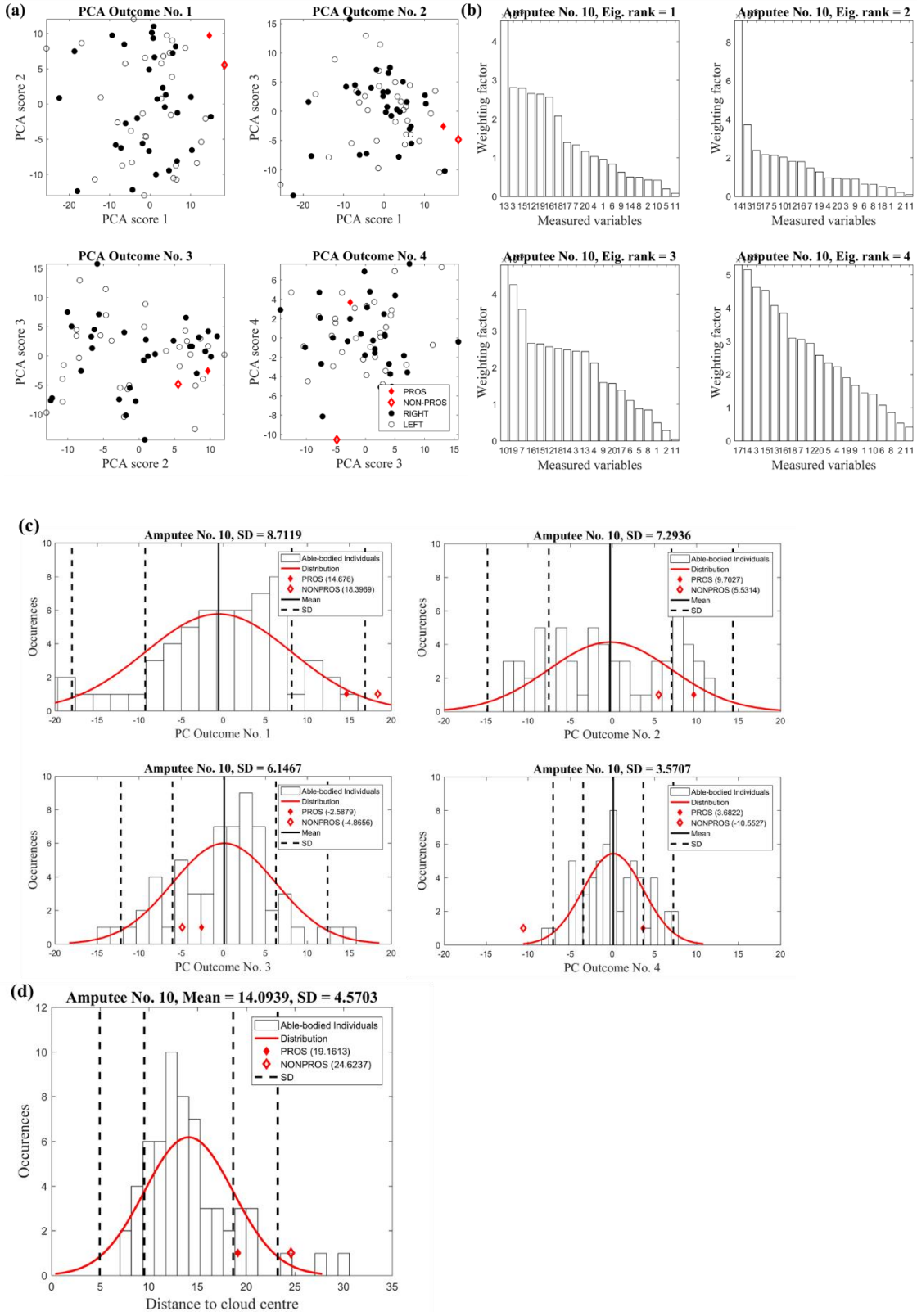

Figure 10.19 PCA outcome using the covariance approach with data normalised to units (a), the corresponding Eigenspectra (b), the Euclidian distance from the origin of the principal component (c) and the Euclidian distance from the centre of the cloud of individual with UTTA number 10.

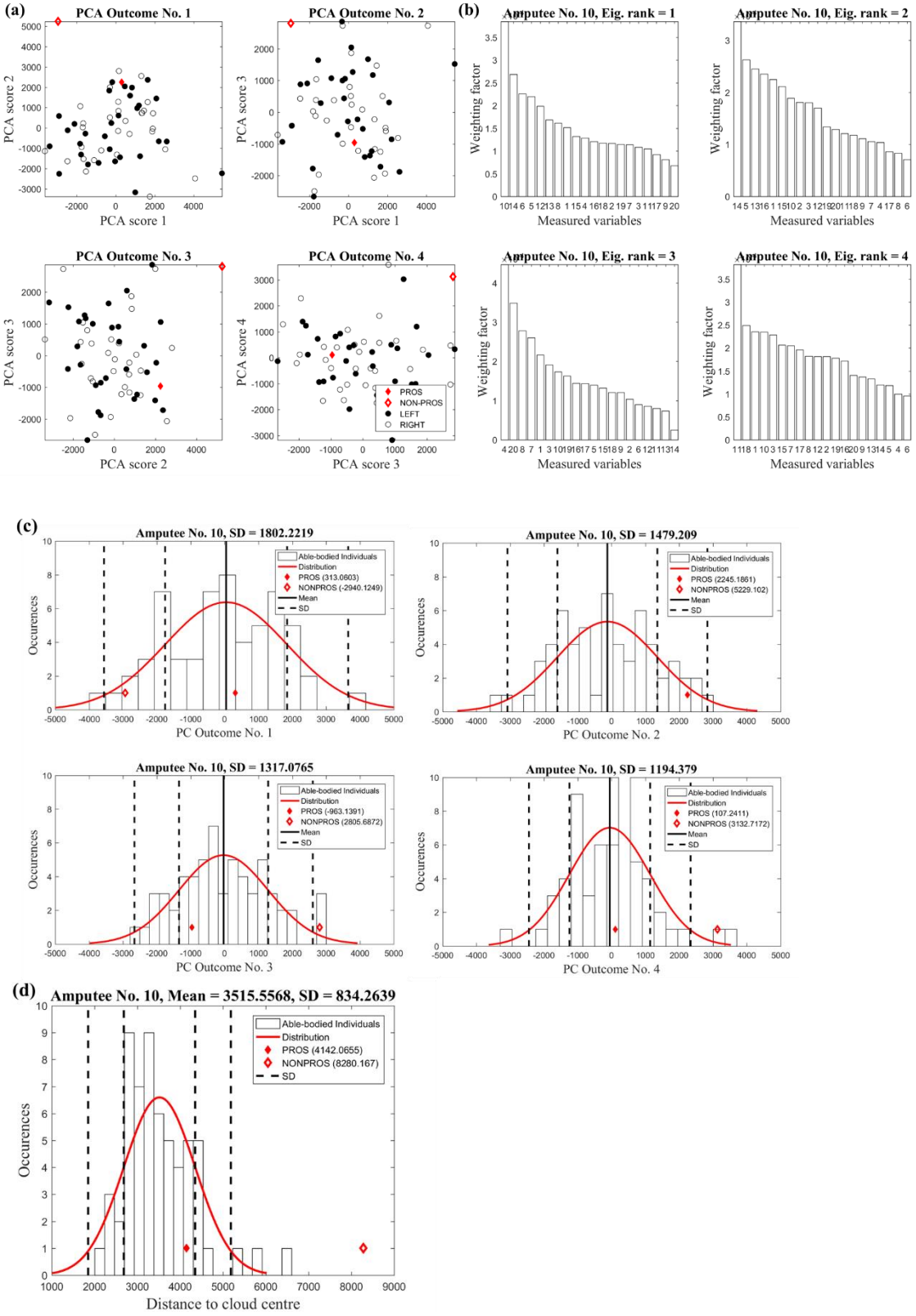

Figure 10.20 PCA outcome using the correlation approach (a), the corresponding Eigenspectra (b), the Euclidian distance from the origin of the principal component (c) and the Euclidian distance from the centre of the cloud of individual with UTTA number 10.

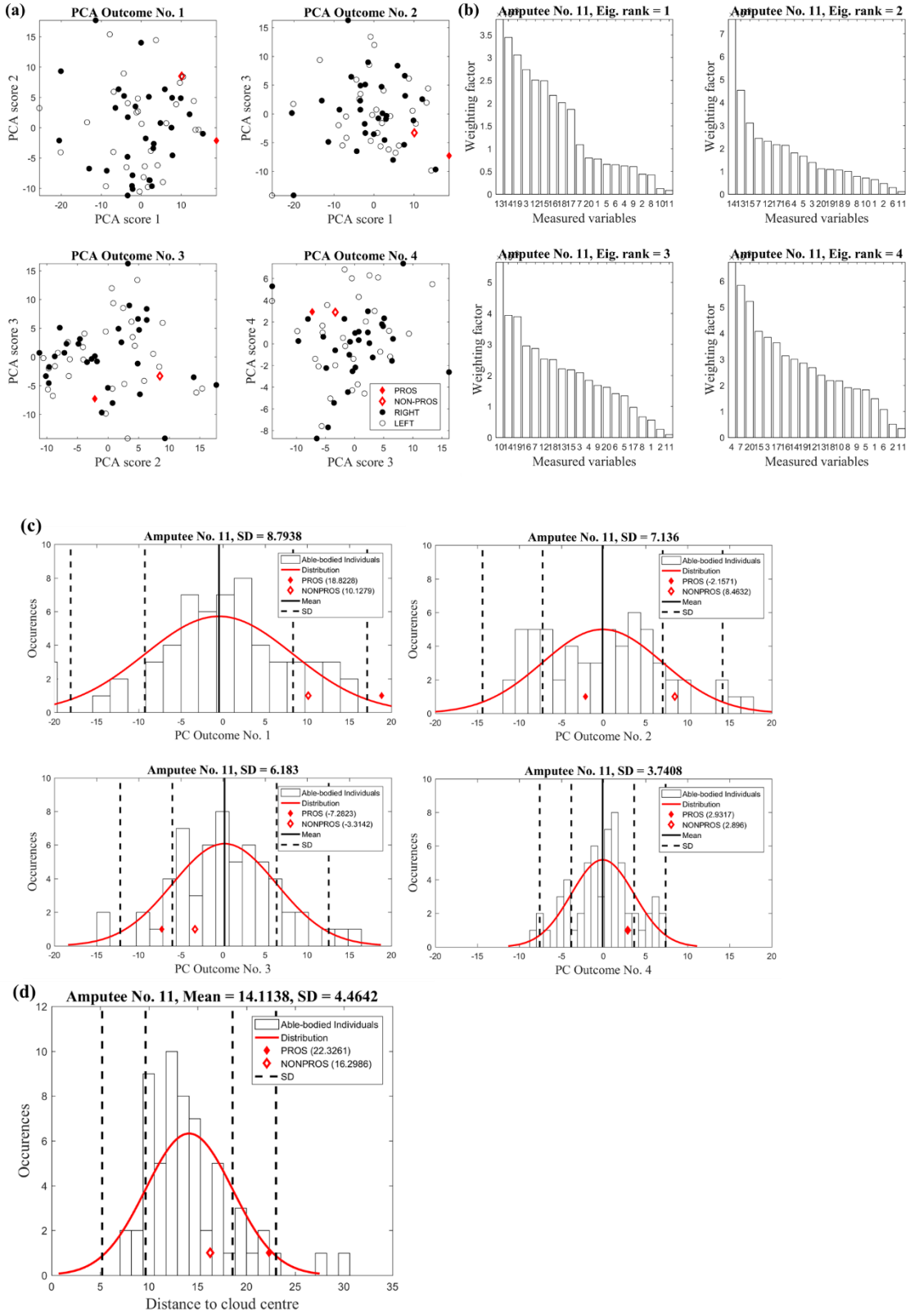

Figure 10.21 PCA outcome using the covariance approach with data normalised to units (a), the corresponding Eigenspectra (b), the Euclidian distance from the origin of the principal component (c) and the Euclidian distance from the centre of the cloud of individual with UTTA number 11.

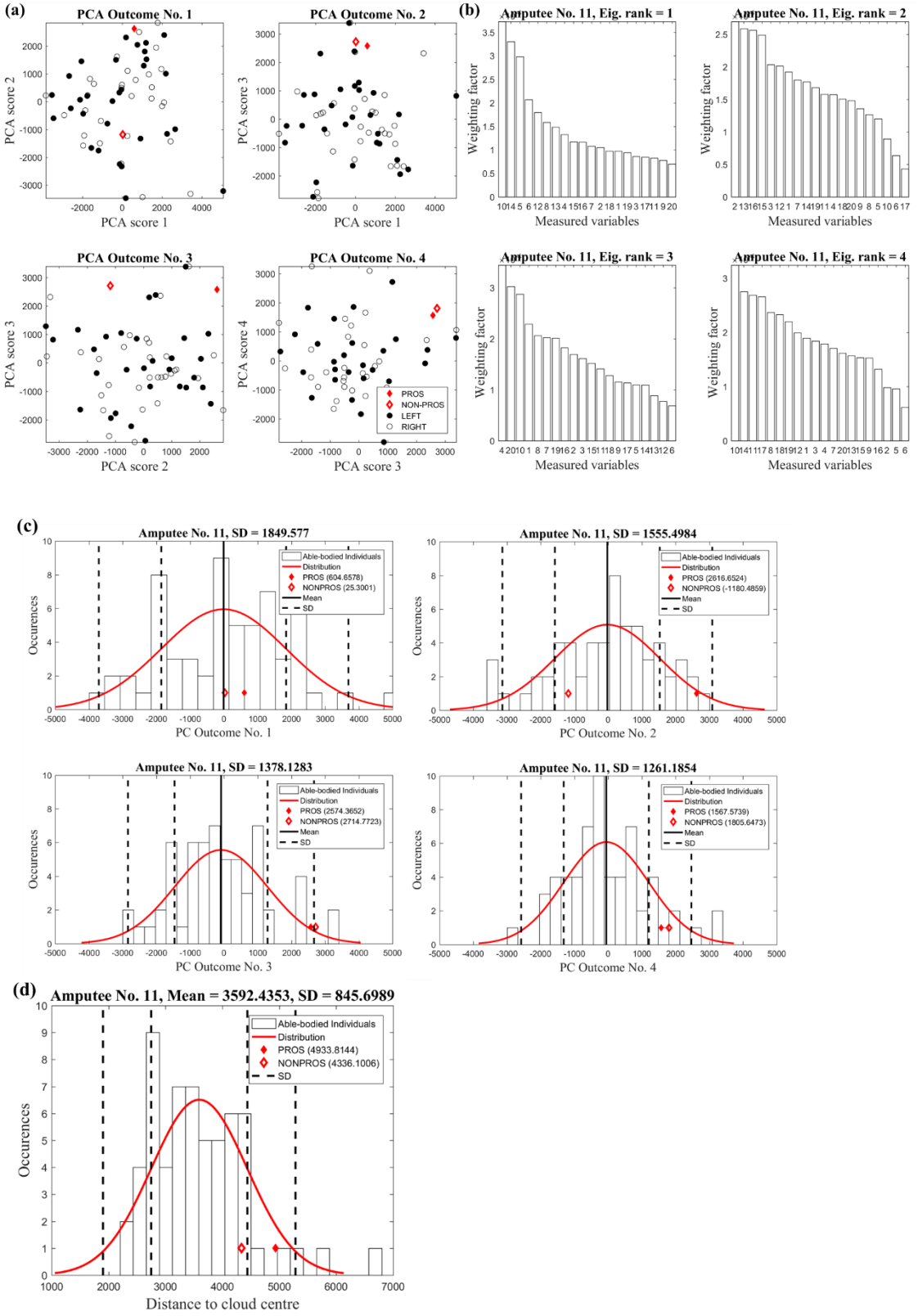

Figure 10.22 PCA outcome using the correlation approach (a), the corresponding Eigenspectra (b), the Euclidian distance from the origin of the principal component (c) and the Euclidian distance from the centre of the cloud of individual with UTTA number 11.

Appendix 4 – Supplementary Results of Study 4 Presented in Chapter 7

Appendix 4.1 – Unilateral Trans-Tibial Amputation During Attempted Symmetrical Step Parameters Compared to Self-Selected Speed

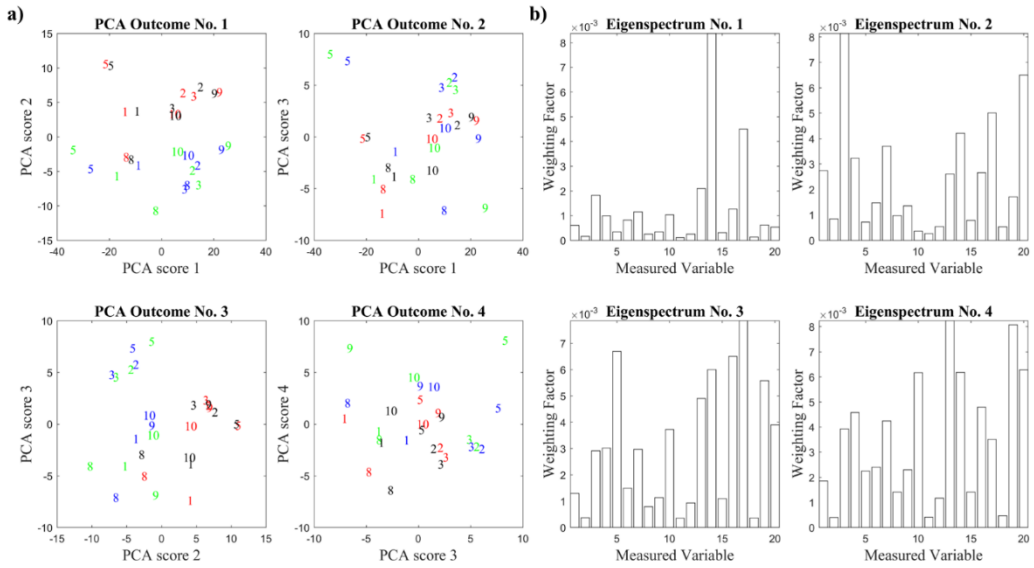

Figure 10.23 PCA outcome (a) and Eigenspectrum (b) using the covariance approach to compare individuals with UTTA at NORM and attempted SYM_{SL}. The different colours indicate the limbs, where the prosthetic limb is shown by green and blue numbers, and intact limb by red and black numbers, where the numbers refer to the individual.

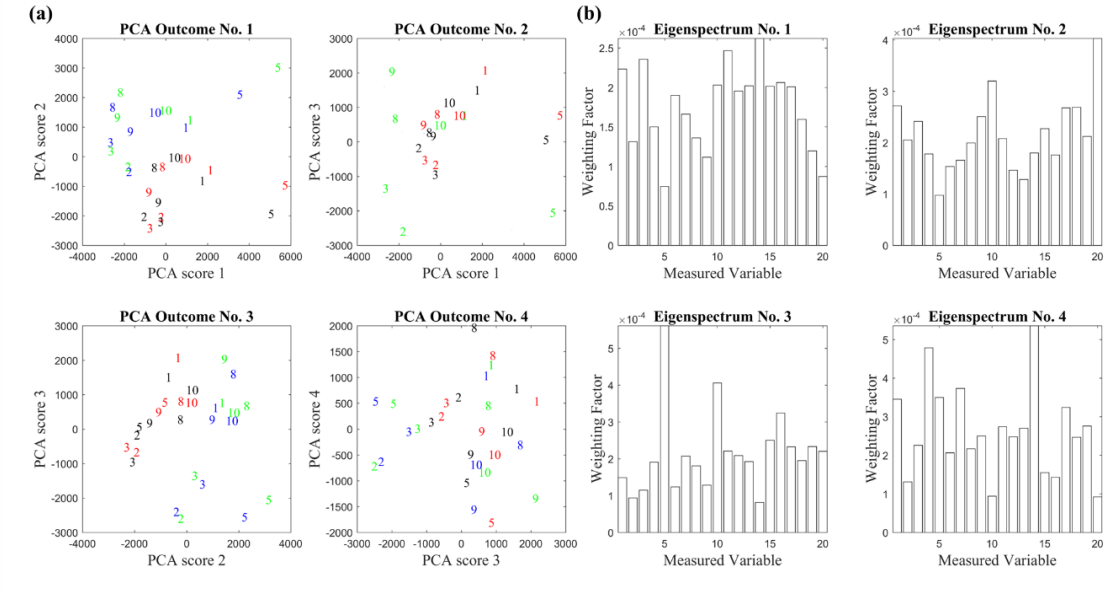

Figure 10.24 (a) PCA outcome and (b) Eigenspectrum using the correlation approach to compare individuals with UTTA at NORM and attempted SYM_{SL}. The different colours indicate the limbs, where the prosthetic limb is shown by green and blue numbers, and intact limb by red and black numbers, where the numbers refer to the individual.

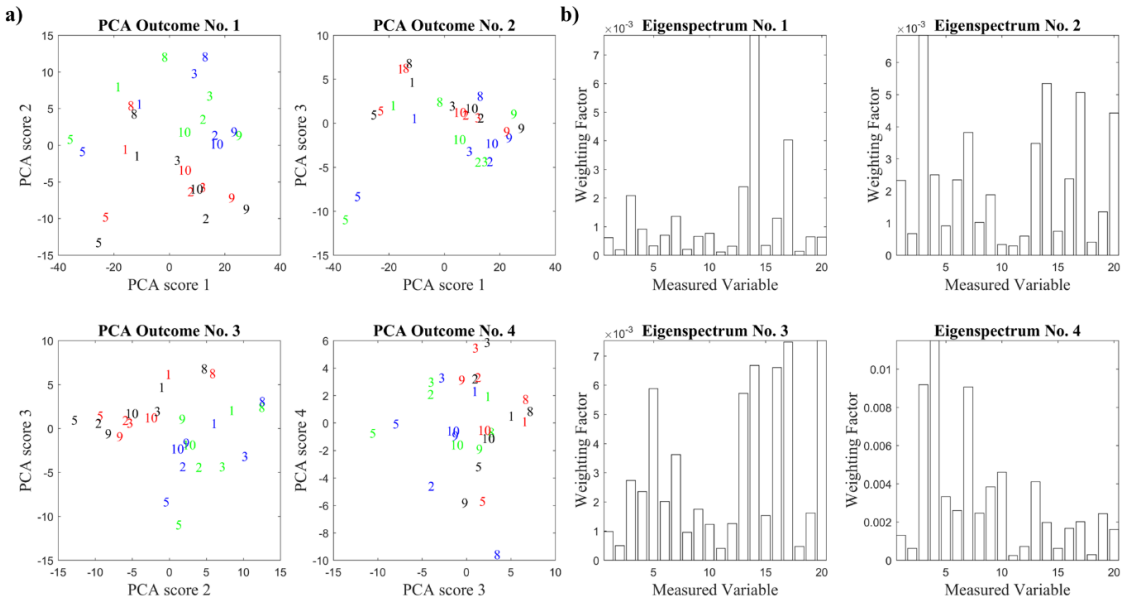

Figure 10.25 PCA outcome (a) and Eigenspectrum (b) using the covariance approach to compare individuals with UTTA at NORM and attempted SYM_{SF}.

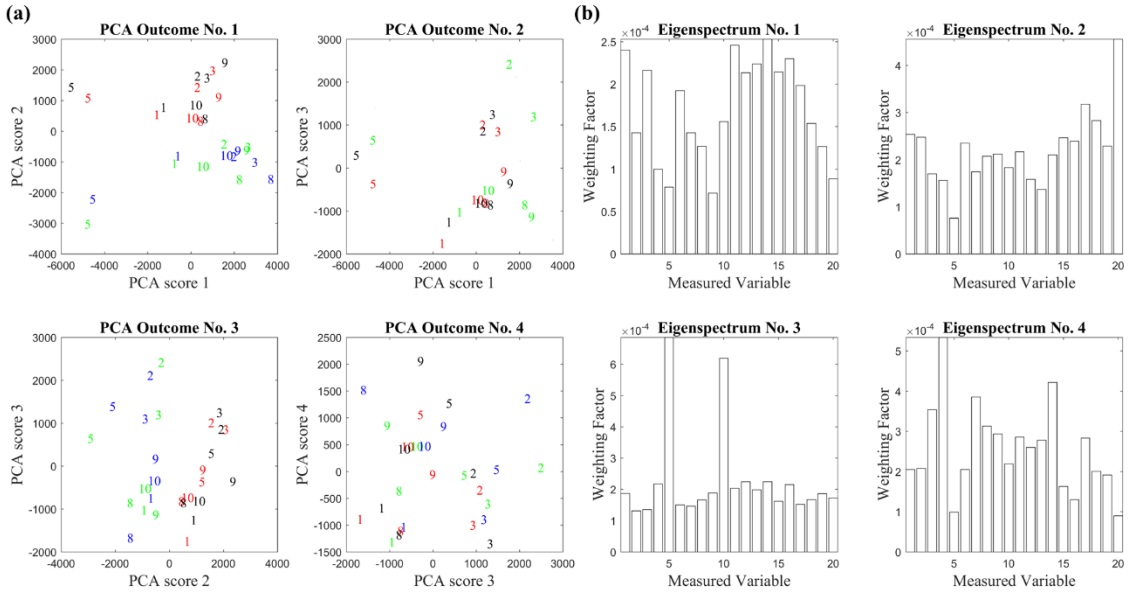

Figure 10.26 PCA outcome (a) and Eigenspectrum (b) using the correlation approach to compare individuals with UTTA at NORM and attempted SYM_{SF}.

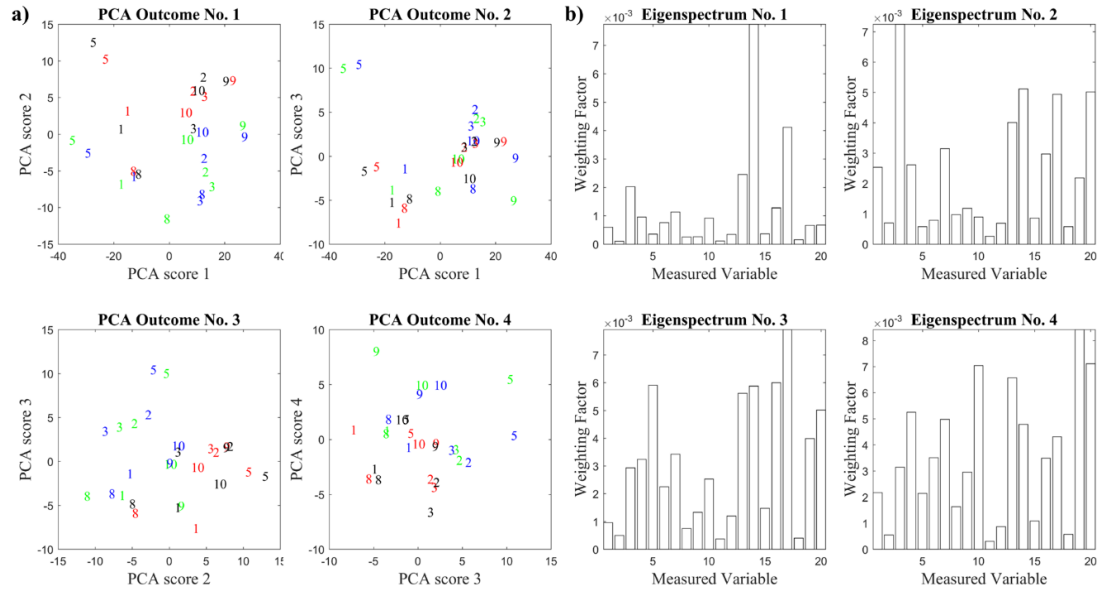

Figure 10.27 PCA outcome (a) and Eigenspectrum (b) using the covariance approach to compare individuals with UTTA at NORM and attempted SYM_{SL+SF}.

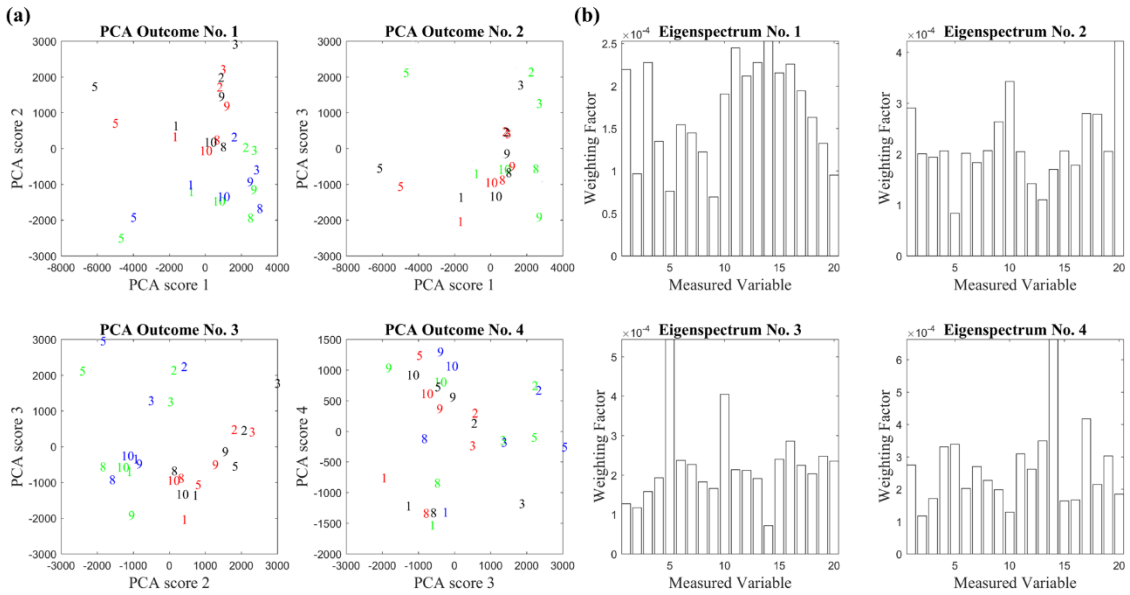

Figure 10.28 PCA (a) outcome and Eigenspectrum (b) using the correlation approach to compare individuals with UTTA at NORM and attempted SYM_{SL+SF}.

Appendix 4.2 – One Individual with a Unilateral Trans-Tibial Amputation During Symmetrical Step Length Compared to a Group of Individuals with a Unilateral Trans-Tibial Amputation During Self-Selected Walking Speed.

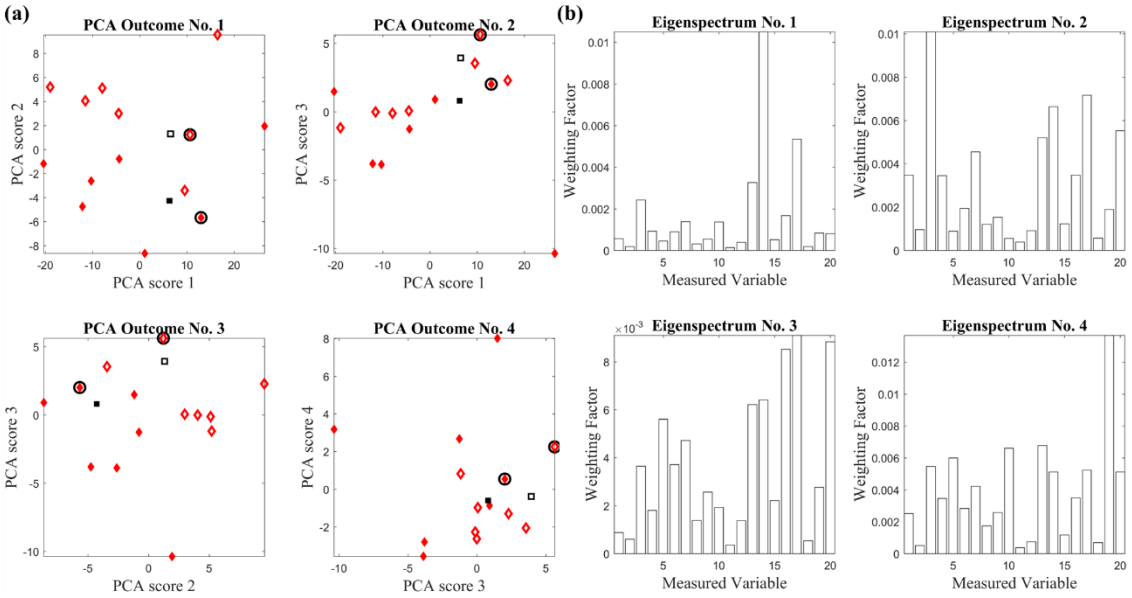

Figure 10.29 Individual with UTTA number 1 discriminated using the covariance matrix during attempted SYM_{SL} (black squares) from a group of individuals with UTTA during NORM (red diamonds). Diamonds with black circle illustrate the NORM trial of the individual with UTTA number 1.

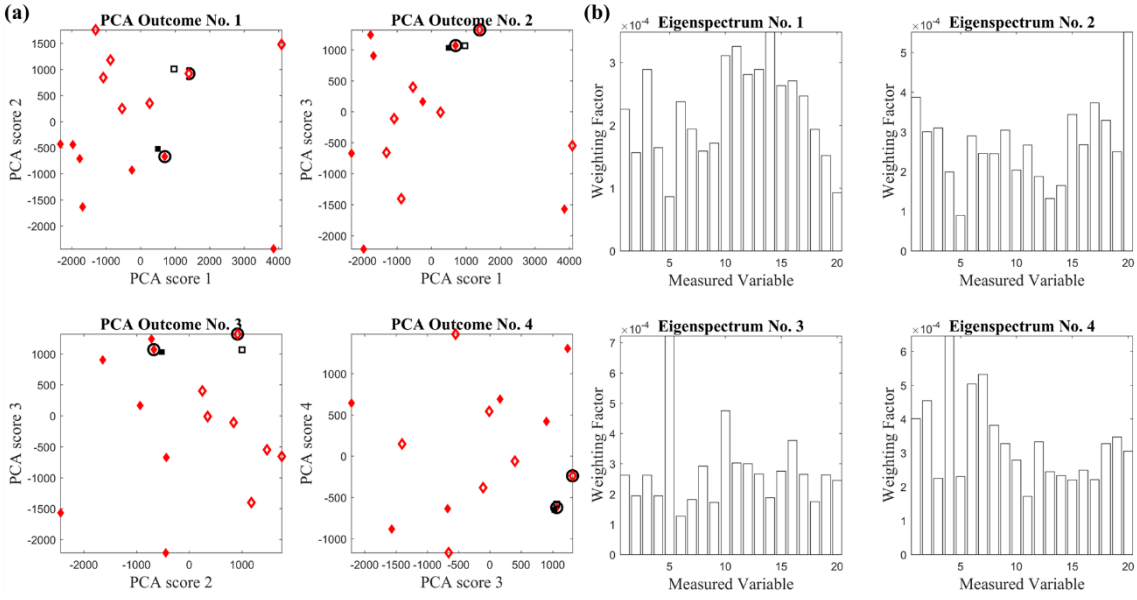

Figure 10.30 Individual with UTTA number 1 discriminated using the correlation matrix during attempted SYM_{SL} (black squares) from a group of individuals with UTTA during NORM (red diamonds). Diamonds with black circle illustrate the NORM trial of the individual with UTTA number 1.

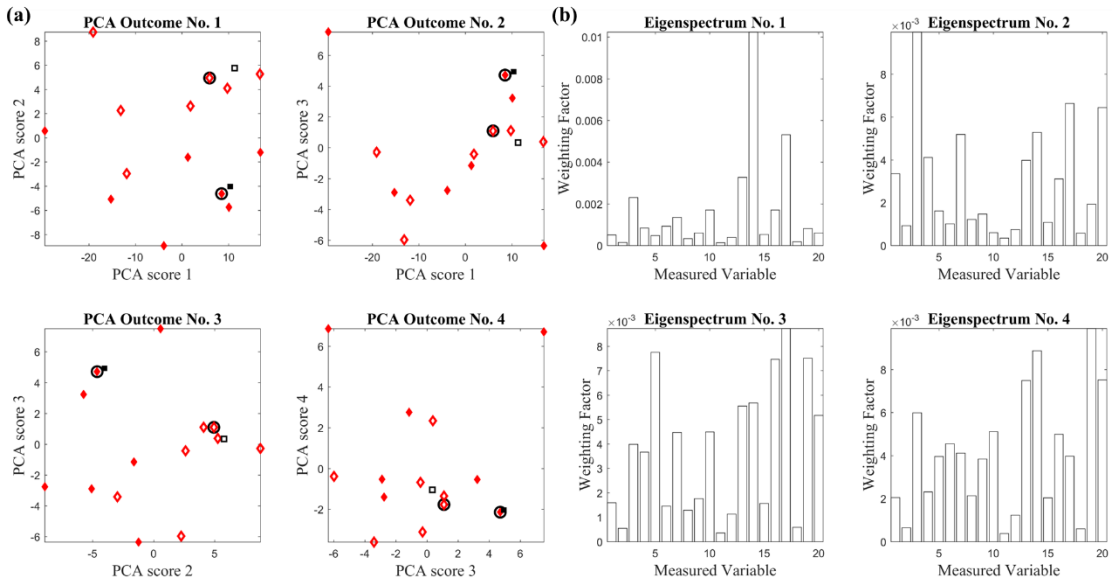

Figure 10.31 Individual with UTTA number 2 discriminated using the covariance matrix during attempted SYM_{SL} (black squares) from a group of individuals with UTTA during NORM (red diamonds). Diamonds with black circle illustrate the NORM trial of individual with UTTA number 2.

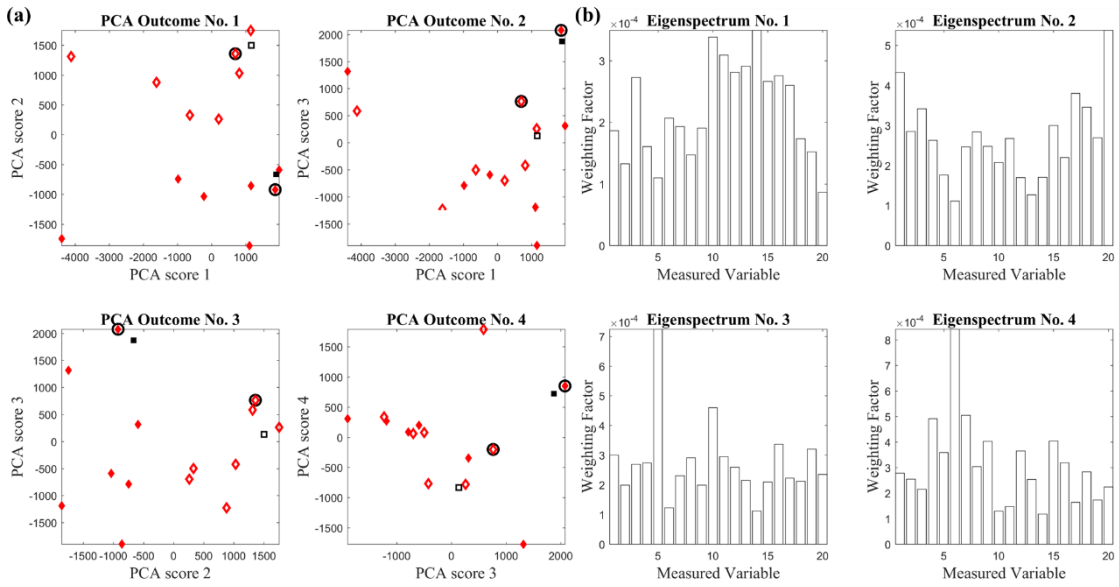

Figure 10.32 Individual with UTTA number 2 discriminated using the correlation matrix during attempted SYM_{SL} (black squares) from a group of individuals with UTTA during NORM (red diamonds). Diamonds with black circle illustrate the NORM trial of individual with UTTA number 2.

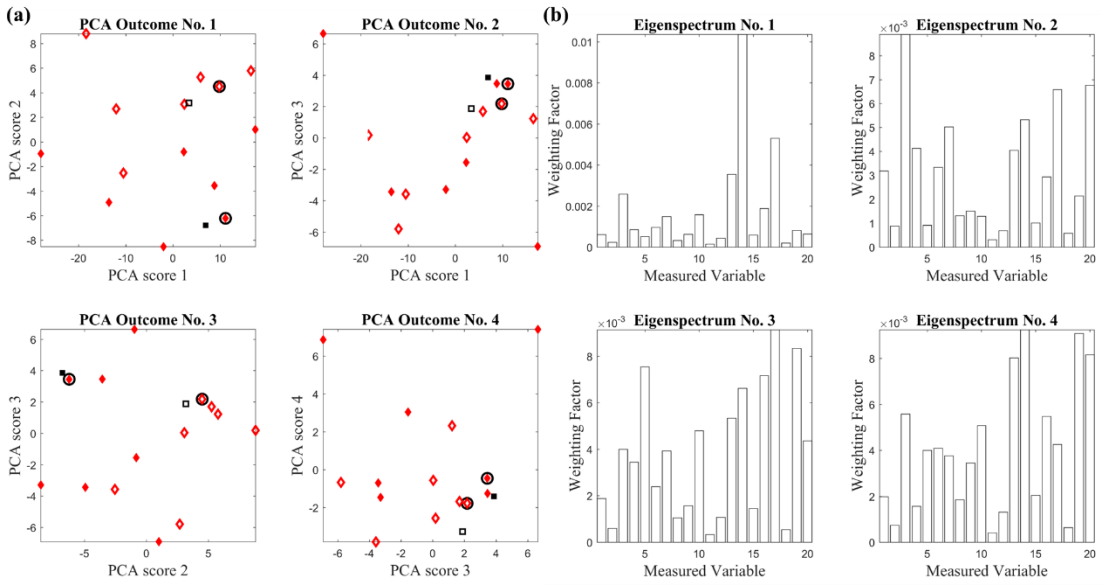

Figure 10.33 Individual with UTTA number 3 discriminated using the covariance matrix during attempted SYM_{SL} (black squares) from a group of individuals with UTTA during NORM (red diamonds). Diamonds with black circle illustrate the NORM trial of individual with UTTA number 3.

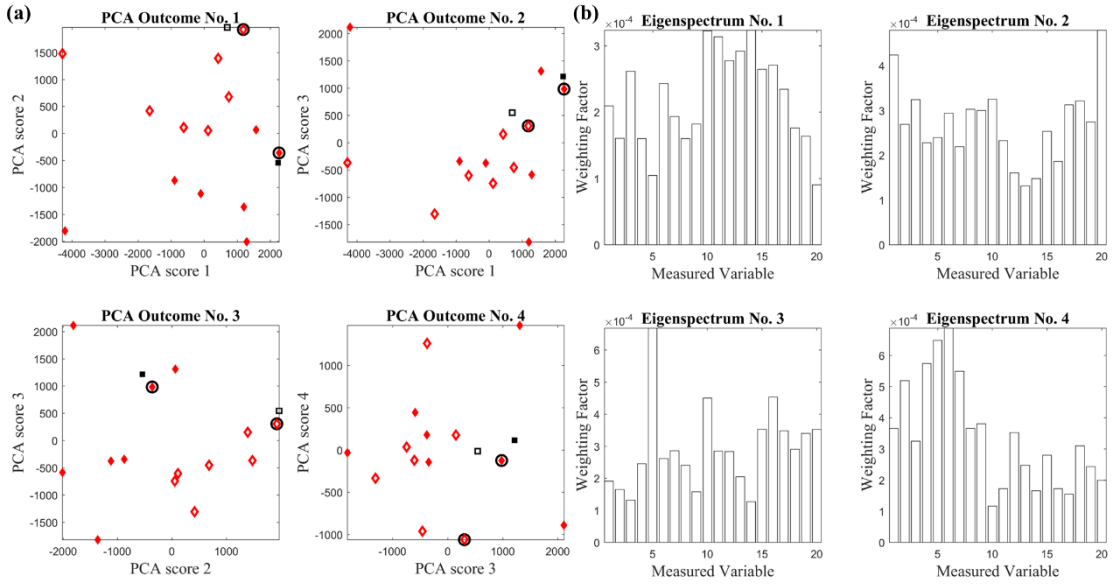

Figure 10.34 Individual with UTTA number 3 discriminated using the correlation matrix during attempted SYM_{SL} (black squares) from a group of individuals with UTTA during NORM (red diamonds). Diamonds with black circle illustrate the NORM trial of individual with UTTA number 3.

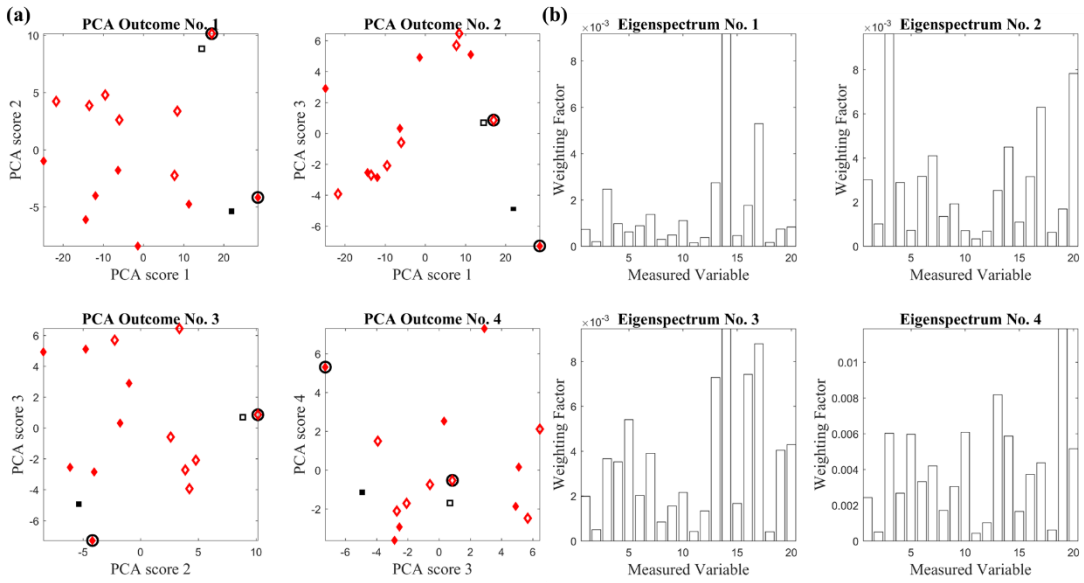

Figure 10.35 Individual with UTTA number 4 discriminated using the covariance matrix during attempted SYM_{SL} (black squares) from a group of individuals with UTTA during NORM (red diamonds). Diamonds with black circle illustrate the NORM trial of individual with UTTA number 4.

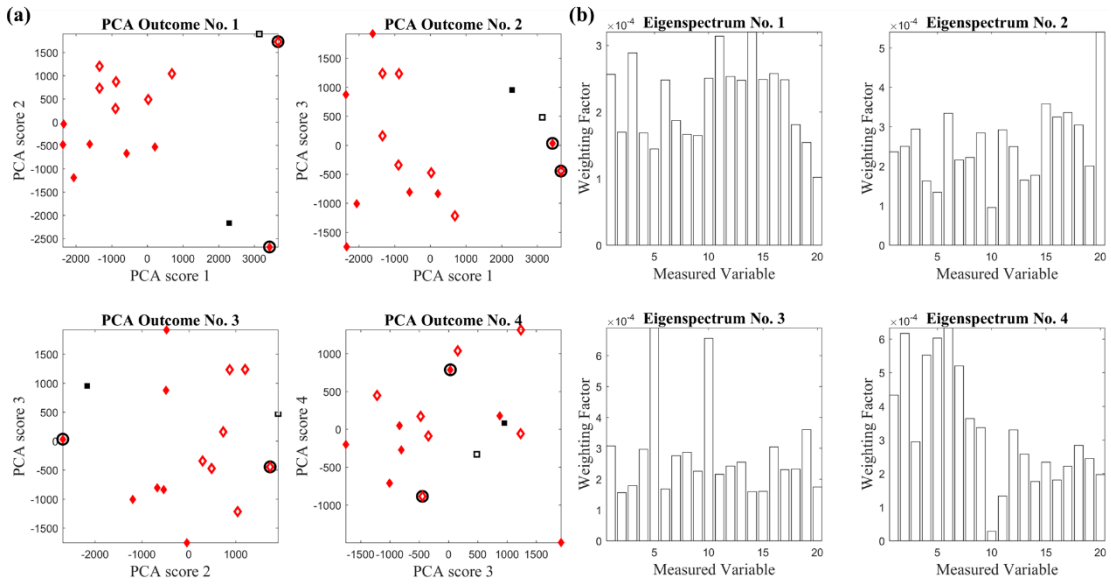

Figure 10.36 Individual with UTTA number 4 discriminated using the correlation matrix during attempted SYM_{SL} (black squares) from a group of individuals with UTTA during NORM (red diamonds). Diamonds with black circle illustrate the NORM trial of individual with UTTA number 4.

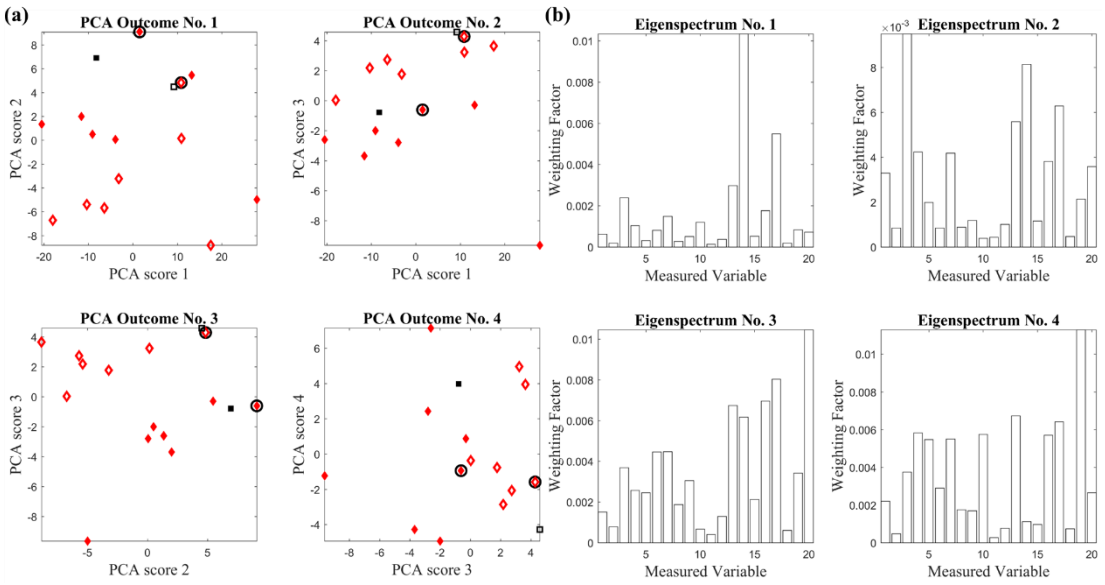

Figure 10.37 Individual with UTTA number 5 discriminated using the covariance matrix during attempted SYM_{SL} (black squares) from a group of individuals with UTTA during NORM (red diamonds). Diamonds with black circle illustrate the NORM trial of individual with UTTA number 5.

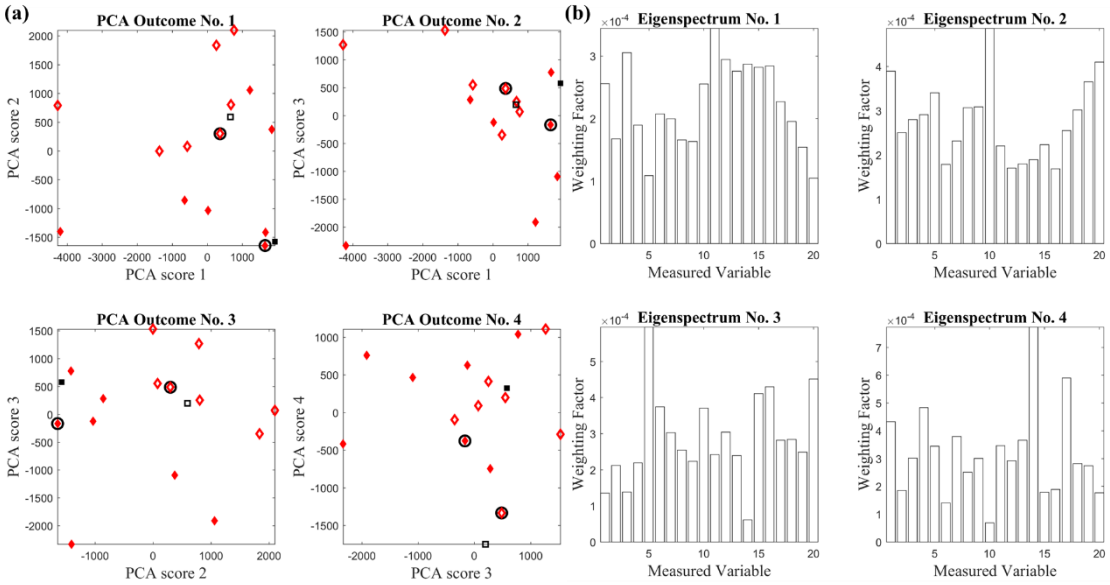

Figure 10.38 Individual with UTTA number 5 discriminated using the correlation matrix during attempted SYM_{SL} (black squares) from a group of individuals with UTTA during NORM (red diamonds). Diamonds with black circle illustrate the NORM trial of individual with UTTA number 5.

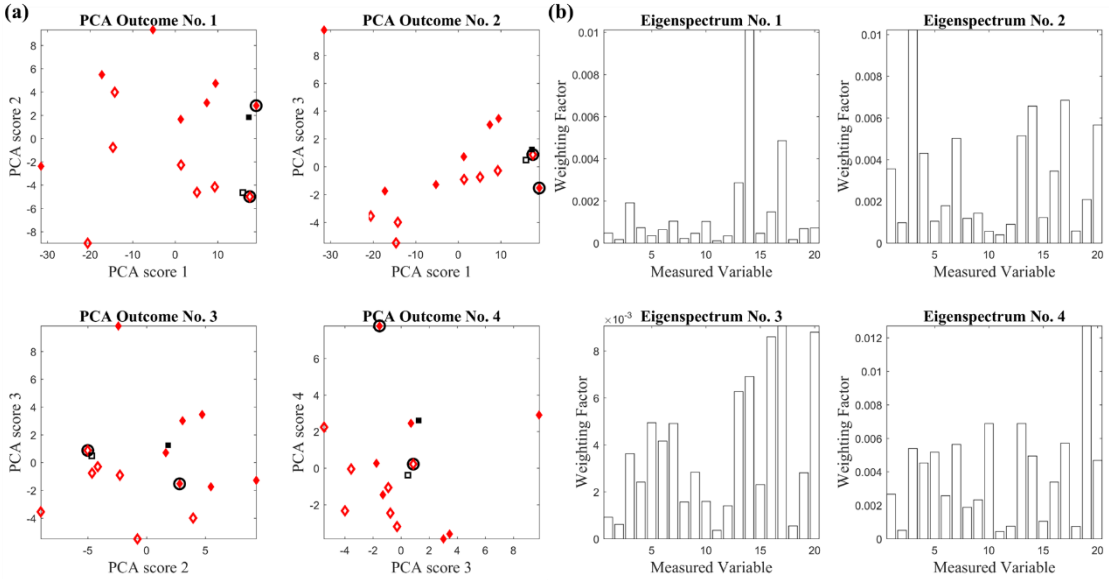

Figure 10.39 Individual with UTTA number 6 discriminated using the covariance matrix during attempted SYM_{SL} (black squares) from a group of individuals with UTTA during NORM (red diamonds). Diamonds with black circle illustrate the NORM trial of individual with UTTA number 6.

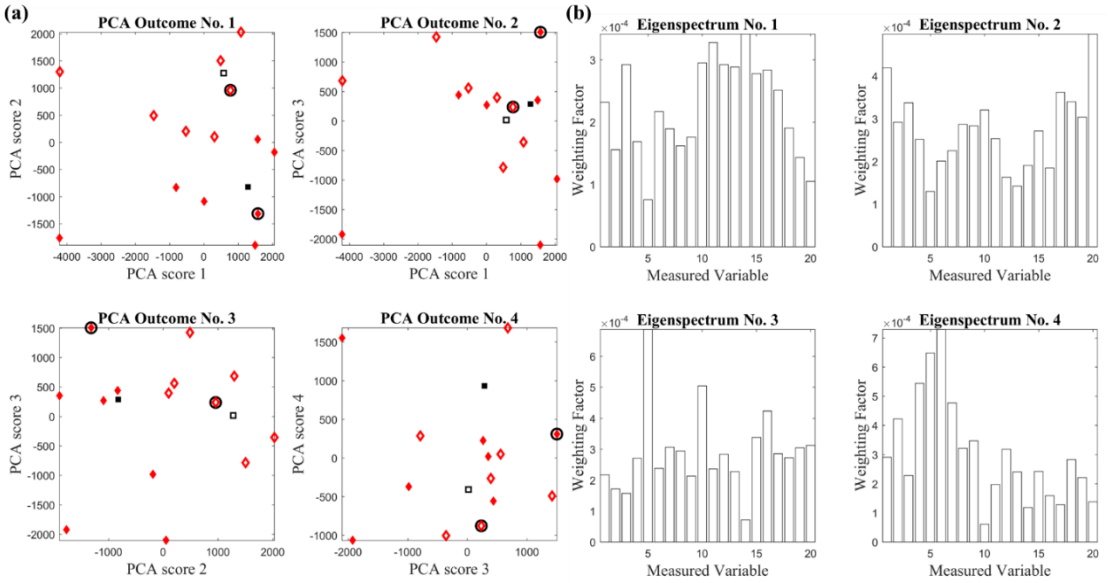

Figure 10.40 Individual with UTTA number 6 discriminated using the correlation matrix during attempted SYM_{SL} (black squares) from a group of individuals with UTTA during NORM (red diamonds). Diamonds with black circle illustrate the NORM trial of individual with UTTA number 6.

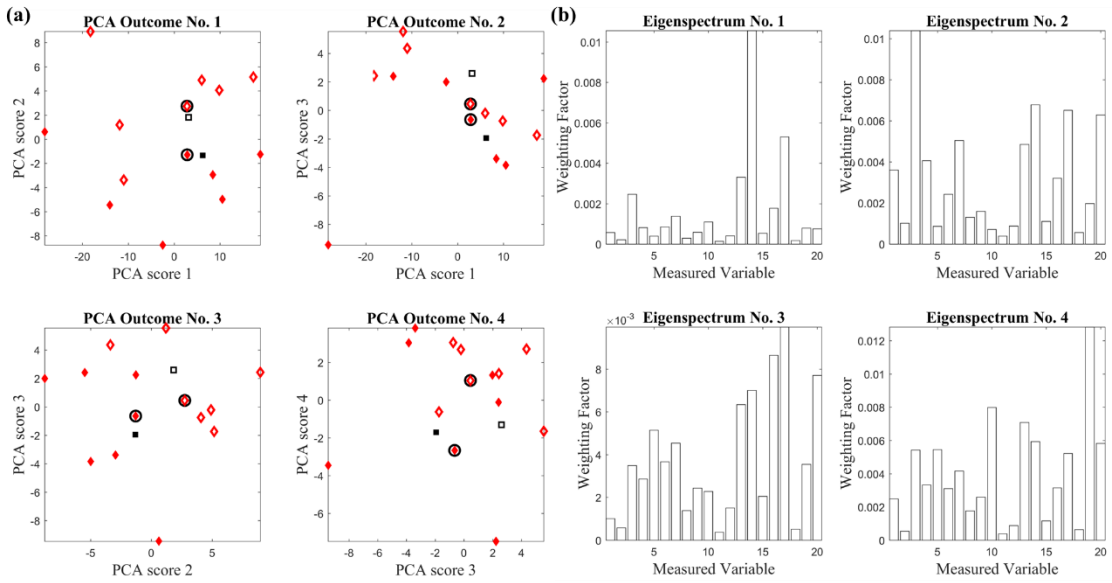

Figure 10.41 Individual with UTTA number 7 discriminated using the covariance matrix during attempted SYM_{SL} (black squares) from a group of individuals with UTTA during NORM (red diamonds). Diamonds with black circle illustrate the NORM trial of individual with UTTA number 7.

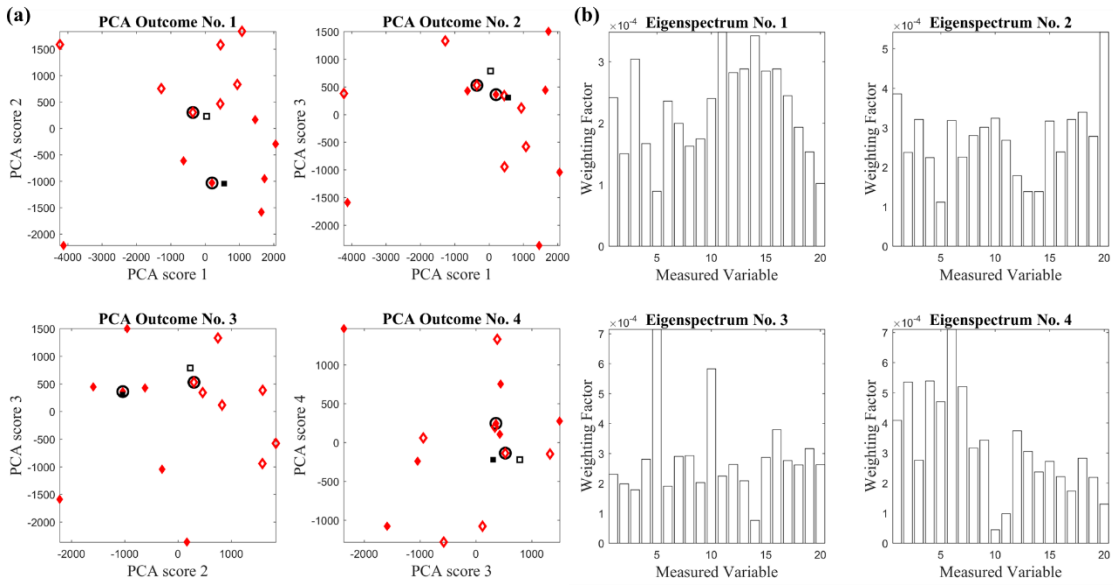

Figure 10.42 Individual with UTTA number 7 discriminated using the correlation matrix during attempted SYM_{SL} (black squares) from a group of individuals with UTTA during NORM (red diamonds). Diamonds with black circle illustrate the NORM trial of individual with UTTA number 7.

Appendix 4.3 – One Individual with a Unilateral Trans-Tibial Amputation During Symmetrical Step Frequency Compared to a Group of Individuals with a Unilateral Trans-Tibial Amputation During Self-Selected Walking Speed.

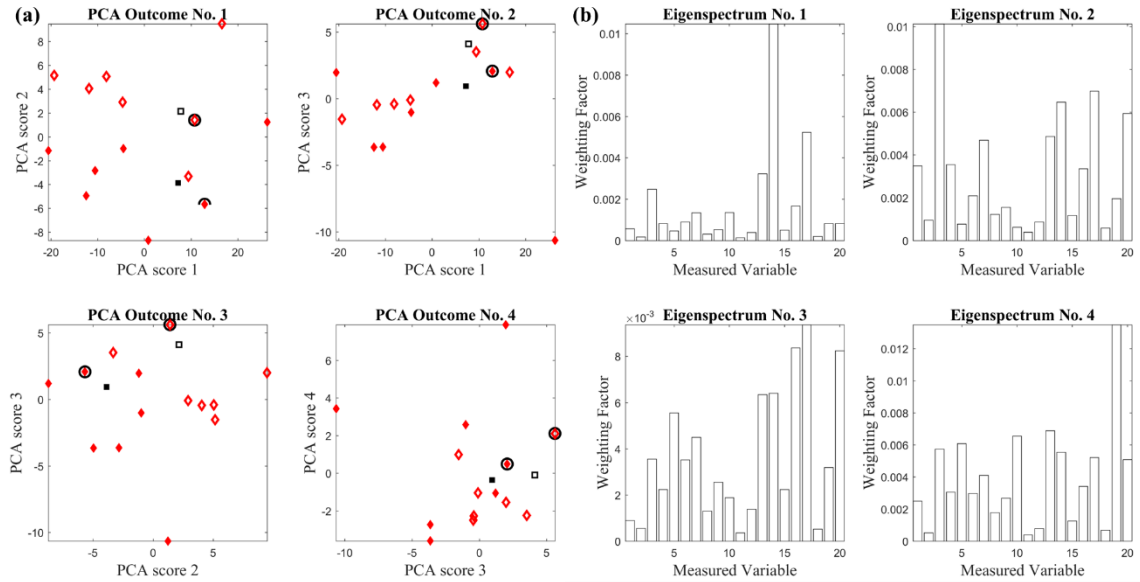

Figure 10.43 Individual with UTTA number 1 discriminated using the covariance matrix during attempted SYM_{SF} (black squares) from a group of individuals with UTTA during NORM (red diamonds). Diamonds with black circle illustrate the NORM trial of individual with UTTA number 1.

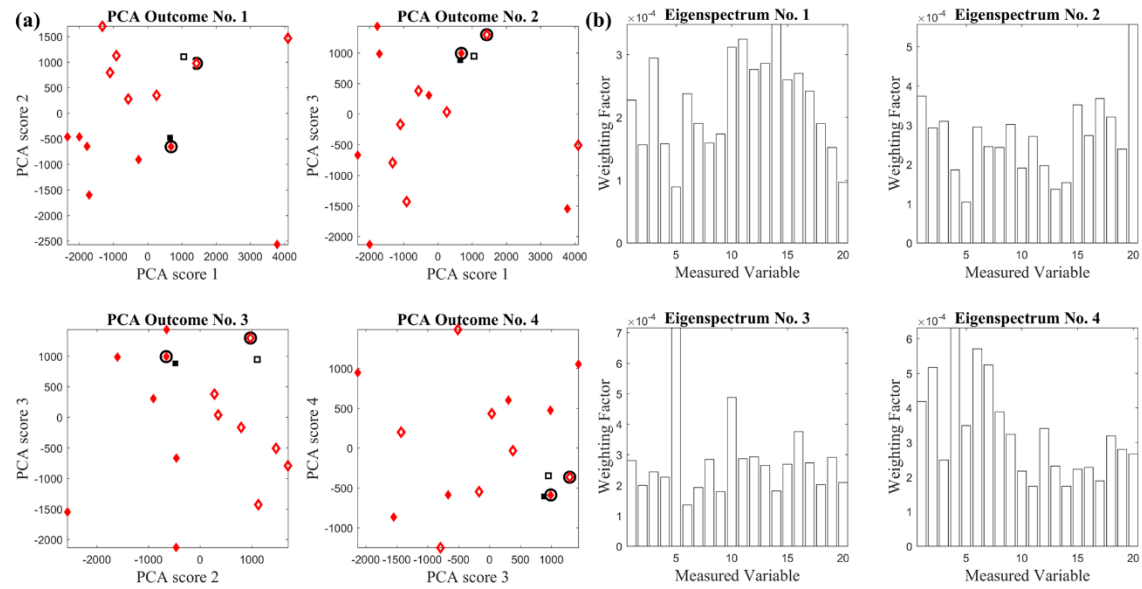

Figure 10.44 Individual with UTTA number 1 discriminated using the correlation matrix during attempted SYM_{SF} (black squares) from a group of individuals with UTTA during NORM (red diamonds). Diamonds with black circle illustrate the NORM trial of individual with UTTA number 1.

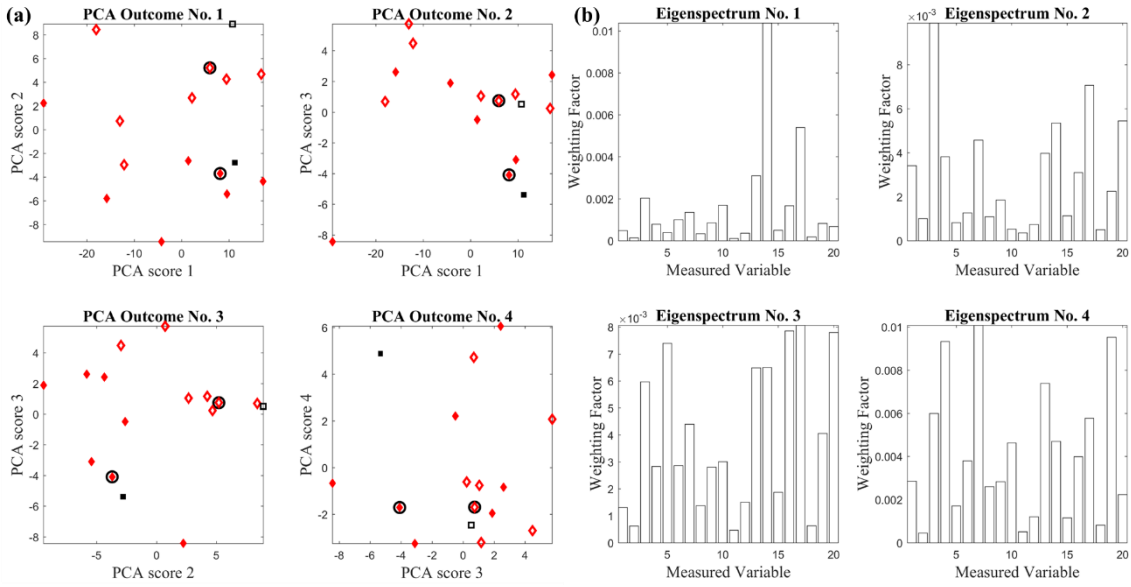

Figure 10.45 Individual with UTTA number 2 discriminated using the covariance matrix during attempted SYM_{SF} (black squares) from a group of individuals with UTTA during NORM (red diamonds). Diamonds with black circle illustrate the NORM trial of individual with UTTA number 2.

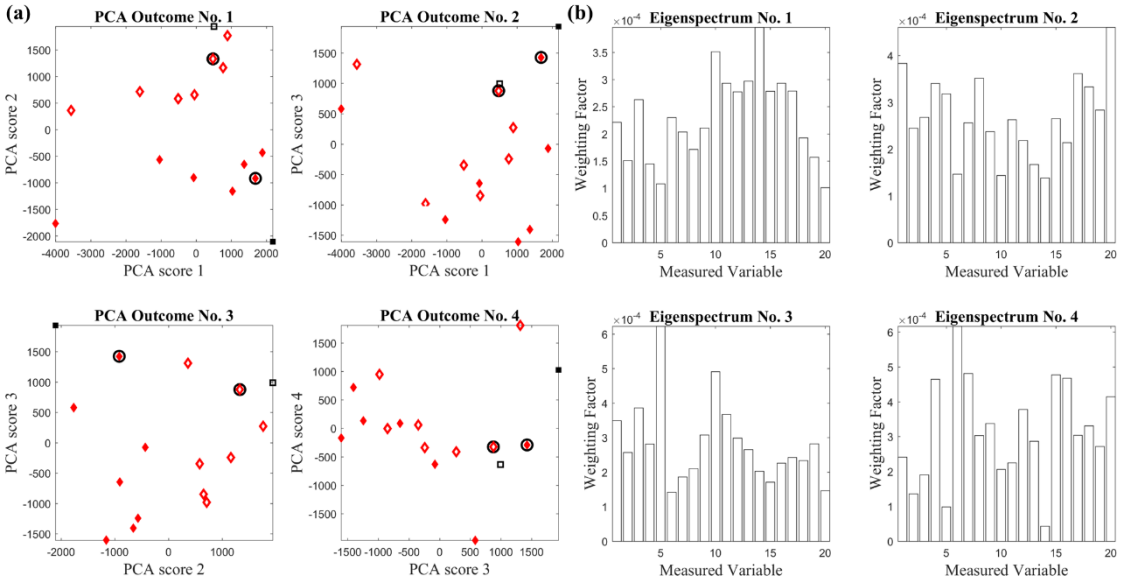

Figure 10.46 Individual with UTTA number 2 discriminated using the correlation matrix during attempted SYM_{SF} (black squares) from a group of individuals with UTTA during NORM (red diamonds). Diamonds with black circle illustrate the NORM trial of individual with UTTA number 2.

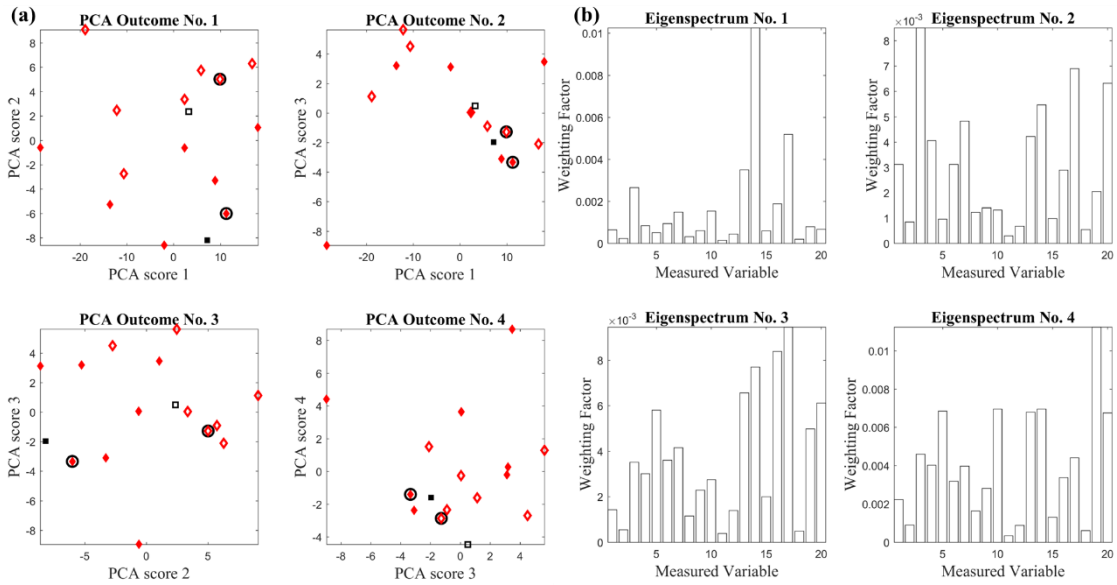

Figure 10.47 Individual with UTTA number 3 discriminated using the covariance matrix during attempted SYM_{SF} (black squares) from a group of individuals with UTTA during NORM (red diamonds). Diamonds with black circle illustrate the NORM trial of individual with UTTA number 3.

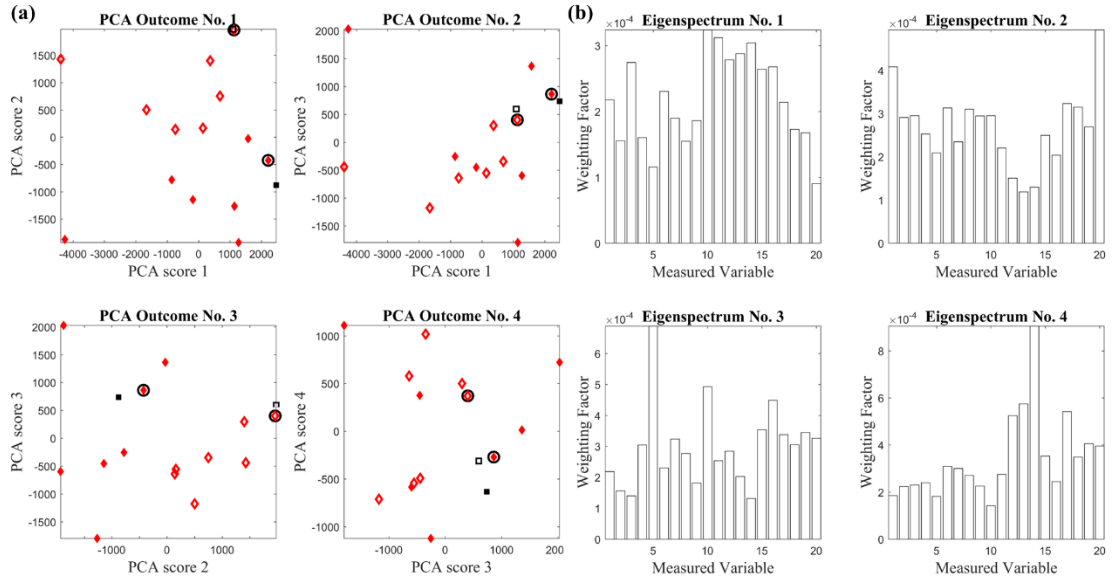

Figure 10.48 Individual with UTTA number 3 discriminated using the correlation matrix during attempted SYM_{SF} (black squares) from a group of individuals with UTTA during NORM (red diamonds). Diamonds with black circle illustrate the NORM trial of individual with UTTA number 3.

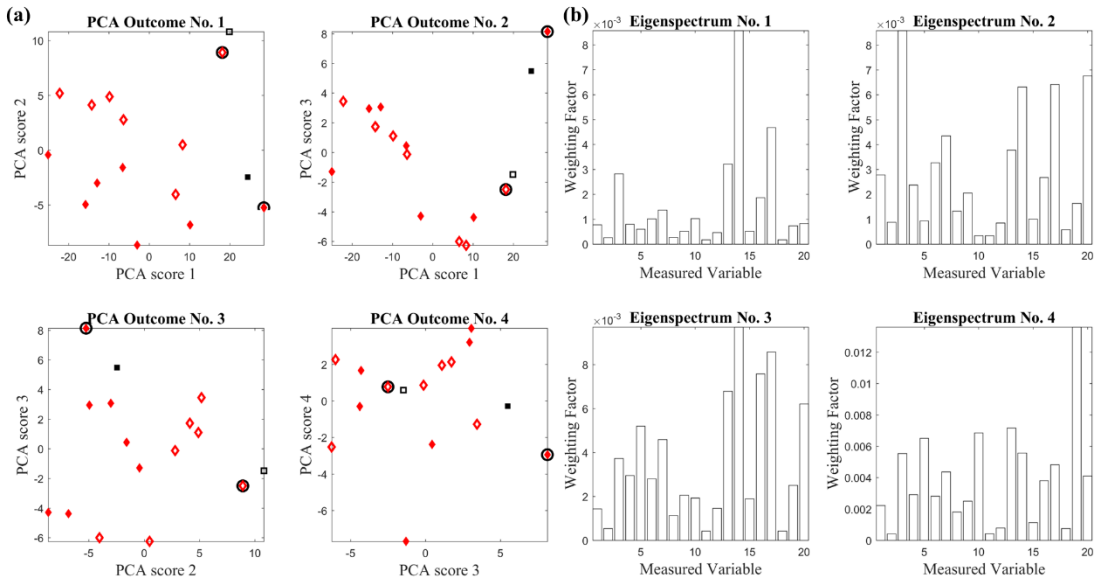

Figure 10.49 Individual with UTTA number 4 discriminated using the covariance matrix during attempted *SYM*$_{SF}$ (black squares) from a group of individuals with UTTA during NORM (red diamonds). Diamonds with black circle illustrate the NORM trial of individual with UTTA number 4.

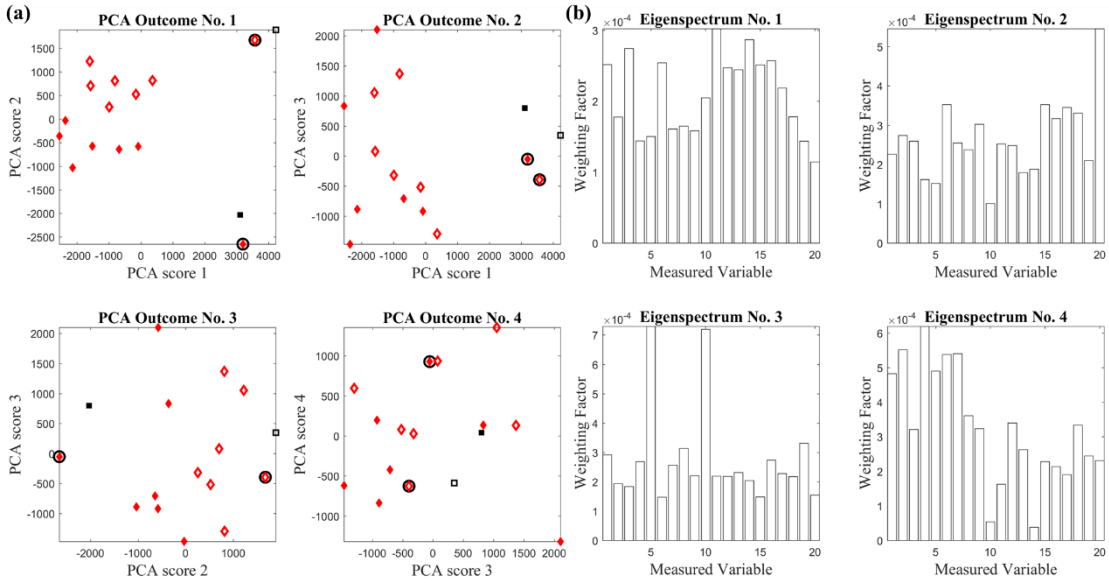

Figure 10.50 Individual with UTTA number 4 discriminated using the correlation matrix during attempted *SYM*$_{SF}$ (black squares) from a group of individuals with UTTA during NORM (red diamonds). Diamonds with black circle illustrate the NORM trial of individual with UTTA number 4.

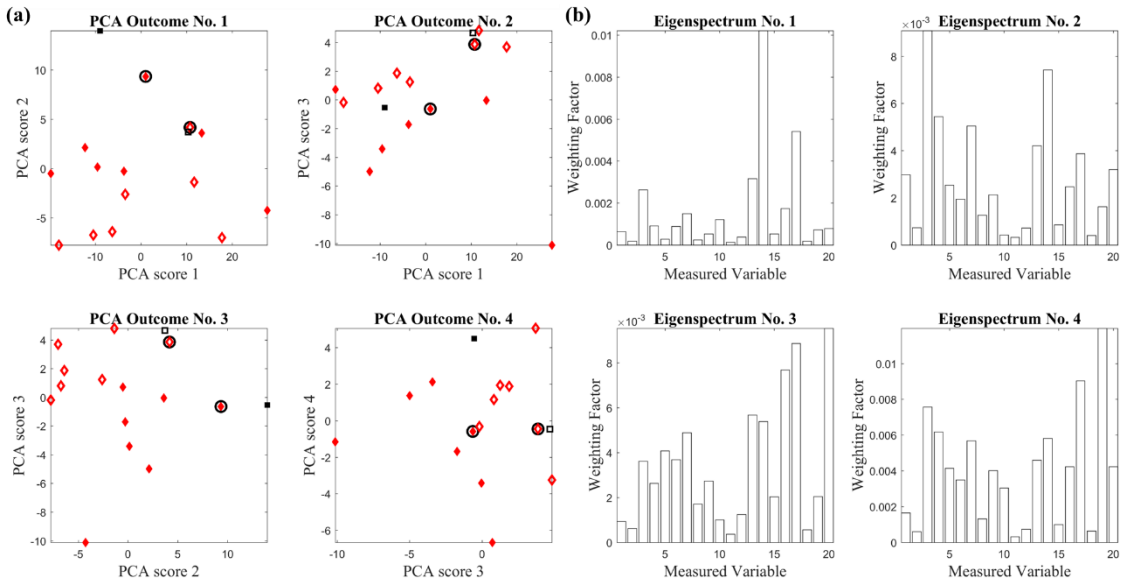

Figure 10.51 Individual with UTTA number 5 discriminated using the covariance matrix during attempted SYM_{SF} (black squares) from a group of individuals with UTTA during NORM (red diamonds). Diamonds with black circle illustrate the NORM trial of individual with UTTA number 5.

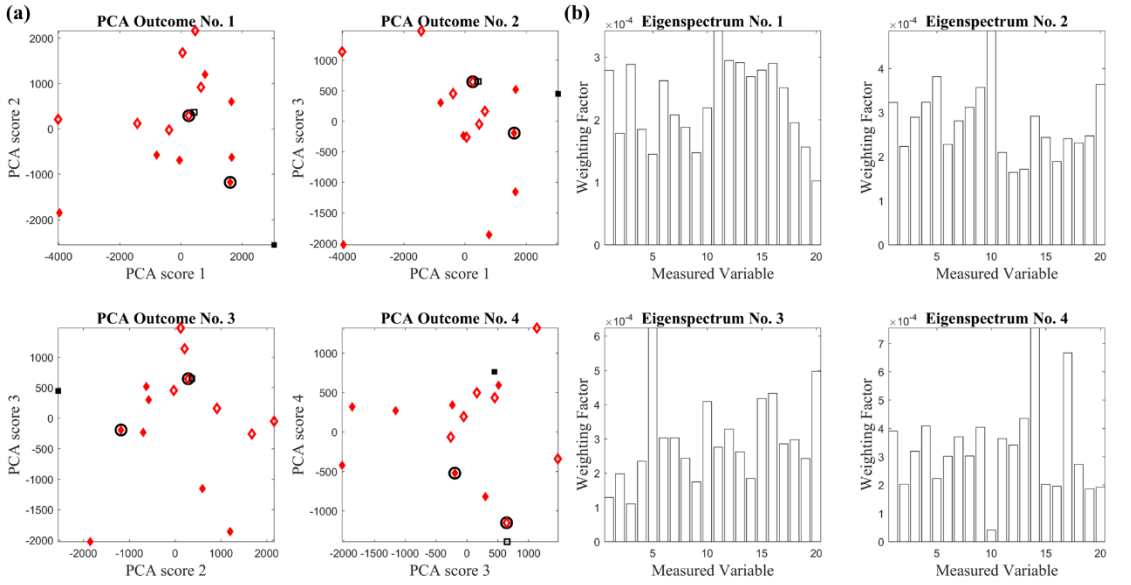

Figure 10.52 Individual with UTTA number 5 discriminated using the correlation matrix during attempted SYM_{SF} (black squares) from a group of individuals with UTTA during NORM (red diamonds). Diamonds with black circle illustrate the NORM trial of individual with UTTA number 5.

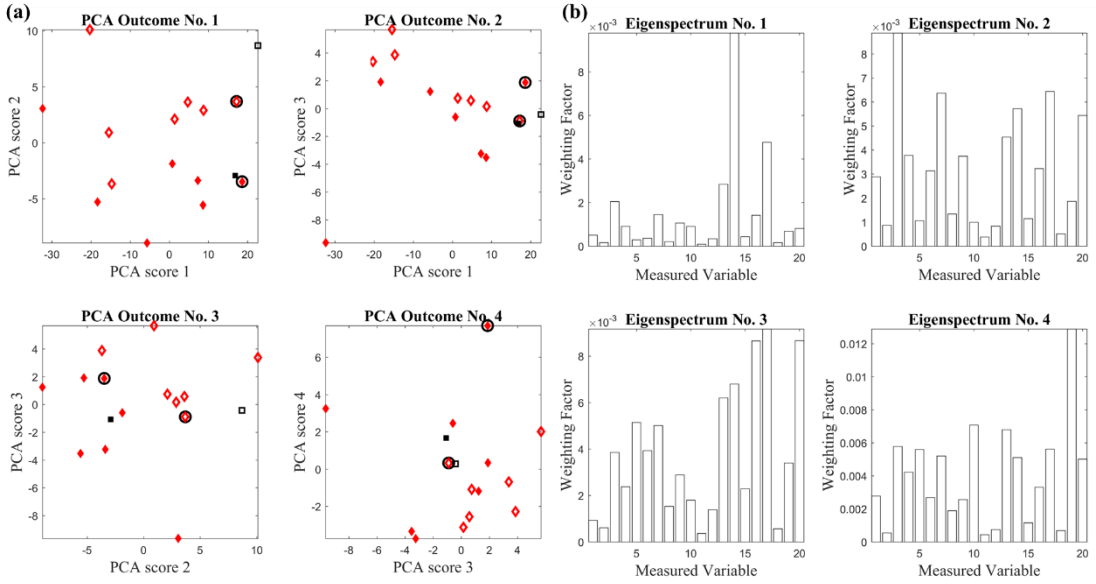

Figure 10.53 Individual with UTTA number 6 discriminated using the covariance matrix during attempted SYM_{SF} (black squares) from a group of individuals with UTTA during NORM (red diamonds). Diamonds with black circle illustrate the NORM trial of individual with UTTA number 6.

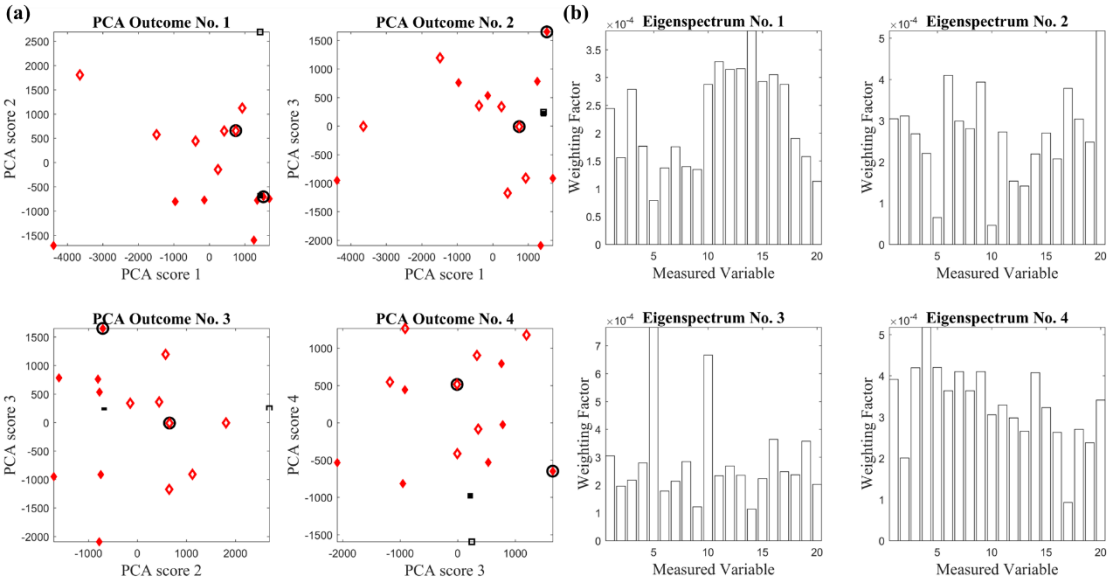

Figure 10.54 Individual with UTTA number 6 discriminated using the correlation matrix during attempted SYM_{SF} (black squares) from a group of individuals with UTTA during NORM (red diamonds). Diamonds with black circle illustrate the NORM trial of individual with UTTA number 6.

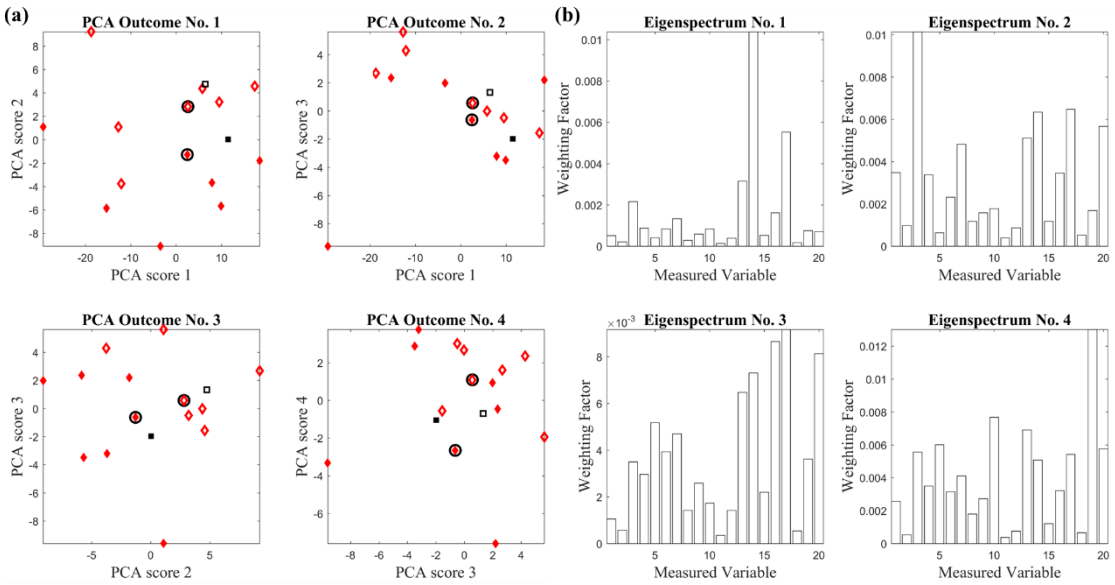

Figure 10.55 Individual with UTTA number 7 discriminated using the covariance matrix during attempted SYM_{SF} (black squares) from a group of individuals with UTTA during NORM (red diamonds). Diamonds with black circle illustrate the NORM trial of individual with UTTA number 7.

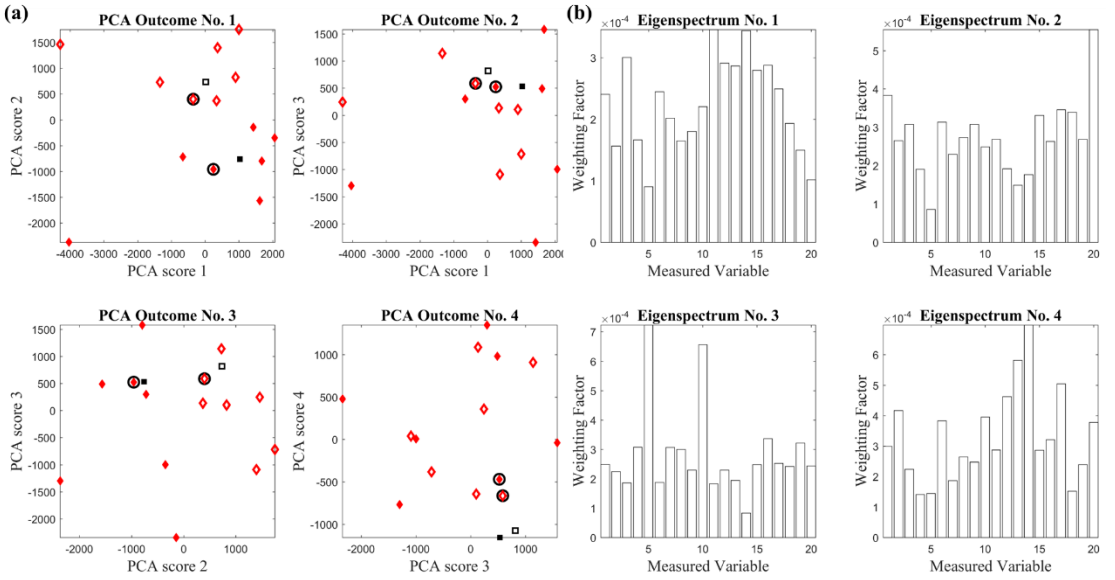

Figure 10.56 Individual with UTTA number 7 discriminated using the correlation matrix during attempted SYM_{SF} (black squares) from a group of individuals with UTTA during NORM (red diamonds). Diamonds with black circle illustrate the NORM trial of individual with UTTA number 7.

Appendix 4.4 – One Individual with a Unilateral Trans-Tibial Amputation during Symmetrical Step Length and Step Frequency compared to a Group of Individuals with a Unilateral Trans-Tibial Amputation during Self-Selected Walking Speed.

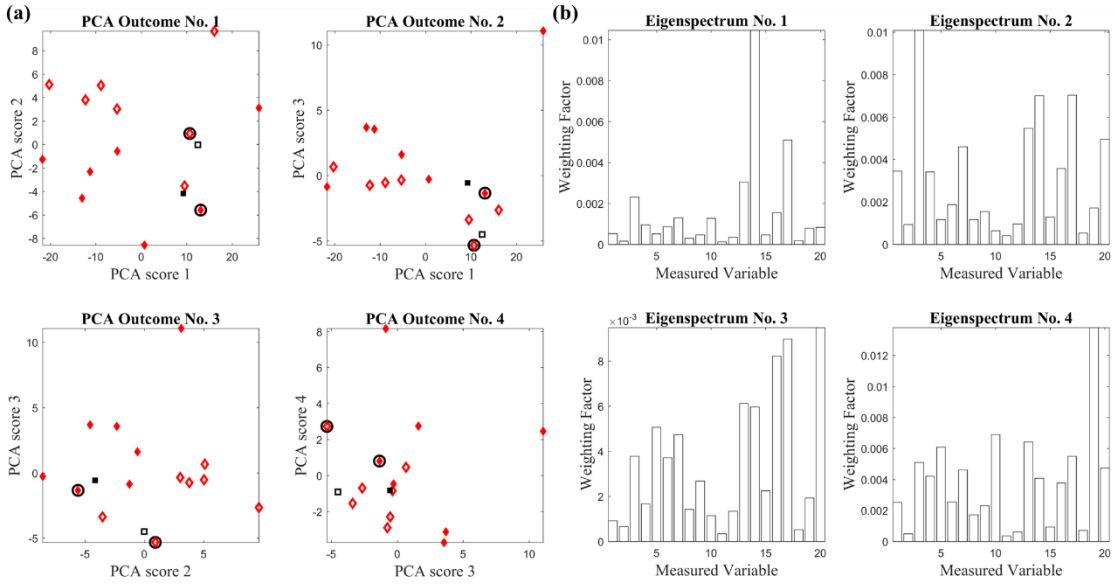

Figure 10.57 Individual with UTTA number 1 discriminated using the covariance matrix during attempted SYM_{SL+SF} (black squares) from a group of individuals with UTTA during NORM (red diamonds). Diamonds with black circle illustrate the NORM trial of individual with UTTA number 1.

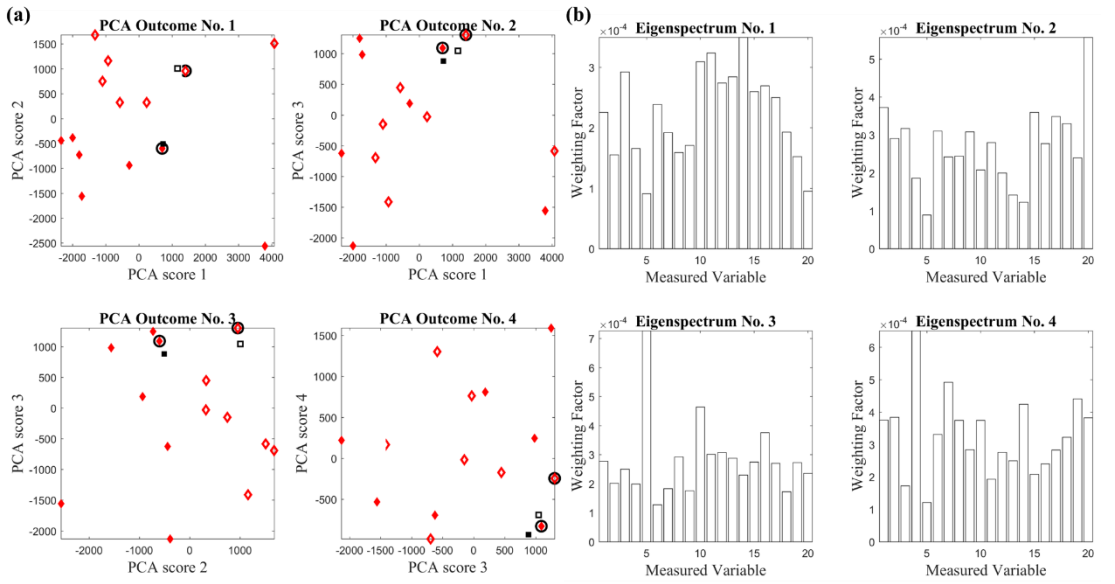

Figure 10.58 Individual with UTTA number 1 discriminated using the correlation matrix during attempted SYM_{SL+SF} (black squares) from a group of individuals with UTTA during NORM (red diamonds). Diamonds with black circle illustrate the NORM trial of individual with UTTA number 1.

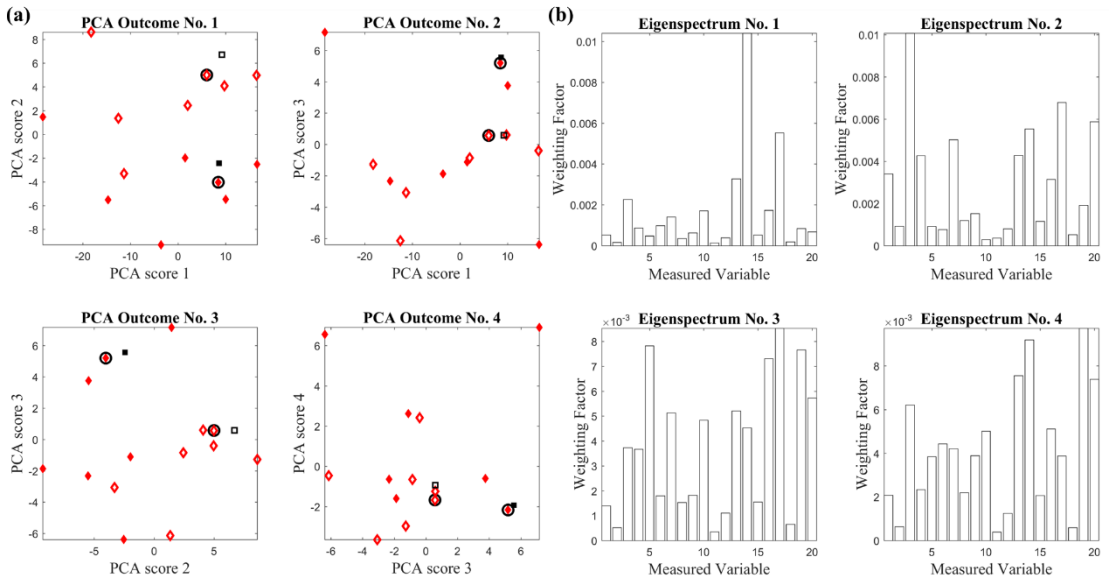

Figure 10.59 Individual with UTTA number 2 discriminated using the covariance matrix during attempted SYM_{SL+SF} (black squares) from a group of individuals with UTTA during NORM (red diamonds). Diamonds with black circle illustrate the NORM trial of individual with UTTA number 2.

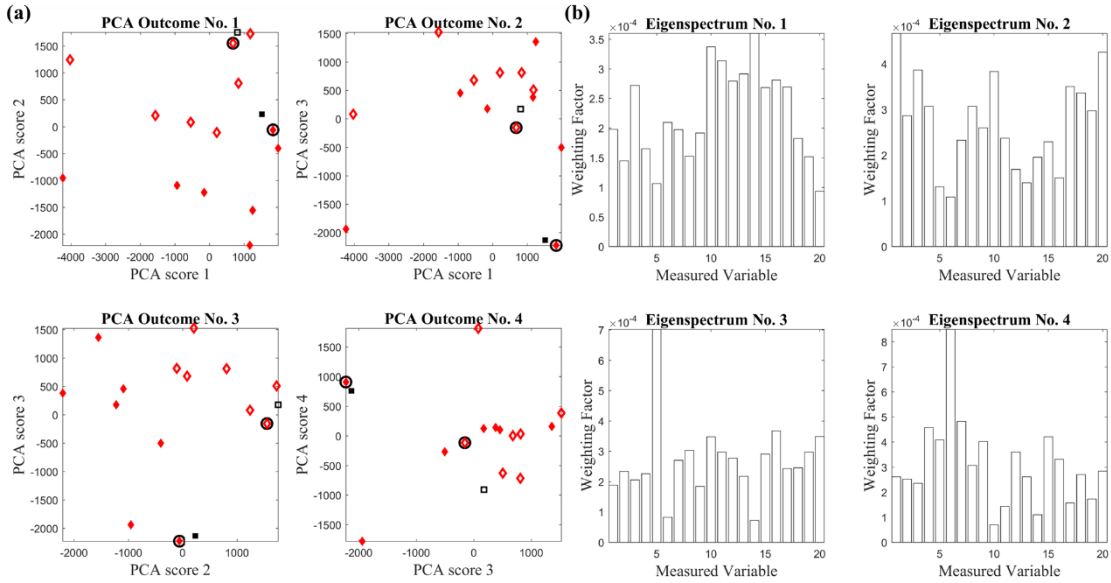

Figure 10.60 Individual with UTTA number 2 discriminated using the correlation matrix during attempted SYM_{SL+SF} (black squares) from a group of individuals with UTTA during NORM (red diamonds). Diamonds with black circle illustrate the NORM trial of individual with UTTA number 2.

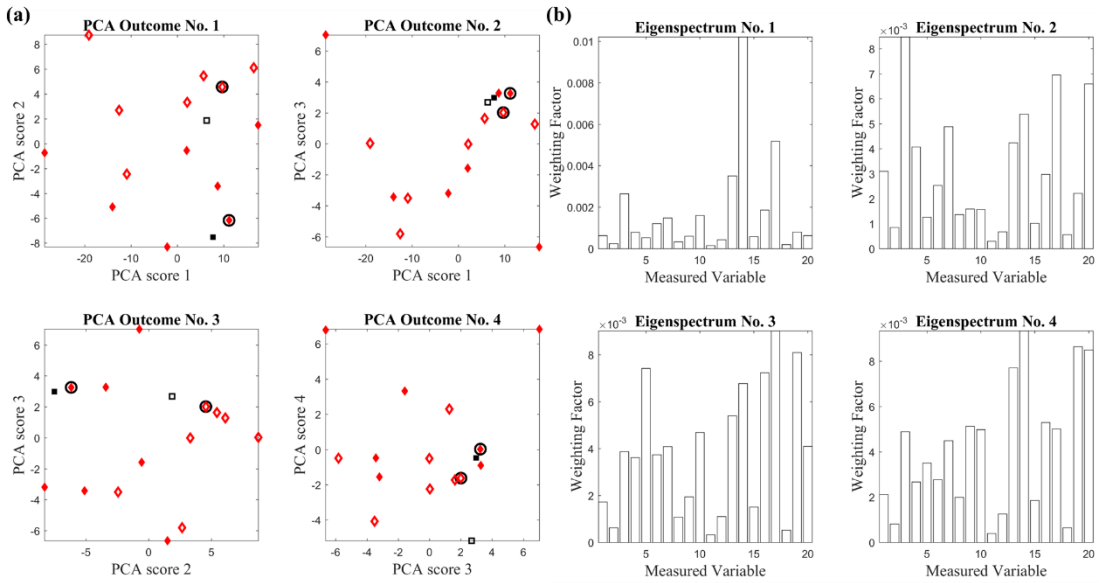

Figure 10.61 Individual with UTTA number 3 discriminated using the covariance matrix during attempted SYM_{SL+SF} (black squares) from a group of individuals with UTTA during NORM (red diamonds). Diamonds with black circle illustrate the NORM trial of individual with UTTA number 3.

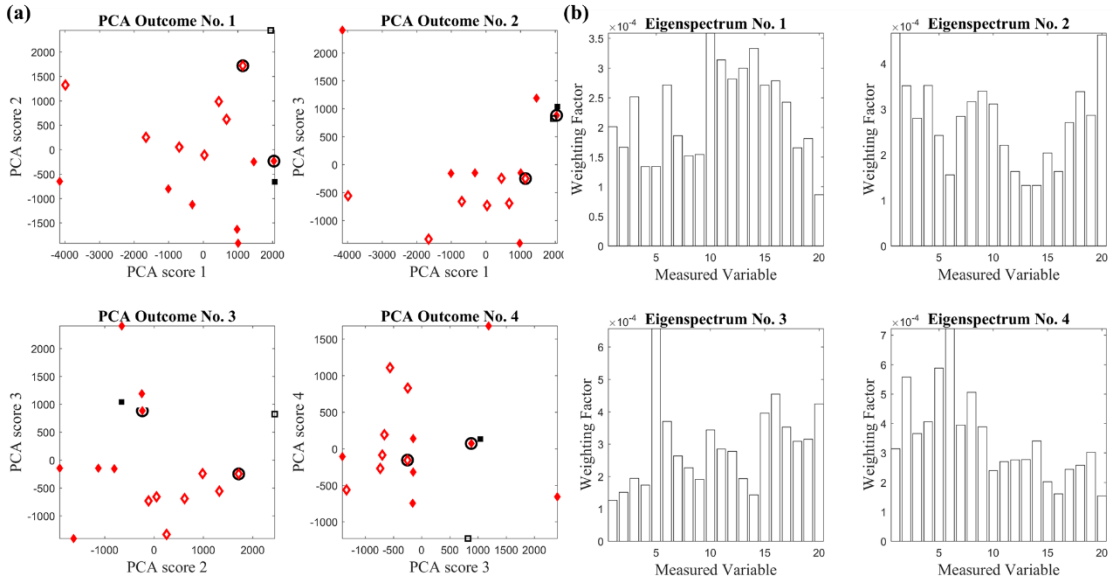

Figure 10.62 Individual with UTTA number 3 discriminated using the correlation matrix during attempted SYM_{SL+SF} (black squares) from a group of individuals with UTTA during NORM (red diamonds). Diamonds with black circle illustrate the NORM trial of individual with UTTA number 3.

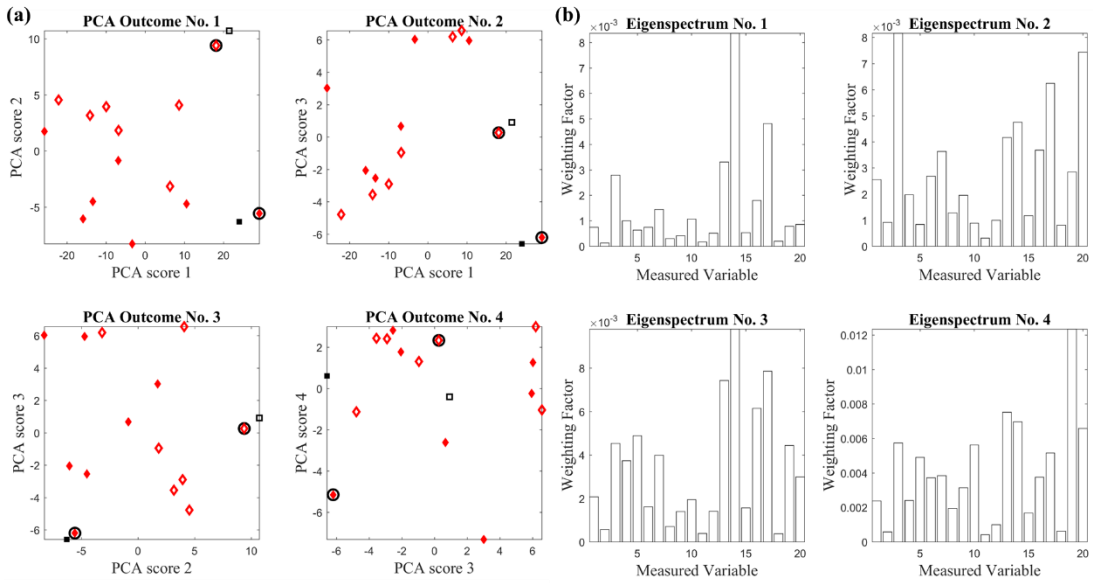

Figure 10.63 Individual with UTTA number 4 discriminated using the covariance matrix during attempted SYM_{SL+SF} (black squares) from a group of individuals with UTTA during NORM (red diamonds). Diamonds with black circle illustrate the NORM trial of individual with UTTA number 4.

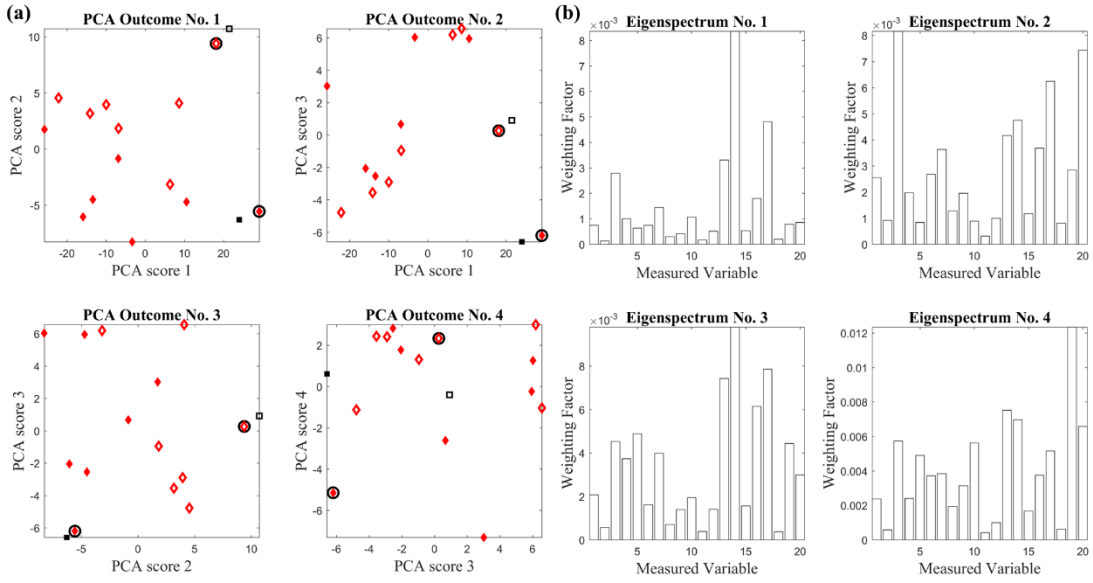

Figure 10.64 Individual with UTTA number 4 discriminated using the correlation matrix during attempted SYM_{SL+SF} (black squares) from a group of individuals with UTTA during NORM (red diamonds). Diamonds with black circle illustrate the NORM trial of individual with UTTA number 4.

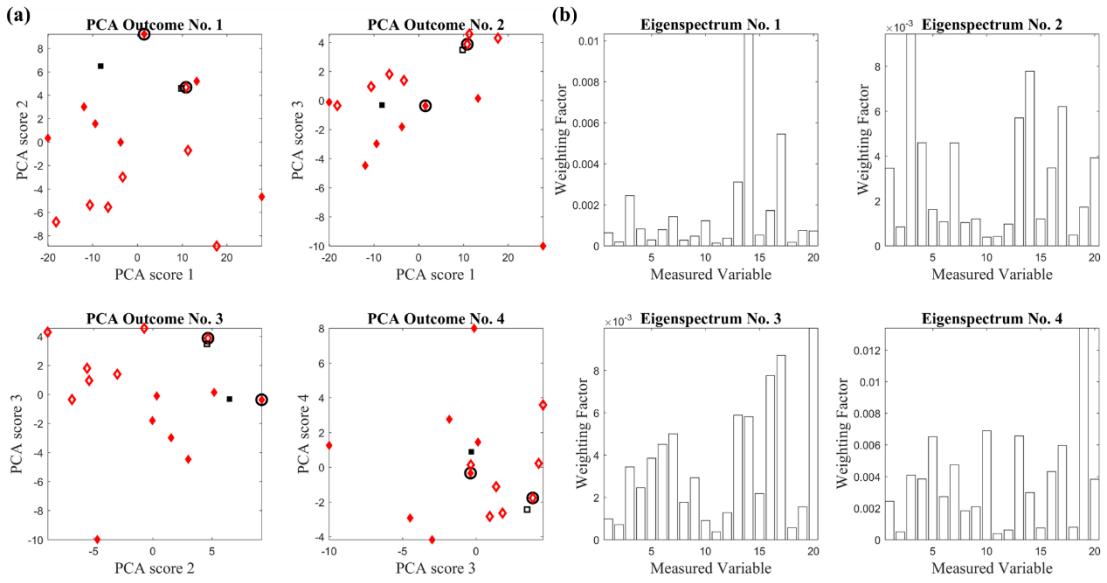

Figure 10.65 Individual with UTTA number 5 discriminated using the covariance matrix during attempted SYM_{SL+SF} (black squares) from a group of individuals with UTTA during NORM (red diamonds). Diamonds with black circle illustrate the NORM trial of individual with UTTA number 5.

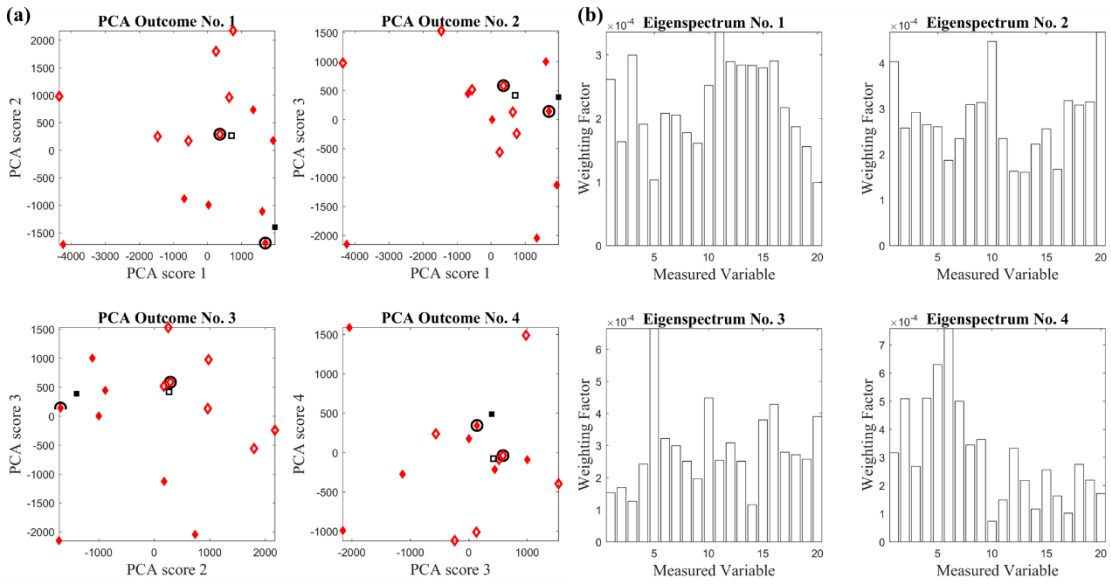

Figure 10.66 Individual with UTTA number 5 discriminated using the correlation matrix during attempted SYM_{SL+SF} (black squares) from a group of individuals with UTTA during NORM (red diamonds). Diamonds with black circle illustrate the NORM trial of individual with UTTA number 5.

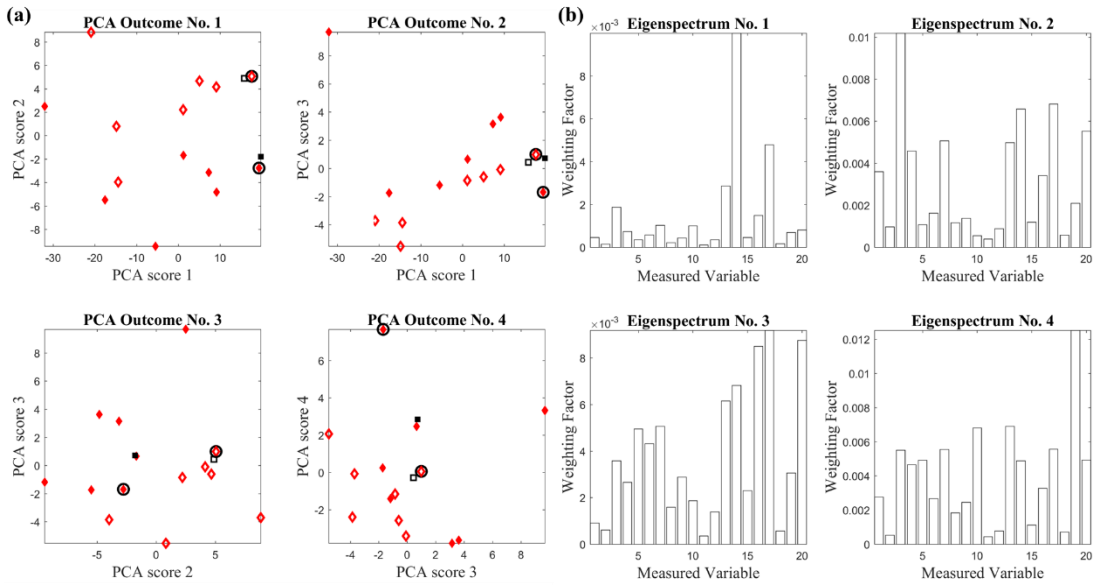

Figure 10.67 Individual with UTTA number 6 discriminated using the covariance matrix during attempted SYM_{SL+SF} (black squares) from a group of individuals with UTTA during NORM (red diamonds). Diamonds with black circle illustrate the NORM trial of individual with UTTA number 6.

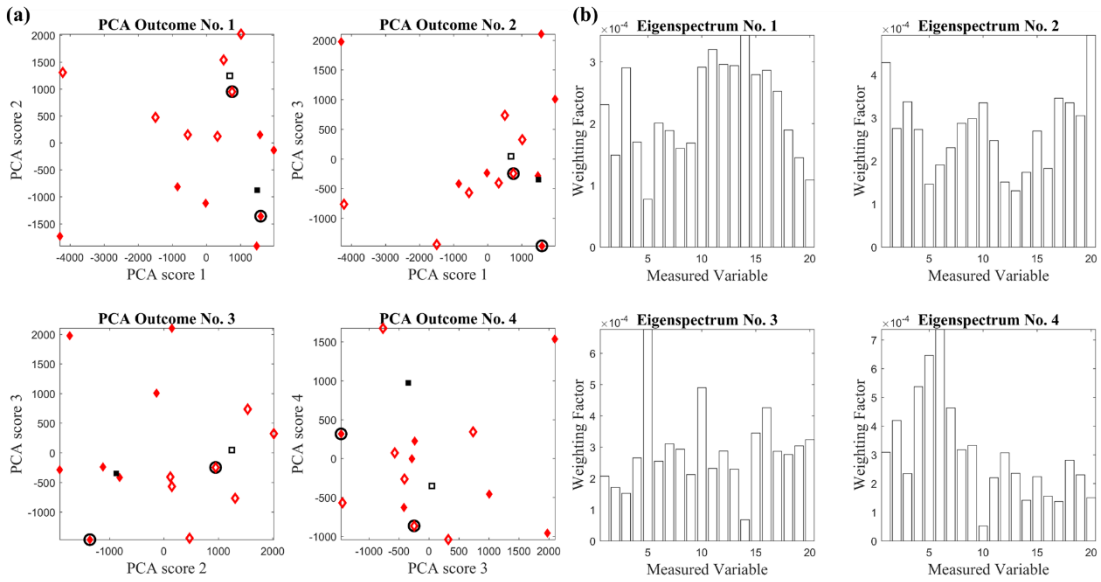

Figure 10.68 Individual with UTTA number 6 discriminated using the correlation matrix during attempted SYM_{SL+SF} (black squares) from a group of individuals with UTTA during NORM (red diamonds). Diamonds with black circle illustrate the NORM trial of individual with UTTA number 6.

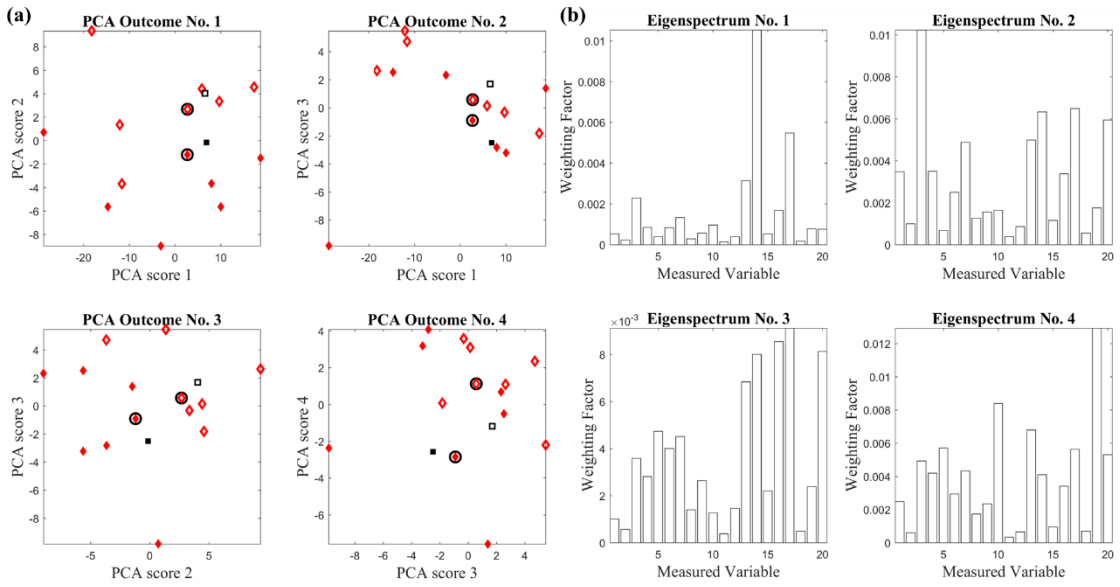

Figure 10.69 Individual with UTTA number 7 discriminated using the covariance matrix during attempted SYM_{SL+SF} (black squares) from a group of individuals with UTTA during NORM (red diamonds). Diamonds with black circle illustrate the NORM trial of individual with UTTA number 7.

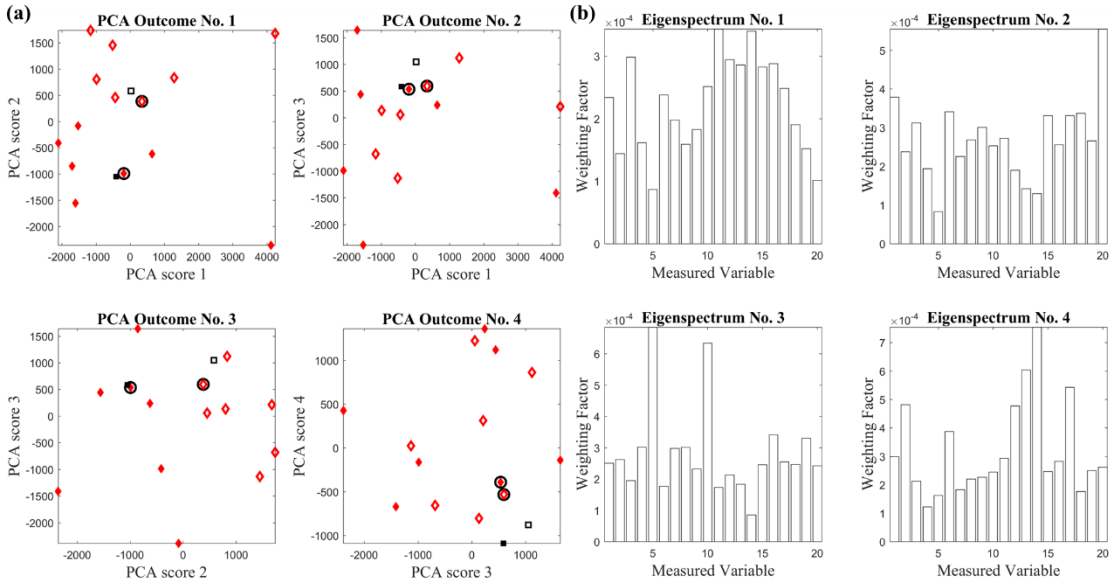

Figure 10.70 Individual with UTTA number 7 discriminated using the correlation matrix during attempted SYM_{SL+SF} (black squares) from a group of individuals with UTTA during NORM (red diamonds). Diamonds with black circle illustrate the NORM trial of individual with UTTA number 7.

Appendix 5 - Participant Information Sheet for and Consent Form for Study 1 Presented in Chapter 4

Appendix 2a

Participant Statement of Consent to Participate in the Investigation Entitled:

Biomechanical adaptations to barefoot running in habitually shod runners.

1) I, _____agree to partake as a participant in the above study.

2) I understand from the participant information sheet, which I have read in full, and from my discussion(s) with_____ that this will involve me running in three conditions: with your normal running shoes (SHOD), with minimal shoes i.e. plimsolls (MIN) and without shoes i.e. barefoot (BRFT) and then a repeat of these conditions with a change in direction, in the biomechanics laboratory on three occasions for duration of approximately one hour.

3) It has also been explained to me by_____that the risks and side effects which may result from my participation are as follows: allergic reaction to sticky tape, falling from a treadmill and muscle pain and/or strain due to exercising.

4) I confirm that I have had the opportunity to ask questions about the study and, where I have asked questions, these have been answered to my satisfaction.

5) I undertake to abide by University regulations and the advice of researchers regarding safety.

6) I am aware that I can withdraw my consent to participate in the procedure at any time and for any reason, without having to explain my withdrawal and that my personal data will be destroyed.

7) I understand that any personal information regarding me, gained through my participation in this study, will be treated as confidential and only handled by individuals relevant to the performance of the study and the storing of information thereafter. Where information concerning myself appears within published material, my identity will be kept anonymous.

8) I confirm that I have had the University's policy relating to the storage and subsequent destruction of sensitive information explained to me. I understand that sensitive information I have provided through my participation in this study, in the form of personal contact details and motion capture data will be handled in accordance with this policy.

9) I confirm that I have completed the health questionnaire and know of no reason, medical or otherwise that would prevent me from partaking in this research.

Participant signature: Date:

Independent witness signature: Date:

Primary Researcher signature: Date:

Appendix 6 – Participant Information Sheet for Studies 2-4 Presented in Chpaters 5-7

Appendix 6.1 – Participant Information Sheet for Prosthetic User

NOTTINGHAM TRENT UNIVERSITY

PARTICIPANT INFORMATION SHEET FOR PROSTHESIS USER

Title of Project: Understanding the influence of symmetry manipulations on lower limb amputee walking gait and dynamic stability.

IRAS ID: 203582

Name of Researcher: Miss Maria Bisele

Contact Details: Email maria.bisele2014@my.ntu.ac.uk

We would like to invite you to take part in a research study. Before you decide, we would like you to understand why the research is being done and what it would involve for you.

Please take time to carefully read the following information and talk to others about the study if you wish.

Part 1 will tell you about the purpose of the study and what will happen if you decide to take part.

Part 2 gives you more detailed information about the conduct of the study.

Please ask us if there is anything that is not clear or if you would like more information. We would like to know if you would like to take part in this research study. You have up to two weeks following your appointment to decide whether or not you would like to take part.

PART 1

What is the purpose of this study?

People with a lower limb amputation have been shown to fall more often when compared to age-matched individuals without lower limb amputation. Prosthesis users adopt certain compensatory mechanisms to have more efficient gait. Rehabilitation intervention are aimed to re-educate amputees to abandon these mechanisms and walk in a manner similar to non-amputees. However it has become apparent that these mechanisms facilitate the amputee's balance thus changing them would result in the reduction of balance leading to an increased risk of falling. Therefore, the aim of this study is to investigate whether walking in a manner which is similarly to non-amputees causes a reduction of balance in amputees.

Why have I been invited?

You have been invited to take part in this study as you fit the criteria required to participate in this study.

Do I have to take part?

No. Participation in this study is entirely voluntary.

If you do decide to take part in this study, you will be free to stop taking part at any time without giving a reason. This will not affect your care, your future treatment or your legal rights in any way.

What will happen if I decide to take part?

If you decide to take part in the study then great! You will need to contact Miss Maria Bisele (maria.bisele2014@my.ntu.ac.uk, Dr. Cleveland Barnett 01158483824) to let her know you are keen to take part and you will then be invited to the Biomechanics Laboratory, at Nottingham Trent University. You will be asked to bring along a pair of shorts, a t-shirt or vest and some comfortable shoes you can walk in. No high heels are permitted in the laboratory. If you do not have shorts, they will be provided for you. You are also advised to bring along food and drink.

When you arrive, you will be asked to change into your shorts and t-shirt. Reflective markers will be placed on your skin with double sided sticky tape. The markers are about the size of a marble, made of polystyrene and covered in reflective tape. Electromyography electrodes will also be placed on your skin. To place these a standardised skin preparation will be performed during which the area of interest will be shaved until free of hair, the surface will then be lightly abrading to remove dead skin cells and wiped clean with alcohol to remove oils from the skin. Once markers and the electrodes are in place you will be asked to perform a gait analysis task (which is described in more details in the Section '*What do I have to do*').

Are there any costs involved?

No. The University will reimburse any costs that you incur as a result of travelling to the University at a standard University rate of **25p** per mile travelled if coming by car. Your fare will be reimbursed if you come by train or taxi.

What do I have to do?

The testing will be conducted over seven visits, you will be asked to attend the first two sessions for a gait analysis test and if you feel fit to it you will be asked to attend an additional five sessions for a dynamometer test. The overall time commitment of the your visits should not exceed 32 hours in a four week period.

During visit 1.(gait analysis) you will be walking across a 15m walkway at self-selected speed. This will be repeated for each leg five times. You are then asked to repeat these trials at both self-selected slow and self-selected fast speeds.

If you are a non- prosthesis user, you will be equipped with an ankle-foot orthosis and the same tasks are repeated.

During visit 2. (gait analysis) step length and step frequencies measured during the visit 1. are altered by the researcher so that you will follow a walking pattern which is not habitual to you.

If you are used to conducting vigorous-intensity activity without experiencing any complications and distress, and you decide you will carry on, you will be asked to come in for an additional five visits to conduct a dynamometer test using an isokinetic dynamometer as displayed below in Figure 1. During this test maximum strength of hip, knee and ankle joints are measured. However if you do not wish to conduct any further testing, it is not a problem. Participation in this study is entirely voluntary and you are free to withdraw at any time without giving a reason.

During visit 3. and 4. you will be familiarised with the use of the dynamometer. During visit 5., 6. and 7. you will perform the test. The dynamometer test involves you being tightly strapped into a chair whilst pushing or pulling your leg with full force against the resistance of the crank arm which extends from the dynamometer. The strength exerted during the actions of pulling and pulling are recorded. This process will be repeated for the extension and flexion of hip, knee and ankle joints and in various seating positions e.g. upright and lying down flat on your back.

Figure 1. Dynamometer.

Are there any risks involved?

When performing the gait analysis tasks, you may feel unstable. However, you will not be asked to perform any tasks that you feel are not within your capabilities.

It is extremely rare but one possible side effect of sticky tape being placed on the skin is a skin reaction to the tape. Your skin will be checked when the markers have been removed and, if there has been any reaction, appropriate treatment would be recommended. There is also a miniscule risk of an infection because of the skin preparation which is done to place the EMG electrodes, however new equipment will be used during each session to minimise the chance of this happening.

You may experience fatigue or tiredness associated with walking so you will be advised to bring along food and drink, and will be afforded generous rest periods in order to recuperate.

Prosthesis users may experience abrasion at the socket-residuum interface. Thus you will be asked to bring your usual sock and liner and you will be able to remove/attach your prosthetic at your leisure.

Non- prosthesis user may experience musculoskeletal soreness and abrasions from the use of the ankle-foot orthosis. You will be afforded generous rest periods in order to recuperate.

When performing the dynamometer testing, you will be required to exert multiple maximal voluntary hip, knee and ankle extension and flexion tasks which may result in some fatigue. You may also feel short of breath after efforts and may feel some delayed muscle soreness following each session. You will be afforded generous rest periods in order to recuperate and will be invited to stop the data collection sessions if abrasions occur and impact upon your ability to perform the tasks pain free.

Being tightly constrained by straps keeping you in place and repeated application of force may result in soreness, which will be prevented or reduced by providing additional cushioning.

There is a risk that you may faint or experience a heart attack during the dynamometer testing due to the nature of the physical activity, however it is very unlikely assuming you meet the required inclusion criteria. First aiders are available during the duration of the testing protocol in the events of any unexpected emergencies. If you are suffering from any cardiovascular complaints you do not meet the inclusion/exclusion criteria and are unable to participate in this study due to the risks involved with exercising on a dynamometer.

The correct health and safety measures are taken at all times in the Biomechanics Laboratory and first aiders from the sport's department are on site at all times during the testing period. First aider will be sampled from the following list of current first aiders within the department and on site: Terry Campion (Laboratory Technician in Sport Science, First Aid Certificate), Alan MaNally (Reader in Bioscience, First Aid Certificate), Paul Lester (PhD Student and Hourly Paid Lecturer in in Sport and Exercise Science, TQUK Level 2 Award in Emergency First Aid at Work (QCF)).

What happens when the research study stops?

The results from the study will be published in scientific and clinical publications as well as being presented at international conferences. You will not be identified in any of this material to preserve your confidentiality. You may request a copy of any published results from Miss Maria Bisele.

What if there is a problem?

Any complaint about the way you have been dealt with during the study or any possible harm you might suffer will be addressed. Please contact Professor Mary Nevill, Head of Department of Sport Science (mary.nevill@ntu.ac.uk, 011584883918) if this is the case.

If the information in Part 1 has interested you and you are considering taking part in the study, please read on to Part 2 for additional details.

PART 2

Confidentiality

All information and data from the study will be kept strictly confidential., Your name and details will not be disclosed at any time and you will be assigned a code number to identify you in the study. All data and information will be kept on record electronically on a password protected computer and in locked filling cabinets.

Miss Maria Bisele has responsibility to safeguard the data and information and only those individuals involved with the study will have access to these sources.

All data and information will be kept by Miss Maria Bisele at Nottingham Trent University for the duration of the study and 5 years beyond as to conform with regulations related to challenges that could be made in terms of publication of data stemming from this study.

In case that you withdraw from the study, data already collected with consent will be retained and used in the study.

Please be aware that, when giving consent to participate, you are agreeing with the conditions outlined above.

Your Rights

Your participation in this study is voluntary. You are allowed to withdraw from the study at any time without reason. This will not affect any future treatment or any legal rights. Withdrawal is totally without prejudice.

For more advice on the project please contact Miss Maria Bisele, email maria.bisele2014@my.ntu.ac.uk.

Trial-Related Injury

It is unlikely that you will experience an injury or illness as a result of taking part in this research study. However, indemnity is provided by the Nottingham Trent University and any compensation will be as per the University's usual standards. For more information please contact Miss Maria Bisele.

Who is organising the study?

Miss Maria Bisele, School of Science and Technology, Nottingham Trent University.

Thank you for your time and I look forward to speaking to you soon.

Miss Maria Bisele
School of Science and Technology
Nottingham Trent University

Appendix 6.2 – Participant Information Sheet for Non-Prosthetic User

NOTTINGHAM TRENT UNIVERSITY

PARTICIPANT INFORMATION SHEET FOR NON-PROSTHESIS USER

Title of Project: Understanding the influence of symmetry manipulations on lower limb amputee walking gait and dynamic stability.

IRAS ID: 203582

Name of Researcher: Miss Maria Bisele

Contact Details: Email maria.bisele2014@my.ntu.ac.uk

We would like to invite you to take part in a research study. Before you decide, we would like you to understand why the research is being done and what it would involve for you.

Please take time to carefully read the following information and talk to others about the study if you wish.

Part 1 will tell you about the purpose of the study and what will happen if you decide to take part.

Part 2 gives you more detailed information about the conduct of the study.

Please ask us if there is anything that is not clear or if you would like more information. We would like to know if you would like to take part in this research study. You have up to two weeks following your appointment to decide whether or not you would like to take part.

PART 1

What is the purpose of this study?

People with a lower limb amputation have been shown to fall more often when compared to age-matched individuals without lower limb amputation. Prosthesis user adopt certain compensatory mechanisms to have more efficient gait. Rehabilitation intervention are aimed to re-educate amputees to abandon these mechanisms and walk in a manner similar to non-amputees. However it has become apparent that these mechanisms facilitate the amputee's balance thus changing them would result in the reduction of balance leading to an increased risk of falling. Therefore, the aim of this study is to investigate whether walking in a manner which is similar to non-amputees causes a reduction of balance in amputees.

Why have I been invited?

You have been invited to take part in this study as you fit the criteria required to participate in this study.

Do I have to take part?

No. Participation in this study is entirely voluntary.

If you do decide to take part in this study, you will be free to stop taking part at any time without giving a reason.

What will happen if I decide to take part?

If you decide to take part in the study then great! You will need to contact Miss Maria Bisele (maria.bisele2014@my.ntu.ac.uk, Dr. Cleveland Barnett 01158483824) to let her know you are keen to take part and you will then be invited to the Biomechanics Laboratory, at Nottingham Trent University. You will be asked to bring along a pair of shorts, a t-shirt or vest and some comfortable shoes you can walk in. No high heels are permitted in the laboratory. If you do not have shorts, they will be provided for you. You are also advised to bring along food and drink.

When you arrive, you will be asked to change into your shorts and t-shirt. Reflective markers will be placed on your skin with double sided sticky tape. The markers are about the size of a marble, made of polystyrene and covered in reflective tape. Electromyography electrodes will also be placed on your skin. To place these a standardised skin preparation will be performed during which the area of interest will be shaved until free of hair, the surface will then be lightly abrading to remove dead skin cells and wiped clean with alcohol to remove oils from the skin. Once markers and the electrodes are in place you will be asked to perform a gait analysis task (which is described in more details in the Section '*What do I have to do*').

Are there any costs involved?

No. The University will reimburse any costs that you incur as a result of travelling to the University at a standard University rate of **25p** per mile travelled if coming by car. Your fare will be reimbursed if you come by train or taxi.

What do I have to do?

The testing will be conducted over seven visits, you will be asked to attend the first two sessions for a gait analysis test and if you feel fit to it you will be asked to attend an additional five sessions for a dynamometer test. The overall time commitment of the your visits should not exceed 32 hours in a four week period.

During visit 1.(gait analysis) you will be walking across a 15m walkway at self-selected speed. This will be repeated for each leg five times. You are then asked to repeat these trials at both self-selected slow and self-selected fast speeds.

If you are a non- prosthesis user, you will be equipped with an ankle-foot orthosis and the same tasks are repeated. An ankle-foot orthosis is a brace, made of plastic (as seen in Figure 1.), which holds the lower leg and the foot in place to limit movement at the ankle.

Figure 1. Ankle-Foot Orthosis.

During visit 2. (gait analysis) step length and step frequencies measured during the visit 1. are altered by the researcher so that you will follow a walking pattern which is not habitual to you.

If you are used to conducting vigorous-intensity activity without experiencing any complications and distress, and you decide you will carry on, you will be asked to come in for an additional five visits to conduct a dynamometer test using an isokinetic dynamometer as displayed below in Figure 2. During this test maximum strength of hip, knee and ankle joints are measured. However if you do not wish to conduct any further testing, it is not a problem. Participation in this study is entirely voluntary and you are free to withdraw at any time without giving a reason.

During visit 3. and 4. you will be familiarised with the use of the dynamometer. During visit 5., 6. and 7. you will perform the test. The dynamometer test involves you being tightly strapped into a chair whilst pushing or pulling your leg with full force against the resistance of the crank arm which extends from the dynamometer. The strength exerted during the actions of pulling and pulling are recorded. This process will be repeated for the extension and flexion of hip, knee and ankle joints and in various seating positions e.g. upright and lying down flat on your back.

Figure 2. Dynamometer.

Are there any risks involved?

When performing the gait analysis tasks, you may feel unstable. However, you will not be asked to perform any tasks that you feel are not within your capabilities.

It is extremely rare but one possible side effect of sticky tape being placed on the skin is a skin reaction to the tape. Your skin will be checked when the markers have been removed and, if there has been any reaction, appropriate treatment would be recommended. There is also a miniscule risk of an infection because of the skin preparation which is done to place the EMG electrodes, however new equipment will be used during each session to minimise the chance of this happening.

You may experience fatigue or tiredness associated with walking so you will be advised to bring along food and drink, and will be afforded generous rest periods in order to recuperate.

Prosthesis users may experience abrasion at the socket-residuum interface. Thus you will be asked to bring your usual sock and liner and you will be able to remove/attach your prosthetic at your leisure.

Non- prosthesis user may experience musculoskeletal soreness and abrasions from the use of the ankle-foot orthosis. You will be afforded generous rest periods in order to recuperate.

When performing the dynamometer testing, you will be required to exert multiple maximal voluntary hip, knee and ankle extension and flexion tasks which may result in some fatigue. You may also feel short of breath after efforts and may feel some delayed muscle soreness following each session. You will be afforded generous rest periods in order to recuperate and will be invited

to stop the data collection sessions if abrasions occur and impact upon your ability to perform the tasks pain free.

Being tightly constrained by straps keeping you in place and repeated application of force may result in soreness, which will be prevented or reduced by providing additional cushioning.

There is a risk that you may faint or experience a heart attack during the dynamometer testing due to the nature of the physical activity, however it is very unlikely assuming you meet the required inclusion criteria. First aiders are available during the duration of the testing protocol in the events of any unexpected emergencies. If you are suffering from any cardiovascular complaints you do not meet the inclusion/exclusion criteria and are unable to participate in this study due to the risks involved with exercising on a dynamometer.

The correct health and safety measures are taken at all times in the Biomechanics Laboratory and first aiders from the sport's department are on site at all times during the testing period. First aider will be sampled from the following list of current first aiders within the department and on site: Terry Campion (Laboratory Technician in Sport Science, First Aid Certificate), Alan MaNally (Reader in Bioscience, First Aid Certificate), Paul Lester (PhD Student and Hourly Paid Lecturer in in Sport and Exercise Science, TQUK Level 2 Award in Emergency First Aid at Work (QCF)).

What happens when the research study stops?

The results from the study will be published in scientific and clinical publications as well as being presented at international conferences. You will not be identified in any of this material to preserve your confidentiality. You may request a copy of any published results from Miss Maria Bisele.

What if there is a problem?

Any complaint about the way you have been dealt with during the study or any possible harm you might suffer will be addressed. Please contact Professor Mary Nevill, Head of Department of Sport Science (mary.nevill@ntu.ac.uk, 011584883918) if this is the case.

If the information in Part 1 has interested you and you are considering taking part in the study, please read on to Part 2 for additional details.

PART 2

Confidentiality

All information and data from the study will be kept strictly confidential., Your name and details will not be disclosed at any time and you will be assigned a code number to identify you in the study. All data and information will be kept on record electronically on a password protected computer and in locked filling cabinets.

Miss Maria Bisele has responsibility to safeguard the data and information and only those individuals involved with the study will have access to these sources.

All data and information will be kept by Miss Maria Bisele at Nottingham Trent University for the duration of the study and 5 years beyond as to conform with regulations related to challenges that could be made in terms of publication of data stemming from this study.

In case that you withdraw from the study, data already collected with consent will be retained and used in the study.

Please be aware that, when giving consent to participate, you are agreeing with the conditions outlined above.

Your Rights

Your participation in this study is voluntary. You are allowed to withdraw from the study at any time without reason. Withdrawal is totally without prejudice.

For more advice on the project please contact Miss Maria Bisele, email maria.bisele2014@my.ntu.ac.uk.

Trial-Related Injury

It is unlikely that you will experience an injury or illness as a result of taking part in this research study. However, indemnity is provided by the Nottingham Trent University and any compensation will be as per the University's usual standards. For more information please contact Miss Maria Bisele.

Who is organising the study?

Miss Maria Bisele, School of Science and Technology, Nottingham Trent University.

Thank you for your time and I look forward to speaking to you soon.

Miss Maria Bisele
School of Science and Technology
Nottingham Trent University

Appendix 7 – Participant Consent Form experimental for Studies 2-4 Presented in Chapters 5-7

Appendix 7.1 – Participant Consent form for Prosthetic User

NOTTINGHAM TRENT UNIVERSITY

Patient Identification Number for this trial:

CONSENT FORM FOR PROSTHESIS USER

Title of Project: Understanding the influence of symmetry manipulations on lower limb amputee walking gait and dynamic stability.

IRAS ID: 203582

Name of Researcher: **Miss Maria Bisele**

Please initial all boxes

1. I confirm that I have read and understand the information sheet dated ____/____/____ (version **PIS006_PROS**) for the above study. I have had the opportunity to consider the information, ask questions and have had these answered satisfactorily. ☐

2. I understand that my participation is voluntary and that I am free to withdraw at any time without giving any reason, without my medical care or legal rights being affected. ☐

3. I understand that relevant Sections of my medical notes and data collected during the study, may be looked at by individuals from **Nottingham Trent University and The Mobility Centre, Nottingham University Hospitals NHS Trust**, from regulatory authorities or from the NHS Trust, where it is relevant to my taking part in this research. I give permission for these individuals to have access to my records. ☐

4. I agree to take part in the above study. ☐

Name of Participant	Date	Signature
Name of Person taking consent	Date	Signature

A copy of this form will be retained by the researchers, a copy will be given to the participant and a copy will be placed in the medical notes of the prosthetic user.

Appendix 7.2 – Participant Consent form for Prosthetic User

NOTTINGHAM TRENT UNIVERSITY

Patient Identification Number for this trial:

CONSENT FORM FOR NON-PROSTHESIS USER

Title of Project: Understanding the influence of symmetry manipulations on lower limb amputee walking gait and dynamic stability.

IRAS ID: 203582

Name of Researcher: **Miss Maria Bisele**

Please initial all boxes

5. I confirm that I have read and understand the information sheet dated ____/____/____ (version **PIS007_CON**) for the above study. I have had the opportunity to consider the information, ask questions and have had these answered satisfactorily. ☐

6. I understand that my participation is voluntary and that I am free to withdraw at any time without giving any reason, without my medical care or legal rights being affected. ☐

7. I understand that relevant Sections of my data collected during the study, may be looked at by individuals from **Nottingham Trent University and The Mobility Centre, Nottingham University Hospitals NHS Trust**, from regulatory authorities or from the NHS Trust, where it is relevant to my taking part in this research. I give permission for these individuals to have access to my records. ☐

8. I agree to take part in the above study. ☐

Name of Participant	Date	Signature
Name of Person taking consent	Date	Signature

A copy of this form will be retained by the researchers and a copy will be given to the participant.

Appendix 8 – Participant Health Screen for Studies 2-4 Presented in Chapters 5-7

NOTTINGHAM TRENT UNIVERSITY

Patient Identification Number for this trial:

Date:

PARTICIPANT DETAILS OF PROSTHESIS USER

Information with regards to Limb-Loss

Date of Amputation _____

Side of Amputation (Right or Left Limb): _____

Amputation Level (Above knee or Below knee): _____

Reason for amputation_____

Do you experience any phantom limb pain? _____

Frequency/intensity of pain? _____

Information with regards to Prosthesis

How long have you been using your current prosthesis?_____

Socket type _____

Liner type _____

Suspension type _____

Prosthetic components _____

Residuum Dimension: _____

Proximal circumference _____

Distal circumference _____

Length (from knee joint centre to tip) _____

Do you sometimes use any ambulatory aids (ie: walker, crutches, etc.)? How frequently?

_____

Do you have any issues in relation to the non- prosthetic limb e.g. osteoarthritis in knee?

_____

Exercising Details

Do you do any exercise?

_____

How many days during the week do you exercise?

_____

For how many hours does your exercise session last on average?

_____

Do you do any vigorous-intensity activity?

_____

Have you previously performed a maximum strength test using a dynamometer?

_____

NOTTINGHAM TRENT UNIVERSITY

Patient Identification Number for this trial:

Date:

PARTICIPANT DETAILS OF NON-PROSTHESIS USER

Exercising Details

Do you do any exercise?

_____

How many days during the week do you exercise?

_____

For how many hours does your exercise session last on average?

_____

Do you do any vigorous-intensity activity?

_____

Have you previously performed a maximum strength test using a dynamometer?

_____

NOTTINGHAM TRENT UNIVERSITY

Patient Identification Number for this trial:

MEDICAL AND HEALTH SCREEN

Please complete this brief questionnaire to confirm fitness to participate:

1. In general, how would you describe your health?

Excellent ____ Very good ____ Good ____ Fair ____ Poor ____

2. **At present,** do you have any health problem for which you are:

(a) on medication, prescribed or otherwise Yes ☐ No ☐

(b) attending your general practitioner (GP) Yes ☐ No ☐

(c) on a hospital waiting list Yes ☐ No ☐

If **YES**, please describe the condition(s):

_____

_____

3. Do you **currently** :

(a) Have a pace maker Yes ☐ No ☐

(b) Take medication **daily** (i.e. hypertension, oestrogen replacement therapy Yes ☐ No ☐

(c) Suffer from high blood pressure Yes ☐ No ☐

(d) Have any physical disabilities (e.g. visual or hearing problems) Yes ☐ No ☐

(e) Use an assistive device for walking Yes ☐ No ☐

(f) Sustain any regular limb pain when performing daily movement tasks Yes ☐ No ☐

(g) Have osteoporosis Yes ☐ No ☐

(h) Numbness, tingling, swelling or arthritis in hands or feet Yes ☐ No ☐

(i) Any other illness or condition that affects your general health or interferes with your mobility and may affect your participation in this study? Yes ☐ No ☐

Smoke cigarettes Yes ☐ No ☐

- If NO, have you ever smoked? Yes ☐ No ☐
- How many years? _____
- How many years since stopped _____
- Number formally smoked on an average day _____

3. **In the past five years,** have you had any illness which require you to:

(a) consult your GP Yes ☐ No ☐

(b) attend a hospital outpatient department Yes ☐ No ☐

(c) be admitted to hospital Yes ☐ No ☐

If **YES**, please describe the condition(s):

_____

_____

4. **Have you ever** had any of the following?

(a) Airway/chest problems or significant breathing difficulties Yes ☐ No ☐
(e.g. bronchitis, asthma or wheezy chest)?

(b) Allergy to nuts, alcohol etc Yes ☐ No ☐

(c) Back problems Yes ☐ No ☐

(d) Blood/blood vessel disorders Yes ☐ No ☐
(e.g. thrombosis, aneurysm, stroke, blood clots)

(e) Bone problems (e.g. osteoporosis, loss of height) Yes ☐ No ☐

(f) Broken or fractured any bones Yes ☐ No ☐

(g) Cerebrovascular disease Yes ☐ No ☐

(h) Convulsions/epilepsy Yes ☐ No ☐

(i) Diabetes or any other metabolic disease (please state if insulin dependent) Yes ☐ No ☐

(j) Disturbance of balance /coordination Yes ☐ No ☐

(k) Disturbance of vision Yes ☐ No ☐

(l) Ear /hearing problems Yes ☐ No ☐

(m) Emotional distress or psychiatric problems Yes ☐ No ☐
(worse than mild anxiety or depression)

(n) Head injury Yes ☐ No ☐

(o) Heart problems (inc. heart attack, valve disease, palpitations, serve angina) Yes ☐ No ☐

(p) Joint surgery Yes ☐ No ☐

(q) Kidney or liver problems Yes ☐ No ☐

(r) Major illness now or in the last 20 years Yes ☐ No ☐
(e.g. rheumatoid arthritis, blood disorders, cancer)

(s) Problems with bones or joints Yes ☐ No ☐

(t) Suffered from significant memory loss Yes ☐ No ☐

(u) Thrombophlebitis or pulmonary embolus Yes ☐ No ☐

(v) Thyroid problems Yes ☐ No ☐

If yes to **ANY** of the above questions, please provide details on condition(s)

_____

_____

5. **Has any,** otherwise healthy, member of your family under the age of 50 died

Yes ☐ No ☐

suddenly during or soon after exercise?

6. Has a **close relative** had a heart attack before age 55 (father or brother)

Yes ☐ No ☐

or before age 65 (mother or sister)? If YES, who and at what age: _____

7. Have you had a cold, flu or any flu like symptoms in the last month?

Yes ☐ No ☐

9. Have you had febrile illness within the previous 6 months

Yes ☐ No ☐

9. Have you lost any mobility for greater than 1 week in the previous 6 months,

Yes ☐ No ☐

or greater than 2 weeks in the previous year?

If yes to **ANY** of the above questions, please provide details on condition(s)

_____

_____

10. Lifestyle and Exercise

Work

Does your work involve vigorous-intensity activity that causes large increases in breathing or heart rate like [carrying or lifting heavy loads, digging or construction work] for at least 10 minutes continuously?

Yes ☐ No ☐

In a typical week, on how many days do you do vigorous intensity activities as part of your work?

How much time do you spend doing vigorous-intensity activities at work on a typical day?

Does your work involve moderate-intensity activity, that causes small increases in breathing or heart rate such as brisk walking [or carrying light loads] for at least 10 minutes continuously?

Yes ☐ No ☐

In a typical week, on how many days do you do moderate intensity activities as part of your work?

How much time do you spend doing moderate-intensity activities at work on a typical day?

Activities

Do you do any vigorous-intensity sports, fitness or recreational (leisure) activities that cause large increases in breathing or heart rate like [running or football] for at least 10 minutes continuously?

Yes ☐ No ☐

In a typical week, on how many days do you do vigorous intensity sports, fitness or recreational (leisure) activities?

How much time do you spend doing vigorous-intensity sports, fitness or recreational activities on a typical day?

In a typical week, on how many days do you do moderate intensity sports, fitness or recreational (leisure) activities?

How much time do you spend doing moderate-intensity sports, fitness or recreational (leisure) activities on a typical day?

11. Women only

Are you pregnant, trying to become pregnant or breastfeeding?

Yes ☐ No ☐

If YES to any question, please describe briefly if you wish (e.g. to confirm problem was/is short-lived, insignificant or well controlled.

_____

Participant Name (Please print):

_____

Signature: _____ Date:_____

Researcher Name (Please print):

_____

Signature: _____ Date:_____

Thank you for completing this questionnaire.

In case of emergency details:

Name:

_____

Relationship to participant:

_____

Contact detail (1):

_____

Contact detail (2):

_____

Appendix 9 – Journal Article